AIRCRAFT ACCIDENT REPORT 1/2005

Air Accidents Investigation Branch

Department for Transport

Report on the accident to Sikorsky S-76A+, G-BJVX near the Leman 49/26 Foxtrot platform in the North Sea 16 July 2002

AIRCRAFT ACCIDENT REPORT 1/2005

Air Accidents Investigation Branch

Department for Transport

Report on the accident to
Sikorsky S-76A+, G-BJVX
near the Leman 49/26 Foxtrot platform
in the North Sea
16 July 2002

This investigation was carried out in accordance with
The Civil Aviation (Investigation of Air Accidents and Incidents) Regulations 1996

© *Crown Copyright 2005*

Published with the permission of the Department for Transport (Air Accidents Investigation Branch).

This report contains facts which have been determined up to the time of publication. This information is published to inform the aviation industry and the public of the general circumstances of accidents and serious incidents.

Extracts can be published without specific permission providing that the source is duly acknowledged.
Published 28 February 2005.
Produced from camera ready copy supplied by the Air Accidents Investigation Branch.

Printed in the United Kingdom for the Air Accidents Investigation Branch

RECENT AIRCRAFT ACCIDENT AND INCIDENT REPORTS
ISSUED BY THE AIR ACCIDENTS INVESTIGATION BRANCH

THE FOLLOWING REPORTS ARE AVAILABLE ON THE INTERNET AT
http://www.aaib.gov.uk

3/2003	Boeing 747-2B5F, HL-7451 near London Stansted Airport on 22 December 1999	July 2003
4/2003	McDonnell-Douglas MD-80, EC-FXI at Liverpool Airport on 10 May 2001	November 2003
1/2004	BAe 146, G-JEAK during descent into Birmingham Airport on 5 November 2000	February 2004
2/2004	Sikorsky S-61N, G-BBHM at Poole, Dorset on 15 July 2002	April 2004
3/2004	AS332L Super Puma, G-BKZE on-board the West Navion Drilling Ship 80 nm to the west of the Shetland Islands on 12 November 2001	June 2004
4/2004	Fokker F27 Mk 500 Friendship, G-CEXF at Jersey Airport, Channel Islands on 5 June 2001	July 2004
5/2004	Bombardier CL600-2B16 Series 604, N90AG at Birmingham International Airport on 4 January 2002	August 2004

Department for Transport
Air Accidents Investigation Branch
Berkshire Copse Road
Aldershot
Hampshire GU11 2HH

January 2005

The Right Honourable Alistair Darling
Secretary of State for Transport

Dear Secretary of State

I have the honour to submit the report by Mr J J Barnett, an Inspector of Air Accidents, on the circumstances of the accident to Sikorsky S-76A+, which occurred approximately 0.8 nm north west of the Leman 49/26 Foxtrot platform in the Leman Offshore Gas Field of the North Sea on 16 July 2002.

Yours sincerely

Ken Smart
Chief Inspector of Air Accidents

Contents

ANNEXES

GLOSSARY OF ABBREVIATIONS USED IN THIS REPORT

AAIB	Air Accidents Investigation Branch
AD	Airworthiness Directive
ADELT	Automatically Deployable Emergency Locator Transmitter
agl	above ground level
amp(s)	ampere(s)
ASB	Alert Service Bulletins
asl	above sea level
ATC	Air Traffic Control
BIM	Blade Inspection Method
BTE	Break Through Equivalent (a through-crack)
CAM	Cockpit Area Microphone
CMM	Composite Materials Manual
CVFDR	Combined Voice and Flight Data Recorder
DAPU	Data Acquisition and Processing Unit
EI	Engineering Instructions
ELT	Emergency Locater Transmitter
ETA	Estimated time of arrival
FAA	Federal Aviation Administration
FDR	Flight Data Recorder
FEM	Field Emission (Scanning Electron) Microscope
g	normal acceleration
HLO	Helicopter Landing Officer
hrs	hours (time)
HUMS	Health and Usage Monitoring System
IFR	Instrument Flight Rules
IHUMS	Integrated Health and Usage Monitoring System
KIAS	knots indicated airspeed
kt	knot(s)
lb	pound(s)
lbf	pounds force
MAPS	Movement and Personnel System
MAUW	Maximum all-up weight
MBPG	Minimum [Blade] Pitch on Ground
mins	minutes
mm	millimetres
MRB	Main Rotor Blade
NDT	Non-destructive test
nm	nautical mile(s)
Nr	Helicopter main-rotor RPM
NUI	Normally Unmanned Installation
ORIs	Overhaul and Repair Instructions
PC	Personal Computer
psi	pounds per square inch
QA	Quality Assurance
QFE	pressure setting to indicate
QNH	corrected mean sea level pressure
ROV	Remotely Operated Vehicle
RPM	revolutions per minute
RT	Radio transmission
RTB	Rotor track and balance
RTF	Radiotelephony
sec	second(s)
SEM	Scanning Electron Microscope
SRAM	Static Random Access Memory
TEM	Transmission Electron Microscope
TRB	Tail Rotor Blade
UK	United Kingdom
UKOOA	UK Offshore Operators Association
USA	United States (of America)
UTC	Universal Time Co-ordinated
VHF	Very high frequency
°C ºF ºM	Degrees Celsius, Fahrenheit, Magnetic

Air Accidents Investigation Branch

Aircraft Accident Report No: 1/2005 (EW/C2002/07/04)

Operator:	Bristow Helicopters Limited
Aircraft Type and Model:	Sikorsky S-76A+
Nationality:	British
Registration:	G-BJVX
Location:	Approximately 0.8 nm north west of the Leman 49/26 Foxtrot platform in the Leman Offshore Gas Field of the North Sea Latitude 53° 07' N Longitude 002°03' E
Date and Time:	16 July 2002 at approximately 1844 hrs UTC All times in this report are UTC

Synopsis

Lowestoft Coastguard notified the accident to the Air Accidents Investigation Branch (AAIB) at 2000 hrs on 16 July 2002 and the investigation began that same day. The following Inspectors participated in the investigation:

Mr J Barnett	Investigator-in-Charge
Mr N Dann	Operations
Mr K Conradi	Operations
Mr R Parkinson	Engineering
Mr S Moss	Engineering
Mr R Vance	Flight Data Recorders
Mr A Foot	Flight Data Recorders

The aircraft operator's base at Norwich operates S-76 helicopters in support of offshore oil and gas operations in the southern North Sea. On the evening of the accident the aircraft departed Norwich to complete a scheduled flight consisting of six sectors in the southern

North Sea offshore gas fields. The first four sectors were completed without incident but whilst en-route between the Clipper, an offshore production platform, and the Global Santa Fe Monarch, a drilling rig, the aircraft suffered a catastrophic structural failure. The helicopter's main rotor assembly separated almost immediately and the fuselage fell to the surface about 0.8 nm north-west of the Global Santa Fe Monarch which at the time was attached to the Leman 49/26 Foxtrot platform, a normally unmanned installation. Witnesses reported hearing a single or double muffled bang or boom, and seeing the aircraft fall into the sea. The fuselage disintegrated on impact and the majority of the structure sank. Fast rescue craft launched from the Putford Achilles, a multipurpose standby vessel, arrived at the scene of the accident within a few minutes. There were no survivors amongst the nine passengers and two crew.

The investigation identified the following causal factors:

i) A manufacturing anomaly created an area of reduced insulation between a main rotor blade's spar and one section of its two-piece leading edge erosion cover.

ii) The affected blade had been struck by lightning.

iii) Electrical energy from the lightning strike exploited the manufacturing anomaly and caused microstructural damage that was not detectable when the blade was returned to its manufacturer for assessment.

iv) The blade was repaired before being returned to service and a fatigue crack in the spar originated from the microstructural damage.

v) An opaque protective patch applied to the erosion cover's scarf joint hid exterior symptoms of the developing spar crack that appeared before the accident.

vi) The helicopter's proprietary onboard Health and Usage Monitoring System (IHUMS) did not provide sufficient warning of impending blade failure in time to avert the accident.

vii) There were no in-flight symptoms of impending blade failure that the pilots should have recognised.

Six safety recommendations have been made.

1 Factual Information

1.1 History of flight

1.1.1 Background

On the day of the accident the aircraft was scheduled to complete five flights from Norwich. The first two flights were completed by an early shift crew. The accident crew reported for duty at 1100 hrs UTC and had been rostered to fly the remaining three flights. They completed the first two flights without incident.

The fifth and final flight of the day was scheduled to depart Norwich at 1700 hrs UTC. Included in this flight was a passenger and article of freight destined for the Maersk Enhancer drilling rig. Due to the late arrival of this freight it was decided to put both the passenger and freight on a later flight, and the Maersk Enhancer was dropped from the route. As a result of these changes the aircraft was delayed and finally departed at 1732 hrs.

1.1.2 Facility Descriptions

Norwich - an International Airport.

Santa Fe Britannia - a four-leg Jack Up rig located, at the time of the accident, alongside the 'Skiff' Normally Unmanned Installation (NUI) in the Sole Pit field.

Shell Clipper - a manned gas production platform, the nodal platform for the Sole Pit field.

Shell Barque PL - a NUI in the Sole Pit field

Santa Fe Monarch - a three-leg Jack Up rig located, at the time of the accident, alongside the Leman 49/26 Foxtrot NUI.

1.1.3 Route details

The aircraft was scheduled to operate the offshore shuttle flight Number 1800, scheduled in the Movement and Personnel System (MAPS) as Flight 2-1800. The planned route was as follows:

Norwich-Britannia-Clipper-Barque PL-Clipper-Santa Fe Monarch-Norwich

The route flown together with the sector distances and times is shown in the diagram at Annex A. The relevant times and distances are shown in the table below:

Table 1 – Sector Distances and Times

Sector	Departure Time (UTC)	Arrival Time (UTC)	Flight time (hrs:mins)	Sector Distance (nm)
Norwich to Britannia	1732	1757	0:25	51
Britannia to Clipper	1801	1806	0:05	6
Clipper to Barque PL	1808	1814	0:06	7
Barque PL to Clipper	1817	1823	0:06	7
Clipper to Santa Fe Monarch	1831	N/A	0:13	24
Totals			0:55	95

1.1.4 Conduct of the flight

Prior to the final departure the crew carried out their normal pre-flight planning and were seen by several witnesses to complete a full walkround check of the aircraft. The passenger bags and freight were loaded on the aircraft before the five passengers arrived from the airport terminal by bus. After a short wait they boarded the aircraft.

The aircraft start-up appeared normal to the start-up engineer who was monitoring the start from outside the aircraft; however, two passengers stated that it seemed to take longer than usual for the rotors to reach their normal speed. The same passengers also stated that they heard unusual noises during rotor start likened to an engine running with low oil.

After start the aircraft taxied from the eastern apron onto the Bravo Taxiway. This taxiway was closed at holding point B1 due to work in progress and the aircraft hover taxied around the holding point directly to the runway. This took it over an area of recently cut grass and two passengers reported seeing grass being lifted by the rotor downwash.

The passengers who commented on the long start and unusual noises also stated that the hover at this point seemed to be laboured, described as like a car being driven with its handbrake half on.

The aircraft then took off from Runway 27.

1.1.5 Offshore witness information

Interviews were carried out with passengers who travelled on the aircraft during the sectors prior to its final departure from the Clipper. Helideck crews were also interviewed at all the installations visited on these sectors. Everyone interviewed offshore described the aircraft's operation as completely normal.

On the sector from the Barque PL to the Clipper one passenger stated that he sat in the row directly behind the pilots and was able to observe the pilot in the left-hand seat (the co-pilot's seat). He stated that this pilot was flying the aircraft and that during the flight he noticed the speed was 120 kt. He continued to watch as the helicopter slowed down to start its approach to the Clipper until it was at 80 kt; he then diverted his attention elsewhere. He could not remember any of the other indications on the instruments, but commented that the pilots did not appear to be dealing with any particular problems during the flight.

On arrival at the Clipper from the Barque PL all the passengers, with the exception of one, disembarked from the aircraft; the transit passenger occupied the front row right-hand seat. The bags from the Barque PL were offloaded and the bags for the next sector, including some surveying equipment, were loaded into the baggage compartment. A further eight passengers then boarded and the aircraft departed for the Global Santa Fe Monarch. The helideck crew reported that the takeoff appeared normal.

The installation crew on the Global Santa Fe Monarch were not expecting any more flights to arrive that day and were surprised to receive a radio message from the aircraft requesting wind information for their landing on the Monarch. The Monarch helideck crew was hastily assembled and the Helicopter Landing Officer (HLO) recalled seeing the aircraft commence its approach. At this point it appeared to be perfectly normal, but he then lost sight of the aircraft behind the rig structure. Witnesses report that there was either a single or double muffled bang or boom, although no one was actually watching the aircraft at this point. On hearing the bang the witnesses turned around and saw the aircraft falling into the sea. One witness reported that it was tumbling but intact and that the main rotors appeared to be going round slowly enough to make out each individual blade. Another reported seeing the aircraft dive steeply towards the water rolling to the left. A third witness reported seeing the main rotor "flutter down like a sycamore seed" behind the main body of the helicopter as it hit the water.

The impact of the aircraft with the water created a large splash. When the splash had subsided, the aircraft had vanished from view although two objects resembling life rafts or floats could be seen on the surface. The alarm was raised and the witnesses kept pointing at and watching the wreckage, as they had been trained to do, until fast rescue craft launched from the Achilles arrived at the scene.

1.2 Injuries to persons

Injuries	*Crew*	*Passengers*	*Others*
Fatal	2	9	0
Serious	0	0	0
Minor/None	0	0	

1.3 Damage to the aircraft

The helicopter was destroyed.

1.4 Other damage

There was no other damage.

1.5 Personnel Information

1.5.1 Commander

Age:	42 years	
Licence:	Airline Transport Pilot's Licence	
Aircraft Ratings:	Sikorsky S-76 series, Bell 212/412 and Bell 47 series	
Last Licence Proficiency Check:	18 April 2002	
Last Instrument Rating Renewal:	18 April 2002	
Last Line Check:	18 February 2002	
Last Medical:	26 February 2002	
Emergency and Safety Equipment Check	30 September 2001	
Flying Experience	Total all types:	8,585 hours
	Total on type	>2,318 hours[1]
	Last 90 days:	135 hours
	Last 28 days:	35 hours
	Last 24 hours:	3 hours
Previous rest period:	23 hours	

[1] Minimum figure and may have been slightly greater but not all the commander's logbooks were available

1.5.2 Co-pilot

Age:	32 years
Licence:	Commercial Pilot's Licence
Aircraft Ratings:	Sikorsky S-76 Series, Robinson R22
Last Licence Proficiency Check:	13 March 2002
Last Instrument Rating Renewal:	13 March 2002
Last Line Check:	10 November 2001
Last Medical:	5 April 2002
Emergency and Safety Equipment Check	16 June 2002
Flying Experience:	Total all types 590 hours
	On Type: 420 hours
	Last 90 days: 97 hours
	Last 28 days: 8 hours
	Last 24 hours: 3 hours
Previous rest period:	6 days and 8 hours

1.6 Aircraft Information

1.6.1 General information

Manufacturer:	Sikorsky Aircraft Corporation
Type:	S-76A+
Aircraft serial No:	760100
Date of construction:	15 November 1980
Powerplants:	Two Turbomeca Arriel 1S turboshaft engines
Total airframe hours:	15,959 hours
Total airframe cycles:	48,057
Certificate of Registration:	UK Registered on 15 January 1982
Certificate of Airworthiness:	Certificate of Airworthiness in the Transport Category (Passenger), issued by the UK Civil Aviation Authority on 24 March 2000 and expiring on 23 March 2003.
Certificate of Release to Service:	Issued on 31 March 2002

1.6.2 S-76 helicopter description

The Sikorsky S-76 is a general-purpose all-weather helicopter. It is used extensively for offshore oil support, corporate executive transport and general utility operations. A photograph of G-BJVX is shown below.

The S-76 benefits from the design, research and development work carried out on the dynamic system of Sikorsky's UH-60A Black Hawk. Its main rotor is a scaled down version of that developed for the UH-60A. Construction of the first prototypes began in May 1976 and the first flight took place in March 1977. Initial deliveries of fully certificated IFR production aircraft began in February 1979.

There are a number of S-76 versions. The original S-76 was the designation of all models delivered before 1 March 1982; these were powered by Allison 250-C30 turboshaft engines. The designation S-76A+ defines a rotorcraft retrofitted with Turbomeca Arriel 1S engines. Models delivered after March 1982 were designated S-76 Mark II. In 1987 the S-76B was produced with many enhancements and Pratt & Whitney PT6B-36A engines. In 1990 the S-76C model was produced with Turbomeca Arriel 1S1 engines. All the models share the same basic main and tail rotor designs.

The normal crew complement is two pilots. The passenger section of the cabin of G-BJVX was configured for a maximum of nine passengers. The helicopter type uses a conventional transmission system with both engines driving through a combiner gearbox to a main gearbox. The main rotor blades are mounted on elastomeric rotor hub bearings with hydraulic dampers. The flight controls and retractable landing gear wheels are hydraulically powered. The fuselage is a composite structure of glassfibre nose, light alloy honeycomb cabin, semi-monocoque light alloy tailcone and 'Kevlar' fairings.

1.6.3 Main rotor blade description

There are four main rotor blades each weighing approximately 97 lb, 19.98 feet (6.089 metres) in length and individually colour-coded yellow, red, blue and black.

The primary structural member of a main rotor blade is the welded titanium spar which provides the majority of the spanwise, torsional, and centrifugal load carrying ability. The manufacturer's drawing of the blade's construction is shown in Figure 1 and photographs of a cross-section of an S-76 blade are shown in Figure 2.

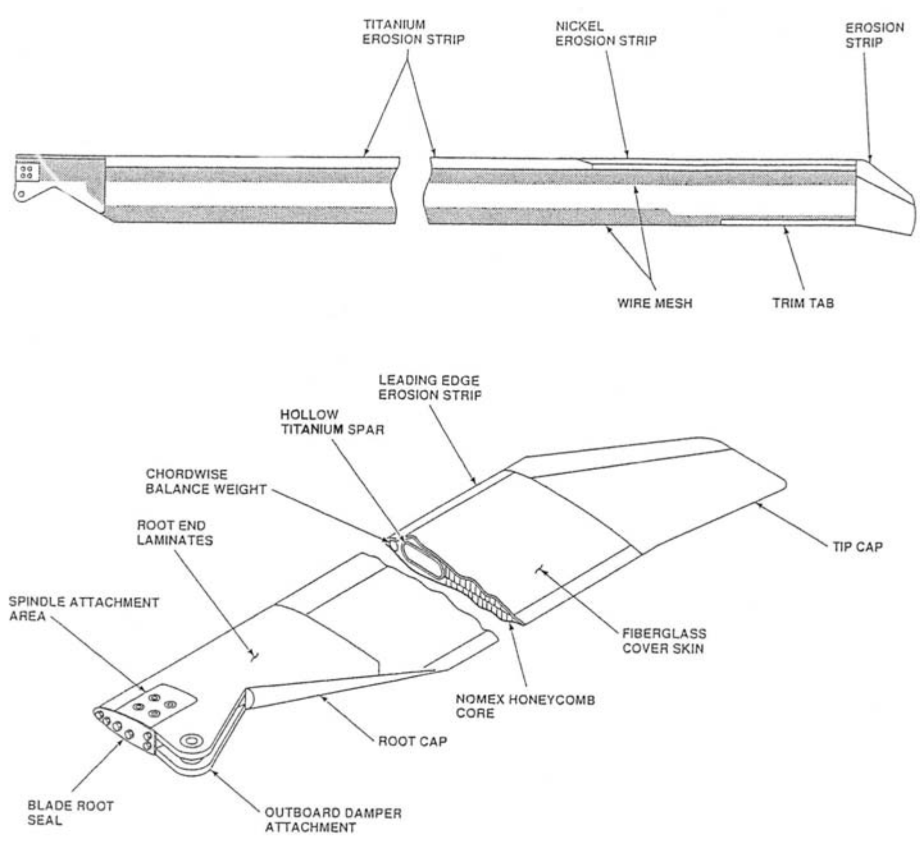

Manufacturer's drawing

Figure 1 - Construction of a main rotor blade

There are four holes with bushings for through-bolts at the root end of the blade for attachment to the rotor head spindle. The skin is made from cross-plied woven fibreglass with graphite trailing edge reinforcing strips. An aluminium wire mesh impregnated into the cover skin provides lightning protection. The leading edge of the blade is protected from erosion by a titanium cover. The early production blades have a two-piece titanium erosion cover, the two pieces

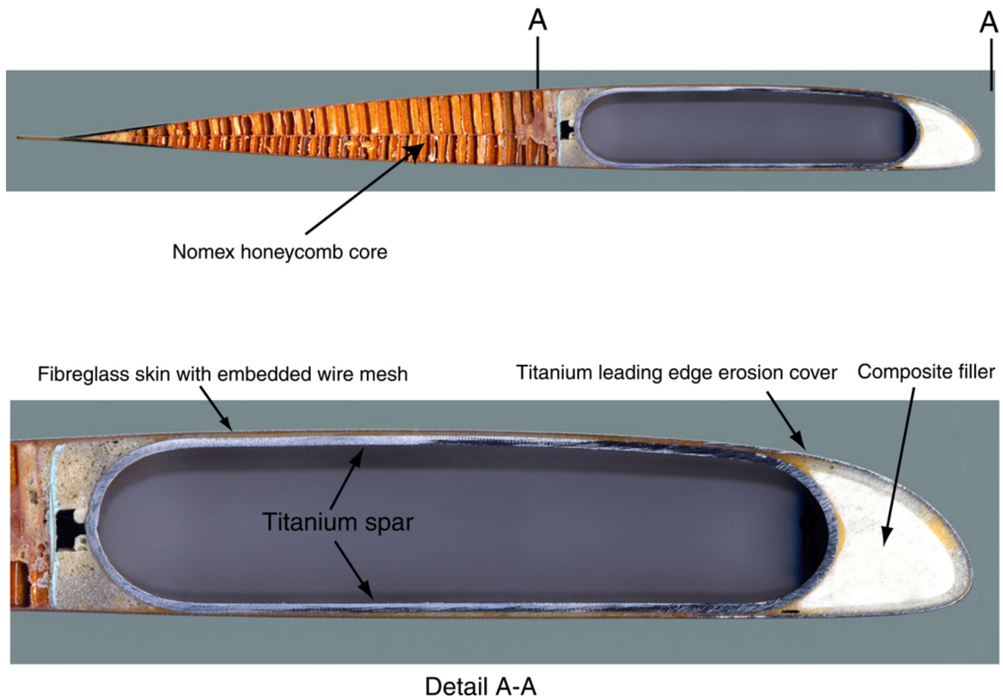

Figure 2 - A chordwise section through a main rotor blade

coming together at a scarf joint the centre of which is located approximately 13.37 feet (4.075 metres) from the blade tip. A total of approximately 2,800 S-76 main rotor blades have been manufactured; of this total there are between 1,600 and 1,675 main rotor blades in-service that were manufactured with the two-piece erosion cover. From 1989 onwards, all new blades were manufactured with a one-piece titanium erosion cover.

The outboard 6.95 feet (2.12 metres) of the blade leading edge has a nickel erosion strip bonded onto the top of the titanium erosion cover. A 'Nomex' honeycomb core supports the cover skin aft of the spar. Balance weights made from fibreglass and lead rods are bonded to the spar leading edge for chordwise balance. At the spar tip end, spanwise and chordwise shim weights are attached during blade manufacture for final blade balance. A replaceable 'Kevlar' tip cap with a swept leading and trailing edge is attached to the blade.

1.6.4 Details for the yellow colour-coded main rotor blade

Manufacturer:	Sikorsky Aircraft Corporation
Part number:	76150-09100-041
Serial number:	A086-00741
Date of construction:	19 March 1981
Hours since manufacturer:	9,665.10
Hours at lightning strike:	8,261.45
Date fitted to G-BJVX:	June 2001
Hours when fitted to G-BJVX:	8,262.10
Date of lightning strike:	17 November 1999
Hours since lightning strike:	1,403.25

1.6.5 Main rotor blade manufacturing process

The blade spar was made from titanium alloy Ti-6AI-4V plate that was cold-formed into a cylinder, then plasma arc butt welded into a tube. A hot-forming operation was used to make the round tube into an aerofoil contour. The two sections of the titanium leading edge erosion cover were manufactured and joined in the area of the scarf joint by a composite doubler, which was located inside the contour of the erosion cover. Due to the geometry of the erosion cover, the composite doubler did not support the rear edges of the 0.020 inch thick titanium. The erosion cover sub-assembly, together with the trailing edge 'nomex' honeycomb sub-assembly were push-fitted with a solid film epoxy structural adhesive onto the titanium spar in a compaction fixture into which the blade's upper surface woven fibreglass skin with the impregnated aluminium wire mesh had been laid. The compaction fixture held the blade in a near horizontal upside-down configuration. The blade's lower woven fibreglass skin was then applied. The blade was moved from the compaction fixture, wrapped, and placed in a bonding fixture, where the upper surface of the blade was again placed on the lower surface of the fixture. In the bonding fixture, the erosion cover was forced into conformance with the blade's surface by pressure applied by the fixture. The bonding fixture was placed in an autoclave which applied heat and pressure to cure the epoxy structural adhesive. The epoxy structural adhesive then encapsulated the scarf joint and faired in any gaps on the trailing edge of the erosion cover and the leading edge of the 'nomex' honeycomb sub-assembly. Following removal from the autoclave, the hardened excess adhesive was removed to form a smooth aerofoil profile. The majority of the blades manufactured did not require the hardened adhesive sanded back to the extent that exposed the area of the tangs at the rear of the scarf joint of the titanium erosion cover. Following this manufacturing process the blade was subjected to a finishing process, part of which involved painting the upper and lower surfaces including the trailing edges of the titanium erosion cover.

During the spar's manufacturing process 15 different inspections of every spar were carried out prior to blade assembly. These inspections were intended to ensure that the final shot-peened titanium spar was fabricated to design requirements and that no damage had been incurred during the manufacturing process. Thereafter a spar was deemed fully compliant and damage free. It was then assembled with other components to become a full blade assembly. The assembly process cocooned a spar thereby precluding damage during the remainder of the blade manufacturing process.

Quality Assurance (QA) inspections (also known as Quality Control) were conducted during each phase of the blade assembly but there was no specific requirement for a pre or post autoclaving inspection of the tangs for correct orientation. The QA inspection procedures culminated in a Fluoroscope inspection of the entire blade (for a description of fluoroscopy see paragraph 1.18.3.3.2).

1.6.6 Main rotor blade maintenance requirements

1.6.6.1 Manufacturer's routine inspection requirements

The helicopter's manufacturer specifies the routine inspection procedures and intervals for the main rotor blades in Chapters 4 and 5 of the applicable S-76 Airworthiness Limitations and Inspections Requirements Manual. Section 5-20-00 specifies that an inspection of the main rotor blades is required to be carried out during every pilot's pre-flight check and at 50, 340, 500, 900 and 3,000 flying hour intervals and every 3 years, the details of which are shown in Annex B. The 340 hour inspection did not apply to any of the blades fitted to G-BJVX because they were all fitted with tip plate retention bolts part number 79790H-4-5. The 3,000 hour and 3-yearly inspections only apply to blades that have completed 11,750 flight hours; none of the blades fitted to G-BJVX had reached this milestone.

1.6.6.2 Manufacturer's special inspection and repair requirements

The manufacturer's detailed inspection requirements, acceptance and rejection criteria for damage and repair limits for the main rotor blades is specified in their Composite Materials Manual (CMM), Publication No SA 4047-76-5 and their Engineering Instructions (EIs). The acceptance and rejection criteria for main rotor blades as described in the CMM are shown at Annex C on pages C-2 to C-4.

1.6.6.2.1 Cracks in the leading edge erosion cover

Partial and complete chordwise cracks in the titanium leading edge erosion cover were allowed providing there was no more than four inches of disbond adjacent to the crack. Cracks were to be covered with tape in accordance with Repair Procedure No 6 in the CMM. Pages C-5 and C-6 of Annex C describe Repair Procedure No 6.

Before this accident there were no special inspections associated with any tape repairs to the leading edge erosion cover. After this accident, Table 3-1 in the CMM dated 'Dec 23/02' specified the ongoing inspection requirements once a crack has been observed and 'repaired'. The revised procedure stated that where the disbond is less than two inches either side of the crack then a polyurethane patch is applied over the crack to prevent moisture ingress and a re-inspection is required every 300 hours. Where the disbond is between two and four inches a polyurethane patch is applied and a re-inspection is required every 50 hours. Where the disbond is in excess of 4 inches the blade must be removed and sent to an approved repair facility.

The approved patch materials were listed with other consumable materials on page 1-1-13 of the CMM under Item No 28 (see Annex C page 1). Three tape materials were approved and all were described as 'Abrasion Resistant Polyurethane – Adhesive – Coated'. Two of the tapes were identified by thickness (0.014 inches), vendor part number (8671 & 8681), width (suffix -2.00 or -6.00 specifying width in inches) and a textual description. The descriptions related the width as applicable to TRB or MRB (Tail or Main Rotor Blade) and further specified the material as 'Clear (Transparent)' or 'Matte (Transparent)'. Both vendor part numbers were also listed as compliant with specification SS9538. A third part number, 8663, was identified as '0.18 Thick'; no surface finish, colour, width, applicability to MRB/TRB, or specification were listed. All three tapes were available from the same vendor.

Within the instructions for Repair Procedure No 6 on page 1-4-24 of the CMM (see Annex C page 5) the three part numbers were repeated. On this page part numbers 8671-6.00 and 8681-6.00 did not specify the tape surface finish or colour in the text.

Tape 8671 was only available as a clear material whereas tape 8681 was available from the vendor in both clear and a grey colour. The third patch material, described as an alternative to the first two, was part number 8663 and identified as transparent. However, the vendor also supplied tape 8663 in black.

1.6.6.2.2 Scarf joint patch

There was no stated requirement for a polyurethane patch to be applied to the area of the scarf joint between the two sections of the erosion cover.

1.6.6.2.3 Post lightning strike inspections

Engineering Instruction (EI) E76-762-10-1331, dated 22 January 1991, (see Annex D) detailed the 'Recommended Post Lightning Strike Inspection For Main & Tail Rotor Blades'. EIs were (and still are) intended for internal use by the manufacturer and so are not included in the CMM. Occasionally EIs and other internal documents such as Overhaul and Repair Instructions (ORIs) were issued to overhaul facilities fully-licensed by the aircraft manufacturer.

1.6.6.2.4 Alert Service Bulletins and Customer Service Notices

Prior to the accident, five Alert Service Bulletins (ASB) had been issued that were applicable to S-76 main rotor blades. Two of the ASBs were not applicable, by the blade serial numbers and time in-service, to any of the four blades fitted to G-BJVX. One ASB was applicable only to the blue colour-coded blade. Another ASB (76-65-51) requiring a root end spar inspection for evidence of cracking was applicable to all four blades. The fifth ASB (76-65-34A) requiring a blade tip spar inspection for evidence of cracking was applicable to the yellow, blue and red colour-coded blades.

On 13 November 1990 the manufacturer issued Customer Service Notice 76-167B (revised 25 May 1993) which introduced a modification to the tip cap retention area of the blade.

1.6.6.3 FAA mandatory inspection requirements

The FAA issued Airworthiness Directive (AD) 84-10-02, amended on 18 June 1984, which required an inspection of the main rotor blade spar for evidence of cracking in the area of the root end. Following the initial inspection it required that a repeat inspection be carried out at intervals not exceeding 500 hours time in service. This AD was applicable to all four blades fitted to G-BJVX.

1.6.6.4 Operator's inspection requirements

In addition to the manufacturer's and the FAA's inspection requirements, the operator had instigated additional local inspection procedures. Prior to each flight that originated from their maintenance base at Norwich, a pre-flight/turnround inspection was carried out by an operator's authorised aircraft engineer following which the aircraft's technical log was signed by that engineer. Within this pre-flight/turnround procedure was a requirement for the engineer to inspect the top surfaces of the main rotor blades for obvious signs of damage or disbonding. To achieve this, the engineer had to stand on the left side transmission deck and look along each blade's surface. For the average height person this would give a viewing angle of the area of the scarf joint in the titanium leading edge erosion cover of between 17° to 25°. The operator also required that, in addition to the pre-flight/turnround inspection that a daily inspection (A check) was carried out by an authorised aircraft engineer. The daily inspection required that the top surfaces of the main rotor blades were inspected for signs of damage or disbonding. This was also achieved by the engineer standing on the left side transmission deck.

1.6.7 Main rotor blade, colour-coded yellow, maintenance history

The yellow colour-coded main rotor blade was manufactured in March 1981 and delivered as part of a new S-76A helicopter, registration G-BISZ, to a United Kingdom North Sea helicopter operator supporting the oil and gas industry. Over its service life, the blade was fitted to a number of other S-76 helicopters (see Annex E) all of which were operated by the same North Sea helicopter operator in support of the oil and gas industry prior to being fitted to G-BJVX. During this time the blade was maintained in accordance with the manufacturer's and operator's maintenance procedures and all applicable ASB's and FAA AD's.

On the day of the accident four different authorised aircraft engineers had carried out five pre-flight/turnround inspections. The last pre-flight/turnround inspection was carried out 0.92 flight hours and the last daily inspection (A check) 6.25 flight hours prior to the accident. The last 50 hour inspection was carried out on 17 June 2002, 37.05 flight hours prior to the accident. A 500 hour inspection was carried out on 21 February 2002, 422 flight hours prior to the accident and a 900 hour inspection was carried out on 4 February 2002, 509 flight hours prior to the accident.

Two unscheduled maintenance operations took place during the blade's life. In January 1993 there was a maintenance incident involving a flight control function check with hydraulic power selected on and an incorrectly installed main rotor blade damper. This resulted in damage to the blade's damper attachment fitting. The blade was removed and returned to the manufacturer for repair. In 1999 the helicopter to which the blade was fitted, G-BHBF, suffered an in-flight lightning strike that was the subject of an AAIB Investigation (see below).

1.6.8 Lightning damage to main rotor blades on G-BHBF

All four main rotor blades fitted to G-BHBF were damaged by a lightning strike on 17 November 1999; the circumstances were reported in AAIB Bulletin 3/2001. The report concluded that the aircraft was struck by a relatively low magnitude strike.

The damaged blades were initially inspected by the manufacturer's UK-based representative and a rotor blade repair organisation in the UK. The blades were then sent to a blade repair station in the USA for further assessment. The EI which detailed the 'Recommended Post Lightning Strike Inspection For Main & Tail Rotor Blades' had been issued to the USA blade repair station. Its staff inspected the blades in accordance with the EI but did not carry out any repairs. Instead, the repair station forwarded the damaged blades to their original manufacturer. The manufacturer assessed two blades as beyond repair and they were scrapped but the other two were repaired. Component records for the blades that were scrapped were destroyed but photographs of two of the damaged blades were retained and these are shown at Figure 3 below. They are photographs of the two blades colour-coded red and black. The red blade was repaired but the black blade was scrapped. Coincidentally, the blade that subsequently failed on G-BJVX was allocated the 'yellow' colour code on both helicopters. No photographs of this blade or the blue blade were available. Nevertheless, the photographs below illustrate the nature of visible damage inflicted on the red and black blades by a lightning strike.

Black blade upper surface

Red blade upper surface

Figure 3 - Lightning damaged blades fitted to G-BHBF

1.6.9 Lightning damage to subject blade

1.6.9.1 Blade inspection in the UK

In the case of the blade later fitted to G-BJVX the UK repair organisation found evidence of lightning damage on the trailing edge at blade station[1] 122.5 and on the root end laminates, on both upper and lower surfaces, at station 44. It also found cracks in the leading edge sheath and skin delamination damage to the tip cap assembly but these defects were not attributable to lightning damage. The UK repair organization assessed the lightning damage as '*beyond workshop limits*' and returned it to the operator with a recommendation that it be returned to the manufacturer for a full evaluation.

1.6.9.2 Blade inspection by the USA Repair Station

The blade (one of four) was sent to an independent fully-licenced Repair Station in the USA for further assessment. The Repair Station found lightning damage to the conductive aluminium wire mesh between stations 42.5 and 50.5 on both the upper and lower surfaces. There were also defects described as 'arc blow outs' near the leading edge at stations 118.75 and 139.75 on both the upper and lower surfaces. Cracks in the leading edge erosion sheath were identified at stations 112.0, 118.75, 139.75 and 180.25 which were attributed to puncture damage; there was also an 'arc mark' at station 122.75. Voids (areas of disbonding) were found associated with all four cracks using a coin tap test. On the outboard blade section the conductive aluminium wire mesh was burnt on the upper surface between stations 186 to 187.25. Some pitting and arc marks were noted at the root end laminates but no signs of lightning damage were noted in the root end seal, at the root of the spar or at the exposed tip end of the spar.

An internal boroscope inspection of the hollow spar showed a 'black charred mark' in line with the upper trailing edge of the erosion cover at blade station 36.25. 'Pitting/arc marks' in line with the upper trailing edge of the erosion cover were also identified at blade station 48.25. Black streaks aligned with the blade's trailing edge were seen between blade stations 89.25 and 91.0. Black marks aligned with the leading edge were noticed at blade station 98.25 and white streaks were seen aligned with the leading edge between blade station 98.5 and 143.0, extending beyond boroscope range.

The Repair Station assessed the blade as *"Beyond workshop limits. Return to Sikorsky"*, affixed a red rejection tag to the blade and forwarded it to the manufacturer.

[1] A blade station is the distance in inches measured from the blade root towards the tip

1.6.9.3 Blade inspection by the manufacturer

At the manufacturer's facility the blade was visually examined which revealed chordwise cracks in the leading edge sheath at blade stations 111, 118.25, 139.3 and 179.75. (These cracks were also noted by the UK repair organization and not associated with the lightning strike). Patches of water ingress into the Nomex core in the region of tooling holes[1] and the trailing edge pocket in the outboard section were also identified using fluoroscopy. The folded tang of the scarf joint was not detected.

In respect of the lightning strike, the blade was inspected and deemed *"Blade is acceptable to work providing it has passed all inspections called out in Engineering Instruction EI E76-762-10-1331"*. (See Annex D.)

1.6.9.4 Scarf joint damage

No lightning damage was observed in the area of the titanium leading edge erosion cover scarf joint, blade stations 75.75 to 82.75, by the UK repair organisation, the USA Repair Station or the blade manufacturer.

1.6.10 Blade repairs

The blade was repaired by the manufacturer in accordance with the Repair Procedures in the Composite Materials Manual SA 4047-76-5, additional Overhaul and Repair Instructions (ORIs) and other instructions. The detail of the refurbishment was contained in a work pack that was too large to include in this report. In respect of the lightning damage, the disrupted skin areas were removed, the conductive aluminium wire mesh was patch repaired and new skin patches were bonded in place. The trim tab was removed and replaced. Pockets in the blade interior that had absorbed water were emptied by drilling and suction before being sealed with structural adhesive and fibreglass. In addition the manufacturer carried out a number of applicable EI's, AD's and ASB's and a 500 hour inspection. On completion of the repairs, the entire length of the blade was inspected by fluoroscopy.

1.6.11 Blade finishing

Following the manufacturer's repairs the blade was returned to the USA Repair Station where a new tip cap was fitted.

[1] Holes in the blade used during the manufacturing process to locate it accurately in the compaction and bonding fixtures which are filled after the blade has been cured in an autoclave

Before returning the blade to the operator as a serviceable component, the USA Repair Station applied five opaque polyurethane protective patches to the titanium leading edge erosion cover. Four were placed over cracks in the leading edge erosion cover and one was placed over the scarf joint between the two sections of the erosion cover. A similar patch to that placed over the scarf joint is shown in Figure 4.

Figure 4 - Example of an opaque protective patch covering the scarf joint in the titanium leading edge erosion cover

The purpose of this polyurethane patch was to prevent erosion of and moisture ingress into the exposed hardened adhesive filler in the scarf joint. On the upper surface of the blade the similar patch extended approximately 35 mm rearwards from the trailing edge of the titanium leading edge erosion cover. On the underside of the blade the similar patch extended approximately 42 mm rearwards from the trailing edge of the erosion cover. A scarf joint that has been exposed by removing the patch, paint and hardened structural adhesive is shown at Figure 5.

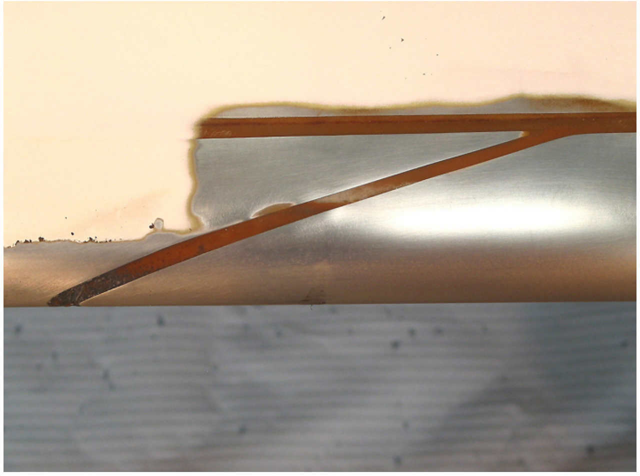

Figure 5 - Scarf joint in a titanium leading edge erosion cover with the protective patch, paint and hardened structural adhesive removed

1.6.12 Rotorcraft weight and balance

Basic weight and balance details for the operator's S-76 aircraft were held on a computerised database known as INTOPS. This system was used by pilots to generate an Initial Load Report for the assigned aircraft by keying in the air temperature and pressure for the point of departure, en-route sectors and for the destinations. The aircraft zero fuel weight included the weight of the two pilots to which was added the passenger, baggage, freight and fuel weights for each sector. Calculated values listing the Restricted Take-off weights for each departure point are listed in Table 2.

Table 2 – Calculated helicopter weight for each departure of last flight

Item/Location	**Norwich Airport**	**GSF Britannia**	**Clipper**	**Barque PL**	**Clipper**
No of passengers on board	5	2	0	8	9
Passenger weight (lb)	980	392	0	1,568	1,764
Baggage weight (lb)	102	47	0	286	290
Freight weight (lb)	115	115	0	10	0
Fuel weight (lb)	1,200	900	820	730	640
Aircraft zero fuel weight (lb)	7,699	7,699	7,699	7,699	7,699
Restricted take-off weight (lb)	10,800	10,800	10,800	10,800	10,800
Actual take-off weight (lb)	10,096	9,153	8,519	10,293	10,393
Margin below MAUW (lb)	704	1,647	2,281	507	407

Allowing for the approximation of fuel consumption on each sector and the fuel used during the final sector from the Clipper to the Santa Fe Monarch, the aircraft's weight at the time of the accident was approximately 10,300 lb and its centre of gravity was within limits.

1.6.13 Recent Flight Activity

A table showing the number of engine starts, landings and flight hours for the final 100 flight hours accrued by G-BJVX is shown at Annex F.

1.6.14 Automatically deployable emergency locator transmitter (ADELT)

The ADELT beacon fitted to G-BJVX was mounted in a carrier located externally at the lower rear section of the tail boom. The ADELT could be deployed by any one of three methods: a cockpit switch; a saline switch in the carrier; and by either of two frangible 'crash switches' mounted in the airframe. The radio transmitter beacon was a conical shaped sealed self-buoyant unit with an antenna system mounted in the upper portion.

The current requirements for an ADELT are specified in EUROCAE [1] document ED-62 dated May 1990. This document supersedes MPS 1/WG4/65, "Minimum Performance for Radio Survival Beacons functioning on VHF" dated July 1965. In respect of current requirements for crash shock resistance, an ADELT should survive a 500g impulse lasting 4 ± 1 milliseconds and a 100g impulse lasting 23 ± 2 milliseconds. Regarding impact shock developed by contact with a hard surface (eg rock, concrete, steel) the ADELT must survive an impact velocity of 25 metres/sec (80 feet/sec) under laboratory conditions. Calculations indicated that the speed of water impact was in the order of 140 kt (72 metres/sec or 236 feet/sec) with the fuselage in a 37° dive.

1.7 Meteorological information

The synoptic situation at 1800 hrs UTC showed a ridge of high pressure over the British Isles with a weak cold front covering Norfolk. The general weather conditions were as shown in Table 3.

[1] The European Organisation for Civil Aviation Equipment

Table 3 – General weather conditions over Norfolk

Height agl	Wind speed and direction	Temperature deg C	Dew Point deg C
Surface	030°/10 kt	16.6	13.0
500 feet	040°/15 kt	18.0	10.5
1,000 feet	040°/15 kt	18.0	10.5
2,000 feet	040°/15 kt	15.5	10.0

The general visibility was 20 km and the cloud was a few cumulus or strato-cumulus at 4,500 to 5,000 feet. The mean sea level air pressure was 1020 millibars. The sea state was recorded as 'slight' with 0.5 metre waves every 3 seconds. The weather observation for Norwich Airport taken 12 minutes before the helicopter's final departure was: mean wind 040°/6 kt varying in direction between 010° and 080°; more than 10 km visibility; broken cloud at 4,500 feet; temperature 18°; dewpoint 14° and QNH 1021 millibars.

The radio operator on the Global Santa Fe Monarch reported the following weather conditions to the crew on first radio contact just prior to the accident:

Wind	345°/8 kt
Visibility	More than 5 km
Cloud	No significant low cloud
Temperature	16.5°C
QFE	1011 millibars

1.8 Aids to navigation

The performance of navigational aids was not relevant to this accident.

1.9 Communications

Transcripts of radio transmissions between the helicopter and other agencies were available but were not required because all the relevant messages were recorded on board the helicopter.

1.10 Aerodrome Information

Aerodrome and offshore helicopter platform information were not relevant to this accident.

1.11 Flight recorders

1.11.1 Introduction

G-BJVX was equipped with a proprietary form of HUMS (Health and Usage Monitoring System) called IHUMS, (the letter 'I' meaning Integrated). IHUMS has three main functions: cockpit voice recording; flight data recording; and maintenance health and usage monitoring. Cockpit voice recording and flight data recording are mandatory requirements that are accomplished using a single Combined Voice and Flight Data Recorder, (CVFDR). The CVFDR retains the time history of the most recent five hours of data and the most recent one hour of audio. The recording medium is an endless loop of plastic tape contained within a crash protected enclosure. Since the year 2000 health monitoring (but not usage monitoring) has also been a mandatory requirement (UK CAA AAD 001-05-99) but the Operator originally introduced the system eight years earlier.

Health and usage data was acquired by a Data Acquisition and Processing Unit (DAPU) and recorded on a PC SRAM (Static Random Access Memory) card unit. The PC card is not crash protected and relies on an internal battery to preserve the recorded data. At the end of each flight the PC card is removed from the aircraft. A replacement card is fitted at the start of the subsequent flight.

1.11.2 Recovery of the flight recorders

The CVFDR was identified within the wreckage of the aircraft fuselage on the morning of Friday 19 July 2002 using a Remotely Operated Vehicle (ROV) camera controlled from the search vessel 'Kommander Subsea'. It was retrieved from the seabed later that day by a diver from the recovery vessel 'DSV Mayo'. It was placed in a water filled container and transported to the AAIB flight recorder replay and analysis laboratory.

The maintenance recorder was recovered with the main wreckage. When the PC memory card was removed from the maintenance recorder in the AAIB laboratory, it was found to be crushed and broken into two parts. Further tests showed that the physical damage to the card had resulted in the loss of all the recorded data.

1.11.3 Configuration of the CVFDR

The CVFDR records audio and data on an endless loop of ¼ inch wide plastic tape. Eight separate tracks are used for the recording. On G-BJVX three tracks were used simultaneously to record three channels of audio information. The track allocation was as follows:

Channel 1 – Commanders 'hot mic' [1]

Channel 2 – Co-pilots 'hot-mic'

Channel 3 – Cockpit Area Microphone (CAM)

The remaining five tape tracks were used sequentially to record flight data. A list of the recorded parameters is included in Annex G. Audio recorded one hour earlier and data recorded five hours earlier respectively are erased and overwritten.

1.11.4 Replay of the CVFDR

The CVFDR was dismantled and the plastic recording tape was removed from its crash protected enclosure. It was cleaned, dried and then spooled onto a standard 3-inch tape reel. The only visible damage to the tape was discolouration and the presence of corrosion deposits where the tape was in contact with metal parts of the tape transport mechanism. The corrosion deposits were most severe on those sections of tape in direct contact with the recording heads. As far as practical, consistent with causing no further damage to the recording tape, the corrosion deposits were neutralised and removed.

The recorded data and audio information were replayed separately using specialist transcription units. The replays showed that the CVFDR and all of its information sources on the aircraft were fully serviceable throughout the recording. The only difficulty encountered during the replay was the corruption of both the audio and data output during the last two seconds of the recordings. This occurred as a consequence of the corrosion deposits described above. Using specialist recovery techniques all but 0.25 seconds of recorded flight data was recovered. The audio information was also recovered although the amplitude of the signal was at a reduced level compared to the rest of the recording. A print from an oscillograph showing the variation in signal levels during the last 0.75 seconds of the recording is at Annex H.

1.11.5 Interpretation of the recordings

The data recording began at 1035 hrs on 16 July 2002. The earliest recorded data was of the aircraft preparing to land on a rig. Recorded data was available from nine complete sectors and the incomplete accident sector. Audio recording began at 1740 hrs whilst the aircraft was en-route to the 'Britannia' platform

[1] A continuously live microphone feed to the CVFDR

from Norwich. Both the audio and data recordings were routine until the sector from the 'Clipper' platform to the 'Monarch' platform: the accident sector. Seven minutes before the end of the recordings the co-pilot, who was the handling pilot for the sector, commented, "GOT A QUITE A VIBRATION THERE". The commander agreed and said, "I'LL JUST DO A ROTOR TRACK AND BALANCE ON IT"[1]. Six seconds later the co-pilot said "OUT OF TRACK"[2]. The commander agreed. There was no evidence on the voice recording that the increase in vibration caused any immediate concern to either pilot and neither commented on the vibration again.

Examination of the data time histories did not indicate any detectable changes during the accident sector. Annex I shows the CVFDR time history of relevant parameters during the accident sector.

Four minutes before the end of the recording the crew began the approach checks. There then followed RT exchanges with the Santa Fe Monarch radio operator that were consistent with the helideck crew not expecting the helicopter and needing time to prepare for its arrival. The only item remaining on the checklist when the recording ended was "DECK CLEARANCE".

The last second of the audio recording contained two loud "crack" sounds. The final samples of data recorded showed that the aircraft experienced normal accelerations varying between 1.5g and 0.26g in the space of ½ second, during which time the aircraft rolled 20° to the right. When the recording stopped at 1841 hrs the aircraft was flying on a heading of 151°(M) at a speed of 94 KIAS and at a height of 323 feet asl. The pitch attitude was 1° nose-up and the roll attitude was +20°, (roll to the right)

1.11.6 Archive recordings

The IHUMS Data Acquisition and Processing Unit (DAPU) acquires maintenance data on every flight and records it on a PC SRAM card. The PC card is removed, by the flight crew, at the end of every flight. Its contents are subsequently transferred to an IHUMS ground station.

The non-mandatory functions of IHUMS are to assist in detecting incipient defects in major components before they become a hazard to the safety of flight, to detect exceedences of maintenance manual limitations and to increase the reliability of equipment by minimising airframe vibrations. IHUMS has two safety aims which are:

[1] This involved pressing a button in the cockpit which initiated a data acquisition process lasting many seconds.
[2] This assessment was almost certainly made visually.

(i) Monitoring known progressive failure modes to detect incipient failures, (health monitoring) and,

(ii) Recording procedures to assist maintaining the aircraft eg component life usage and rotor track and balance diagnostics.

The maintenance data collected during the flight and recorded on G-BJVX's PC card includes:

Exceedence conditions
Rotor track and balance data
Gearbox vibration data
Engine vibration data

The maintenance data recorded on the PC card during flight is processed in the IHUMS ground station and relevant system information is fed into the aircraft and fleet maintenance programme. All the recorded maintenance data is retained and stored in an IHUMS archive.

The content of G-BJVX's IHUMS archive was made available to the investigation. This contained all the IHUMS data except that recorded on the accident flight. Data from the accident flight was not available because the PC card had been destroyed in the accident.

1.11.7 Rotor track and balance (RTB)

Data is captured using a light sensitive sensor, which generates an electrical pulse each time a rotor blade interrupts the ambient light focused on the sensor. A pulse is generated by both the leading and trailing edges of each rotor blade. The time interval between each interruption is captured by the DAPU and recorded by the IHUMS. Data capture is pre-programmed within IHUMS to occur during specific flight regimes. As the position of the sensor is known; the recorded timings enable the speed of the main rotor head, the separation between each rotor blade and the height of each rotor blade above the sensor to be calculated. A detailed description of the rotor track and balance system is provided at Annex J.

The data captured by the IHUMS together with the positional information of the sensor is used by the IHUMS ground station to calculate rotor track data. This is combined with IHUMS airframe vibration measurements and when either track or vibration measurements exceed limits established by the aircraft operator, the ground station generates an alert and, if appropriate, suggests adjustments necessary to achieve optimum rotor track and balance. This is the primary use for the RTB data. Because tracking data capture relies on ambient light, it can only produce data during daylight although the vibration data is unaffected by light conditions; furthermore, tracking data captured during daylight is susceptible to corruption from bright sunlight and unwanted reflections. These factors restrict the reliance that can be placed upon rotor track measurements in service.

In addition to the RTB data captured by the IHUMS, the FDR records rotor track data in an incomplete 'raw' format during periods when the IHUMS is not performing a data capture. The investigation had available data that overlapped the data from the last three IHUMS downloads and importantly from the last flight where IHUMS data was not available. The overlapping data was used to validate the equations necessary to reduce the FDR timings to RTB information.

The complexity of the IHUMS and RTB data was such that the AAIB commissioned an independent analysis from Flight Data Services Ltd to determine whether the data were capable of giving adequate warning of impending blade failure. The results of this analysis are at Annex K.

1.12 Aircraft accident site, wreckage recovery and examination

1.12.1 Accident site

The accident site was located in the southern sector of the North Sea within the Leman Gas Field. The wreckage was found on the seabed, approximately 40 metres below the surface, between the Leman and Ower Banks. The main wreckage of the helicopter was found on a bearing of 295°(M) from the co-located Leman Foxtrot and Santa Fe Monarch installations at a distance of approximately 950 metres. It was spread over a 300 metre trail which was approximately 30 metres wide and lying along a general track of 130°(M). Annex L shows the position of the debris field relative to the co-located installations and the major items found within the debris field. Only those items so dense that they were unlikely to be drifted by the currents are identified on the plot. The majority of the wreckage comprised sections of severely fragmented composite structure.

The first significant piece of wreckage along the trail was the main rotor gearbox complete with the rotor head and the majority of the rotor blades. This was found approximately 1,200 metres from the Santa Fe Monarch and lying slightly to the east of the main wreckage trail track.

1.12.2 Wreckage recovery

The first wreckage recovered was found floating on the surface by the standby vessel Putford Achilles which arrived at the accident location within a few minutes of the accident occurring. This wreckage consisted of light secondary fuselage structure, parts of the rear baggage bay, sections of main cabin seating, liferafts and passenger baggage.

Fragments and components from the main wreckage area were recovered over a period of five days by divers operating from a Diving Support Vessel. It was estimated that 97% of the wreckage by weight was recovered.

1.12.3 Wreckage examination

1.12.3.1 General

The helicopter's airframe was very severely broken-up consistent with a very high energy impact with the sea. Examination of the forward and centre fuselage structures showed that at impact there were very high vertical and forward deceleration forces coupled with a low, right, lateral deceleration force. Examination of the main rotor gearbox, rotor head and blades indicated that they were not attached to the airframe when they impacted the sea. The main rotor gearbox complete with the rotor head and blades was found on the seabed some distance from and up-track of the main wreckage site. Examination of the main rotor blades revealed that three of the blades were only superficially damaged whereas the fourth blade, which was colour-coded yellow, had the outboard 4.15 metres missing. Despite a search of the likely areas, this section of main rotor blade was not located and hence not recovered.

There was no evidence of an airborne collision or in-flight fire.

1.12.3.2 Metallurgical examination of the yellow colour-coded main rotor blade

1.12.3.2.1 Blade spar

The inboard section of the yellow colour-coded main rotor blade was removed from the rotor head and taken to the Structures and Materials Centre at QinetiQ Limited for a detailed metallurgical examination and analysis. The body of QinetiQ's report is shown at Annex M.

In summary QinetiQ's examination and analysis showed that the main rotor blade failed due to fatigue in the titanium spar. The fatigue crack grew through approximately 50% of the spar prior to a single catastrophic overload failure of the remaining 50%. The fatigue crack initiated from an area where there had been a change in the titanium's microstructure from a normal equi-axed alpha-beta microstructure to martensite (see Figure 6).

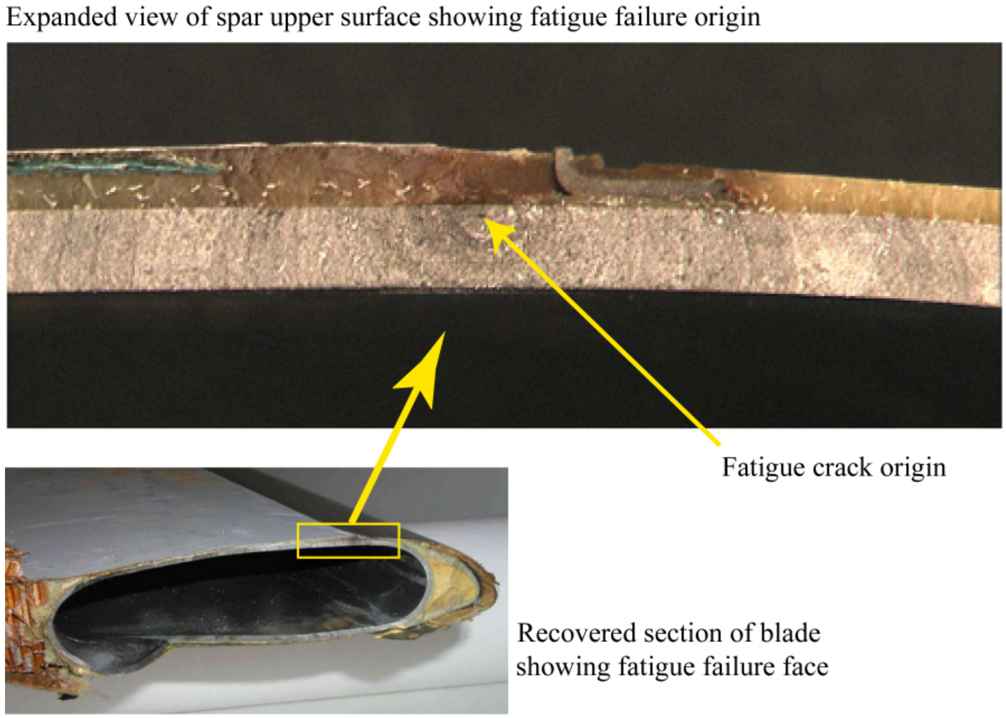

Figure 6 - Fatigue crack origin

The temperature required to produce the microstructural change was in excess of 995°C. This martensitic transformation would have altered the beneficial compressive residual stress from shot-peening, and probably resulted in an unfavourable, localised, residual tensile stress. The untempered martensitic material is also somewhat softer then the normal alpha-beta material. (Note that this is opposite to the effect seen in martensitic steels.) These localised changes resulted in greater susceptibility to fatigue initiation. The area where the change in the microstructure had occurred was where the tip of the tang of the inboard end of the outboard titanium leading edge cover had come into contact with or extremely close to the spar. There was no evidence to indicate whether the tip had or had not contacted the spar. The defect had arisen because of a manufacturing anomaly which had caused the tang to become folded under the outboard end of the inboard leading edge cover (see Figure 7).

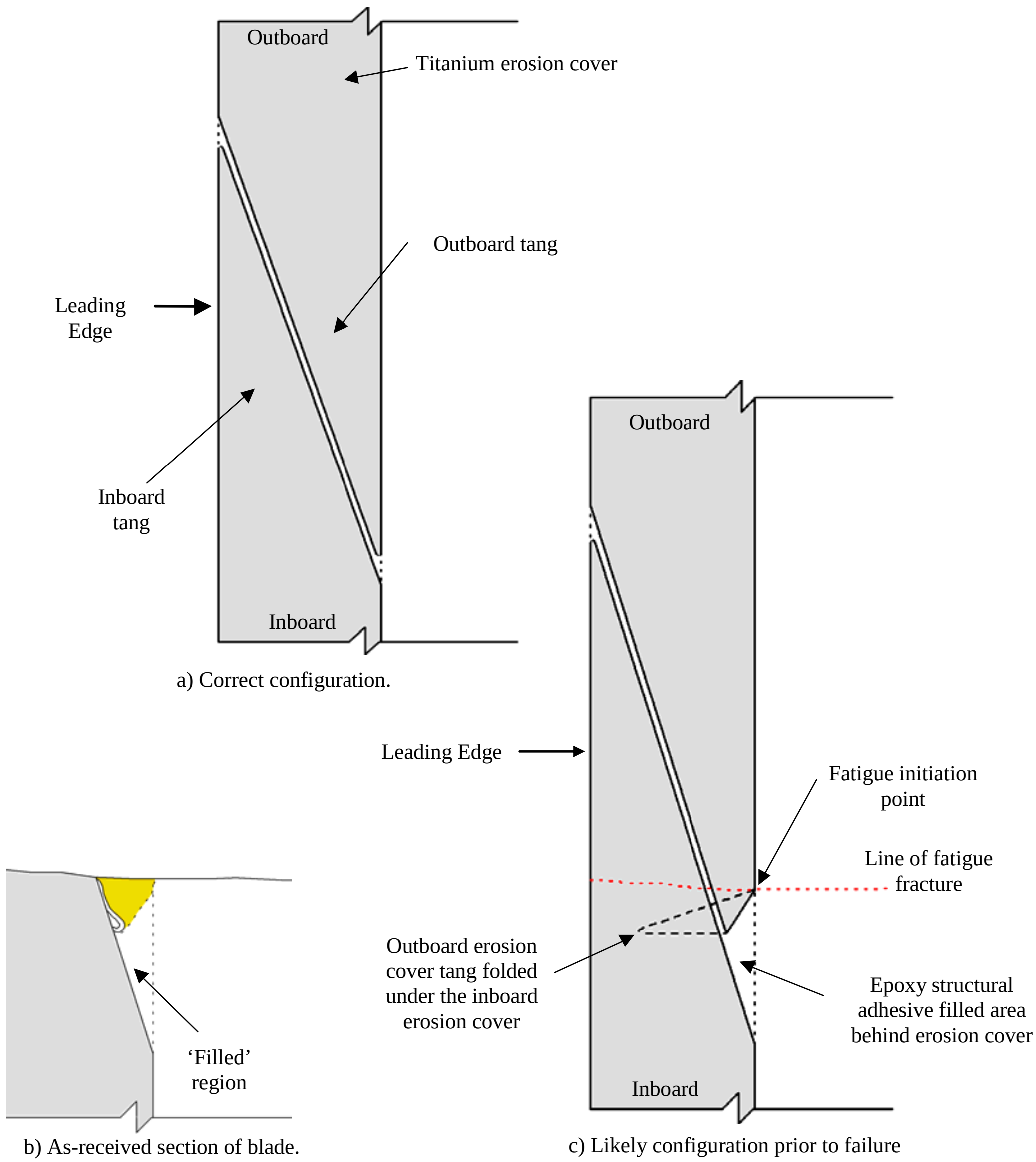

Figure 7 - Scarf joint configuration.

The manufacturing anomaly had been present since the blade was manufactured in 1981, some 21 years prior to the accident. There was very good evidence to indicate that the titanium microstructure change had been caused by very rapid localised heating of the spar at the point where the tip of the tang had come into contact or extremely close to it, followed by rapid cooling. This evidence was in a form that resembled an electrical spot weld. The heat discoloration at the surface of the spar adjacent to the origin and the heat affected microstructure indicated a possible scenario whereby electrical current flow during a lightning strike had been able to pass from the titanium leading edge cover to the titanium spar through the folded tang.

1.12.3.2.2 First fatigue striation count

The first fatigue striation count was undertaken by QinetiQ Limited in an attempt to estimate the length of time in flight hours for the fatigue crack to progress from initiation to final failure.

Striation measurements were carried out at differing distances from the fatigue origin. The striations were clearly visible across the majority of the fracture surface towards the ends of the cracks but closer to the origin the striations became less obvious. From the origin to a distance of approximately 14 mm the striations were not clearly visible. However, approximately 14 mm from the origin to the ends of the cracks, sufficient striations were observed to estimate the total number of load cycles that the blade had encountered for crack growth between these points. Using a main rotor blade RPM of 304, it was estimated that the time required for crack growth from approximately 14 mm from the origin to final failure was about 8.1 flight hours. A 'best-fit' curve for the distance between striations was plotted and extrapolated back to 0.6 mm from the origin to estimate the total number of load cycles for crack growth. It was estimated that the total number of cycles was approximately 1,838,662 which equated to 100.8 flight hours.

The macro examination of the fracture surface identified areas where the crack propagation rate slowed down, arrested, restarted or accelerated; these areas produced a series of bands. Each of these bands was the result of a decrease in the forces on the blade which slowed down or arrested the crack propagation rate followed by an increase in the forces which restarted or accelerated the crack propagation. A total of 62 bands were counted; of these 33 appeared to be larger and more pronounced.

The first two graphs at Annex N show the approximate crack progression in millimetres, both forward and rearward from the initiation point, in relation to the aircraft's flying hours. The third graph is derived from addition of the two progression rates and illustrates the total crack length in relation to the aircraft's flying hours.

1.12.3.2.3 Second fatigue striation count

In early 2004 the aircraft manufacturer requested the opportunity to carry out a striation count using a different technique to QinetiQ's. The main differences were the use of a Transmission Electron Microscope (TEM) instead of a Scanning Electron Microscope (SEM) and the examination was of acetate replicas taken from the original fracture face. The results of this second striation count were made available to the investigation and are included in this report at Annex O.

The resolution of striations using a TEM is greater than using an SEM (called an FEM in the Annex) but more sub-surface features are resolved in the SEM. Each method has its advantages but the use of the TEM method resolved striations in the early part of the crack between the origin and the start of QinetiQ's physical count that commenced approximately 14 mm on either side of the origin. These refinements suggested that QinetiQ's curve projection method significantly over-estimated the number of striations in this region but slightly underestimated the number of striations between the 14 mm points and the two ends of the fatigue crack.

QinetiQ accepted that Sikorsky's TEM method resolved finer striation densities than their SEM method. However, there were differences between the two parties regarding the end point of the fatigue region on the leading edge of the crack and what constituted a fine striation as opposed to a feature of lamella[1] type structure. The investigation team considered these differences in interpretation far less important than the differences between the two assessments of the total number of striations between the crack origin and the 14 mm points on either side.

Although both parties converted the total striation counts into flying hours on the same basis (one striation per blade revolution), they used different methods for converting the striation densities observed into total striation counts. To facilitate a more meaningful comparison of the differing results, in May 2004 QinetiQ were tasked with re-assessing the flying hours during which crack growth was taking place. The revised assessment amalgamated Sikorsky's striation densities with QinetiQ's mathematical integration method of producing a total striation count. The results of this re-assessment are presented in Annex P.

The most significant finding was a reduction in time between through-crack initiation and spar failure from around 100 flight hours to less than 30 flight hours.

1.12.3.2.4 Crack lengths before flight

From the graphs at Annex P an estimate was made of the crack lengths forward and rearward from the initiation point prior to each flight on the 16 July 2002, the day of the accident. The two dimensions were then added to derive the total crack length as shown in Table 4 below.

[1] *noun* a thin plate or layer

Table 4 – Spar crack length prior to each flight on 16 July 2002

Flights on 16 July 2002	Flight Time Before Failure (hrs:mins)	Towards Leading Edge Crack Length (approx. mm)	Towards Trailing Edge Crack Length (approx. mm)	Total Crack Length (approx mm)
1st	6:14	21	30	51
2nd	4:48	27	38	65
3rd	3:56	30	44	74
4th	2:54	36	52	88
5th	0:55	50	73	123

1.12.3.2.5 Main rotor blade leading edge erosion cover

The piece of the inboard section of the titanium leading edge erosion cover that was recovered with the section of the yellow colour-coded blade was examined by the Structures and Materials Centre at QinetiQ to establish if there was any evidence of fatigue prior to the final failure. The body of QinetiQ's report is included at Annex Q.

In summary, QinetiQ's examination found that the erosion cover showed good evidence that fatigue had occurred prior to the final overload failure. The initiation point of the fatigue was on the inner surface of the erosion cover 6.7 mm forward of the upper trailing edge of the tapered tang. This was approximately 11.7 mm forward of the fatigue initiation point in the titanium spar. From the initiation point the fatigue progressed rearwards to the trailing edge and 64.3 mm forward around the leading edge prior to the final overload failure.

A fatigue striation count was carried out in an attempt to estimate the time, in flight hours, for the crack to propagate from initiation to final failure. During the examination of the fatigue surface, heavy post-failure mechanical damage was observed in the area of the initiation point and up to 18.5 mm from that point. However it was possible to carry out a striation count from the 18.5 mm point to the final failure and using that data a 'best fit' curve was plotted. Extrapolation of the 'best fit' curve back to the point of initiation gave a total number of load cycles of approximately 133,444 which, when assuming a main rotor RPM of 304, gave an approximate flight time of 7.3 hrs from crack initiation in the erosion cover to final failure of the blade.

It was observed during the examination that there had been three static jumps which indicated that the crack propagation mechanism had changed from fatigue to overload and back to fatigue for short periods of time. These static overload jumps were ignored from the total load cycle estimations. It is possible that these static jumps could have increased the time taken for the crack to propagate to final failure because the fatigue crack would take time to re-initiate after the static jump.

This section of erosion cover was also examined for traces of residues from the adhesive that had been used to bond the polyurethane protective patch over the scarf joint between the two sections of the erosion cover. Positive traces of the adhesive were found on both the upper and lower surfaces. Traces of the adhesive were also found on the upper and lower painted areas of the blade's surfaces immediately to the rear of the erosion cover but they were extremely small in quantity when compared to those found on the erosion cover.

1.12.3.2.6 Internal inspection of main rotor blade spar

The recovered portion of the main rotor blade, less the fracture face which was removed from its outboard end, was internally inspected by boroscope. Unidentified marks were noted on the internal surfaces of the spar so the blade was sectioned lengthwise to expose these surfaces. There were marks on the inside of the spar; some were patches of oily contaminant and one appeared to resemble green chromate paint. There were no apparent defects and no marks consistent with the likely effects of a lightning strike on the spar's interior surfaces.

1.12.3.3 ADELT

When recovered the ADELT (Automatically Deployed Emergency Location Transmitter) beacon did not appear to have deployed when the helicopter struck the sea surface. It was recovered from the main wreckage site together with its carrier into which it appeared to be loosely fitted. The beacon launcher had been torn away from its mounting position at the lower rear part of the tailboom. The beacon deployment springs mounted within the launcher unit were extended. The electrically initiated explosive squib was not recovered. The radio transmitter beacon had been severely damaged during the impact rendering it unserviceable electrically and non-buoyant.

The launcher unit and the beacon were physically examined and there were no obvious defects that would have prevented deployment of the beacon.

The mechanical firing mechanism was dismantled and no fault was found with any of the mechanical parts. The lithium battery was tested and found to be well below its minimum charge which was consistent with its submersion in water for a period of time. The electric charge within the battery indicated that there had not been a defect and that it had not suffered a short circuit. The battery was found to be well within its service calendar life.

The examination of the launcher mechanism, which did not include the explosive squib, concluded that there was no evidence of a pre-impact defect or failure that would have prevented deployment of the beacon.

The launcher and the aircraft mounting bracket were taken to an explosives laboratory for chemical analysis. The results of this analysis detected traces of the explosive used in the electrically initiated squib, which indicated that the squib had fired.

1.13 Medical and pathological information

Of the 11 occupants, five bodies were recovered by the Putford Achilles shortly after the accident and five were recovered by divers from the sea bed in the vicinity of the wreckage. Despite a thorough surface and underwater search of the area surrounding the wreckage, the eleventh body was not found.

Thorough autopsies, including full body radiological and toxicological examinations were carried out by a team led by an experienced aviation pathologist. The pathologist concluded that everyone had died from multiple injuries consistent with a high vertical impact loading with some forward motion. There was no medical evidence of pre-impact fire or explosion.

1.14 Fire

There was no fire.

1.15 Survival aspects

The accident was not survivable.

1.15.1 Search and Rescue

At the time of the accident, the multi-role vessel Putford Achilles was fulfilling the role of standby vessel to the Santa Fe Monarch. The role of a standby vessel is primarily to provide rescue cover for helicopter operations but the crew of the Putford Achilles, believing flying to be finished for that day, was not expecting any more helicopter traffic. The vessel had moved away from her flying standby position and was stationed approximately one mile to the south of the Santa Fe Monarch, heading into the current on a course of 140° and so facing away from the platform.

The crash alarm was raised initially by the radio operator on the Santa Fe Monarch, alerting Great Yarmouth Coastguard and the Putford Achilles. On receiving the alert, the Putford Achilles turned towards the accident site and launched its two fast rescue craft. These arrived in the area of wreckage approximately seven minutes after the initial alarm and began a search for survivors. Initially four bodies were recovered from the sea surface and taken to the Putford Achilles which was, by then, also in the accident area.

Initial reports from the Santa Fe Monarch were that this was the total number on board the helicopter and the search then concentrated on collecting the light wreckage remaining on the surface. About 15 minutes later the Santa Fe Monarch reported that there were in fact 11 persons on board the helicopter and the search for survivors resumed, recovering one further body.

The surface search continued during the evening with an RAF Search and Rescue helicopter, the Cromer lifeboat and about 10 other vessels on task. The search for survivors continued through the night until 0800 hrs the following morning when the search activity was scaled down. During the daylight hours of the day after the accident, the Trinity House vessel Patricia continued searching the local area around the Santa Fe Monarch and an aerial search was carried out over a wider area. No more bodies were found during these surface searches.

1.16 Tests and research

1.16.1 Crack relationship testing

The helicopter manufacturer tested a specimen section of main rotor blade to establish if there was any relationship between a titanium spar crack and an induced crack in the blade skin immediately adjacent to the titanium spar crack (ie a 'sympathetic' crack).

A flat section of spar from the underside of a blade manufactured at about the same time as the yellow colour-coded blade was deliberately 'notched' so as to induce a fatigue crack under repetitive loading. Cyclic loading was applied by a servo-hydraulic fatigue test machine for a total of 483,106 cycles. Initially, when a sympathetic crack in the fibreglass skin and paint layers first appeared, it was about half the size of a 2-inch (50 mm) crack in the titanium. However, within a few hundred cycles it grew to a size which was consistently about 0.1 inches (2.5 mm) shorter than the titanium crack. This size relationship (ie approximately 0.1 inches shorter) was maintained until the test specimen failed in fatigue.

1.16.2 Main rotor blade tip droop

To determine if the amount of blade tip droop changed with increasing crack length, one of the three remaining main rotor blades that had been fitted to G-BJVX at the time of the accident and that had remained relatively intact was taken to QinetiQ's Structures and Materials Centre for testing.

The blade root was securely clamped with the blade mounted approximately horizontal. A cut representing a crack at different stages of propagation was progressively introduced at the fatigue crack initiation location identified on the yellow colour-coded accident blade. This representative crack was introduced by making a progressive chordwise cut into the titanium spar using a thin high-speed cutting wheel and a small hacksaw. Annex R shows the results of this test.

There were a number of factors that were not representative of the failure to the yellow colour-coded accident blade. The blade used in the test was approximately 10 lb heavier than a standard blade due to the ingress and retention of seawater that may have increased the tip droop observed. The representative crack was substantially wider than a fatigue crack which may also have increased the amount of tip droop observed. In order to cut the varying crack lengths into the titanium spar, it was necessary to cut into the external wire mesh impregnated composite layer and the titanium leading edge erosion cover. It is not known if or when a crack occurred in the wire mesh impregnated composite layer of the yellow colour-coded blade but the formation of such a crack seems very likely once the spar crack exceeded 50 mm in length. Before the composite layer cracked or if it did not crack, it would have provided some resistance to the tip droop.

In summary, this test indicated that approximately 5.33 flying hours prior to the accident (at the time of the inspection carried out by an authorised aircraft engineer after the last flight of the previous flying day) there would have been no increase in blade tip droop. Approximately 1 flying hour prior to the accident (at the time of the final pre-flight/turnround inspection carried out by an authorised aircraft engineer) the static blade tip may have drooped by as much as an additional 23 mm.

1.16.3 The fatigue implications of the manufacturing anomaly

There was no indication of any mechanical rubbing between the folded tang of the yellow colour-coded blade and its spar. However, the aircraft manufacturer calculated the potential reduction in fatigue life of a similarly anomalous blade assuming that the spar was being abraded by contact with a folded tang. This calculation assumed that only the ground-air-ground blade loading cycle was damaging and that this cycle occurred at the FAA approved statistical rate of 450 cycles per 100 flying hours.

The calculations indicated that the fatigue life for this potential failure mode was in excess of 100,000 flight hours whereas the maximum permitted service life of a main rotor blade spar is 37,000 hours. Consequently, the service life and airworthiness of a main rotor blade with a folded erosion cover tang in contact with its spar would not be compromised by spar abrasion damage.

1.16.4 Titanium thermal discoloration

The aircraft manufacturer conducted an experiment to establish the persistence of titanium spar surface discoloration due to overheating. A section of spar was subjected to a spot welding heat source that generated a number of burn marks varying in diameter between 0.05 and 0.2 inches. The colours of the burn marks varied from dark grey in their centres through blue to a yellowish straw colour at their periphery. The spar sample was then cleaned without etching, primed and cured at a temperature of 250ºF (121ºC). The spar sample was then bonded to a layer with structural adhesive and cured once more at the same temperature. This state was representative of the interface between the spar and the adjacent components of a completed blade.

Next the spar sample was subjected to a 'tear down' process to simulate removal of the bonded components during a notional blade repair operation during which the surface of the titanium spar would be exposed. The sample was heated to 400ºF (204ºC) for 30 minutes before the structural adhesive was scraped off by hand using a beryllium copper scraper. The burn marks were still visible at this time but a spar would not have been inspected until the adhesive and primer residues had been removed. These residues were removed by immersion in a molten salt bath for five minutes followed by rinsing in cold and hot water. After drying the spar was inspected. All traces of discoloration from the burn marks had been removed with the primer layer.

In the process of replicating the thermal discoloration it was noted that the sample exhibited melted regions of titanium that did not exist on the failed spar of the yellow colour-coded blade. From this it was concluded that the minimum settings of the spot welding machine used on the sample created a heat effect greater than the lightning induced thermal damage to the failed spar.

1.16.5 Fatigue spectrum

In late 2003 a theoretical study of the effects of variations in blade loading on fatigue crack growth was proposed by the helicopter manufacturer. Detailed flight data was accumulated from the operator's technical records but the project was later abandoned.

1.17 Organisational and management information

1.17.1 Flight planning

Flights within the southern North Sea operating to offshore installations owned or controlled by Shell are co-ordinated using their Movement and Personnel System (MAPS). This is a computer based system which allows authorised users to book equipment and personnel on to flights, the flights themselves being operated to a previously arranged schedule. On offshore installations it is normally the radio operator who inputs the required bookings into MAPS, and as a result the system is usually kept in the radio room. As MAPS can also be used to track the progress of a flight, the radio operator is able to summon the helideck crew into position prior to the aircraft's arrival.

MAPS is a passive system in that no acknowledgement needs to be made that a flight is expected by its intended destination. Because the destination is usually the source of the flight booking, this normally causes no problem. On this occasion, however, the flight booking to disembark a passenger at the Santa Fe Monarch had been made by a Shell representative without the knowledge of the Santa Fe Monarch's radio operator. The individual who made the booking had then left the drilling platform without informing the radio operator of his action. Consequently, no one on board the Santa Fe Monarch was expecting a helicopter movement and so the arrival of G-BJVX came as a surprise.

1.17.2 Flight-following

In the context of this report, the term 'flight-following' means monitoring the progress of a multi-sector flight. In one sense it is a safety measure implemented to ensure that if an aircraft does not arrive at its destination, appropriate action may be taken and if necessary, search and rescue resources may be deployed without delay. In another sense it is the system used to prepare offshore installations and their safety assets for the arrival and departure of helicopter flights.

At the time of this accident, flight-following was accomplished by a mix of MAPS updating and radio telephony between the flight crew, the operator, onshore Air Traffic Control (ATC) agencies and the offshore installations.

Flights departing from or inbound to onshore destinations are normally in contact with ATC and receiving a radar service. Flights between installations are often of short duration, flown at low altitude and occasionally beyond or beneath radar coverage. Consequently, flight-following for these sectors depends heavily on the installation radio operators. These operators exchange RTF messages with the helicopters and they are normally responsible for updating MAPS. Some 'in field' transits are made between manned and normally unmanned installations and so unbroken radio contact with the radio operator based on the manned or 'nodal' installation is vital for flight-following.

During the accident flight, when transiting between installations, the pilots were always in radio contact with either Anglia Radar (based at Aberdeen but using the Cromer and Claxby radar heads) or with a manned offshore installation, and sometimes in contact with both simultaneously using two radios. Before departing a helideck, they passed details of their next destination, en-route altitude and persons on board to the radio operator. Once they had departed, the installation radio operator updated MAPS. During the final leg of the accident flight, the pilots established contact with Anglia Radar before ceasing communications with the Clipper's radio operator. Next they established contact with the Santa Fe Monarch radio operator before ceasing communications with Anglia Radar.

1.18 Additional Information

1.18.1 Operating regime of G-BJVX

The recent operational life of G-BJVX involved numerous short flights between Norwich Airport and various offshore gas exploration and production installations. A large number of the flights flown were of short duration that did not require the engines to be shut down between flights.

The operating procedure for this helicopter was, following first engine start, the main rotor was accelerated fairly quickly up to 65-75% Nr (100% Nr is 293 RPM). Following system and control checks the rotor was then accelerated to 97% Nr and the second engine started, after which the rotor speed was stabilised at 99% Nr. In the cruise, rotor speed was maintained at 103-104% Nr. During the approach and landing phase of flight the rotor speed was kept at 107% Nr. After landing, the rotor speed was reduced to 100% Nr, but could in exceptional circumstances be reduced to 70% Nr. In high wind conditions the rotor speed was kept at 107% Nr after landing.

1.18.2 Fatigue crack characteristics

Fatigue cracks occur in three distinct phases, each of which can be governed by different factors;

Stage I - Initiation region – large influence of i) microstructure, ii) mean stress and iii) environment.

Stage II - Steady growth (striations) – little influence from i) microstructure, ii) mean stress, iii) environment and iv) thickness.

Stage III - Tending towards 'Static mode' failure (ie overload) - large influence of i) microstructure, ii) mean stress and iii) thickness. Little influence from iv) environment.

It is the stage II striations that can be interpreted to determine the crack life. The stage I occurs over a very small crack length and the stage III occurs relatively instantaneously; therefore, an estimate of the time taken for stage II to occur can give a good approximation of the length of time that the crack has been present.

The steady state growth is assumed to produce one striation (ie increment of crack growth) on each load cycle. An assumption has to be made as to what constitutes one load cycle. Determining the total number of striations on the fracture surface coupled with an assumption of the constitution of a load cycle enables the time for stage II crack growth to be determined.

The propagation rate of a fatigue crack is controlled by the stress intensity at the crack tip, which can be a function of the loads imposed and the crack length. The stress intensity at the crack tip will increase with an increase in applied loads and/or crack length. At short crack lengths, and hence low stress intensity, the crack will propagate over a shorter distance than a longer crack for the same load cycle. This can be seen on a fracture surface, as the striations at the start of a crack are usually much closer together (ie small crack propagation between load cycles) than those at the end of a crack where the stress intensity at the crack tip is larger and therefore the propagation per cycle is longer. In most situations, fatigue cracks tend to propagate slowly at the start, increasing in growth rate as the crack length progresses.

1.18.3 Non-destructive inspection techniques

There are a number of non-destructive inspection techniques that may have detected the fatigue crack in the main rotor blade spar prior to the final failure.

1.18.3.1 Eddy current

This technique uses a probe that contains two coils. An alternating current applied to the primary coil induces an alternating magnetic field in the item being examined which in turn generates an alternating current of a similar frequency in the receiver coil. The current in the receiver coil is affected by any changes in the physical properties of the item being examined. The probe containing the two coils has to be in very close proximity to the material being examined to be effective. This technique can be used to detect cracks on the upper and lower surfaces of the blade spar. However, it would not be effective in detecting cracks in the leading or trailing edges of the spar due to the blade's aerofoil shaped construction in those areas. The difference between the blade and spar profiles in these regions would increase the distance between probe and spar sufficiently to render this technique ineffective. Moreover, both the titanium leading edge erosion cover and the aluminium wire mesh lightning strike protection layer would cause major problems when using this technique to detect short length cracks. Generally the probe size, and therefore the swept area, has to be one-third the size of the minimum crack length that is to be detected. This results in a very time consuming operation when a large item such as a rotor blade is being examined.

1.18.3.2 Ultra sonic

This technique uses a probe that emits high frequency sound, which can be used to detect cracks on the upper and lower surfaces of the blade spar. This technique, like that using eddy currents, requires the probe to be in very close proximity to the spar material and therefore would not be effective in detecting cracks in the leading or trailing edges of the spar due to the way that the blade is constructed in those areas. Both the titanium leading edge cover and the foam filling within the blade cannot be penetrated using this technique. Also any porosity (bubbles of air) within the bonding materials will result in false returns. As with the eddy current technique, the probe size, and therefore the swept area, has to be one-third the size of the minimum crack length that is to be detected. This technique is more labour intensive than that of using eddy currents.

1.18.3.3 Radiography

1.18.3.3.1 X-ray photography

This technique uses very high frequency waves in the Gamma area of the electromagnetic spectrum to penetrate materials and produce a photographic negative image. Visual examination of the negative image is used to detect anomalies in a material. This technique can be used to detect cracks throughout all the spar material and is not affected by the titanium leading edge erosion cover or the wire mesh lightning protection layer. However, because of the physical size of a main rotor blade and strict health and safety considerations, there are very few facilities that would have the capability of conducting x-ray examinations of an entire blade.

1.18.3.3.2 Fluoroscopy

Fluoroscopy uses the same system as the X-ray technique but instead of the X-rays producing an image on a photographic negative, they are converted into a digital image using a photocathode. This enables both still and dynamic images to be observed in real time and still images can be digitally stored. However, the resolution of fluoroscopy images is considerably lower than those obtained using the X-ray technique with photographic negatives. There are very few facilities worldwide that have a fluoroscopy capability for large items the size of a helicopter main rotor blade.

1.18.3.4 Non-destructive testing resource implications

All of these techniques are very time consuming and can take up to eight hours per blade to conduct satisfactorily. They also require the use of specialist equipment and specially trained personnel to carryout the inspections. The eddy current and ultra sonic techniques can be used in the field whereas generally, the X-ray and fluoroscopy techniques can only be used at purpose built facilities.

1.18.4 Blade Inspection Method (BIM)

A number of helicopter manufacturers, including the manufacturer of the S-76, incorporate into some of their main rotor blades a special feature for alerting flight crew and ground staff to the early indications of cracks developing in the blade's spar. Sikorsky's proprietary technology is known as the Blade Inspection Method and is normally abbreviated to BIM. The hollow main rotor spar is sealed at both ends and pressurised, normally with nitrogen, to approximately 10 psi. The BIM device monitors the nitrogen pressure and the technology includes an elaborate venting system to allow the gas to escape from a crack in a spar whilst that spar is cocooned within the sealed blade assembly. A pressure indicator is mounted at the root end of the blade's spar and will give an alert indication when the pressure within the spar drops below a preset value. This pressure drop could indicate if a small crack had developed or if there was a seal leak.

Some helicopters are fitted with a cockpit BIM warning system. This system gives the flight crew an in-flight indication that one or more of the main rotor blade spar pressures has dropped below their preset values.

There was no BIM system fitted to any main rotor blades of Sikorsky's range of S-76 helicopters.

The BIM system is fitted to the main rotor blades of the Sikorsky H-60 (Blackhawk) range of helicopters which have successfully indicated the presence of a crack on two occasions (see paragraph 1.18.7). Over the service life of the H-60 there have been in excess of 100 false indications generated by the BIM system that have been reported to the manufacturer. The manufacturer is of the opinion that there have been many other BIM system false indications that have not been reported.

1.18.5 Safety Actions taken

1.18.5.1 Initial safety action by the helicopter manufacturer

On 25 July 2002 the helicopter manufacturer issued Alert Service Bulletin 76-65-55A which required the identification and removal from service of all model S-76 main rotor blades that had suffered damage by lightning and to remove from service any main rotor blade that suffers damage by lightning after the date of issue of the ASB. As a result of this ASB, 26 main rotor blades were removed from service. Of these, 17 were removed as a result of Log Card entries stating that there had been lightning strike damage and 9 where there had been incomplete Log Card histories.

1.18.5.2 Further safety action taken by the helicopter manufacturer

On 9 August 2002 the helicopter manufacture issued Alert Service Bulletin 76-65-56 which required a one-time inspection of all model S-76 main rotor blades that have two piece titanium leading edge covers for evidence of tangs that may have folded under themselves or the adjacent leading edge cover. Of the 1,600 to 1,675 blades affected, only 310 reports were received by the manufacturer, each of which reported no anomaly.

In November 2002 the manufacturer issued a revision to their Composite Materials Manual for the model S-76. A section of this revision introduced an inspection requirement, acceptance and rejection criteria and repair action for damage caused by a lightning strike.

1.18.5.3 Safety action by the helicopter operator

On the 22 July 2002 the operator issued Alert Message AM S76/02/001 to all its engineering bases worldwide requiring a detailed inspection of the flying control and power transmission systems and a close monitoring of the IHUMS data.

On the 30 July 2002 the operator issued Alert Message AM S76/02/004 to all its engineering bases world-wide requiring inspection of all main rotor blades that have two piece titanium leading edge covers for evidence of tangs that may have folded under themselves or the adjacent leading edge cover.

1.18.6 Main rotor out-of-balance forces

The manufacturer carried out calculations to determine the magnitude of the lateral forces that would be generated when the outer 4.15 metres of a main rotor blade separates in-flight. These calculations estimated that the out-of-balance lateral force generated would be in the region of 27,000 lbf. The main rotor gearbox to fuselage mountings are designed to accept lateral forces up to +/- 3g, which is approximately 5,800 lbf. These figures indicate that with 4.15 metres of a main rotor blade missing, the out-of-balance forces would be about 4.5 times greater than the design lateral loading of the main rotor gearbox to fuselage mounting points.

1.18.7 Previous titanium main rotor spar failures and spar cracking

The helicopter manufacturer produces three types of main rotor blade that utilise a titanium spar: one for the S-76; one for the H-60 range (including the S-70 export version); and one for the S-65 (H-53). There have been no known failures of main rotor blade titanium spars fitted to any of these helicopter types.

The helicopter manufacturer was unaware of any previously identified cracking in the main body of any S-76 main rotor blade titanium spar but cracks were found at the blade ends. Specific inspections were introduced to detect cracking in these areas. Some 80 cracks have been found at the root ends in the areas of the holes for the rotor hub attachment bolts and several at the tip ends in the area of the tip cap attachment bolts. All of these cracks were assessed as benign and/or in areas of redundant structure.

There have been two identified cracks in the spars of the main rotor blades fitted to the H-60 helicopter range (a UH-60 and an HH-60J). On the UH-60 the crack originated from electrical arc damage from the de-ice mat which had previously been disrupted by a bullet. On the HH-60J the crack originated at the BIM fitting in the spar in the cuff area of the blade where there was a redundant load path. Both cracks were detected by the BIM system.

There has been one identified crack in the spar of the main rotor blade fitted to the CH-53 helicopter that originated from a tip block attachment hole where there was a redundant load path. This was detected during a routine visual inspection which involved removal of the tip cap thus exposing the end of the spar.

1.18.8 Total service life of Sikorsky titanium spared main rotor blades

To date there has been only one failure of a titanium spar of a S-76 main rotor blade. That failure is the subject of this investigation.

The total time in service of S-76 main rotor blades is approximately 12.8 million flying hours.

The total time in service of all titanium sparred main rotor blades manufactured by Sikorsky is approximately 40 million flying hours.

1.18.9 Previous folded tang on the titanium erosion cover

About six to eight months after the manufacture of the yellow colour-coded blade that was fitted to G-BJVX at the time of the accident, the manufacturer found, during the manufacturing process, a blade that had a folded tang at the scarf joint of the two-piece titanium erosion cover. The folded tang was found during the fluoroscope inspection. The manufacturer formed an internal Material Review Board to assess the manufacturing anomaly. The Material Review Board assessed the anomaly as not structurally significant and required that the blade be re-worked; this decision was sent to the appropriate Airworthiness Certification Office to allow FAA oversight. The blade re-work consisted of trimming off the folded tang section of the erosion cover and filling the void. No requirement was issued for a retrospective inspection of previously manufactured main rotor blades.

2 Analysis

2.1 Catastrophic failure

The accident occurred when the outer portion of the yellow colour-coded main rotor blade separated as the helicopter was approaching to land on the Santa Fe Monarch. A fatigue crack, originating from the combination of a manufacturing anomaly and the effects of a lightning strike, had progressed, very slowly at first, in a chordwise direction, both forwards and rearwards from an initiation point on the upper surface of the blade's titanium spar.

A few hours before the catastrophic failure, the crack propagation rate accelerated markedly and the crack grew to about half the blade spar's cross-section before the various forces acting on the spar were sufficient to overcome its residual strength and the outer two thirds of the blade separated. The main rotor blades rotate at about 304 RPM and the centrifugal force imbalance created by the missing blade section was about 27,000 lbf. This imbalance exceeded the design requirements for the main rotor gearbox attachment fittings by a factor of more than four. Consequently, the gearbox, together with the three intact blades and the stub of the broken blade, tore away from the helicopter's fuselage. This probably happened a fraction of a second after the blade failed. Even if the gearbox had been retained, the helicopter would have been uncontrollable and the environment for its occupants would probably have been unsurvivable. Therefore, separation of the main rotor gearbox had no appreciable effect on the outcome.

The gearbox separated when the helicopter was travelling at about 94 kt airspeed and at a height of 323 feet. After the main rotor gearbox separated, drive to the tail rotor would have been lost and so there would have been no tendency for the helicopter's fuselage to rotate due to tail rotor yaw force. With an initial airspeed of 94 kt and with the fin in place and largely undamaged, the fuselage probably fell nose-first in a ballistic curve, accelerating until it struck the sea surface. The combination of forward and vertical speeds was responsible for the severe disintegration of the fuselage and the immediate fatal injuries suffered by everyone on board.

The gearbox, with three intact rotor blades plus the inboard stub of the yellow coded blade fell to the sea, probably in a manner somewhat resembling a sycamore seed as reported by one of the few eye witnesses. As it fell, the main rotor assembly, which was also no longer supporting the weight of the fuselage, would have lost most of its forward speed and much of its rotational speed. These factors explain the relatively superficial damage to the assembly compared to the remainder of the helicopter and why it was found some distance from the main debris field.

Search and Rescue assets at sea and ashore were deployed without delay but there was nothing that could be done to save any of the 11 persons on board.

2.2 Scope of analysis

This was the first known in-flight fatigue failure of a titanium sparred main rotor blade manufactured by Sikorsky and so, from the outset, it seemed likely that exceptional circumstances were involved in this failure. The origin of the crack in the yellow colour-coded blade was beneath the tang of one section of the two-piece titanium erosion cover. This tang had been inadvertently distorted during blade manufacture in 1981, resulting in a small malformation of the scarf joint between the two pieces of the erosion cover. Although the malformation went unnoticed for 18 years, it seems to have had no material effect on the integrity of the blade until it was exploited by an electrical pulse that can be attributed to a low-magnitude lightning strike (less than 10,000 amps) in 1999. The electrical discharge passed between the two sections of erosion strip via the tang, which at the fold line, was either in contact with the spar or very nearly so, and the spar itself. This momentarily created sufficient heat to change the material properties of the titanium spar in a small elliptical region probably less than 2 mm wide. The reasons why the manufacturing anomaly was not noticed and rectified during blade manufacture, and had apparently not been noticed during subsequent inspections and blade repairs, deserve an explanation.

An electrically conductive path (bonding[1]) giving some protection against lighting strikes had been built into the blades. However, there was no deliberate electrical bonding path between the upper and lower conductive aluminium wire meshes and the titanium erosion cover although the gap between these components appeared to be very small (significantly less than 1 mm). Some burning of this aluminium wire mesh was visible but not in the area of the scarf joint. In this region an electrical discharge passed between the malformed tang and the spar. Had the spar damage been detected (or as will be explained later, detectable) when, following the lightning strike, the blade was returned to its manufacturer for assessment, this accident might have been avoided. However, it is appropriate to review the assessment in the context of that time, when the potential for microstructural damage through this mechanism was not appreciated, perhaps principally because it had not previously occurred.

[1] Joining together all major metal parts of an aircraft, especially an aircraft not of all–metal construction, to ensure low-resistance electrical continuity throughout. Bonding is necessary for Earth–return systems and to dissipate lightning strikes and other electrical charges safely with no tendency to arcing

After refurbishment the blade was returned to service in 2001 having accumulated 8,261 flying hours but it did not fail until some 1,400 flying hours later. Current estimates of the crack propagation rate suggest that a through-crack[1] did not form until between 21.3 and 29.8 flying hours before complete failure. This analysis will examine the symptoms of imminent blade failure during this latter period and what, if anything, could have been done to detect an imminent failure in time to prevent the accident.

There were three basic means by which the crack might have been detected; by visual inspection; by non-destructive testing; and by trend analysis using data recorded on board the helicopter. The potential for each of these basic means will be examined. Finally, the analysis concludes with a review of the safety actions taken, assessing whether these are sufficient to prevent a similar accident, and whether the current blade inspection, testing and crack detection processes might be adapted to better detect fatigue cracks in spars.

2.3 Interim Safety Action

Representatives from the helicopter manufacturer and the Federal Aviation Administration of the USA were incorporated into the investigation team as advisers to the Accredited Representative from the USA. As soon as the investigation team was certain that the fatigue crack emanated from the combination of a folded tang and thermal damage by a lightning strike, the aircraft manufacturer issued an Alert Service Bulletin (ASB). This ASB, issued nine days after the accident, required the identification and removal from service of all S-76 main rotor blades that had suffered a lightning strike and any which in future might be similarly affected. The next day, 26 July 2002, the AAIB sent an interim safety recommendation identified as 2002-25 to the FAA recommending that:

> *The Federal Aviation Administration mandates appropriate action to ensure the continued airworthiness of Sikorsky S-76 main rotor blades which have either:*
>
> *a. A two-piece leading edge titanium sheath (erosion strip).*
> *or*
> *b. Have suffered a lightning strike.*
>
> (Safety Recommendation 2002-025)

That same day the FAA acted by giving mandatory status to the manufacturer's ASB through an FAA Airworthiness Directive. Subsequently, on 9 August 2002 the manufacturer issued another ASB requiring a one-time

[1] The point at which the embryonic crack in the spar's outer surface reached the spar's inner surface.

inspection of the scarf joint on all S-76 main rotor blades fitted with a two-piece leading edge erosion cover. This inspection required removal of any patches, paint, primer and adhesive covering the scarf joint and inspection for a folded tang. No more folded tangs were found.

2.4 The manufacturing anomaly

2.4.1 Blade manufacture

The techniques and materials used for manufacturing the S-76 main rotor blades were very similar to those used for manufacturing blades for the larger H-60 and H-53 helicopters, the main differences being those of scale. The blades all have titanium spars and all are made at the same facility using much the same processes carried out by the same skilled workforce.

The plasma arc butt welding process used to join the rolled titanium plate is partially automated and carefully controlled making stray thermal damage unlikely. The weld is then subjected to rigorous inspection, both internally and externally, throughout its length before the tube is flattened leaving the weld at the centre of curvature facing the trailing edge of the blade. Consequently, any stray thermal damage during the welding process should be detected but if not, it would be near the trailing edge side of the spar and well away from the area beneath the scarf joint. Plasma arc butt welding was the only high temperature process during blade manufacture so the heat damage near the spar's leading edge could not have been inflicted during the blade's manufacture.

The blade components were assembled by hand and most were joined using structural adhesive bonding. The tooling used to hold the blade during assembly generally supported it inverted at a height above the ground that was a few inches above the average man's waist height. The convention of keeping the blade inverted arose because the shape of the upper surface of the blade is aerodynamically more critical than the underside. By assembling the blade inverted, the upper surface of the blade lay on the rigid metal former and the slightly flexible caul was placed on top of the assembly which by then was the underside of the blade. The assembled blade was transferred from the compaction fixture to the bonding fixture by an overhead crane that needed to raise the blade by only a few inches to move it. Consequently, the upper surface of the blade was always on the underside throughout the assembly and curing processes. In that orientation, the scarf joint anomaly was unlikely to be observed since it was facing the ground and well below eye level.

The uncured epoxy structural adhesive used to bond the erosion strip to the blade was very 'sticky' to touch. It seems likely that the unsupported rear edge of the thin metal tang on the outboard section of the erosion cover was gripped by the adhesive before the assembly was pressed fully home in the compaction fixture. As the assembly was pressed home, the gripped tang folded backwards into alignment with the direction of compaction. Being underneath the blade and a little above waist height, it was not obvious to the technicians that this had occurred. The remaining components of the blade were added and the whole assembly was then transferred to the bonding fixture before curing in an autoclave. Sufficient adhesive was used to be sure of high quality bonding and the filling of any minor voids before being exuded from the interior. This excess adhesive was sufficient to fill a small depression left in the surface of the blade by the folded tang and its opacity was sufficient to hide the anomaly.

Although the quality control process during blade assembly was extensive, it did not include a specific check of the scarf joint prior to autoclaving and hence the anomaly was not noticed during the manufacturing process. There was however, one final chance to detect the anomaly before the blade was released to service. Each new blade is examined across its entire width and length by fluoroscopy (described in paragraph 1.18.3.3.2). This examination was capable of revealing the folded tang had the operative been searching for such a flaw but the search objectives were the detection of foreign objects and correct assembly of the internal metallic parts, particularly at the root and tip ends of the blade.

All S-76 main rotor blades manufactured since 1989 have a one-piece erosion cover that is far less susceptible to assembly distortion. Moreover, the manufacturer now uses improved tooling and a greater degree of automation to attach the erosion cover assembly to the leading edge.

2.4.2 Other folded tangs

Some months after the yellow blade was constructed, a similar deformation of one tang was discovered during manufacture of an S-76 blade (see paragraph 1.18.9). Although the defect was discovered, the mechanism by which it arose was unknown. A Material Review Board assessed the defect as 'not significant' and this blade was re-worked, principally by cutting out the folded tang and filling the void created. Had the same anomaly been discovered during manufacture of the yellow blade, it seems probable that a similar decision would have been taken.

After this accident, a check of all S-76 main rotor blades bearing a two-piece erosion strip was initiated by the manufacturer. The check required a one-time inspection of the scarf joint for a deformed tang. Of the 1,600 to 1,675 blades affected only 310 reports were received by the manufacturer, each of which reported no anomaly. It is likely that many more blades were examined but, having found no anomalies, the examiners declined to submit reports to the manufacturer. Since no other instances of folded tangs were reported it appears likely that the yellow colour-coded blade fitted to G-BJVX was the only one blade to enter service with a folded tang.

2.4.3 Airworthiness of the yellow blade

There was no evidence on the recovered section of the blade of mechanical interference between the deformed erosion cover tang and the spar. Nevertheless, even if the tang had been rubbing the spar's surface, given the calculations conducted by the manufacturer, there is no reason to suppose that the anomaly would have had any impact on the airworthiness or service life of the blade, unless it was exploited by another damage mechanism. This investigation determined that it was exploited by a lightning strike.

2.5 Thermal damage to the spar

2.5.1 Lightning strike examinations

Although two of the blades damaged by the lightning strike suffered by G-BHBF were photographed before removal, no photographs of the blade that features in this investigation could be found. The only records of the damage suffered were the written records retained by the UK repair organization, the USA Repair Station and the helicopter manufacturer.

It seems clear from all three sets of records that the blade exhibited conspicuous external signs of lightning damage. The signs included burning of the aluminium wire mesh embedded in the upper and lower surface skins at blade station 44 which is inboard of the scarf joint and in a similar location to the strikes on the blades photographed after the strike to G-BHBF. There were also arc marks and abnormal features described as 'blow out' marks on the leading edge near the erosion strip. Nevertheless, although there were obvious lightning strike marks on the blade, there were none in the region of the scarf joint. The areas with conspicuous damage were repairable in accordance with procedures in place at the time.

The two repair agencies that examined the blade before the manufacturer declined to repair it but found no signs of damage to the blade spar, although one organisation recorded visible marks inside the hollow spar. After the accident only two of those marks could be assessed since the remainder were inside the outboard portion of the blade that was not recovered. These marks were difficult to identify using a boroscope but after blade sectioning and closer inspection, they were thought to be marks left by solidified contaminants such as oil, grease, paint and possibly dirt. These contaminants were almost certainly harmless and were probably introduced when the blade was in service, making their way along the inside of the spar under the influence of centrifugal forces. Certainly, there were no signs of lightning induced or any other mechanical damage inside the recovered section of spar.

The authority for the final decision as to whether the blade was repairable was vested in the manufacturer's engineering staff. There were no prescribed limits for the size or extent of any lightning damage. As the Engineering Instruction (Appendix C) makes clear, the assessment ('disposition') had to be made by experienced engineers using their engineering judgement. They had examined other blades struck by lightning and had amassed relevant experience. Some of these blades were scrapped but some were repaired and returned to service. Damage due to wear and tear on the blade (eg water ingress) was detected during the blade receipt fluoroscopy inspection (which was not part of the EI lightning strike inspection but a more general examination of the internal condition of the blade). However, the presence of the folded tang was not detected. The engineering assessment was that the yellow blade was repairable provided that it passed all the detailed inspections stipulated in the Engineering Instruction. Other minor defects that had arisen during normal in-service operation were also identified as requiring repair.

2.5.2 Detection of thermal damage

Inspection of the blade by its manufacturer was unlikely to have revealed the folded tang unless it was noticed during either the receipt or release fluoroscope inspections. These radiographic inspections were not intended to detect such flaws; their purpose was to detect foreign objects, internal metallic damage or incorrect assembly of metallic parts, and to inspect the interior for water ingress. These aims were achieved; water ingress was identified during the incoming inspection but not metallic damage or incorrect assembly. Moreover, throughout the inspection and refurbishment processes, the damage to the spar was thermal and not mechanical. The size, shape and thickness of the spar metal in the area beneath the scarf joint would have been unaltered by the thermal damage. There was no crack in the spar and so there was no prospect of detecting the small area of thermal damage beneath the folded tang using fluoroscopy.

As the QinetiQ report at Appendix L makes clear, the fatigue crack initiated from a localised change in the microstructure of the titanium metal. After cleaning the fracture area, the change was visible on the spar's surface as a small region of discolouration but to identify the extent of the damage, QinetiQ had to use a scanning electron microscope. The region of changed microstructure within the recovered half of the fracture face was a semi-elliptical shape 1.23 mm wide and 0.23 mm deep.

There is no known non-destructive method for detecting such small and localised changes in the microstructure of a large metallic component that is encased within layers of fibreglass, sheet metal or metallic mesh, and epoxy adhesive. In areas where there was suspicion that the spar might have been damaged, it would have been possible to remove the damaged skins, expose the spar and chemically clean the epoxy adhesive and primer paint layer from the spar surface. However, the etching agent used to remove the adhesive and primer residues would also have removed the tinted layer on the titanium surface. Since there was no physical deformation of the metal, the small area of microstructural damage would then have been invisible.

The spar of the blade was the primary load bearing structure and therefore critical to its continued airworthiness. The assessors made a judgement that being encased in secondary structure, the spar was unlikely to be damaged in areas where that secondary structure was undamaged. There was no visible damage in the scarf joint area (blade stations 75.25 to 82.75). The nearest visibly damaged area was a crack in the leading edge erosion cover at blade station 112 which was 29.25 inches from the scarf joint. That defect was not attributable to lightning damage. The nearest burn damage to the blade's skin was 36 inches from the scarf joint at station 118.75. Consequently, there was no realistic prospect of detecting the thermal damage in the spar before the blade was repaired.

2.5.3 Blade refurbishment

The actions taken to refurbish the blade were extensive and detailed but the focus of the repairs was remote from the scarf joint area. The manufacturer had earlier used a splicing process to repair cracks in the leading edge erosion covers but this practice was no longer invariably used when the blade was repaired. Unless an area of disbonding wider than four inches from the crack was found, approved 'repairs' to the erosion cover were achieved by covering them with plastic tape in accordance with a procedure listed in the manufacturer's Composite Materials Manual.

Had cracked sections of the two-piece leading edge erosion strip been removed and replaced, the folded tang might have been discovered since the epoxy adhesive filled void might have been exposed. The void would have been exposed if the entire erosion cover had been replaced by a new one-piece unit. The manufacturer determined that because any disbonding was within limits, the cracks could be covered with tape in accordance with the Composite

Materials Manual. The blade manufacturer did not carry out these patch 'repairs'. They were deferred for corrective action by the customer (the USA Repair Station) as part of the blade finishing process that was carried out before the repaired blade was returned to the operator.

All the cracks in the erosion cover were outboard of the scarf joint and the nearest was 29 inches away. Consequently, it seems unlikely that any splice repair which physically replaced sections of cracked metal would have involved disturbing the scarf joint, so the change in repair method probably had no effect on the prospects of discovering the folded tang. Nevertheless, had the scarf joint been disturbed during refurbishment, the epoxy filled void and possibly the discoloration beneath the folded tang might have been noticed by a technician and reported to engineering for 'disposition'. This was the only method by which the thermal damage might have been detected and assessed during blade refurbishment.

2.6 Fatigue crack formation

2.6.1 Crack initiation

The failed blade had been subjected to flight loads for 1,403.6 hours since refurbishment. At some indeterminate stage during that period, the crack formed. Cyclic loading of the blade was responsible for the crack. This cyclic loading arises mainly from changes in blade lift, blade flapping, blade bending and blade lead/lag motions. Centrifugal on-off cycling is also a significant fatigue inducing load.

Many materials under the influence of cyclic loading are susceptible to fatigue. In this case, the spar surfaces were shot-peened to produce compressive residual stresses in the spar surface and so reduce the likelihood of fatigue initiation within the design life of the blade. The thermal damage caused by the lightning strike removed the beneficial effects of the shot peening and changed the microstructure of the metal to a structure more susceptible to fatigue initiation. After the thermal damage had occurred, cyclic loading in the blade initiated a fatigue crack at this point within the design life of the blade.

The crack took several hundred hours to materialise after the lightning strike. This is a typical feature of fatigue cracks. The nucleation of a fatigue crack absorbs the majority of the fatigue life of a component in that initiation can take significantly longer than propagation. Initially the crack direction was from the outside of the spar towards the inside until a through-crack formed. This initial through-crack growth was likely to be different from the crack growth in the two opposite propagating crack fronts.

2.6.2 Spar crack striation counts

The AAIB employed the QinetiQ materials laboratory to analyse the fracture face. QinetiQ's assessment of the crack comprised three sectors:

1. From the origin to a length of about 0.6 mm in each direction (a total crack length of 1.2 mm). This sector was associated with through-crack growth and the elapsed time for this sector was indeterminate.

2. From about 0.6 mm to about 14 mm from the origin in both directions (a total crack length of 28.3 mm). The elapsed time for this sector was calculated by extrapolation of the striation count in the third sector. This technique produced an estimate of around 1.7 million striations in these sectors (1,689,429 for the trailing edge and 1,691,669 for the leading edge).

3. From about 14 mm either side of the origin to a total crack length of 143 mm. The striation densities in this sector were measured and represent a good estimate of the crack growth. Within this sector there were 158,824 striations towards the trailing edge and 137,402 striations towards the leading edge and around the nose curvature of the spar.

This early work was later reviewed in the light of Sikorsky's striation count. Their assessment estimated the number of striations inside 14 mm from the origin by measuring striation density and not by graphic extrapolation. The striation density measurements were combined with QinetiQ's power curve mathematical method to estimate the number of striations in this region. The results were a very significant reduction from about 1.7 million to about 244,000 on either side of the fatigue origin.

Interpolation of the graph at Figure 4 of Annex P shows that in the regions from about 14 mm either side of the origin to the ends of the fatigue region, the Sikorsky striation density measurements also produced increases in the striation counts in the order of 25%. However, there were surface features that were counted as valid fatigue striations by Sikorsky's assessments of crack face replicas but not by QinetiQ who assessed the original crack face. Given that these differences cannot be resolved without a great deal of further work, the investigation team considered it reasonable to combine Sikorsky's striation density measurements inside 14 mm from the origin, where the TEM method was superior, with QinetiQ's striation densities beyond 14 mm, where the SEM method was more than adequate and the crack itself was assessed. The results of this combined data assessment are shown in column 3 of Table 5.

Table 5 – Total Striation Count Estimates

	QINETIQ DATA	SIKORSKY DATA	COMBINED DATA
Leading Edge of Crack Origin to end	1,829,071	542,704	**388,025**
Trailing Edge of Crack Origin to end	1,848,253	537,008	**444,712**

2.6.3 Fracture mechanics assumptions

QinetiQ's first striation report at Annex M states*:*

> *'The use of striation counting to estimate crack growth must be used as a guide only. Many assumptions are made about the loading cycle. In this case it has been assumed that each blade revolution produces one striation and that each blade revolution occurs at a speed of 304 RPM. It is possible that some striations are produced by cyclic loads not associated with the blade rotation such as vibration and wind gusts, although in this case that problem was addressed by measuring the distance between the prominent striations and ignoring the 2 to 3 smaller striations that were observed in-between. However, this again is an assumption.'*

It is not possible to calculate the flight hours during which the crack progressed without making some assumptions and QinetiQ were fully aware of the fragility of their initial assumptions. The helicopter manufacturer also cast doubt upon the direct relationship between striations and blade rotations. The company thought the ground-air-ground cycle, during which a blade transitions from producing little or no lift to lift for flight, followed by a reduction to near zero lift after landing, would also have a major effect on crack progression. Additionally, it is possible that the blade accelerate-decelerate cycle, which coincided with engine starts and stops and normally occurred just once per multi-sector flight, might also have had an appreciable effect on fatigue progression. This cycle induces significant changes in centrifugal and lead/lag forces within the blades. Furthermore, there was a possibility of crack progression whilst the rotors were running on the ground or on a helideck; these periods represented 'rotors-running' operations for which flight time was not logged. Unfortunately the study into these potential contributory factors was not completed.

2.6.4 Spar crack progression during final flight

Figure 4 of Annex K (reproduced below) shows little difference in the track of the yellow colour-coded blade during the first three flights on the graph (the second, third and fourth flights of the day) but a change is unmistakeable during the fifth and final multi-sector flight. These changes must be related to spar crack size and so the crack was growing rapidly during this flight.

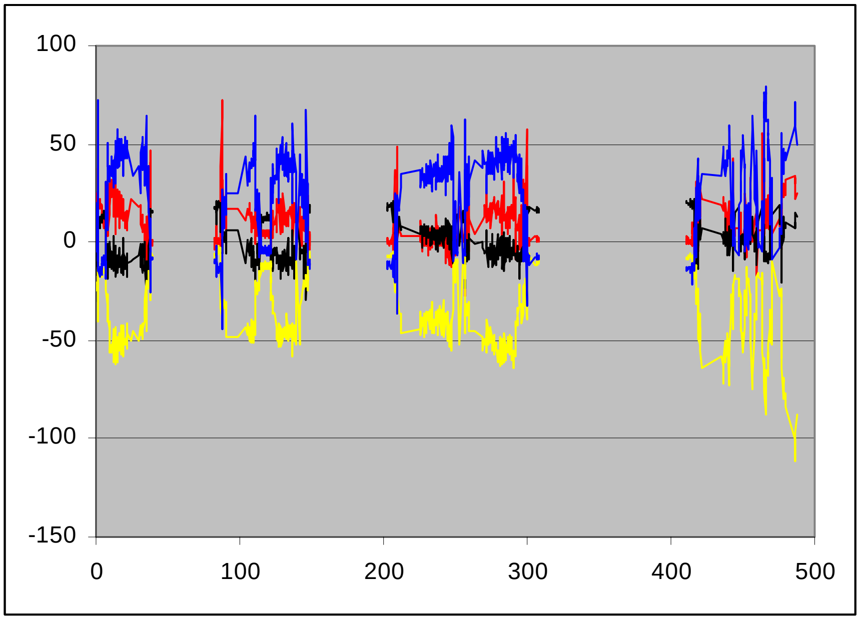

Annex K Figure 4 - Track Data (mm) from FDR vs Pseudo Time (min)

The rapidity of the crack growth during the final five sectors of the last flight is also illustrated by Figure 7 on page 15 of Annex K which shows the yellow blade track changing during each sector departure. This graph also suggests that something significant happened to the blade between the third and fourth sectors; this could, however, have simply been the change in payload from zero to eight and then nine passengers and their baggage for the last two sectors (see Table 2).

All these discernable changes were taking place during a period of just 72 minutes (of which 55 minutes were flight time) which encompassed 5 takeoffs, 4 landings and 1 blade acceleration. Consequently, it seems likely that the crack growth rate during the last few flight hours was driven predominantly if not exclusively by blade rotation. If the ground-air-ground and blade accelerate-decelerate cycles did have an appreciable effect on crack propagation, then it seems likely that their effects were more pronounced during the early stages of crack formation and progression. Therefore, the analysis proceeds on the basis that during the final stages of crack growth, one striation occurred with each blade rotation.

2.6.5 Total time for spar crack propagation

The total time for spar crack propagation can only be estimated by dividing the total number of striations by the in-flight blade rotation speed of 304 RPM (18,240 cycles per hour). The results are shown in Table 6 below. It must be emphasised that of these figures, the combined data represents the minimum period.

Table 6 – Spar crack propagation time estimates

	QINETIQ DATA	**SIKORSKY DATA**	**COMBINED DATA**
Leading Edge of Crack Origin to end	100.3 hours	29.4 hours	24.4.hours
Trailing Edge of Crack Origin to end	101.3 hours	29.8 hours	21.3 hours

The only other clue to the total period is the significance of the 63 'macro bands' in one direction and 61 bands in the other direction observed by QinetiQ which are indicative of a change in circumstances during crack propagation. The record of flight times and sectors flown at Annex F shows that the last 63 sectors were flown over 19.6 flight hours and that the last 63 engine starts took place over 70.4 flight hours. If the macro bands represent engine starts and stops, then the total crack propagation period is likely to be nearer 70 hours than 20 hours. If they represent ground-air or air-ground changes in vertical blade loading, then they correspond to events during the last 19.6 flying hours and so the total period is likely to be nearer 20 hours than 70 hours. Neither correlation seems a good match for any of the data sets in Table 6 although the closest match is the combined data and the ground-air-ground cycles. Consequently, the period of spar crack propagation remains indeterminate but allowing for the different striation counts, it seems very likely that significant spar crack growth began within the final 100 flight hours.

2.6.6 Crack growth rate shortly before the accident

Defining a specific phase of spar crack progression is somewhat subjective but before the external crack formed, there was no visible evidence suggesting internal damage to the spar. Therefore, the start point of the most important phase is taken to be when the sympathetic crack first formed in the blade's exterior close to the crack origin.

During the manufacturer's coupon tests (see paragraph 1.16.1) a sympathetic crack in the fibreglass skin and paint layers first appeared, when the crack in the adjoining titanium spar material was 2 inches (nominal 50 mm) long. Therefore, a crack length of 50 mm appears to be an appropriate start point for analysing the subsequent, rapid growth phase. It also permits a meaningful comparison of QinetiQ's striation count with Sikorsky's count and permits scoping of the likely flight hours during which an exterior surface crack was present.

QinetiQ's graph on page 3 of Annex N suggests that the spar crack length grew from 50 mm to 143 mm (failure) in a little less than 5 flight hours. Interpretation of the combined data, as shown at Figure 4 of Annex P, suggests that it grew the same amount in 6.3 flight hours (21 mm leading edge and 29 mm trailing edge). Consequently, despite the differences in striation counts, both elapsed time assessments were broadly similar for the phase of crack growth from 50 mm to failure.

The major part of the crack was in the upper surface and leading edge of the spar. The trial report at Annex R contains a colour-coded diagram of saw cuts used to simulate the crack size at various stages; this diagram is repeated in Figure 8.

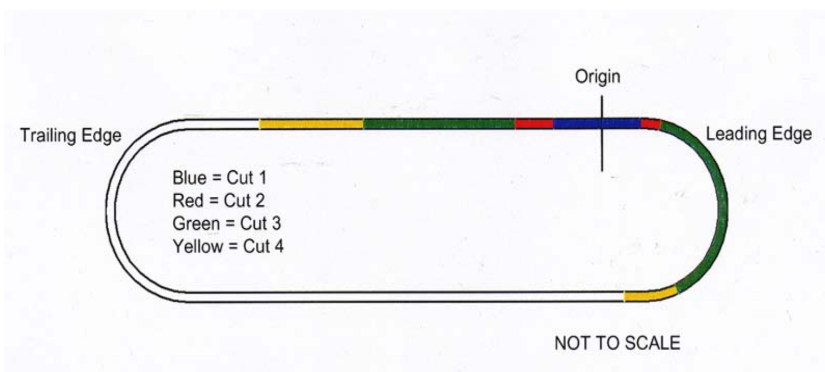

Coloured band(s)	Crack length (mm)	Flight time before failure
Blue	30	9 hrs 30 mins
Blue and red	41	7 hours 35 mins
Blue red and green	102	2 hours
Blue, red, green and yellow	142	0 mins

Figure 8 – Crack growth simulation

The amalgamation of the coloured bands in Figure 8 illustrates the approximate size of the crack at failure. The flight times in the third column have been amended (relative to those in Appendix Q) to conform to the combined data curves in Appendix O.

The data show the spar crack did not reach the underside of the spar until the day of the accident. Had the crack initially formed in the underside of the spar, flight loads would have tended to open the crack and the spar would probably have failed much earlier due to bending loads in the upper surface.

2.6.7 The period between formation of a sympathetic crack and blade failure

A few hours before the accident the spar crack beneath the inboard section of the erosion cover spawned a sympathetic crack in the thin, titanium metal. It was estimated that the flight time required for erosion cover crack growth from approximately 18.5 mm from its origin to final failure was 2.4 hours. Extrapolation of the striation densities using a best-fit curve was plotted to estimate the total number of load cycles for crack growth. The total number of cycles was 133,444, which equates to a time required for crack growth of 7.3 hours. Because of the limitations of striation counting, this should be considered a minimum time and the crack may have formed earlier.

2.6.8 External crack growth

Interpolation of the striation count for the fatigued erosion cover suggests that an external crack was present in the blade's leading edge structure on the morning of 16 July. When applied to the graphs at Appendix O, the result of the crack relationship testing (see paragraph 1.16.1) suggests that an external crack would have formed in the blade's upper skin when the spar crack beneath it extended 50 mm aft of the erosion cover. However, the skin crack might also have formed earlier, particularly if the blade acceleration cycle was tending to open the spar and erosion cover cracks during engine starts.

The spar fatigue origin was 6.7 mm forward of the rear edge of the erosion cover so a skin crack would probably have formed by the time the spar crack front moving towards the blade's trailing edge was 56.7 mm from the origin. Figure 4 of Annex P suggests that this happened about 2.4 flight hours before the accident. Therefore, a crack in the blade's upper skin would most probably have been present on the day of the accident. If a skin crack formed, which seems very likely, the moment that it became visible was when it appeared aft of the polyurethane protective patch.

2.7 Crack detection

2.7.1 Detection opportunities

There was no practical method which the operator could have used to detect the spar crack by visual inspection until a sympathetic crack formed on the blade's exterior. Therefore, exactly how long the spar crack had existed is technically interesting but of limited significance to its discovery. The practicality of timely detection of any exterior crack in the blade's surface is of much greater significance.

Unfortunately, when the sympathetic crack in the erosion cover first appeared, it would have been hidden underneath the black, opaque, polyurethane patch that had been fitted to prevent water ingress into the scarf joint. That patch always hid the crack front that was moving towards the blade's leading edge until the accident. However, the crack front moving towards the trailing edge might have been visible before the blade failed.

2.7.2 Crack detection by routine visual inspection

The last detailed visual inspection of the main rotor blade surfaces was performed during the 50 hour Inspection that was carried out 37 flight hours prior to the accident but there would have been no external symptoms of a crack then. A Daily Inspection was carried out on 11 July on completion of that day's flying and a Pre-flight/turnround Inspection was carried out before each of the five flights on the day of the accident. All six of these inspections required a visual check of the blades' surfaces for obvious signs of damage or disbonding and they were carried out by an authorised engineer (this was the operator's initiative and not an aircraft manufacturer's requirement). The underside of the blades' surfaces would have been inspected whilst standing on the ground whereas their upper surfaces would have been viewed from a position standing on the left side engine decking. Before each flight a pilot may also have inspected the blades but possibly only from a ground viewpoint.

When a main rotor assembly stops rotating after flight, the position of each rotor blade in the horizontal plane will be randomly different. Also, because the main rotor mast is tilted 5° forward from the vertical axis of the helicopter, each rotor blade will adopt a randomly different angle away from the eye of the engineer standing on the left side engine decking. When standing on the ground, the blades can be rotated to improve the view of the underside of each blade but this is not practical when standing on the engine decking. These conditions would make the visual examination and detection of a short, chordwise, crack on a rotor blade's upper surface in the area of the erosion cover's scarf joint, which is approximately 6.61 feet (2.01 metres) from the blade root, extremely difficult, particularly for those blades that came to rest on the starboard side of the machine.

2.7.3 Crack detection through blade droop or discontinuity

The S-76 main rotor blades are flexible and droop when stationary. The experiment report at Annex R shows that in static laboratory conditions a test blade with an undamaged spar drooped 542 mm at the tip. There was no inspection procedure in the Maintenance Manual (nor is there now) that refers to blade droop. The objective of the experiment was to determine whether there would have been appreciable extra droop or a visible discontinuity in the cracked blade's shape when viewed from one end.

The results showed that there was no additional droop when the spar crack was 41 mm long; the crack was about this length when the blade was inspected after flying twice on 10 July. When the blade was inspected during the last Check A on 11 July after the crack had grown significantly, the additional droop was probably about 30 to 40 mm. This much extra droop over the 6,089 mm length of the blade was indiscernible in the laboratory when viewed from either end with the blade stationary. On the airport apron in the open air, the additional droop would have been impossible to see because the blades tend to float up and down in any breeze and the surface wind on 16 July was 6 kt.

2.7.4 The visibility of an external skin crack

The protective patch applied to the area of the scarf joint was not a manufacturer's requirement nor did it conform to any of the transparent tapes specified in the Composite Materials Manual for a repair patch. Nevertheless the fitting of such patches over scarf joints was common practice to prevent the ingress of moisture into the joint.

The patch extended about 35 mm rearwards from the trailing edge of the upper surface of the erosion cover and 42 mm rearwards from the lower trailing edge of the erosion cover. An illustration of the approximate extent of the patch relative to the titanium leading edge erosion cover and its interfaces with the upper and lower fibreglass skins is shown below at Figure 9.

The spar fatigue origin was 6.7 mm forward of the rear edge of the erosion cover so, on the upper surface of the blade, the patch extended at least 41 mm rearwards from the spar crack origin. The graph on page 6 of Annex P shows that at the time of the Daily Inspection, 6.25 flight hours prior to the final failure, the spar crack had progressed approximately 30 mm rearwards from its origin. The crack relationship test showed than any associated skin crack was unlikely to be longer than the spar crack. Consequently, if a skin crack existed at that time, it was invisible.

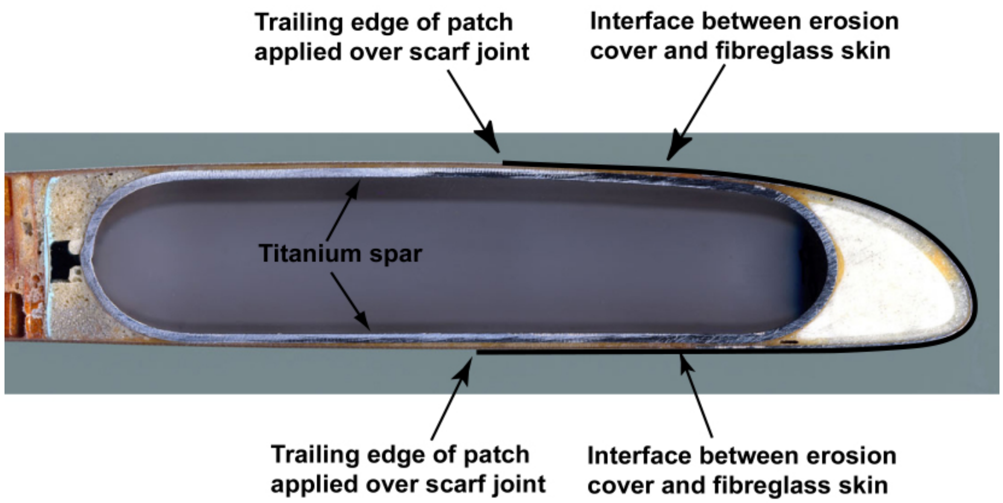

Figure 9 – Approximate extent of polyurethane patch over scarf joint

The graph suggests that the rearward extent of any skin crack did not progress aft of the patch until about 4.3 flight hours before the accident, which encompasses the last three pre-flight checks. Given the inspection difficulties and the few opportunities to see an external crack aft of the patch, if it existed it is not surprising that its existence went unnoticed.

2.7.5 Crack detection by NDT

Since the thermal damage to the blade spar was unlikely to be discovered immediately before or during blade refurbishment, and the operator's opportunities to detect a crack during routine visual inspections were extremely limited, the catastrophic accident could only have been averted if the crack had been detected by NDT before it progressed to failure.

At the time of the accident there had been no known cracking within the body of an S-76 titanium spar and none predicted by the manufacturer. Consequently, there was no requirement for crack detection by NDT. However, in the context of this accident, it is relevant to consider whether there was a realistic opportunity to detect the crack if NDT techniques had been employed during a routine inspection.

The last opportunity when an NDT inspection could have been performed as a routine operation was at the final 50-hour maintenance inspection, which was carried out 37 flight hours prior to the final failure. The graphs at Annex P suggest that the spar crack did not exist when this inspection took place, but if it did, it would have been less than 5 mm long.

The three potential NDT techniques were: eddy current, ultrasonic and radiographic. All three techniques would be very time consuming, they would require removal of the blade from the helicopter, and they would be very much dependent on the expertise of the equipment operator.

It is not easy to determine the size of crack that could be detected without conducting trials using various techniques on a blade with known crack lengths introduced. Both the eddy current and ultrasonic techniques could have detected a 5 mm crack but to enable the techniques to be effective, both would have required removal of the titanium leading edge erosion cover and the wire mesh layer embedded into the surface skins. These operations would be impractical using an operator's expertise and facilities. Every blade would have to be returned to a Repair Station or to the manufacturer for this process. Moreover, to be certain that such inspections were effective, an inspection would have to be carried out at intervals not greater than 20 hours which would be totally impractical and commercially prohibitive.

Since the crack was 'internal', an X-ray technique would be required to detect it in its early stages of propagation without removing the leading edge erosion cover and the embedded wire mesh. In theory, this technique could detect cracks of a few millimetres in length but a general X-ray inspection probably would not reveal a 5 mm crack. The chances of success would be improved if the inspection were focussed on a specific area of the spar using high-resolution equipment. However, the crack may not have grown as far as the through-crack stage at that time and there was no reason to suspect a crack in the scarf joint area. Therefore, X-ray examination was unlikely to have averted the accident.

2.8 Protective patches

Had an opaque patch not covered the scarf joint, the detection of a small crack in the erosion cover at the scarf joint would not necessarily have prompted further investigative action apart from a tap test to check for disbonding on either side of the crack. Assuming that any spanwise disbonding extended less than 4 inches from the crack, and that seems likely, shortly after its discovery the crack would probably have been covered by a patch to prevent water ingress. Consequently, had the scarf joint not been covered by an opaque protective patch before it was returned to service, it is possible that it would have acquired an opaque patch before the accident. Therefore, the fitting of an opaque patch over the scarf joint after the blade was repaired may have had little if any effect on the eventual outcome.

2.8.1 The significance of a crack in an erosion cover

Although the appearance of a crack in an erosion cover is very likely to be benign, it might be the one visible symptom of an underlying crack in the spar or composite structure, especially if the crack spreads into the adjacent composite skin. This feature could have been identified as a symptom of a serious defect prompting blade removal. In this accident, the presence of the patch prevented prompt discovery of the sympathetic crack in the erosion cover. Therefore, in the light of this accident, the addition of patches to the leading edges of main rotor blades should be more rigorously controlled.

Moreover, the crack inspection and monitoring process ought to be more rigorous than a periodic tap test for disbonding on either side of the crack. Once a new crack in the erosion cover is identified, given the knowledge acquired during this investigation, it would seem sensible to monitor the crack's growth frequently, for example before or after every flight, and for a period to be sure that the external crack is only a crack in the erosion cover and not a symptom of a far more serious defect in the spar. It would seem sensible that any spread of a crack into the upper or lower composite skins should prompt immediate withdrawal from service of the affected blade for further investigation.

2.8.2 Patch material

The manufacturer's CMM (Composite Materials Manual) specified the use of transparent patch material in its descriptive list of consumable materials. However, within Repair Procedure No 6, the materials were specified by part number and only one of three part numbers quoted, tape 8663, was identified as transparent.

The USA Repair Station used tape 8663 because it considered it to be more durable due to its greater thickness (0.018 inches versus 0.014 inches for tapes 8761 and 8681). Although both the CMM references to tape 8663 specified the material as transparent, it was available in black and black was used.

Opaque patches were sometimes used because the other approved materials were considered to be less durable. Once a patch is fitted, the recurrent inspection period of an erosion cover crack prompting removal of the patch is never less than 50 hours. If a growing crack is to be visually detected in time to avert an accident, this event demonstrates that a 50 hour interval is too long.

Had there been a requirement to monitor crack growth, an opaque patch would have prevented any further monitoring of the crack size until the patch was removed whereas a transparent patch would have permitted closer monitoring of the crack size during daily and pre-flight inspections. It is accepted that patches placed over the erosion strip are themselves likely to suffer erosion which may render them progressively less transparent. However, a transparent patch, replaced when and if necessary, would better facilitate crack growth assessment during pre-flight inspections until the crack has been confirmed as just a crack in the erosion cover. Thereafter, the crack could safely be covered with a durable polyurethane patch and monitored every 50 or 300 hours as required in the Maintenance Manual. Therefore, it was recommended that:

> The Sikorsky Aircraft Corporation should, within Repair Procedure No 6, clearly specify a durable transparent patch material for covering cracks in the leading edge erosion covers of S-76 main rotor blades. (Safety Recommendation 2004-037).
>
> The Sikorsky Aircraft Corporation should ensure that new cracks in the leading edge erosion covers of S-76 main rotor blades are frequently monitored for growth by an appropriately qualified person and for a suitable period to ensure that the crack is not symptomatic of a deeper flaw within the blade. (Safety Recommendation 2004-038).

2.9 Pre-flight inspections

It is unlikely that an engineer or a pilot would notice a small defect on the upper surface of the blade, protruding from the rear of a patch several feet distant, particularly since there was no requirement specified in the inspection procedures to look specifically for cracks. The only requirement was to inspect for skin disbonding.

Whilst a responsible engineer would investigate or at least draw his superior's attention to a crack in the skin of a main or tail rotor blade, there was no specific written requirement for that to be done. Although such a defect could rightly be considered an aspect of 'general condition', there was no definition of this term. In the context of the blades' external surfaces, the procedure required the checker to look for 'raised skin indicative of a disbond' and there was no mention of cracking.

Maintenance checks of the main rotor blades are required every 50 flight hours but this accident has shown that a sympathetic crack in the blade surface may not appear until a few hours before catastrophic spar failure (in the order of 5 to 10 flight hours). It would not be practicable to increase the frequency of the maintenance inspection to an interval approaching 10 hours, nor is it considered necessary based on this blade failure which was caused by a combination of two controllable factors: the malformed tang and the lightning strike. Nevertheless, an awareness of surface cracks and their significance should be a requirement for both a pilot's pre-flight check and an engineer's 50-hour inspection.

Whilst it is not appropriate that pilots should become responsible for rotor blade integrity, pilots are required to carry out a pre-flight inspection of the main rotor blades on both the upper and lower surfaces (see Annex B page 1). Despite the difficulties for pilots of inspecting all the blades' surfaces (as described in paragraph 2.7.2) they are, nevertheless, potentially able to notice crack growth from the leading edge erosion strip into the composite skin. Such a surface crack may be indicative of spar cracking and it should prompt immediate investigation by an engineer before undertaking the flight. Therefore, the written instructions for the 'Pilot's Pre-flight Check' (see Appendix B page1) and the engineer's '50-Hour Inspection Checklist' (see Appendix B pages 2 and 3) could usefully remind pilots and engineers respectively to inspect for cracks in the blade skin, particularly around the edges of any patches placed on the erosion strip to cover cracks in the strip. Consequently it was recommended that:

> The Sikorsky Aircraft Corporation should amend the S-76 Pre-flight Check and 50-Hour Inspection procedures to include a search for cracks in the upper and lower skins of main rotor blades. The procedures should prompt investigation of the underlying reason(s) for such cracks before the next flight. (Safety Recommendation 2004-039).

2.10 Crack detection by onboard technology

Since the crack was unlikely to be detected visually or by NDT, the sole remaining possibility was to detect it using on-board technology. The helicopter was fitted with flight data recording systems and it might have been possible to predict the development of a crack by regular data processing and analysis. However, the only approved onboard system for detecting cracks is the Blade Inspection Method (BIM). Each of these possibilities is considered.

2.10.1 Flight data recording

2.10.1.1 Conventional flight data

The conventional flight data parameters recorded by the IHUMS were numerous but there were none that related to the main rotor apart from rotation speed and a discrete parameter (on or off) for the rotor brake; both these parameters were in the normal range. The time history of conventional flight parameters at Annex I showed a normal flight until the blade fractured whereupon the recorder stopped. Consequently, these data would be of no use in predicting a blade failure.

2.10.1.2 Rotor Track and Balance Data limitations

The function of the onboard Rotor Track and Balance (RTB) installation is to capture data for analysis by an IHUMS ground station. Consequently, the RTB data gathered by G-BJVX could not be processed in flight.

As Annex K shows, analysis of rotor track and balance data is a complicated and specialist task. Data from the operator's S-76 aircraft was processed at Norwich and the RTB results were also sent to Aberdeen for assessment by the operator's specialist. To avoid acting upon spurious samples, it was normal practice for engineers to wait for consistent RTB data and consult the specialist before making any adjustments. Sometimes data from previous flights was not processed until the next day. Consequently, to be effective, the data would have to show significant signs of abnormal blade behaviour several flying hours before blade failure. The requirement to provide several hours warning is further complicated by the fact that the rotor track sensor only works in daylight. This is seldom a problem in summer but in winter, when daylight represents about one third of the day, this is a significant limitation because flight operations have to take place in darkness. A third limiting factor is false data. Bright sunlight and reflections can corrupt blade track data although corrupted data can sometimes be identified by visual inspection of the conditions.

2.10.1.3 Rotor tracking vibration

All helicopters vibrate in flight and the RTB system is used to tune the main rotor to minimise vibration from this source. Once the blades have been mass balanced, any increase in vibration would probably be caused by a tendency for one or more blades to rotate with a different tip-plane path to the majority of the blades. When this happens the aerodynamic disturbance caused by the 'out of plane' blade or blades creates vibration. Figure 3 on page 11 of Annex K shows that on the day of the accident, the red and black blades were rotating in much the same tip path. However, the blue blade was flying high and the yellow blade was flying low; these blades were adjacent and so immune to cross-coupling. The blue blade was intact but the yellow blade was close to failing so the tendency to fly high or low, in itself, is not a good indication of blade damage.

2.10.1.4 General vibration data

The RTB data from previous recordings was reviewed and compared with that recorded on other S-76 aircraft. This review concluded that, apart from the exceedence described below, all the monitored vibration parameters on G-BJXV were within established limits and its vibration levels were lower than the operator's S-76 fleet average.

2.10.1.5 Exceedence warnings

An exceedence[1] warning was generated by the IHUMS ground station on the day of the accident. The warning related to data downloaded earlier that day and processed during the afternoon. The exceedence automatically generated a diagnostic printout which is reproduced on page 18 of Annex K.

The warning related to rotor track and balance. It was triggered by high vertical vibration whilst the aircraft was on the ground at 1353 hrs. A vertical value of 0.481 at MPOG (Minimum [Blade] Pitch on Ground) exceeded the threshold of 0.400. As explained in the Annex, '*this would not have caused any alarm because occasional spurious outputs are a characteristic of the system*.'

The underlying reason for the vertical vibration would not have been apparent unless the accompanying warning:

> *'MAIN ROTOR: Tracker data suspect at CRUISE. Maximum velocity difference of 39.00 exceeds threshold of 38.00'*

had prompted the IHUMS ground station operator at Aberdeen to produce and study a detailed diagnostic printout for the cruise portion of the flight.

Due to the signal variability and noise in the IHUMS RTB data it was entirely reasonable under the circumstances to wait for more data to see if there was a repeat warning. However, even if the IHUMS technician had considered the warning as genuine and had produced the detailed printout immediately, at that time there was no reason for anyone to presume that a blade was approaching structural failure. Moreover, even if the technician had recognised its significance and decided to contact the maintenance base at Norwich to advise them of the blade's abnormal behaviour, he was unlikely to have completed this process before 1700 hrs. This was the scheduled time for departure for the final flight so it is unlikely that action would have been taken in time to stop the helicopter taking off.

[1] A single event, recordable on all HUM systems, in which an engine or other device suffers an excursion in operating regime that is beyond limits. In this case the limits were set by the aircraft operator.

2.10.1.6 Track, lag and velocity trends

Figure 7 of Annex K plots the track of the yellow blade during the final five accelerations in speed after takeoff from Norwich and each of the four offshore installations. The yellow blade flies significantly lower after each acceleration. This graph shows more vividly than any other, the rapidity at which the defect developed during the final sectors. Such was the rapid propagation of the fatigue crack during the final multi-sector flight, that analysis of the RTB data could not have provided more than about 30 minutes warning of anomalous blade behaviour.

It is important to remember that the practical value of the RTB system is to simplify and accelerate main rotor tuning when components are replaced. It was not designed to predict blade failure. Analysis of the data gathered was incapable of predicting blade failure within a practical timescale of several hours flying. Therefore, there seems to be little if any value in trying to develop the system as a method of warning of impending blade failure.

2.10.2 Crack detection using the BIM system

The BIM system involves pressurising the internal cavity of the spar with a gas and monitoring any decrease in the gas pressure. Any crack that propagated through the spar material from the inner to the outer surface would produce a path for the gas to leak causing a pressure drop which in turn would give a warning to the cockpit crew and/or the maintenance personnel. The rate of pressure drop would vary depending on the length and tightness of the crack and the gas path to atmosphere through the secondary structure surrounding the spar.

If a BIM system had been fitted to the main rotor blade, then a warning that a pressure loss had occurred within the spar would have been given to the cockpit crew and/or the maintenance personnel at least 7.3 flight hours, if not more, prior to the final failure. This could have been sufficient time to investigate the pressure loss, discover the crack and prevent the accident.

2.11 Noises and vibrations in flight

In view of the fact that the RTB system detected a vibration exceedance at the start of the penultimate flight, the reports of unusual noises described by passengers on those flights are not easily dismissed. However, by the nature of their employment, the flight crew were more familiar with the S-76 than any of the passengers and if they heard the same noises, they did not appear to be troubled by them. Most of the noises heard in a helicopter cabin with the engines and gearboxes mounted above, emanate from those components. Apart from the damage to the main rotor gearbox caused by overload failure of its attachment fittings, no pre-impact damage was found within the rotating assemblies inside the engines or gearboxes. Also, there were no indications of abnormal engine or gearbox characteristics within the IHUMS data, so the unusual noises heard during rotor start were probably unrelated to the subsequent blade failure. Equally, the grass lifted by the rotor downwash would have been inconsequential and the laboured hover was probably due to the relatively heavy take-off weight on a warm summer evening. Moreover, everyone interviewed who had travelled on the offshore sectors prior to the helicopter's final departure from the Clipper helideck described the aircraft's operation as completely normal.

The passenger sat immediately behind the pilots during the penultimate flight from the Barque PL to the Clipper described normal operations and pilot behaviour. This impression was supported by the audio recording from the CVFDR. In their dialogue both pilots were behaving responsibly and professionally but in a relaxed manner which suggested there was good rapport and co-operation between them and confidence in each other. The co-pilot was handling the controls for the final sector and the only indication of anything unusual was the shared perception of increased vibration seven minutes before the blade failed. They diagnosed the problem by looking at the main rotor tip path plane and noted a 'ragged' track. They then used the IHUMS cockpit interface to trigger an in-flight recording of the RTB which, when downloaded, would advise the engineer on the action required to restore the blade tracking to symmetry. The pilots then continued the flight without giving any audible perception of further concern in their dialogue, nor was there another mention of the vibration. It is likely that the commander intended to report the vibration due to a blade 'out of track' on their return to Norwich.

2.12 Flight crew's response to increased vibration

All helicopters vibrate in flight and the pilots' shared lack of concern was probably due to having flown other helicopters that vibrated with blades out of track. Blade track can change slowly with time and the fact that a blade is 'out of track' is not necessarily an indication of a serviceability problem. Moreover, as page 25 of Annex K shows, G-BJVX had been operated before *'with an overall track split in excess of 200mm – greater than that immediately preceding the blade failure.'* The reporter also concluded that *'G-BJVX had been operated with higher main rotor vibration'*. Consequently, neither pilot had any particular reason to conclude that the vibration was imminently dangerous.

If they had been concerned and wished to land as soon as practicable, since it takes time to prepare a helideck for an unscheduled landing, they could still have been airborne seven minutes later, waiting for the nearest helideck, probably on the Vulcan 2, to be cleared and ready to accept them. In reality, the Santa Fe Monarch, which they had every right to expect to be ready for them, was probably the earliest suitable place for a planned, precautionary landing.

There was no checklist, advice or previous experience that the pilots could have drawn upon to suspect that a blade might be out of track because of a cracked spar. However, even if they had suspicions and decided to land immediately on the water, it is quite possible that the change in airspeed and blade loading could have precipitated failure before they could accomplish such a landing. The blade failed when they were decelerating for the intended landing on the Monarch's helideck.

2.13 The final events

The flight deck audio recording ended suddenly and without warning about one tenth of one second after the second of two loud 'crack' sounds. These two sounds were separated in time by less than one tenth of one second. Three events could have caused these two sounds; the shock of the rotor blade breaking, the separated section of blade striking the rear fuselage and the gearbox separating from its mountings. It is neither practical nor worthwhile to determine which two of these three events were responsible. All that need be concluded is that, given the industry knowledge at the time, there was no recognisable warning of impending blade failure and nothing the pilots should have done to avert the accident.

2.14 Rotor tracking vibration

With the knowledge gained during this investigation, it is now possible to recognise an increase in vibration coupled with a blade 'out of track' observation as symptoms of impending blade failure. Moreover, although the tracking characteristics of the yellow colour-coded blade were deteriorating relatively quickly during the final flight when compared to the previous flight, the change was still more gradual than sudden. Helicopter vibration can be minimised but not entirely eliminated. It can also have multiple sources and numerous influential factors. Consequently, it is impractical to issue instructions to pilots regarding a threshold level of vibration that is unacceptable and which deserves immediate action; this has to be a subjective assessment. Therefore, no safety recommendation on pilot reaction to vibration is made within this report.

2.15 Modifications to the blade design

The investigation carefully considered whether corrective action, including modification to the S-76 main rotor blade design, should be recommended to prevent a recurrence of crack propagation to in-flight failure.

The spar within the S-76 blade is primary structure with no alternative load path. If the spar fails in flight the result is bound to be catastrophic. Moreover, the external surface of the spar is always submerged in secondary structure which is bonded to it and although hollow, the greater part of the spar's internal surface cannot be seen during periodic inspections because of its length. Consequently, maintainers have to judge the condition of the spar by the condition of the secondary structure which, as this investigation has demonstrated, is an imperfect method.

Although the BIM seems likely to be the best physical method of detecting a crack in time to avert an accident, the disadvantages of retro-fitting the system should be weighed against the probability of a recurrence.

2.15.1 Retrospective fitting of the BIM system

The S-76 main rotor blade was not designed to have a gas-tight spar. Modifications to the root and tip of the blade would be required to make the BIM system work. There would probably be spurious warnings due to gas leaks from imperfect seals and spurious warnings tend to be ignored after a while. Also, the spar itself would have to be drilled to install the BIM detector. Unfortunately, a drilled hole would introduce a stress concentration near the blade root that would enhance the probability of crack development. The end result could be a BIM system that was unreliable but which detected genuine cracks induced by retrospective fitting of a BIM system.

2.15.2 Future blade designs

The consequence of an undetected crack in a main rotor blade can be catastrophic, particularly as in this case when the crack propagates very rapidly in a region where there is no redundant load path. In essence, the design was not damage tolerant as currently specified in Certification Specification 29 applicable to large rotorcraft. However, the development emphasis within the helicopter industry is shifting away from metal sparred blades to composite blades. Such blades are not prone to fatigue cracking. Therefore, it seems unlikely that future helicopter rotor blade designs will have titanium spars but if they do, it would be wise for such blades to be equipped with an automatic onboard crack detection system from the outset. Therefore:

It was recommended to the European Aviation Safety Agency and to the US Federal Aviation Administration that their Airworthiness Requirements for helicopters should ensure that any future design of main rotor blade that incorporates a hollow metal spar should be designed from the outset to incorporate an automatic onboard crack detection system covering spar areas which cannot readily be inspected and are not damage tolerant. (Safety Recommendation 2004-040).

2.16 Probability of a recurrence

This accident was caused by a spar fatigue crack that was positively attributed to a combination of two phenomena: a lightning strike that exploited the area of reduced insulation created by a manufacturing anomaly. At the time the blade was repaired, the potential for this damage mechanism was not known by the blade manufacturer but it is now better understood.

It is difficult to calculate the statistical probability of another S-76 blade failing in flight through spar fatigue due to the small statistical sample (one) and combination of factors. Empirically, the probability would seem to be dependent on four factors: the quality of blade design and manufacture, the likelihood of another blade having a similar or comparable anomaly, the likelihood of a lightning strike and the potential for thermal damage from that strike.

Beginning with blade design and quality, S-76 main rotor blades have accumulated some 12.8 million blade flying hours. Taking the wider view, blades of comparable design and construction fitted to the manufacturer's other H-60 and H-53 helicopter models, including some struck by lightning and repaired, have amassed another 28 million flying hours.

Apart from the yellow blade on G-BJVX, within the 40.8 million flying hours accrued by blades constructed with titanium spars by the same manufacturer, none has failed in flight through spar fatigue. Only two blades have exhibited spar cracking in regions which do not have a redundant load path. The first was the crack in the UH-60 blade attributable to battle damage; the other was the subject of this investigation. Consequently, the quality of spar design and manufacture is satisfactory.

Of the 2,800 S-76 rotor blades manufactured, not more than 1,675 of these have two-piece erosion covers and every blade constructed since 1989 has a one-piece 'jointless' erosion cover. The inspection programme instigated after this accident was likely to be assiduously fulfilled by S-76 operators and did not disclose any more blades with folded tangs. Therefore, the probability of another in-service blade having a similar folded tang is also very low.

Lightning strikes affecting rotor blades are infrequent but more common than manufacturing anomalies. After this accident, 26 S-76 blades were removed from service. Of these, 17 had been struck by lighting and the other 9 had incomplete log card histories. Any indication of burns or pits in a blade requires its removal from service but it is conceivable that there are a small number of blades still in service which have been subjected to an electrical discharge which did not produce burns or pits. A lightning discharge so weak that it did not damage the blade's aluminium wire mesh is unlikely to have been sufficiently powerful to inflict thermal damage to the spar. Moreover, the probability of one of these blades also having a folded tang seems extremely low so the risk inherent in these blades remaining in service is negligible.

2.17 Safety actions taken

On balance, the interim safety recommendation made by the AAIB 10 days after the accident coupled with the two ASB safety actions instigated by the manufacturer have ensured that the circumstances of the failure which occurred in this accident have not been repeated. Moreover, the endorsement by the FAA of the decision to remove lightning damaged blades from service, effectively giving the manufacturer's ASB the force of regulation, should ensure that it will never be repeated on a civilian registered S-76 helicopter.

Although the chance of recurrence appears to be extremely low, it is conceivable that thermal damage inflicted by a lighting strike, perhaps associated with a different manufacturing anomaly such as an area of conductive wire mesh touching the spar, could cause similar damage to that seen on the failed blade. Therefore, it would be unwise to return to service any titanium sparred blades affected by lightning fitted to any type of helicopter unless the entire outer surface of the spar can be inspected for thermal damage. Given the method of blade construction and the potential for microstructural damage, this proposition seems impractical. In the case of the S-76, it is immaterial since an Airworthiness Directive was issued requiring all lightning struck blades to be permanently withdrawn from service.

The only alternative, practical and currently available method of monitoring a blade's structural integrity after a lightning strike would be the retrospective fitting of a BIM system. On balance, this proposition is not warranted provided that all S-76 main rotor blades struck by lightning remain permanently withdrawn from service.

Sikorsky is the only known volume producer of hollow titanium sparred main rotor blades for helicopters. The H-60 and H-53 variants are all in military service leaving the S-76 as the only model in civilian service. Consequently, there was no need to recommend the withdrawal of titanium sparred blades from other public transport helicopter models that had suffered a lightning strike.

2.18 Search and Rescue

Two minor issues arose during the course of the investigation concerning the search and rescue phase immediately after the accident. They were the failure of the ADELT to deploy and indicate the surface position of the crash, and the fact that the crews of the Putford Achilles and the Global Santa Fe Monarch had not anticipated the arrival of G-BJVX.

2.18.1 ADELT

The ADELT beacon, a variant of the more generic ELT (Emergency Locater Transmitter) did not perform its intended functions of automatically marking the crash position of the helicopter and transmitting on international distress frequencies. When found, it was on the sea bed still loosely within its carrier. The launcher squib had fired but the spring ejection mechanism was completely overpowered by the speed and force of the impact. Calculations indicated that the speed of water impact was in the order of 140 kt with the fuselage in a 37° dive.

The beacon itself and its ejector mechanism were probably serviceable before water impact but the equipment specification was probably exceeded by the unforeseen brutality of the water impact.

2.18.2 Unexpected arrival of G-BJVX

Nobody on the Santa Fe Monarch was expecting a helicopter movement because the person who requested the movement left the installation before the helicopter arrived and without informing the radio operator. Although the arrival of G-BJVX came as a surprise, as soon as the helicopter came on frequency the helideck was manned and then prepared for a landing. Had there not been an accident, the effect of this lack of awareness would have been little more than a minor nuisance since the helicopter might have had to 'hold off' for a minute or two. The breakdown in the booking procedure on board the Santa Fe Monarch was a minor mistake which was rapidly addressed soon after the accident by the client company.

In the circumstances, the principal effect of the breakdown in procedure was the status of the standby vessel. She was out of position by a mile or so and facing in the wrong direction for the landing. However, when notified of the accident, her crew lost no time in responding and immediately launched two fast rescue craft. They arrived on scene some seven minutes after the accident but it was not survivable. Had anyone survived and been able to operate their lifejacket, the fast rescue craft would have been able to recover them within minutes and transfer them to the Achilles long before the arrival of any other Search and Rescue assets. Consequently, the fact that the Putford Achilles was out of position for the landing had no effect on the survivability of this accident.

2.18.3 Flight-following

The hypothetical question arises that if nobody on board the Santa Fe Monarch had seen the accident, and it had occurred before contact was established with her radio operator, how much time might have elapsed before anyone appreciated that the helicopter was overdue.

On this flight the pilots were always in radio contact with either a land-based agency or an offshore installation, and sometimes in contact with both simultaneously. Had the helicopter crashed out of sight of the Santa Fe Monarch, one of these agencies might have taken follow-up action if the helicopter failed to notify them of a landing or a frequency change. On the other hand, at long range pilots might lose radio contact with an agency before they have attempted to change frequency and so they are forced to change without prior notification. Taking overdue action each time this happened would be inappropriate.

Flight following could be made more efficient if the departure installation positively contacts the destination installation once the aircraft takes off to ensure that the aircraft is expected and at what time. The destination installation could then relay the same notification to the standby vessel and obtain an acknowledgement. If subsequently the aircraft fails to arrive soon after its ETA, appropriate action could be initiated without undue delay.

These communication procedures are not governed directly by the regulatory body for aviation. However, the UK Offshore Operators Association (UKOOA) is the representative organisation for the UK offshore oil and gas industry. Therefore, it was recommended that:

> The UK Offshore Operators Association should amend its guidelines to include a responsibility on offshore installation operators to ensure that, for all flights between manned offshore installations, radio operators of

such installations establish positive contact with the destination installation immediately after the departure of a helicopter and convey the relevant flight details such as persons on board and estimated time of arrival. (Safety Recommendation 2004-041).

3 Conclusions

(a) Findings

1. The pilots were properly licensed and trained, medically fit and adequately rested to undertake the flight.

2. The aircraft was properly loaded and maintained, and its documentation was in order.

3. Approximately two thirds of the yellow colour-coded main rotor blade separated as the helicopter was preparing to land.

4. A chordwise fatigue crack in the blade's titanium spar grew through approximately 50% of the spar's circumference prior to a single catastrophic overload failure of the remaining 50%.

5. Almost immediately after the blade failed the centrifugal force imbalance created by the missing blade section tore the main rotor gearbox from the fuselage.

6. Impact of the helicopter's fuselage with the sea surface was not survivable.

7. Search and Rescue assets at sea and ashore were deployed without delay.

8. The origin of the fatigue crack in the yellow colour-coded blade was beneath the malformed tang of the outboard section of the two-piece titanium erosion cover at the scarf joint.

9. The scarf joint tang of the outboard section of erosion cover had been unintentionally distorted during blade manufacture in 1981.

10. The scarf joint malformation was not noticed but it had no effect on the structural integrity of the blade until it was exploited by a lightning strike.

11. An electrical discharge passed between the tang, which was either in contact with the spar or very nearly so, and the spar itself, momentarily creating sufficient heat to change the material properties of the titanium spar (microstructural damage) in a small region less than 2 mm wide.

12. There were no prescribed limits for the size or extent of lightning damage and the decision on whether the blade was repairable was based on engineering judgement exercised by the helicopter manufacturer.

13 The judgement was made that being encased in secondary structure, a spar was unlikely to be damaged in areas where the external secondary structure was undamaged.

14 There was no visible damage in the area of the scarf joint and the blade was assessed as repairable and subsequently repaired by its manufacturer.

15 There was no practical method by which the microstructural damage to the yellow colour-coded blade could have been detected during the damage assessment.

16 The repaired blade was later fitted to G-BJVX as the yellow colour-coded blade. It had been flown for 1,403.25 hours since refurbishment.

17 The fatigue inducing effect of the microstructural damage was either dormant or in slow growth for at least 1,300 flight hours.

18 There was no practical method by which the operator's maintenance staff could have detected the microstructural damage during routine inspections.

19 The fatigue crack probably began during the final 100 flight hours and may have progressed from an embryonic through-crack to 50% of the spar's circumference in as little as 24.4 flight hours.

20 A sympathetic crack formed in the recovered section of the erosion cover not less than 7.3 flight hours before the accident.

21 When the sympathetic crack first appeared, it would have been hidden underneath a black, opaque protective patch that had been fitted to prevent water ingress into the scarf joint.

22 The manufacturer's Composite Materials Manual specified the use of a clear patch material but opaque patches were commonly used.

23 A crack in the blade's upper surface skin aft of the protective patch may have existed 4.3 flight hours before the accident but, if it existed, its location rendered it unlikely to be detectable during a normal pre-flight inspection.

24 There was no existing line maintenance inspection that could realistically have detected the spar crack or revealed symptoms of the eventual blade failure.

25 Routine non-destructive testing of main rotor blades was unlikely to have averted this accident.

26 The helicopter's onboard IHUMS system occasionally recorded spurious data due to signal variability and noise and so the exceedance warning generated by the IHUMS ground station on the day of the accident did not result in an immediate investigation of its cause.

27 Analysis of the Rotor Track and Balance data recorded by the onboard IHUMS system could not have provided a warning in time to avert the accident.

28 The impending blade failure would not have been identified by an onboard HUMS system because detecting such failure modes is beyond current system requirements and capabilities.

29 The only symptom of impending blade failure was an increase in vibration during the cruise which was mentioned by the pilots about seven minutes before the accident.

30 Both pilots attributed the increase in vibration to a main rotor blade being 'out of track'.

31 There was no checklist, advice or previous experience that the pilots could have drawn upon to suspect that a blade might be out of track because of a cracked spar.

32 Apart from the yellow colour-coded blade on G-BJVX, within the 40.8 million flight hours accrued by similar and comparable blades constructed with titanium spars by the same manufacturer, none has failed in flight through spar fatigue. Only one blade has exhibited cracking in the main body of the titanium spar in an area where there was no redundant load path. That cracking was attributable to battle damage.

33 The only practical and currently available method of monitoring the structural integrity of an embedded tubular blade spar is by monitoring the pressure of gas trapped within the spar. The helicopter manufacturer's proprietary method of achieving this is the BIM system.

34 The retrospective fitting of the BIM system to all S-76 main rotor blades is not warranted provided that all such blades struck by lightning remain permanently withdrawn from service.

35 The ADELT beacon and its ejector mechanism were probably serviceable before water impact but the equipment's specification was probably exceeded at water impact.

(b) Causal factors

The following causal factors were identified:

1 A manufacturing anomaly created an area of reduced insulation between a main rotor blade's spar and one section of its two-piece leading edge erosion cover.

2 The affected blade had been struck by lightning.

3 Electrical energy from the lightning strike exploited the manufacturing anomaly and caused microstructural damage that was not detectable when the blade was returned to its manufacturer for assessment.

4 The blade was repaired before being returned to service and a fatigue crack in the spar originated from the microstructural damage.

5 An opaque protective patch applied to the erosion cover's scarf joint hid exterior symptoms of the developing spar crack that appeared before the accident.

6 The helicopter's proprietary onboard Health and Usage Monitoring System (IHUMS) did not provide sufficient warning of impending blade failure in time to avert the accident.

7 There were no in-flight symptoms of impending blade failure that the pilots should have recognised.

4 Safety Recommendations

The following safety recommendations have been made:

4.1 **Safety Recommendation 2002-025**: On 26 July 2002 it was recommended that The Federal Aviation Administration mandates appropriate action to ensure the continued airworthiness of Sikorsky S-76 main rotor blades which have either:

> A two-piece leading edge titanium sheath (erosion strip).
> or
> Have suffered a lightning strike.

The FAA acted the same day by issuing an Emergency Airworthiness Directive

4.2 **Safety Recommendation 2004-037**: The Sikorsky Aircraft Corporation should, within Repair Procedure No 6, clearly specify a durable transparent patch material for covering cracks in the leading edge erosion covers of S-76 main rotor blades.

4.3 **Safety Recommendation 2004-038**: The Sikorsky Aircraft Corporation should ensure that new cracks in the leading edge erosion covers of S-76 main rotor blades are frequently monitored for growth by an appropriately qualified person and for a suitable period to ensure that the crack is not symptomatic of a deeper flaw within the blade.

4.4 **Safety Recommendation 2004-039**: The Sikorsky Aircraft Corporation should amend the S-76 Pre-flight Check and 50-Hour Inspection procedures to include a search for cracks in the upper and lower skins of main rotor blades. The procedures should prompt investigation of the underlying reason(s) for such cracks before the next flight.

4.5 **Safety Recommendation 2004-040**: It was recommended to the European Aviation Safety Agency and to the US Federal Aviation Administration that their Airworthiness Requirements for helicopters should ensure that any future design of main rotor blade that incorporates a hollow metal spar should be designed from the outset to incorporate an automatic onboard crack detection system covering spar areas which cannot readily be inspected and are not damage tolerant.

4.6 **Safety Recommendation 2004-041**: The UK Offshore Operators Association should amend its guidelines to include a responsibility on offshore installation operators to ensure that, for all flights between manned offshore installations, radio operators of such installations establish positive contact with the destination installation immediately after the departure of a helicopter and convey the relevant flight details such as persons on board and estimated time of arrival.

J J Barnett
Principal Inspector of Air Accidents
Air Accidents Investigation Branch
Department for Transport
January 2005

ROUTE FLOWN BY G-BJVX DURING ACCIDENT FLIGHT

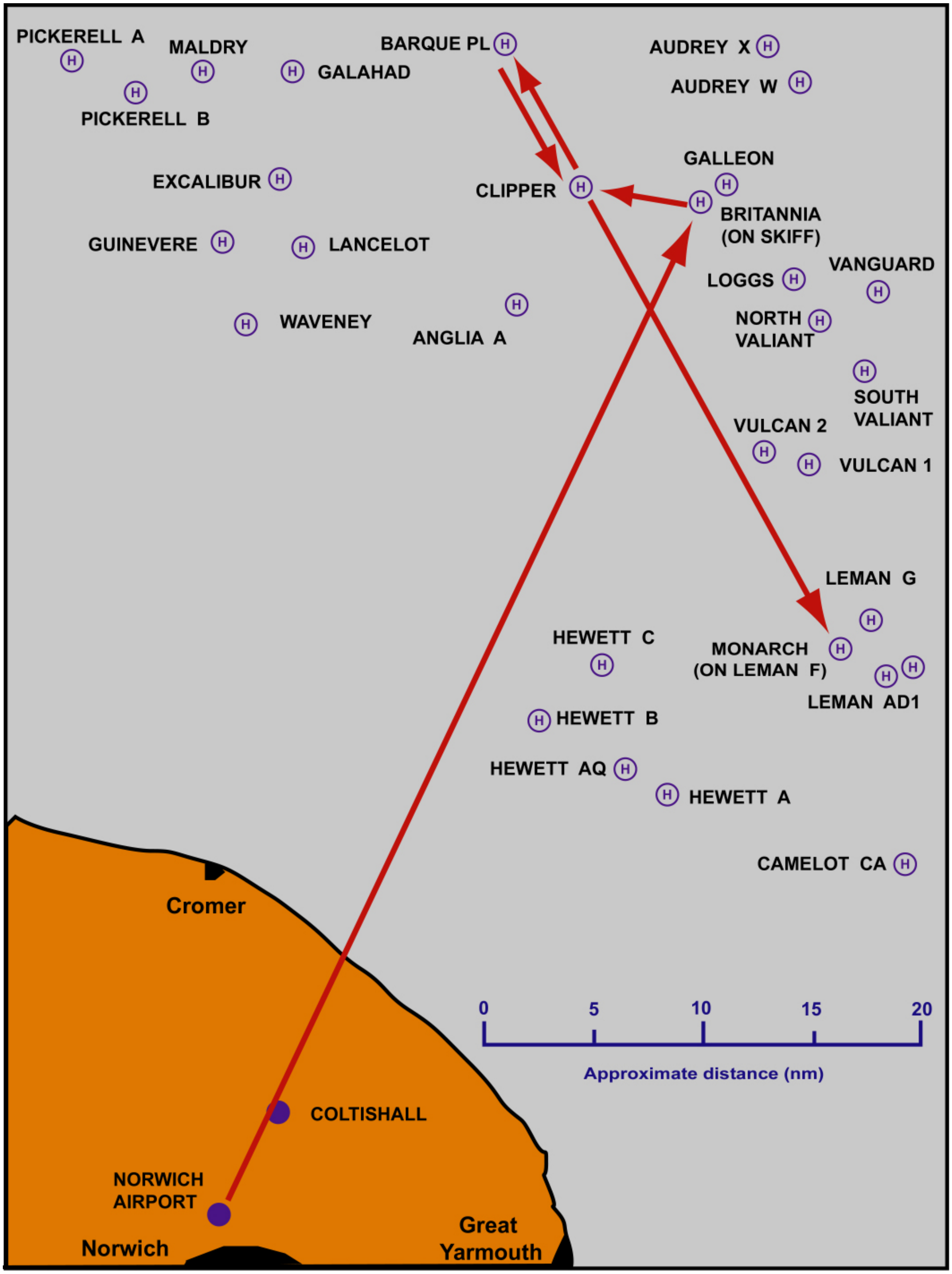

SIKORSKY 76®
SA 4047-76C-2-1

PILOT'S PREFLIGHT CHECK

EXTERIOR CHECK	ITEM	ZONE
CHECK	FOR	
Main Rotor Blades	General condition, tip cap for condition and security; blade upper and lower surfaces for raised skin indicative of disbond. Rotate the rotor system as required to view all blade surfaces and tip caps	5
#Hydraulic Module - First and Second Stages	Proper fluid level, filter button, no leakage	5
#Main Rotor Servos (If helicopter has been non-operational for more than 2 hours in freezing temperatures)	Attempt to manually move input links to forward, lateral, and aft main rotor servos. Input links should move freely with no restrictions approximately 1/4 inch	5

WARNING: Specifically check the security of the aft engine cowl latches and straps just prior to each flight.

All Engine and Transmission Doors and Cowls	Condition, security including hinges, latches, camlocs, and straps	4,5
Main Rotor	Free to turn; walk rotor through 90° to next 45° position, as necessary	5

SIKORSKY 76®
SA 4047-76C-2-1

50-HOUR INSPECTION CHECKLIST	CHAPTER/ SECTION/ SUBJECT	ZONE	INIT	REMARKS
8. Rotating and stationary scissors for bearing wear, security, and general condition. Stationary scissors bracket attachment flange radius and lower link for nicks, cracks, and corrosion. NOTE: Whenever scissors are removed/ disassembled, inspect bolts/studs for corrosion, fretting, scoring, gouging, and other damage.	65-14-01 65-14-02	5		Pay special attention to scissors bearings. If evidence of wear is found, do measurement check per Inspection/Check, 65-14-01 and 65-14-02, as applicable.
9. Check rotational (tangential) play between rotating and stationary swashplate. (a) If less than 0.040 inch, check at next 50 hour interval. (b) If greater than 0.040 inch, but less than 0.070 inch, check rotating scissors bearing wear per Inspection/Check, 65-14-01. Repeat at 50 hour or 25 hour intervals, as required per specified criteria.	65-14-00	5		Refer to Inspection/ Check, 65-14-00.
10. Main rotor dampers for condition and security. Check damper bearings for too much play and wear. Nylon washers (bumpers) for too much wear and secure bond to lugs. Replace if necessary. Tubes and hoses for security, leaks, and general condition.	65-12-09	5		For inspection procedures, refer to Damper Bearings Inspection Procedures, 65-12-09. For Airworthiness Limitations, refer to Chapter 4.
11. Main rotor pitch control rods for condition and security. Rod end bearings for too much play and wear. Check bearing outer race Teflon liners for wear-through, extrusion, or delamination. Replace bearing if any of these conditions exist. Nylon washers (bumpers) for too much wear and secure bond to lugs. Replace if necessary. Pitch control rod attachment lugs on rotating swashplate and spindle horns for scoring caused by disbonding of nylon washers.	65-12-06	5		Do a bearing wear measurement check (0.015-inch maximum) per Pitch Control Rod Bearings Inspection, 65-12-06.
12. Main rotor blade assembly, comprising:	(Page)	5		Refer to Table 2-1, Composite Materials Manual, SA 4047-76-5 for inspection requirements. For Airworthiness Limitations, refer to Chapter 4.

Note: Only pages related to main rotor blade inspection are shown

SIKORSKY 76®
SA 4047-76C-2-1

50-HOUR INSPECTION CHECKLIST	CHAPTER/ SECTION/ SUBJECT	ZONE	INIT	REMARKS
Fiberglass skin/honeycomb core Airfoil contour region (a. through d.) Trailing edge region (a. through d.) Nickel and titanium leading edge abrasion strips (a. through e.) Root cap (a.) Root end laminates (a., b., c.) Trim tab (a.) Tip Cap (a., b., c.)	1-2-2 1-2-2 1-2-2 1-2-3 1-2-4 1-2-4 1-2-5 1-2-5			
13. Tip cap screws for evidence of looseness. Check torque index line through screwheads. Retorque if required.	65-11-00	5		For Airworthiness Limitations, refer to Chapter 4.
14. Tip cap/tip rib for security by visual inspection for cracks while applying upward and downward load on outer end of tip cap by hand. Apply hand pressure to tip cap in area of tip rib and visually check for cracks.	65-11-00	5		
15. Check lubrication/servicing schedule for any requirements that are due.	12-00-00 12-10-00 12-20-00			Refer to Lubrication and Servicing Schedule.
16. Check condition of all access panels, door hinges, and fasteners. Make sure all access panels, doors, cowls, and fairings are closed and secured.				

Note: Only pages related to main rotor blade inspection are shown

SIKORSKY 76®
SA 4047-76C-2-1

11. 340-Hour Inspection Checklist.

340-HOUR INSPECTION CHECKLIST	CHAPTER/ SECTION/ SUBJECT	ZONE	INIT	REMARKS
NOTE: Main rotor blade inspection items 1 and 2 are superseded by the 900-hour inspections for certain main rotor blades modified by CSN 76-167 or later revision (Kit 76070-15003). Refer to 900-Hour Inspection Checklist.				
1. Inspect 76150-09000-045, -047, and -048 main rotor blades. NOTE: Modified blades marked with RS-003 number and also having 79790H-4-5 tip plate retention bolts installed may be inspected every 500 hours per 500-HOUR INSPECTION, item 2.	65-11-00	5		For Airworthiness Limitations, refer to Chapter 4. For inspection procedures, refer to Inspection/Check, paragraph 8.A, 65-11-00.
2. Inspect 76150-09000-046, -049, -050, and 76150-09100-041 through -050 main rotor blades, with tip plate retention bolts (NAS624 series) installed.	65-11-00	5		For Airworthiness Limitations, refer to Chapter 4. For inspection procedures, refer to Inspection/Check, paragraph 8.A, 65-11-00.

Note: Only pages related to main rotor blade inspection are shown

SIKORSKY S-76®
SA 4047-76C-2-1

13. 500-Hour Inspection Checklist.

500-HOUR INSPECTION CHECKLIST	CHAPTER/ SECTION/ SUBJECT	ZONE	INIT	REMARKS
1. Keith air conditioning system compressor motor brushes and evaporator blower motor brushes for wear.	21-50-04 21-53-02	2		Inspect every 500 Hours (compressor motor/ evaporator blower motor operation). Adjust interval per operational experience. In addition, it is recommended that bearings be replaced at this time. Refer to manufacturer's maintenance and overhaul manuals.
NOTE: Main rotor blade inspection items 2 and 3 are superseded by the 900-hour inspections for certain main rotor blades modified by CSN 76-167 or later revision (Kit 76070-15003). Refer to 900-Hour Inspection Checklist.				
2. Inspect 76150-09000-046, -049, -050, and 76150-09100-041 through -050 main rotor blades, with tip plate retention bolts (79790H-4-5) installed and 76150-09000-045, -047, and -048 blades modified by Sikorsky Aircraft and marked with RS-003 number and with tip plate retention bolts (79790H-4-5) installed.	65-11-00	5		For Airworthiness Limitations, refer to Chapter 4. For inspection procedures, refer to Inspection/Check, paragraph 8.A, 65-11-00.
CAUTION: POSITIVE VERIFICATION THAT BOLTS (79790H-4-5) ARE INSTALLED IS REQUIRED. OTHER WISE THESE INSPECTIONS MUST BE DONE EVERY 340 HOURS. RECORD BOLT PART NUMBER IN COMPONENT LOG.				
3. Inspect 76150-09100-051 and -052 blades.	65-11-00	5		For Airworthiness Limitations, refer to Chapter 4. For inspection procedures, refer to Inspection/Check, paragraph 8.A, 65-11-00.
4. Main rotor blade spar for cracks per paragraph 2-7 or 2-7A.	65-11-00	5		Refer to Composite Materials Manual, SA 4047-76-5, for inspection requirements. For Airworthiness Limitations, refer to Chapter 4.

Note: Only pages related to main rotor blade inspection are shown

SIKORSKY 76®
SA 4047-76C-2-1

900-HOUR INSPECTION CHECKLIST	CHAPTER/ SECTION/ SUBJECT	ZONE	INIT	REMARKS
5. Inspect these main rotor blade configurations: 76150-09100-053 and subsequent 76150-09100-051/-052 modified by CSN 76-167 or later revision (Kit 76070-15003) 76150-09000-046/-049/-050 and 76150-09100-041 thru -050 marked RS-004E-II or RS-004F-II or RS-008C-II and modified by CSN 76-167 or later revision (Kit 76070-15003) 76150-09000-045/-047/-048 marked RS-003 and RS-004E-II or RS-004F-II or RS-008C-II and modified by CSN 76-167 or later revision (Kit 76070-15003)	65-11-00	5		This inspection supersedes the 340 Hour Inspection items 1 and 2 and the 500 Hour Inspection items 2 and 3. For Airworthiness Limitations, refer to Chapter 4. For inspection procedures, refer to Inspection/Check, paragraph 8.B, 65-11-00.
6. Remove main rotor blades and inspect main rotor blades comprising (refer to Table 2-1):	(Page)	5		Refer to Composite Materials Manual, SA 4047-76-5, for inspection requirements.
Fiberglass skin/honeycomb core	1-2-2			
Airfoil contour region and trailing edge region (a.)	1-2-3			
Nickel and titanium leading edge abrasion strips (f. and g.)	1-2-4, 1-2-5			
Root end laminate (d.,f., and g.)	1-2-5			
Trim tab (b.)	1-2-5			

Note: Only pages related to main rotor blade inspection are shown

SIKORSKY S-76®
SA 4047-76C-2-1

23. 3000-Hour Inspection Checklist.

3000-HOUR INSPECTION CHECKLIST	CHAPTER/ SECTION/ SUBJECT	ZONE	INIT	REMARKS
1. Remove engine supports (including aft support strut, 0401277930/Post ST20A): Inspect inside and outside surfaces of support tubes for cracks, corrosion, and service-related damage. NOTE: Inspect aft support strut, 0401277170 (pre ST20A) at 1500 hours/2 years interval. (a) Conduct a dye penetrant or magnaflux inspection using 10X glass of support tubes and fittings including weld areas. Refer to Dye Penetrants or Magnetic Particle Inspection, 20-05-00. (b) Inspect airframe mounted fitting lugs for cracks and corrosion using 10X glass. (c) Inspect lower three attachment leg holes of tripod support for cracks, excessive wear, or out-of-round condition. Maximum service wear limit should not be over 0.3130 inch diameter. (d) Inspect front support spherical joints for wear.	71-20-00	4		Inspect every 3000 hours or 4 years since last inspection, whichever occurs first. Coat interior of all engine support tubes per Inspection/ Check, 71-20-00.
2. Main rotor blade root end laminate-to-spar bond per paragraph 2-8.	65-11-00	5		Starting at 11,750 hours, inspect every 3000 hours or 3 years, whichever occurs first. Refer to Composite Materials Manual, SA 4047-76-5, for inspection requirements. For Airworthiness Limitations, refer to Chapter 4.

Note: Only pages related to main rotor blade inspection are shown

SIKORSKY 76®
SA 4047-76C-2-1

CALENDAR INSPECTION CHECKLIST	FRE-QUENCY: HOURS/ CAL-ENDAR	CHAPTER/ SECTION/ SUBJECT	ZONE	INIT	REMARKS
40. Proof pressure test of landing gear emergency blowdown bottle.	3 Years	32-31-01	1		3 Years from date of initial pressurization. Refer to manufacturer's recommendations.
41. Separate rotating and stationary swashplates and inspect all surfaces for signs of nicks, gouges, corrosion, or wear. Clean duplex bearings by wiping with a clean cloth only, and turn by hand to determine if ratcheting or roughness exists.	3 Years	65-14-00	5		Refer to Inspection/ Check, 65-14-00. When reinstalling swashplate, make sure stationary swashplate is properly shimmed per Removal/ Installation, 65-14-00. Also, refer to 5-50-00, Chapter 65, item 9 and item 13 Conditional Maintenance Checks.
42. Remove and inspect specified main rotor head components and bolts for corrosion, fretting, scoring, gouging, and other damage.	3 Years	65-12-00	5		For specific requirements and allowable repairs, refer to Inspection/ Check, 65-12-00. Also, refer to 5-50-00, Chapter 65, item 9, item 10, and item 12, and Chapter 67, item 2, Conditional Maintenance Checks.
43. Starting at 11,750 hours, inspect main rotor blade root end laminate-to-spar bond per 3000-HOUR INSPECTION, Item 2.	3 Years	65-11-00	5		This inspection is not required if the 3000-Hour main rotor blade root end inspection has been accomplished within the 3 year period.
44. Inspect main rotor spindle threads and nut for corrosion per 1250-HOUR INSPECTION, Item 1.	3 Years	65-12-02	5		This inspection is not required if the 1250-Hour main rotor spindle inspection has been accomplished within the 3 year period.

Note: Only pages related to main rotor blade inspection are shown

EXTRACT FROM COMPOSITE MATERIALS MANUAL

SIKORSKY 76

COMPOSITE MATERIALS MANUAL, SA 4047-76-5

TABLE 1-2. LIST OF CONSUMABLE MATERIALS (Cont)

ITEM NO.	NOMENCLATURE	SPECIFICATION
23.	Tongue Depressor	LLL-S-007-20
	ABRASIVES, PAPER, PLASTICS, AND MISCELLANEOUS	
24.	Tape, Masking	UU-T-106
24A.	Tape, Polyester, P/N 8901, 3M Company, 0.001 inch thick. P/N 8902, 3M Company, 0.002 inch thick.	
25.	Cloth, Crocus	P-C-458
26.	Abrasive Paper, 120-, 150-, 180-, 220-, 240-, 320-, 360-, 400-, and 420-Grit, Wet or Dry Type, Commercial Grade	P-P-121 and P-P-101
27.	Cloth, Cheesecloth Type 2, Class B	CCC-C-440
28.	• Tape, Clear (Transparent) Abrasion Resistant Polyurethane - Adhesive - Coated, 0.014 Thick	SS9538
	• Tape, Matte Abrasion Resistant Polyurethane - Adhesive - Coated, 0.014 Thick	SS9538
	Vendor P/N: 8671-2.00 (TRB) Clear (Transparent) P/N: 8671-6.00 (MRB) Clear (Transparent) (SS9538-002A) P/N: 8681-2.00 (TRB) Matte (Transparent) P/N: 8681-6.00 (MRB) Matte (Transparent) (SS9538-003)	
	• Tape, Transparent Abrasion Resistant Polyurethane - Adhesive - Coated, 0.018 Thick (3M P/N 8663)	
	Vendor: 3M International Specialties Div. 15 Henderson Drive West Caldwell, NJ 07006	
	NOTE A list of commercial products conforming to the specifications listed may be obtained by contacting Commercial Product Support, Sikorsky Aircraft.	
29.	Abrasive Pad, Scotch-Brite or equivalent	
30.	Cleaner, Ahco-187B or equivalent	

TABLE 3-1. MAIN ROTOR BLADE ACCEPT/REJECT CRITERIA AND REPAIR ACTION (CONT)

MAIN ROTOR BLADE COMPONENT	TYPE AND SIZE	REPAIR ACTION	REPAIR LOCATION ON A/C	REPAIR LOCATION OFF A/C
Nickel and Titanium Leading Edge Strips (cont) (See Figures 3-3, 3-4, and 3-4A)	- Chordwise cracks with multiple branches up to 1 in. wide. No limit on number of cracks and branches.	Repair per procedure No. 6.		X
	- Partial to complete chordwise cracks with up to 8 square in. of edge bond separation	Repair by adhesive injection per procedure No. 2. Doubler patch per procedure No. 6 is optional.		X
	- Partial to complete chordwise cracks with more than 8 square in. of edge bond separation	Not acceptable. Replace blade. Send damaged blade to Sikorsky Aircraft.		X
	- Partial to complete chordwise cracks with up to 8 square in. internal bond separation.	Acceptable per Note 8.	X	
	- Partial to complete chordwise cracks with more than 8 square in. internal bond separation.	Not acceptable. Replace blade. Send damaged blade to Sikorsky Aircraft.		X
	- Up to 3 in. spanwise maximum 1/2 in. from leading edge	No repair required.	X	
	- Greater than 3 in. spanwise or more than 1/2 in. from leading edge	Not acceptable. Replace blade. Send damaged blade to Sikorsky Aircraft.		X

TABLE 3-1. MAIN ROTOR BLADE ACCEPT/REJECT CRITERIA AND REPAIR ACTION (CONT)

MAIN ROTOR BLADE COMPONENT	TYPE AND SIZE	REPAIR ACTION	REPAIR LOCATION ON A/C	REPAIR LOCATION OFF A/C
Nickel and Titanium Leading Edge Strips (cont) (See Figures 3-3, 3-4, and 3-4A)	- Slight fractures, cracks, and/or disbonds inboard end at radial station 180	Repair by blending to smooth edge and locally filling with adhesive per procedure No. 1.		X
	Broken/Missing (Nickel Strip)			
	- Up to 8 in. portion of abrasion strip missing.	Repair per procedure No. 6.		X
	- Greater than 8 in. missing.	Not acceptable. Replace blade. Send damaged blade to Sikorsky Aircraft.		X
	Cracks (Titanium Strip)	NOTE: Strip splice repair joints performed per ORI 76150-008, Section III, shall be considered to be cracks for the purposes of these criteria.		
	- Partial or complete chordwise crack with edge disbond less than 2 inches on either side of crack.	Repair per procedure No. 6.	X	
	- Partial or complete chordwise crack with edge disbond greater than 2 inches on either side of crack.	Not acceptable. Replace blade.		X

SIKORSKY 76®

COMPOSITE MATERIALS MANUAL, SA 4047-76-5

TABLE 3-1. MAIN ROTOR BLADE ACCEPT/REJECT CRITERIA AND REPAIR ACTION (CONT)

MAIN ROTOR BLADE COMPONENT	TYPE AND SIZE	REPAIR ACTION	REPAIR LOCATION ON A/C	OFF A/C
Nickel and Titanium Leading Edge Strips (cont) (See Figures 3-3, 3-4, and 3-4A)	- Partial or complete chordwise crack with skin disbond less than 4 inches on either side of crack.	Repair per procedure No. 6.	X	
	- Partial or complete chordwise crack with skin disbond greater than 4 inches on either side of crack.	Not acceptable. Replace blade.		X
	- Up to 4 in. spanwise maximum of 1.5 in. from leading edge.	Repair per procedure No. 6.	X	
	- More than 4 in. spanwise or more than 1.5 in. from leading edge	Not acceptable. Replace blade. Send damaged blade to Sikorsky Aircraft.		X
	- Chordwise cracks with multiple branches up to 2 in. wide	Repair per procedure No. 6.		X

4-9. REPAIR PROCEDURE NO. 6.

a. Main Rotor Blade Leading Edge Polyurethane Tape Repair.

(1) This procedure is to be used for repairing damage to titanium and nickel leading edge strips from punctures, and for complete cracks to titanium leading edge strips.

(a) Mask off damaged area for at least 1-3/4 inch on either side (spanwise) and at least 1-1/4 inch aft of titanium trailing edge.

(b) Deleted

(c) Clean area with MEK; wipe dampened area with dry cheesecloth before dampness evaporates.

(d) Spray or brush on adhesion promoter (primer) No. 86 on blade bond area. Allow primer to set for approximately five minutes.

(e) Cut tape, 8671-6.00 or 8681-6.00, to size required, peel off backing and apply to main rotor blade leading edge.

NOTE

3M transparent tape, P/N 8663, may be used as an alternate.

NOTE

The polyurethane repair patch is to be cut and positioned 1/4 inch inside the masking tape on all sides.

(f) Working from one edge only, tack edge of polyurethane sheet to primed surface along its total length, making sure that remainder of sheet does not touch any primer.

(g) Lightly smooth tacked area of polyurethane sheet into position by hand rubbing, using a clean, low-lint cloth.

(h) Continue to lightly smooth tape in a similar manner, across width of sheet, avoiding entrapment of air, until fully positioned.

(i) Firmly apply adhered polyurethane sheet by hand rubbing it down.

NOTE

An alternate method of application is available (steps (j) through (l)) which will eliminate the possibility of trapped air bubbles, but it requires a 24 hour drying time. This method may be used in conjunction with, or as a substitute for, use of the #86 adhesion promoter.

Engineering Instruction E76-762-10-1331

Recommended Post Lightning Strike Inspection For Main & Tail Rotor Blades

REF. EPM 9.7

SIKORSKY AIRCRAFT ENGINEERING INSTRUCTION

CONTRACT	CHARGE NO.	CMRA	EI NUMBER E76-762-10-1331

CP	MODEL	EFFECTIVITY	PRIORITY	DATE 1/22/91
	S-76A/B	IMMEDIATELY AT O&R	URGENT II	PAGE 1 OF 2

TO:

SUBJECT:

Recommended Post Lightning Strike Inspection
For Main & Tail Rotor Blades

The following inspections are to be performed, and any evidence of arcing/burns be reported to Engineering for main rotor blades.

1. Visually inspect entire blade for any evidence of arcing/burn marks paying particular attention to: a) tip cap assy - nickel abrasion strip and steel doublers, b) leading edge assy - titanium sheath, nickel abrasion strip, c) trim tab, d) wire mesh, e) any exposed areas of titanium spar, i.e. at tip and root ends, f) root end bushings. g) root end shims, h) tip end hardware, i) surfaces of root plate

2. Coin tap entire blade checking for disbonds.

3. Disassemble root end and inspect spar inboard holes and all exposed spar surfaces for arcing damage.

4. Disassemble tip end hardware and inspect spar 'C' block attachment holes and all exposed spar surfaces for arcing damage.

5. Disposition of any lightning strike damage will be made by Engineering, and procedures will be provided for that which can be repaired.

6. Ultrasonically inspect root end laminates for disbonds.

	TYPED NAME	SIGNATURE	DATE
PREPARED BY			
AUTHORIZED BY			
APPROVED BY			
CONFIG. MGT.			
RECORDED BY			

Page 2
E76-762-10-1331
January 22, 1991

The following inspections are to be performed, and any evidence of arcing/burns be reported to Engineering for tail rotor blades.

1. Fluoroscope both pockets to ensure that aluminum core is not damaged.

2. Visually inspect pockets for any evidence of arcing/burn marks paying particular attention to: a) nickel abrasion strip, b) Horn, and attached hardware, c) wire mesh

3. Remove pockets from spar.

4. Inspect d) spar attachment bolts, e) internal horn hardware, f) pivot retainers, g) spar center plug for any evidence of lightning strike damage, h) ultrasonically inspect spar for delaminations.

5. Disposition of any lightning strike damage reported will be made by Engineering, and procedures will be provided for that which can be repaired.

HISTORY OF THE YELLOW COLOUR-CODED MAIN ROTOR BLADE

Aircraft Registration	Date Installed	Date Removed	Component Time	Reason for Installation/ Removal
G-BISZ	2 March 1981		New	
G-BISZ		22 Sept 1988	1,636.00	Operational requirement.
G-BJGX	23 Sept 1988		1,636.00	
G-BJGX		3 June 1989	2,196.55	Operational requirement.
G-BJFL	3 June 1989		2,196.55	
G-BJFL		23 Aug 1989	2,355.40	Operational requirement.
G-BISZ	3 Sept 1989		2,355.40	
G-BISZ		31 Jan 1993	4,553.30	Removed having suffered root end damage following a maintenance incident. Blade returned to manufacturer for repair.
	October 1993 – February 1996		4,553.30	In storage
G-BHBF	16 Feb 1996		4,553.30	
G-BHBF		15 Dec 1999	8,261.45	Removed following lighting strike damage. Blade returned to manufacturer for inspection and repair.
G-BHZS	30 Jan 2001		8,261.45	
G-BHZS		16 Feb 2001	8,262.10	Operational requirement (found to be incompatible with the other blades).
G-BJVX	13 June 2001		8,262.10	Fitted during ‘C’ Check after the yellow blade that was fitted to the G-BJVX required repair.
G-BJVX		16 July 2002	9,665.10	Accident

G-BJVX - Recent Flight Activity

Date	Landings	Total Landings	Engine starts	Total Engine starts	Flight Hours	Total Flight Time hrs:mins	Total Flight Time hours
16-Jul	4	4	1	1	0:55	0:55	0.92
16-Jul	7	11	1	2	1:59	2:54	2.90
16-Jul	2	13	1	3	1:02	3:56	3.93
16-Jul	2	15	1	4	0:52	4:48	4.80
16-Jul	2	17	1	5	1:26	6:14	6.23
11-Jul	4	21	1	6	1:00	7:14	7.23
10-Jul	2	23	1	7	1:26	8:40	8.67
09-Jul	6	29	2	9	4:02	12:42	12.70
07-Jul	8	37	1	10	0:47	13:29	13.48
07-Jul	10	47	1	11	0:24	13:53	13.88
07-Jul	1	48	1	12	1:31	15:24	15.40
06-Jul	2	50	2	14	0:46	16:10	16.17
05-Jul	7	57	1	15	1:15	17:25	17.42
05-Jul	2	59	1	16	0:40	18:05	18.08
05-Jul	2	61	1	17	0:40	18:45	18.75
05-Jul	2	63	2	19	0:57	19:42	19.70
05-Jul	11	74	1	20	1:49	21:31	21.52
04-Jul	4	78	1	21	1:34	23:05	23.08
04-Jul	2	80	1	22	0:46	23:51	23.85
03-Jul	6	86	1	23	1:06	24:57	24.95
03-Jul	2	88	1	24	0:55	25:52	25.87
03-Jul	10	98	1	25	1:19	27:11	27.18
03-Jul	6	104	1	26	1:19	28:30	28.50
02-Jul	12	116	3	29	4:23	32:53	32.88
27-Jun	10	126	2	31	1:53	34:46	34.77
26-Jun	2	128	1	32	0:28	35:14	35.23
24-Jun	6	134	1	33	1:49	37:03	37.05
14-Jun	10	144	4	37	3:20	40:23	40.38
13-Jun	22	166	4	41	6:09	46:32	46.53
12-Jun	15	181	6	47	5:22	51:54	51.90
11-Jun	16	197	3	50	3:56	55:50	55.83
10-Jun	12	209	2	52	2:48	58:38	58.63
06-Jun	15	224	4	56	4:49	63:27	63.45
05-Jun	4	228	2	58	2:16	65:43	65.72
04-Jun	13	241	2	60	2:08	67:51	67.85
03-Jun	14	255	1	61	0:53	68:44	68.73
03-Jun	2	257	1	62	0:39	69:23	69.38
03-Jun	3	260	1	63	0:59	70:22	70.36
31-May	21	281	2	65	3:01	73:23	73.38
30-May	8	289	1	66	1:54	75:17	72.28
29-May	1	290	1	67	0:36	75:53	75.88
24-May	12	302	2	69	2:58	78:51	78.85
23-May	27	329	4	73	6:03	84:54	84.90
22-May	23	352	6	79	7:49	92:43	92.72
21-May	13	365	4	83	3:27	96:10	96.17
20-May	11	376	4	87	4:23	100:33	100.55

DATA FRAME LAYOUT

Analogue parameters

IHUMS Ref.	Parameter	First Word	Words/Second
	Synchronisation	1	2
A1	Frame Count LSB	2	0.5
A1	Frame Count MSB	130	0.5
A2	Pressure Alt coarse	113	1
A2	pressure Alt fine	116	1
A4	Indicated Airspeed	19	1
A4	Heading	18	1
A6	Normal acceleration	5	8
A7	Pitch Attitude	22	4
A8	Roll Attitude	23	4
A9	Engine 1 Nf	24	2
A10	Engine 1 Torque	25	2
A12	Engine 2 Nf	40	2
A13	Engine 2 Torque	26	2
A15	Main Rotor Speed (NR)	8	2
A16	Collective Pitch	10	4
A17	Fore/Aft Cyclic	11	4
A18	Lateral Cyclic	12	4
A19	Tail Rotor Pitch	13	4
A21	Outside Air Temperature	115	0.5
A22	Main gearbox Oil Pressure	34	0.5
A23	Main Gearbox Oil Temp.	35	0.5
A28	Radio Altitude	50	2
A29	ILS Glideslope	52	1
A30	ILS Localiser	51	1
A50	Engine 1 Ng	16	4
A51	Engine 2 Ng	32	4
A52	Engine 1 T4	27	2
A53	Engine 2 T4	28	2
A128	Alt Rate	3	2

Discrete Parameters

1	Pilots R/T Key	14
2	Co-Pilots R/T Key	14
3	Rotor Brake	14
154	Red warning Eng 1 out	14
5	RH Hydraulic 2 Off	14
29	Master Warning	14
32	MGB Oil Press Low	14
34	Cargo Hold Fire	14

36	Battery overtemp	14
48	Fuel 1 Low Press	14
38	Engine 2 Oil Press. Low	14
43	DC Gen. 1 Hot	14
44	DC Gen 2 Hot	30
155	Red warning Eng 2 out	30
7	Lane 1 Pitch Engaged	30
161	Weight on Wheels	30
8	Lane 1 Roll Engaged	30
9	Lane 1 Yaw Engaged	30
50	MGB Oil Hot	30
37	Engine 1 Oil Press. Low	30
49	Fuel 2 Low Press.	30
10	Lane 2 Pitch Engaged	30
11	Lane 2 Roll Engaged	30
14	Mode Engaged IAS	30
31	Eng 2 Fire Warning	46
70	Gear selected up	46
71	Left Gear Down	46
72	Right Gear Down	46
73	Nose Gear Down	46
152	Engine 1 Bleed	46
153	Engine 2 Bleed	46
25	A/P Coupled	46
174	No 2 DC Gen Failed	46
15	Mode Engaged Alt	46
17	Mode Engaged Alt	46
30	Engine 1 Fire Warning	62
162	No 1 DC Gen Failed	62
167	FDR Failed	62
168	CVR Failed	62
12	Lane 2 Yaw Engaged	62
174	Arriel/Allison Engine	62
163	Floatation Gear	62
26	Airways Marker Beacon	62
27	Middle Marker Beacon	62
28	Outer Marker Beacon	62

Variation in Signal Levels During Final 0.75 Seconds of Cockpit Voice Recording

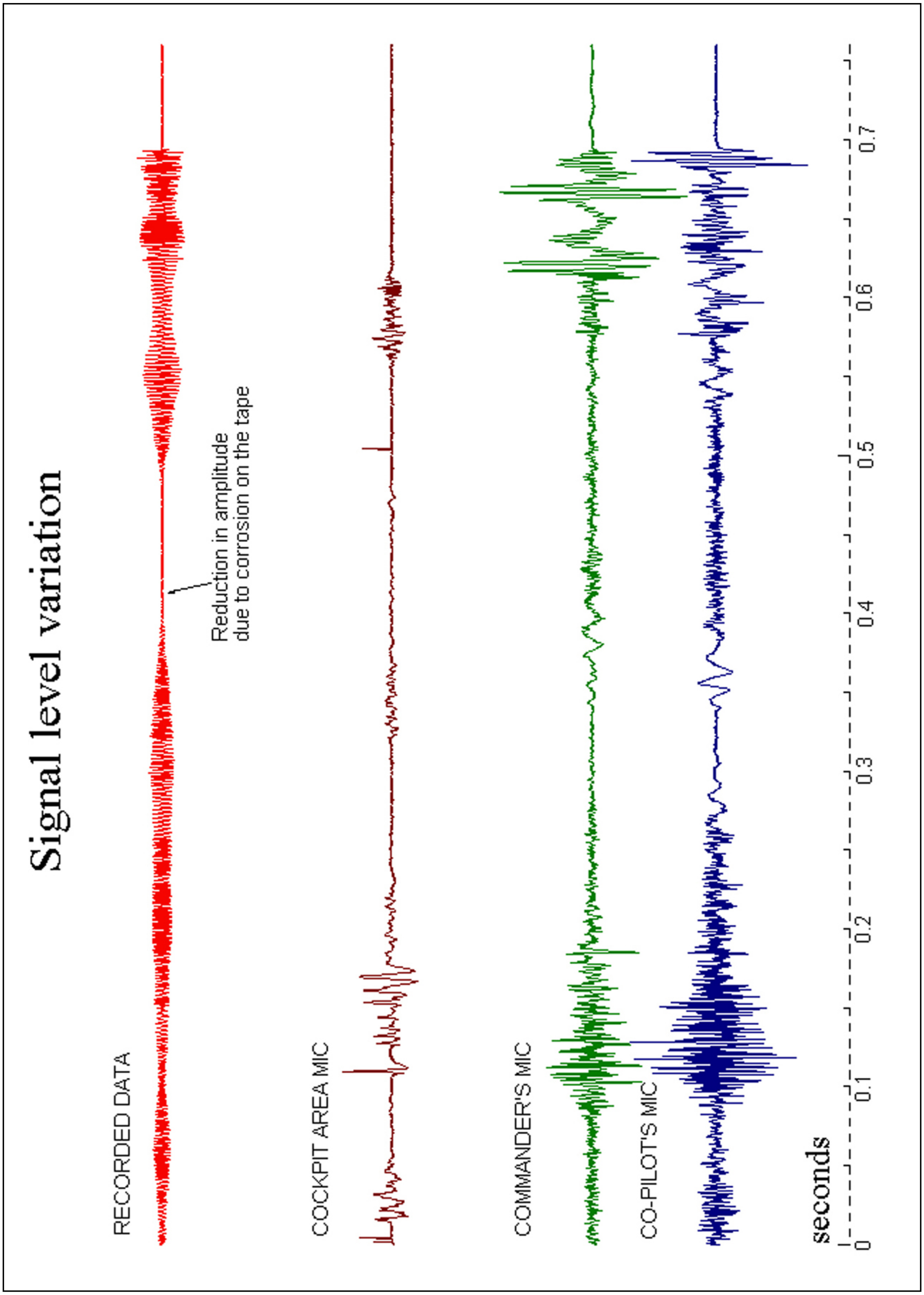

Time History of CVFDR Parameters

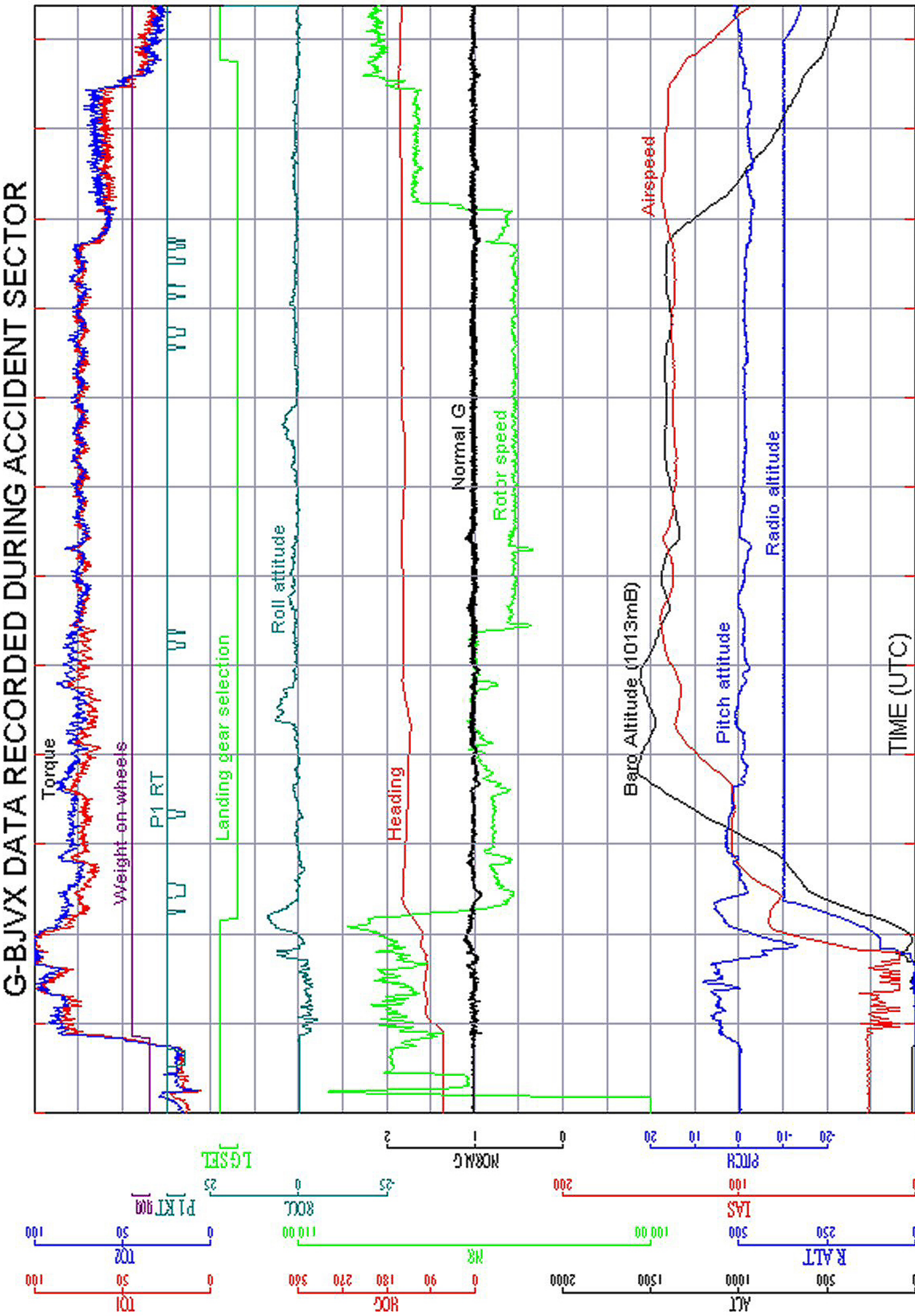

How a Rotor Tracker Works

In the early days of helicopter engineering, rotor tracking only took place on the ground, using a flag or brush to check the blade heights.

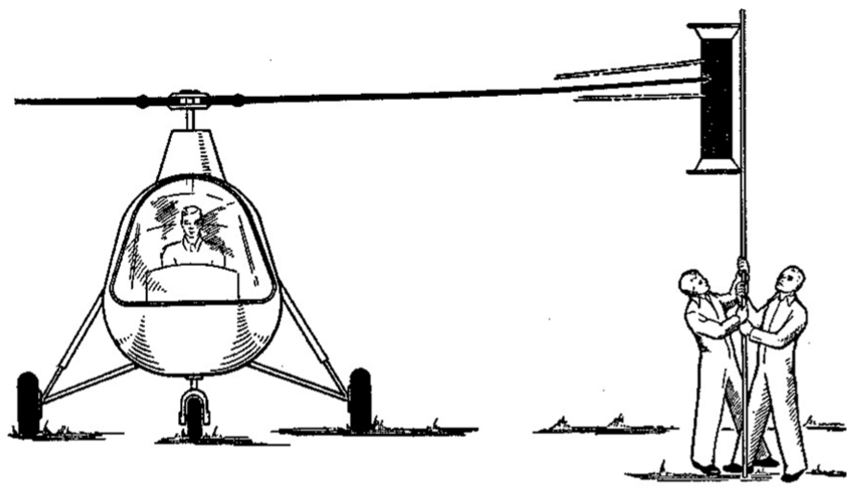

Each blade was marked with coloured chalk and when the blade tips struck the flag, they left corresponding marks. It is for this reason that rotor blades were originally identified by colour, and this has persisted in most operations.

Contemporary Rotor Blade Trackers

There are a number of different types of rotor blade tracker in existence, but all the trackers used by the IHUM system are of the two-beam type. In this design, originally developed by the Stewart-Hughes company in the UK, a lens is placed on the aircraft looking up into the rotor disk. Light passing from the bright sky through the disk is focussed onto two phototransistors, which pulse as the dark blades cross their line of sight.

Each phototransistor gathers light from a line that extends from the tracker up into the sky.

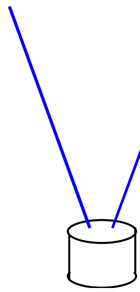

As the rotor blade passes through the two beams, pulses are produced as the (1) leading edge cuts the first beam, (2) leading edge cuts the second beam and (3) trailing edge cuts the second beam.

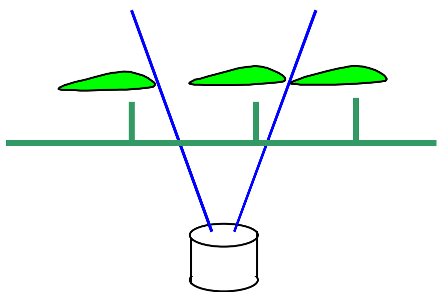

The angle between these “beams” means that the distance between the beams is proportional to the height of the rotor blade. If the blade flies higher, the time between the first two pulses will be greater.

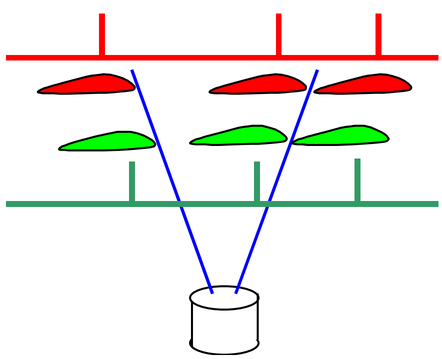

After that, geometry is used to convert pulse timings into blade positions.

The Geometry of an S76

The important geometrical aspects for working out the rotor track are the distance from the rotor hub to the tracker and the angle of tracker elevation.

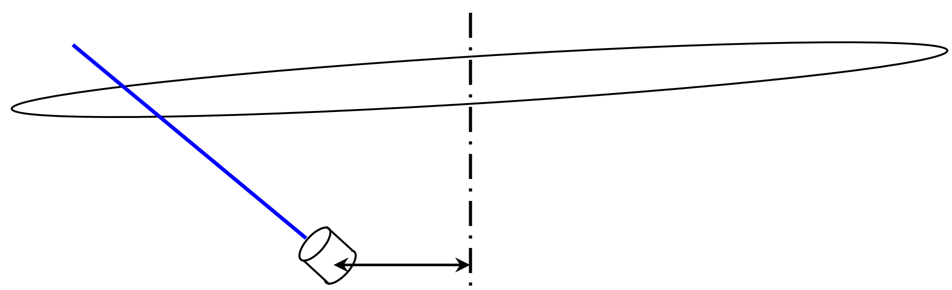

Once this angle and distance are known, the height of the rotor above the tracker can be deduced.

In the case of the S-76, the IHUMS ground station tables contain values of 4.57m and 40 deg respectively. While the angle is reasonable, the tracker position is in error. The operator was asked to double check these data and the resulting discrepancy is described in Appendix A to this Annex. Suffice to say the tracker is 3.42m forward of the rotor hub, pointing at an elevation of 40deg.

The tracker is mounted to the left of the centreline, and it 'looks' radially out from the rotor hub, so all calculations actually relate to a point fractionally before the blade passes over the nose of the aircraft.

Mathematics

There are two alternative ways of converting the track data into blade positions. In one case, the rotor blades are considered to rotate at a constant speed, whereas the more involved formula takes into account the variations in blade velocity. If we are dealing with a three-pulse tracker, it is possible to accommodate individual blade speed variations, but if the tracker only generates two pulses it is not possible to accommodate these variations.

2-Pulse Formulae

The angle ρ between the tracker 'beams' is set at 11.2 degrees by design and manufacture. The ratio between the slant distance from the tracker to the blade, l, and the distance the blade passes from one beam to the next, d, is computed by splitting the tracking triangle in half:

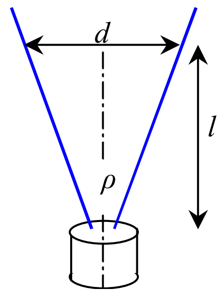

Equation 1

$$\tan\left(\rho/2\right) = \frac{d/2}{l}$$

which can be arranged in two ways:

$$d = 2.l.\tan\left(\rho/2\right)$$

$$l = \frac{d}{2.\tan\left(\rho/2\right)}$$

We also need to know the radius at which the tracker 'sees' the blade. This is not at the tip, firstly because the rotor coning angle changes will cause changes in the tracking distance and, more importantly, because the blade tip cap is not parallel.

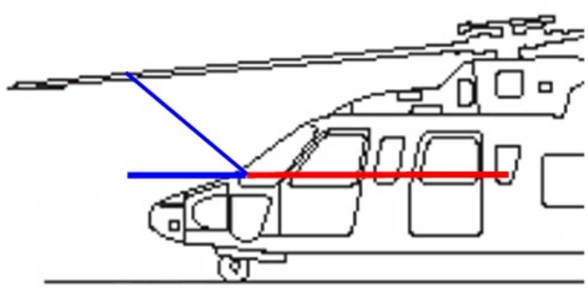

In the diagram above, a thin blue line has been drawn to represent the slant distance from the tracker to the blade, *l*, as used in the previous formula. The rotor tracking radius is then computed by adding the red 'Hub to Tracker' distance, *X,* to the thick blue forward component of *l*. With a tracker installation angle of Φ, we have:

Equation 2

$$r = X + l\cos\Phi$$

Similarly, the blade height above the tracker is determined by

Equation 3

$$H = l \sin \Phi$$

$$or$$

$$l = \frac{H}{\sin \Phi}$$

All this geometry is fine, but we need to relate this to the tracker timings. If the rotor rotational speed is Ω (radians per second) then the velocity of the blade at the radius where it cuts the tracker beams is $\Omega.r$. The distance it travels is the velocity times the time, so it covers the distance, *d*, in the time taken to pass between the beams, *T*(seconds):

Equation 4

$$d = \Omega T r$$

From equation 4, and substituting for d using equation 1 and r using equation 2, we have:

Equation 5

$$2.l.\tan\left(\rho/2\right) = \Omega T X + \Omega T.l.\cos(\Phi)$$

Rearranging to solve for *l*;

Equation 6

$$l = \frac{\Omega T X}{2.\tan\left(\rho/2\right) - \Omega T \cos(\Phi)}$$

Substituting for l from equation 3 and rearranging gives the result we need:

Equation 7

$$\frac{H}{\sin \Phi} = \frac{\Omega T X}{2.\tan\left(\rho/2\right) - \Omega T \cos(\Phi)}$$

$$or$$

$$H = \frac{\Omega T X \sin \Phi}{2.\tan\left(\rho/2\right) - \Omega T \cos(\Phi)}$$

3-Pulse Formulae

For three-pulse trackers, it is possible to carry out a similar derivation of blade position involving mean rotor speeds, however, a simpler and more elegant solution can be generated if the rotor chord at the tracking radius is reasonably constant. This relies upon the fact that the blade chord is known, with it's related time to pass the tracker. Using this fact, we can produce a formula for the distance, d, based solely upon the blade chord and the two time gaps.

If T_d is the time taken for the blade to pass across the tracker beams, and T_c is the time for the chord to pass a single beam, then:

Equation 8

$$\frac{d}{c} = \frac{T_d}{T_c}$$

or

$$d = \frac{c.T_d}{T_c}$$

Using equation 3 for *H*, and substituting for *l* from equation 1 and for *d* from equation 8 we get:

Equation 9

$$\begin{aligned} H &= l \sin \Phi \\ &= \frac{d.\sin \Phi}{2.\tan\left(\rho/2\right)} \\ &= \frac{T_d}{T_c}.\frac{c.\sin \Phi}{2.\tan\left(\rho/2\right)} \end{aligned}$$

This formula does not rely upon computation of the mean rotor speed however it is dependent upon three individual measurement points to generate a result (compared with two for the previous formula) and so will tend to be more slightly prone to spurious readings.

Comparison of Results

The two formulae give similar results, and there is no way of determining which is the more correct. Taking just the 145 knot cruise condition, here are the averaged data values obtained on the four downloads earlier on the day of the accident.

	BLK	BLU	RED	YEL
6910A	7.7	37.7	-8.9	-36.5
6910B	7.7	31.6	0.8	-40.2
6910C	3.2	27.4	6.9	-37.4
6910D	10.3	25	-3.2	-32.1

A section of data from the FDR taken from one of these downloads has been processed using both 2-pulse formulae (2P) and 3-pulse formulae (3P).

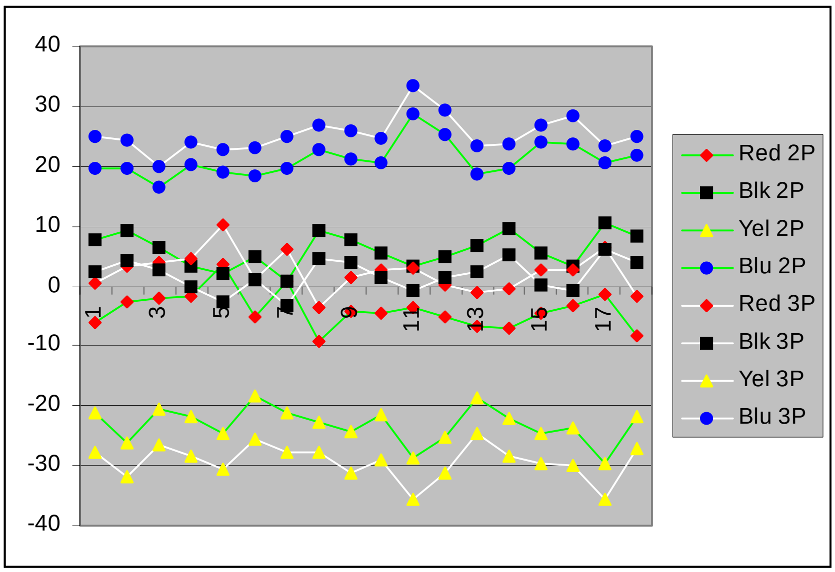

The results are similar, with slightly larger values obtained from the 3-pulse formula. However, the general agreement with the downloaded (averaged) data can be seen, and this also provides an indication of the level of variation in track that occurs due predominantly to turbulence in cruising flight.

The data analysed during this investigation has been checked, and the same pattern of a falling yellow blade and a rising blue blade confirms the blade sequence of Red / Black / Yellow / Blue as the blades pass the tracker.

In line service, the main thrust is to produce track measurements that are immune from stray results, and to this end all track measurements are averaged over many revolutions of the rotor. The individual blade velocity is computed, but used as a data validity check – not to compute the blade position. Data is then statistically treated to accommodate individual flight variations (the median over nine flights is usually taken) and adjustments are then based upon a number of flight conditions taken together.

Conversely, for accident investigation we are purposefully examining individual measurements from the rotor and so for our purposes the 3-pulse formula is the more suitable.

One other issue is relevant when looking at the tracker formulae. We know that the tracker operates at about 5 m from the rotor hub, but that the blades are 6.7 m long. Therefore the blade tip variation will be proportionately larger than that at the tracking position. This must be considered when considering what the pilot might see when looking at the rotor, because the aircrew can only see variations in tip position. For this reason, when analysing the final stages of the flight, the analyst used the 3-pulse formula with an amplification of 6.7/5 to relate the values to the rotor tips.

Appendix A – Tracker Position

The measured position of the track sensor and rotor hub are (in inches):

	Tracker	Rotor hub
Station	68	200
Waterline	85	175
Butt Line	26L	0

The tracker is therefore 132 inches forward of the rotor and 26 inches left of the centreline. (The formulae do not use the rotor hub height, as the blade top height is computed relative to the tracker).

Taking a plane perpendicular to the horizontal datum of the aircraft, passing through the tracker and rotor hub, the tracker is 134.5 inches forward of the rotor. This is 3.42m – well short of the 4.57m listed in the ground station datasheet.

To confirm this, a measurement from the aircraft drawings shows the co-pilot windscreen extending at most 3.5 metres forward of the rotor, and the tracker points up through the base of this transparency, whereas 4.57m extends well into the radome which is not where the tracker is installed.

For the purposes of this report, 3.42 m has been used for the hub to tracker distance.

EXTRACT FROM FLIGHT DATA SERVICES LTD REPORT

Contents

Figures

Abbreviations

1R	Vibration at the first harmonic of the main rotor frequency. About 5Hz for an S786
AC	Alternating Current
DAPU	Data Acquisition and Processing Unit
FDSL	Flight Data Services Limited
IHUMS	Integrated Health and Usage Monitoring System
IPS	Inches per Second; vibration amplitude
M/s	Meters per second
RTB	Rotor Track and Balance

Introduction

FDSL were commissioned by the Air Accidents Investigation Branch of the Department for Transport to assist in the investigation into the loss of the Sikorsky S-76 A+ aircraft, G-BJVX.

Specifically, FDSL were requested to examine the available FDR recordings and data from the Integrated Health and Usage Monitoring (IHUM) system to determine whether there was any evidence of the onset of the problem prior to the accident.

At the start of this work, evidence from the wreckage pointed strongly to a probable defect with the yellow main rotor blade.

Data Available

Two key sources of raw data were used in this study, namely historical records of RTB data from the IHUM system over the time that the suspect blade was in service, and track data written by the IHUMS Data Acquisition and Processing Unit (DAPU) to the FDR on the last five hours of flight before the accident.

An "overlapping" set of IHUMS data is available for three downloads that had been completed safely on the day of the accident, and these have been used to compare with the data from the FDR with the groundstation records.

Historical RTB Data

Bristow Helicopters, through their Aberdeen-based rotor track and balance specialist, provided a set of RTB data tables covering the periods when the aircraft was in service and data was being transferred to Aberdeen for monitoring. In total, data was available for 1347 downloads extending back to January 2000. This start date preceded installation of the Yellow main rotor blade, 00582, on 19th January 2000.

A breakdown of the number of downloads for each month is provided below:

	2000	2001	2002
January	12	5	74
February	70	8	37
March	56		75
April	53		90
May	76		71
June	50	30	24
July	35	88	24
August	65	74	
September	50	57	
October	29	63	
November	23	84	
December	17	7	

Table 1 Available RTB Data Downloads

Associated with the track and vibration for this period were the maintenance and adjustment records for the main rotor.

Data Manipulation

The data was provided in the form of a "Smart" spreadsheet. Ken uses the Smart software as this spreadsheet allows him to have larger tables (i.e. more columns) than can be manipulated with other tools. In each row of the table, vibration data for the main and tail rotors, for each of five harmonics, in amplitude and phase, together with rotor track and lag data is stored for each of the eleven flight regimes recognised by IHUMS. The first action was to prune this to a more manageable size by removing all the tail rotor data and the harmonics higher than 1R. This was done using an old copy of Smart (which runs under DOS) and writing a macro to strip out the unwanted records from each month's file of data.

Once the data was in smaller spreadsheets, these were written out as text files and read into Excel where the months were "stiched" together to form a single spreadsheet of data 188 columns wide by 1347 downloads deep.

A "sanity check" of the available dates and download numbers shows that in early 2001, when no data was available, the download numbers did not increase. As the downloads increment for each new flying day we can conclude that the aircraft did not fly over this period. The slight sawtooth effect at about 800 days into the sample is caused by the groundstation download number being revised to bring it into line with the paper technical log sheets. This is normal and causes no significant problems.

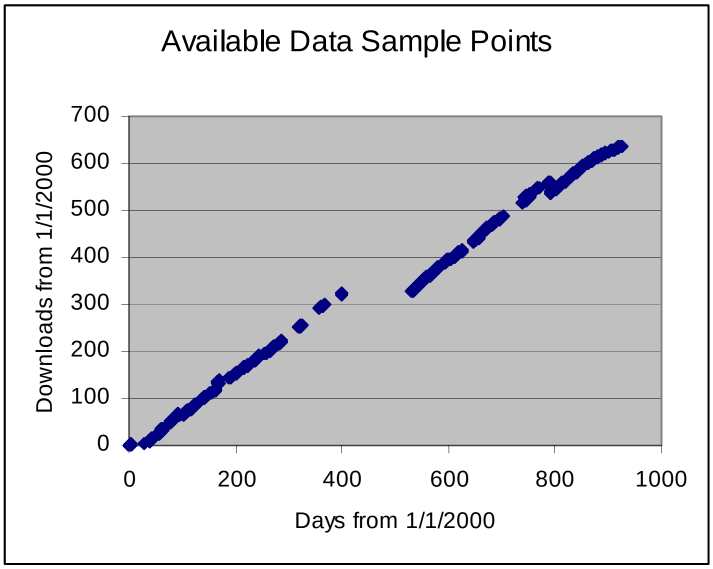

It is unfortunate that the airframe hours is not available in the data presented, however for the purposes of this study it is considered satisfactory to assume an approximately equal flying time per sortie (after all, the distance to the oil rigs is not varying) and if a detailed investigation of specific samples is indicated, the airframe hours for those samples can be extracted from the IHUMS groundstation database. In the analysis, therefore, data is plotted on a per-download timebase.

Data from the Flight Data Recorder

Data was supplied first as a part of a spreadsheet, and later a complete FDR download file became available and a more comprehensive examination was carried out.

Assessment of data supplied in spreadsheet format

The FDR on IHUMS installed aircraft records rotor track on an intermittent basis. Whenever the IHUMS DAPU is processing aircraft vibration, it's acquisition circuitry is dedicated to that task. However, there are large periods when the vibration and rotor track acquisition circuitry is not gathering data (i.e. the aircraft is not flying in the right part of the flight envelope for data capture or a complete set of data has already been acquired). In these "quiet" periods, the DAPU recognises the start of an FDR data frame and gathers one revolution of track data, which is then processed and stored in a subsequent frame. The interval depends upon the software cycle and hardware set-up time, but the combined effect of these is to store a fresh sample typically every eight seconds as illustrated in the following table.

Seconds between track samples	Frequency of Occurrence
2	2
4	1
6	9
8	214
10	36
12	12
14	20
16	9
18	1
22	4
26	1
32	1
34	4
36	2
38	1
40	1
48	1
50	1
54	1
66	1
94	1
117	1
406	1
846	1

For an S-76 with a rotor speed of just over 4 revolutions per second, this means that track data for about one revolution in thirty is being stored. As the tracker is passive, no valid data is acquired by night and there are certain difficult lighting conditions (twilight, pointing the tracking camera straight into the sun) where invalid data can be gathered.

On one hand, it is fair to say that an intermittent acquisition of data, that may be invalid and which is inevitably sparse, is less than ideal. However, given the constraints of an FDR data stream and the DAPU processing hardware this was the best practical solution available. As far as the author is aware, this is still unmatched anywhere else in the world.

Processing of this data started by writing a short procedure that read in the comma separated values supplied by AAIB and stripping out all the clearly invalid data and repeated values, caused by the DAPU software continuing to output the last measured values. From the 2440 frames supplied, 324 frames with valid RTB track data were identified. (It is from this work that the data for the preceding table was obtained).

Unfortunately, one of the larger gaps, 812 seconds long, occurs shortly before the end of the flight and there are only four, widely spaces samples after this. It follows that the track data needs to be plotted against a true timebase for these last samples to be taken in context.

Assessment of the Associated Flight Parameters

From a visual inspection of the flight data, it was clear that false data was present, and it took little time to identify this as relating to low rotor speed conditions when running on the ground (or on an oil rig). This is to be expected as the AC generators are frequency wild and will drop out at low Nr, causing the attitude synchros to adopt meaningless (usually –90 deg pitch, 180 deg roll) values. For this reason, frames where the rotor speed was below 90% were rejected.

Data from ground running was also found to be highly variable, and as the height of the rotor disk can be varied by the pilot (there are particular concerns about the low height of the front of an S76 rotor disk when passengers are approaching the aircraft) this data was also rejected.

Assessment of data supplied in FDR file format

The data from the flight data recorder was supplied by email, having been compressed using FDSL software. The compressed file of 1,456,604 bytes expanded to 4,696,032 bytes.

The file was scanned for valid frames (based only upon the presence of synch words) and 9073 valid subframes were identified. At 2 seconds per frame, this is fractionally over the nominal 5 hour recording duration for this type of recorder.

From the work on the partial data spreasheet, a similar process was undertaken, where only frames with fresh RTB data in excess of 90% Nr were examined. Of these, a few frames had a corruption where an individual value would have a value in excess of 4095, which was clearly in error and so these frames were also rejected. No effort was spent trying to identify the source of the corruption.

A pseudo-timebase was generated automatically from the hours and minutes parameters, with 8 seconds added between samples with the same hours and minutes fields. This provided a time scale that accurately represented the larger gaps in the data and avoided dual samples with the same time-stamp.

The resulting set of data samples is shown illustratively as a plot of altitude points against the pseudo-timebase. The individual flight sectors can be seen, and there are a good number of individual track measurements available.

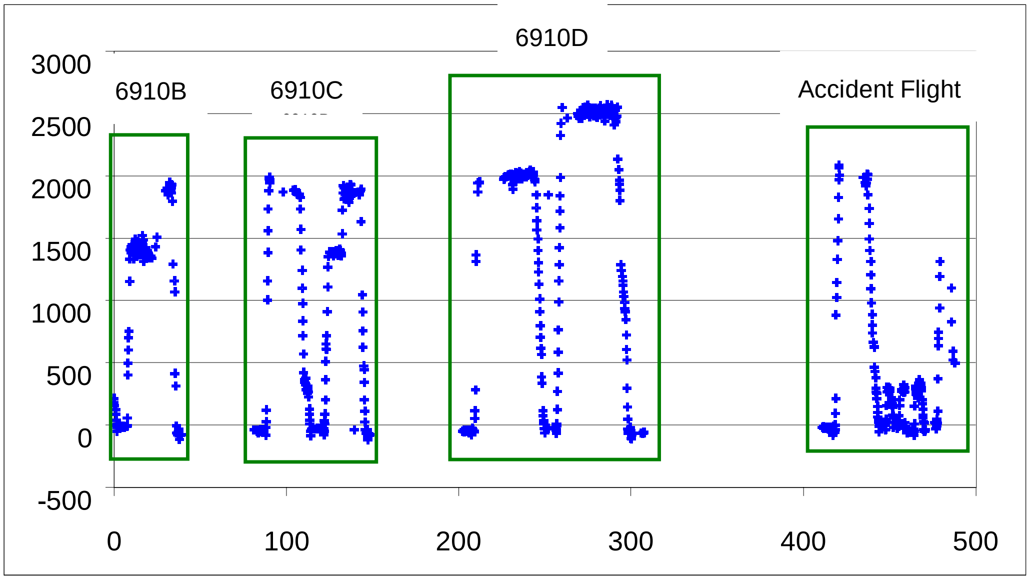

Figure 1 Altitude (ft) vs Pseudo-Time (min) showing IHUMS Downloads

The available data from the last operation has been expanded and plotted using airspeed, as this more clearly shows the rig hopping:

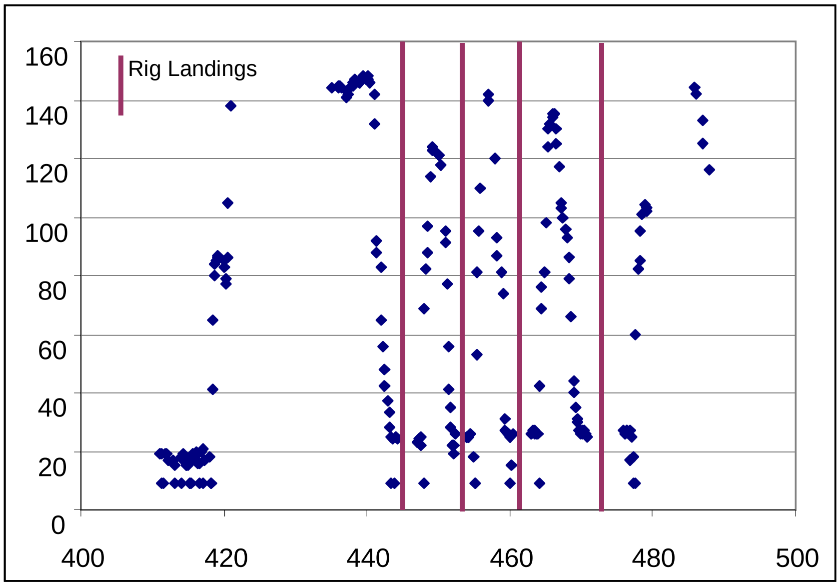

Figure 2 Airspeed (kt) vs Pseudo Time (min) for Final Operation

The track data measured during the first four flights of 16th July was downloaded into the groundstation. IHUMS identifies these by a date code (6910) and a letter sequence. 6910A and the first sector of 6910B were overwritten, so the available data can be related to the sectors flown thus:

Download	Time (from IHUMS log)	Minutes (from FDR)	Comment
6910 B	10:35	0	Land on at rig
6910 B	10:40	5	Take-off
6910 B	11:11	38	Land at EGSH
6910 C	12:00	82	Take-off
6910 C	12:27		Land on at rig
6910 C	12:35		Take-off
6910 C	13:00	148	Land at EGSH
6910 D	14:01	204	Take-off
6910 D	14:43		Land on at rig
6910 D	14:50		Take-off
6910 D	15:33	300	Land at EGSH
		418	Take-off from EGSH
		444	Land on 1st Rig
		447	Take-off 1st rig
		452	Land on 2nd rig
		455	Take-off 2nd rig
		460	Land on 3rd rig
		464	Take-off 3rd rig
		470	Land on 4th rig
		477	Take-off 4th rig
		488	Last sample

Data from the Day of the Accident

IHUMS measures RTB data in eight different regimes, but by chance, no data from a right hand turn was acquired on 16th July. This is not remarkable, as the aircraft has to be in a stable turn for some time to achieve an RTB acquisition. The remaining regimes are:

Sequence	Regime
1	MPOG
2	HOVER
3	DESCENT
4	CLIMB
5	BANK L
6	115 Kts
7	135 Kts
8	145 Kts

Data downloaded on 16th July is plotted against the regimes in sequence, MPOG at the left and Descent at the right, in the graph below. The colours are according to blade sequence, Red, Black, Yellow, Blue.

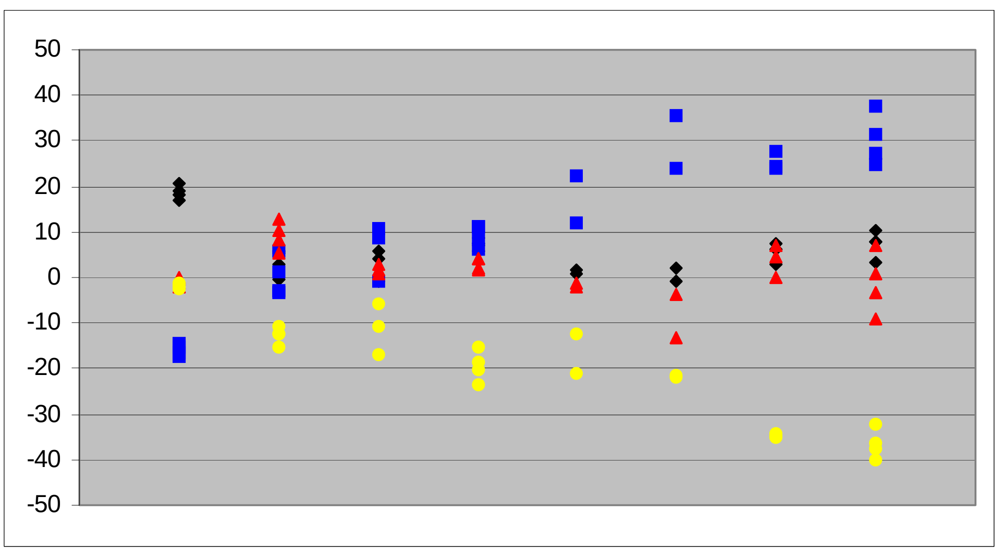

Figure 3 Blade Track (mm) plotted for RTB Flight Regimes

The trend of blades rising or falling with increasing airspeed is typical of an aircraft in service and this range of track splits would not give rise to concern.

The key feature of this data for this investigation is that at highest airspeeds, the yellow blade is clearly lower than the red and black, and the blue blade is higher.

Analysis of the Data

Having converted the data into meaningful parameters and checked that the data being examined was valid, analysis then started in earnest. The analysis started with the FDR records, working from the time of the accident backwards. The findings were then compared to the long term historical trends to provide context to the data.

Track, Lag and Velocity Data from the Day of the Accident

The RTB data downloaded into the groundstation has been shown at Figure 3 Blade Track (mm) plotted for RTB Flight Regimes. It was described previously as not particularly unusual for a helicopter to have a track variation like that.

If we examine the track variation for the day of the accident from the FDR data, the reason for this becomes immediately apparent:

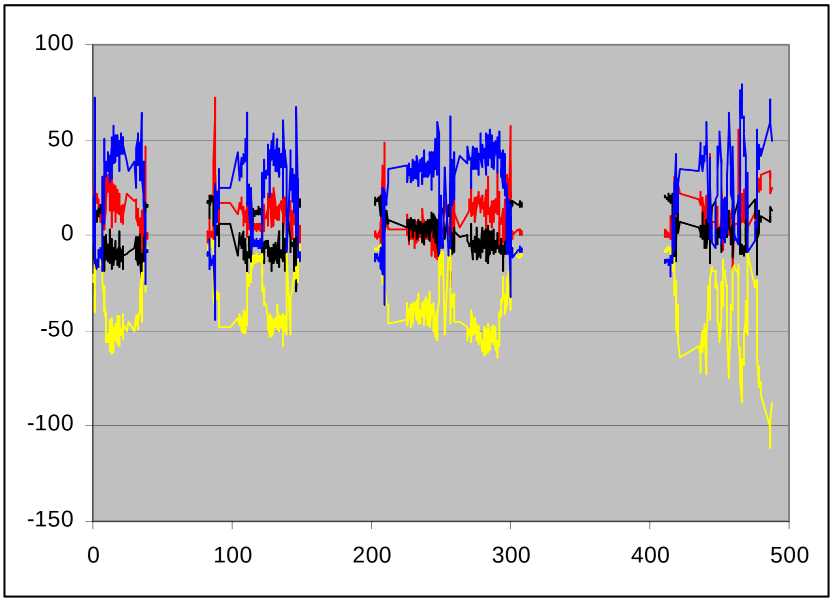

Figure 4 Track Data (mm) from FDR vs Pseudo Time (min)

This is one of the key graphs in this analysis. From the figure above the track pattern on the latter half of the second flight of the day (0 to 40 minutes) and the third and fourth flights (80 to

300 minutes) can be seen to be fairly stable. On each sector, the aircraft accelerates and decelerates, so the normal track variations with airspeed cause the blue blade to rise and the yellow blade to fall at high speed, returning to a smaller track split as the airspeed decreases. The main observation is that the overall track split did not increase during these flights.

On the final sortie, (400 to 500 minutes with many takeoffs and landings) the yellow blade can be seen to dive progressively on each sector flown. This type of graph is plotted with a mean track of zero, hence an apparent increase in red, blue and black track.

There is a similar pattern visible in the lag data, although here the degradation on the second half of the fourth operation of the day (250 to 300 minutes) appears clearer.

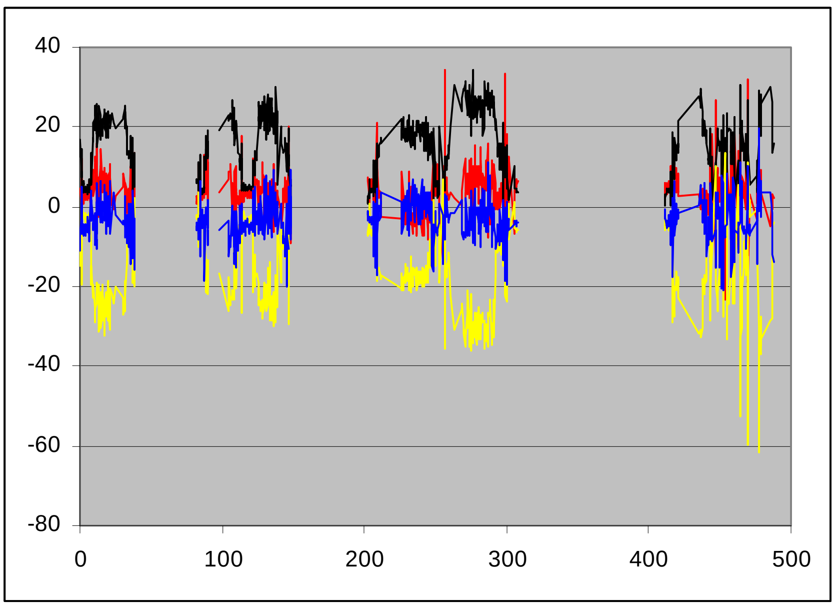

Figure 5 Blade Lag Data (mm) from FDR vs Pseudo Time (min)

What is very clear from these two graphs is that the degradation of the yellow blade occurred on the final operation, progressing as each leg was flown.

Data from the Final Flight

To illustrate the progression of the defect during the last operation, the data from Figure 4 Track Data (mm) from FDR vs Pseudo Time (min) has been expanded to cover just the last operation and drawn with track measurements shown individually.

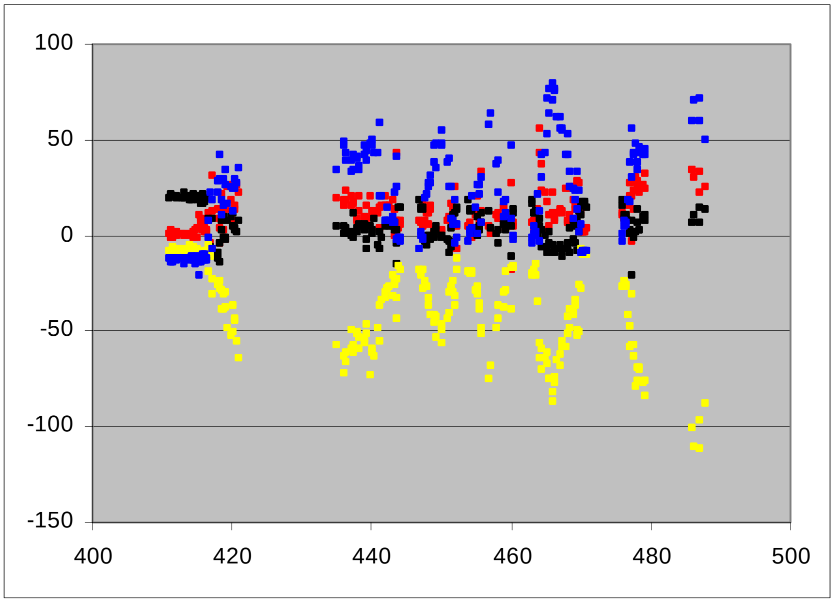

Figure 6 Track Data (mm) vs Pseudo Time (min) for Final Operation

The gap between 420 and 435 minutes corresponds to the period when the IHUM system is busy gathering gear vibration data and acquiring RTB data for the FDR is suspended.

As can be seen from this plot, each time the aircraft accelerated the yellow blade track went down, but the track split became progressively worse each time. Plotting the yellow blade track against airspeed for the five accelerations illustrates this:

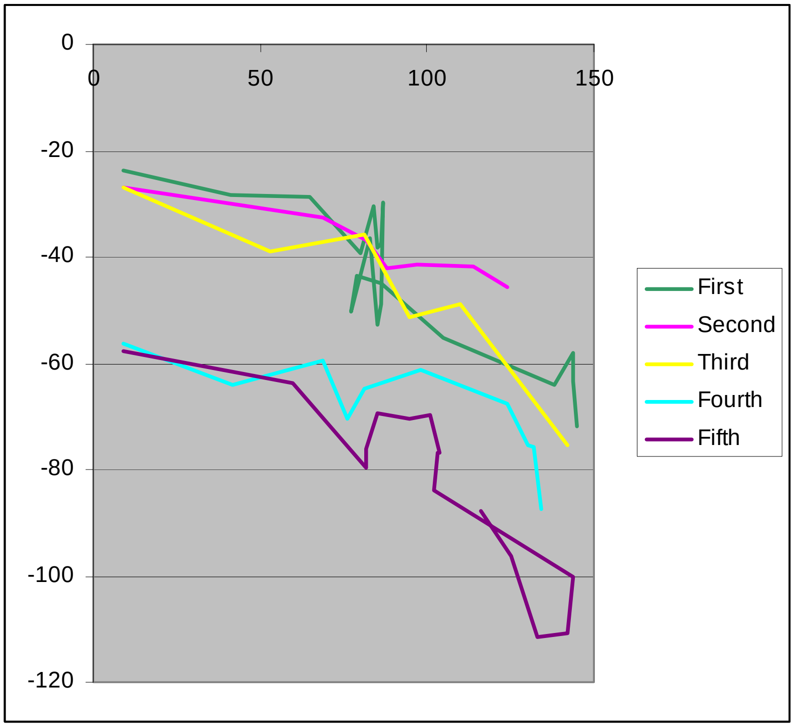

Figure 7 Yellow Blade Track (mm) during Five Accelerations on Last Operation, Plotted vs Airspeed (kt)

This graph shows, more vividly than any other, the speed at which the defect developed on these final sectors. While the pattern of flights earlier in the day had reached typically –45 to -50mm yellow blade height, the first and third sectors flown on this last operation were clearly worse and this became significantly more severe on the fourth sector and the final acceleration.

Assessment of the Groundstation Diagnostics

When the data from the fourth sortie of the day was downloaded into the groundstation, an IHUMS alert for RTB was generated. There is, clearly, a question about whether this was related to the damage that propagated to failure on the following sortie.

IHUMS RTB Diagnostic Processing

On each flight, data is automatically gathered whenever the IHUMS Data Acquisition and Processing Unit (DAPU) recognises that an RTB flight condition is being flown. The resulting data is downloaded and the groundstation carries out a number of data validity checks. The resulting data, in the form of main rotor track data and vibration measurements from the RTB accelerometers is then stored into the groundstation database.

The RTB data is then used in two ways. Firstly, it is tested to see whether any IHUMS limitations have been exceeded. It is important to recognise that these are IHUMS limits, based where possible upon maintenance manual values but applied following every flight. By comparison, the normal maintenance manual limits would only be applied following a pilot complaint for high vibration or disturbance of the main rotor components caused by periodic maintenance actions.

Secondly, data from the current flight is merged with data from up to eight preceding flights (using a median process for each test point and data measurement) to form a composite measurement. This process does not extend across recorded maintenance actions, so, for example, if an adjustment had been made four flights ago, only the most recent four flight of data would be used in the median process.

The composite maintenance record is then used as the basis for calculating the optimal adjustment that will reduce the vibration on the helicopter while maintaining a modest track split. This recommended adjustment is available for the maintainer to view for each download.

If the initial test of vibration and track parameters indicates that adjustment is necessary, then the groundstation printout includes a statement alerting the maintainer and providing the calculated adjustment.

IHUMS Printout in Tech Log 6910D

The RTB adjustment following the fourth flight of the day would not have caused any alarm because occasional spurious outputs are a characteristic of the system. It is usual to wait until a pattern of similar adjustments have been prompted before taking maintenance action, and in particular the S76 diagnostics from IHUMS have a very poor reputation in the field. There had been no RTB adjustments earlier in the day and the normal expectation would have been that the next download would probably have been clear.

We know from the earlier pages that the yellow blade was low, and diving with increasing speed, so one might expect to see some adjustment of the yellow blade tab; in fact the adjustment was:

	Red	Blue	Yellow	Black
Track Rod		-5 clicks	+1 click	
Mass	+2.6 lb			+1.6 lb
Tabs		4 thou Up		4 thou Down

The most conspicuous part of this is the large mass adjustment, which is typical of the ill-favoured S76 IHUMS RTB diagnostics.

RTB Exceedance Tests

Of greater potential significance is the cause of the alert. This came about because of a high vertical vibration on the ground. There was also an unusual spread in blade velocities in the cruise. These can be found in the detailed diagnostic printout (accessible to the maintainer, but not automatically generated).

A copy of the printout, with each point discussed, follows:

Diagnostic Output	Discussion
`RTB Detailed Diagnostics Report`	Heading

`Aircraft     : G-BJVX`
`Tech Log     : 6910D`
`Flight No    : 1500`
`IFN          : 5885`
`Flight Date  : 16/07/02`
`Flight Time  : 13:53`
`Airframe Hrs : 15973`
`Modstate     : 0702 (JI)`
`Report created : 16/07/02 at 16:46:42`
	Documentary data
	IFN = Internal Flight Number (database reference)
	Modstate = diagnostics configuration

`DATA PREPARATION & GROUNDSTATION WARNINGS`	Heading
`(NONE)`	All data was valid; no groundstation software errors were encountered.
`DIAGNOSTIC DATA INTEGRITY WARNINGS`	Heading
`MAIN ROTOR: Tracker data suspect at CRUISE. Maximum velocity difference of 39.00 exceeds threshold of 38.00.`	This is discussed in detail below.
`DIAGNOSTIC DATA EXCEEDANCE WARNINGS`	Heading
`MAIN ROTOR: 1 Main rotor vert value of 0.481 at MPOG exceeds threshold of 0.400.`	This is the test that caused the main rotor data to be printed.
`DIAGNOSTIC ADJUSTMENTS`	Heading
`RTB Diagnostics computed from 9 flights of main rotor data and 9 flights of tail rotor data.`	Statement of how many records were used in the Composite Record assembly. Four of these nine data sets had been gathered on this day, the other five extending back over the preceding week.

Diagnostic Output	Discussion
`MAIN ROTOR: Analysis mode = 2. Data subset = 0. Faults = Pitch Link, Mass, Tabs.`	Definition of the adjustment computation processing. Other modes are available if only partial data sets are available, but this is the normal diagnostic configuration.

`MAIN ROTOR Pitch Link: Lengthen YEL by 1 clicks.`
`AND : Shorten BLU by 5 clicks.`
 	
`MAIN ROTOR Mass: Add 2.6 lbs to RED.`
`OR : Subtract 2.6 lbs from YEL.`
`AND : Add 1.3 lbs to BLK.`
`OR : Subtract 1.3 lbs from BLU.`
 	
`MAIN ROTOR Tabs: Bend down BLK by 4 thou.`
`AND : Bend up BLU by 4 thou.`
	Results of the computation, as in the groundstation printout.

`TAIL ROTOR: Analysis mode = 1. Data subset = 0. Faults = Tail Mass.`	Similar statement of tail rotor adjustment computation

`TAIL ROTOR Tail Mass: Add 3.5 gms to BLU.`
`OR : Subtract 3.5 gms from BLK.`
`AND : Subtract 5.5 gms from YEL.`
`OR : Add 5.5 gms to RED.`
	Adjustment calculated, but not printed as there was no tail rotor exceedance.

Data Integrity Check

The data integrity check "Tracker data suspect at CRUISE" clearly only just breaks the threshold and, in any other circumstances, would be ignored. The significance of this parameter is considered by looking at a plot of blade velocities, using the same graph format as used for the track and lag plots earlier.

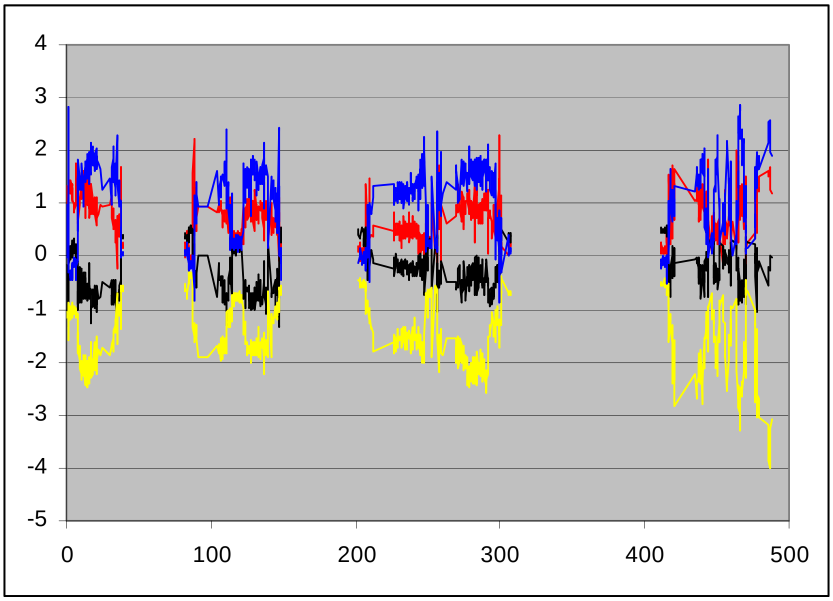

Figure 8 Blade Velocity Variation (m/s) vs Pseudo-time (min)

The increased blade velocity variation in the cruise during the fourth operation of the day was in fact measured at 14:06, corresponding to 211 minutes on the graph scale used here. At this time, the velocity split was not significantly worse than on previous sectors flown that day.

(N.B. The units on this graph are m/s, extrapolated to the rotor tip, with a mean of around 175 m/s in the cruise. The velocity units used in the groundstation have not been identified.)

Trackers compute blade velocity from the time the chord takes to pass one of the tracker "beams" and it only takes a shiny leading edge or glinting lighting conditions to fool the tracker, and this can occur at random under normal circumstances.

Diagnostic Data Exceedance Warnings

There is no vibration data stored on the FDR, so to consider this alert we need to look at the IHUMS groundstation records.

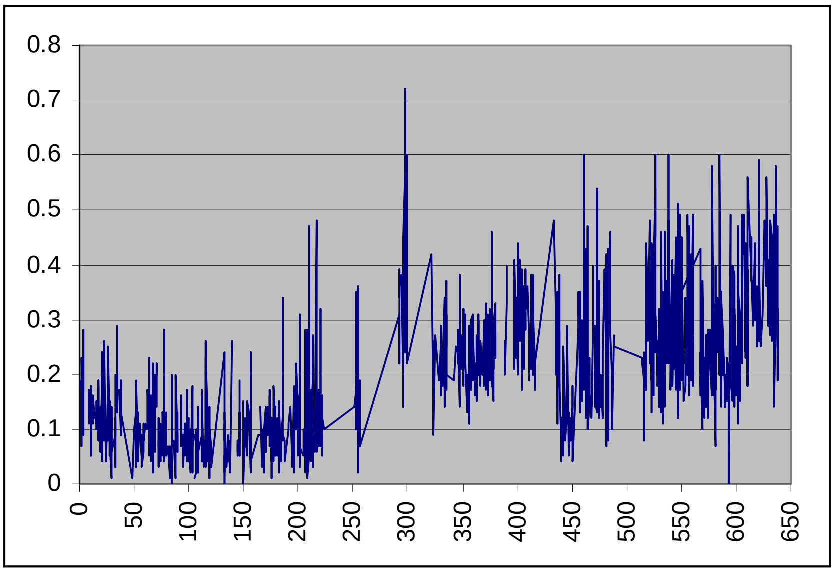

Figure 9 Pilot Vertical 1R Vibration at MPOG (IPS) vs Flying Days

It can be seen from the previous graph, which starts at the beginning of 2000, that it is commonplace for the 1R vibration at MPOG to exceed the threshold of 0.4 IPS.

There are two reasons why this is considered acceptable. Firstly, the parameter is being measured and the maintainers are in a position to identify the cause of any persistent exceedance and secondly because the aircraft spends most of it's time in the cruise, where vibration levels are kept low – to some extent at the expense of higher vibration on the ground.

Looking at the more important cruise vibration level in Figure 10 above, the 0.1 IPS level maintained by this aircraft was very good.

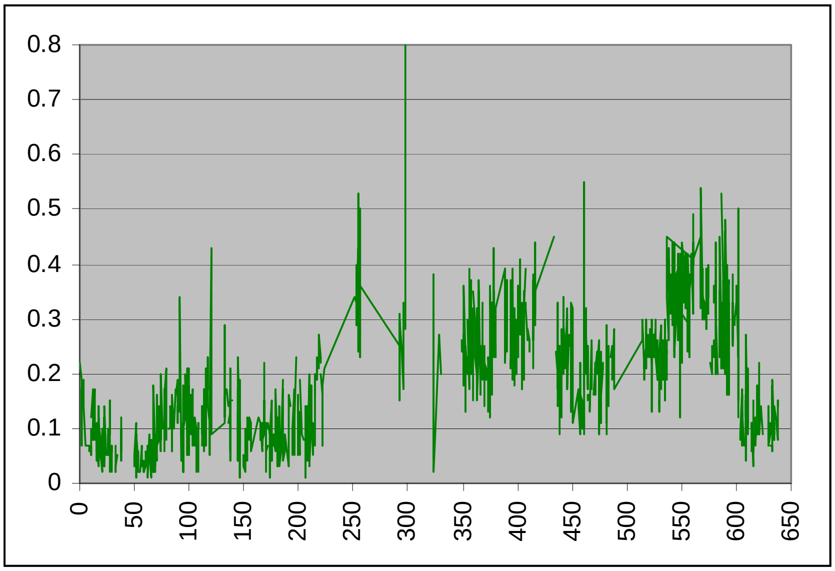

Figure 10 Pilot Vertical 1R Vibration at Cruise (IPS) vs Flying Days

Historical Data

We have already looked at some of the historical records of vibration levels in order to understand the significance of the RTB alerts generated on the last download. In this section, the historical track records are examined.

The question arises whether the rotor behaviour of the final flight is abnormal, or if any similar occurrence has been seen in the past. To do this, a plot of the track of the four blades in the cruise condition is presented below.

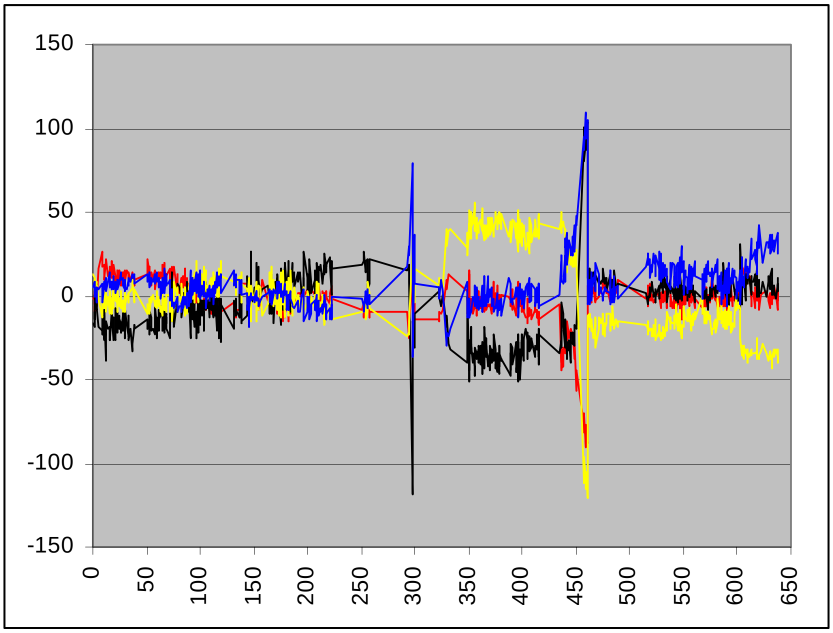

Figure 11 Blade Track in Cruise (mm) vs Flying Days

The calendar period covered by the graph above is two and a half years, with probably 1500 flight hours.

Two aspects of this graph are of interest. The normal characteristic of track patterns that vary slowly over time can be seen, with step changes at maintenance or adjustment points.

The single large black vs blue track split at 300th flying day is curious, but as this is a single value it may be from a test flight or relating to maintenance activity in some other way.

Of greater interest is the developing track split at around 450 flying days, and this section has been expanded below:

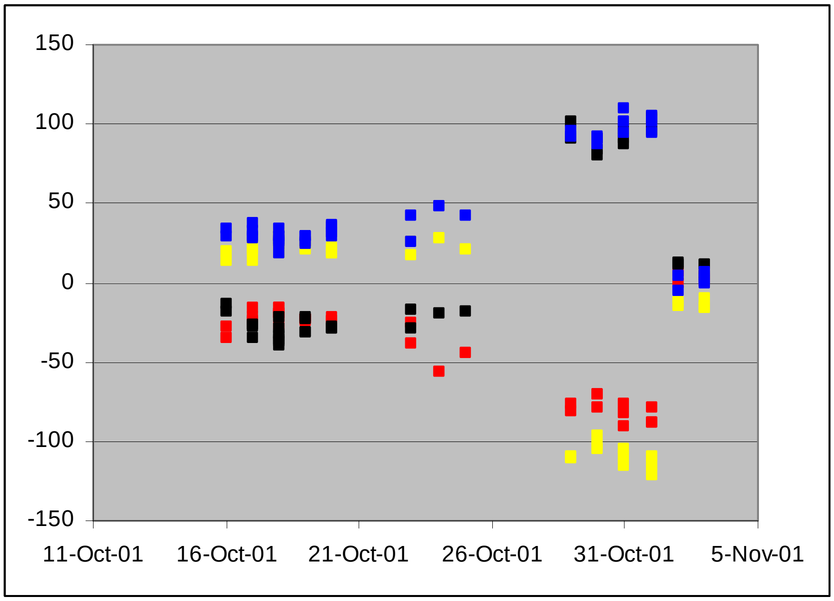

There are multiple downloads on each flying day, hence the multiple sample points on each daily "slice" of data.

As can be seen, around 26th October something happened which caused a significant change in track pattern and this was present in eleven samples taken between 29th October to 1st November. Maintenance records include the following:

15 Oct	Excessive 1R at cruise at high AUW...Yellow (?) pitch links adjusted
23 Oct	Red blade tip cap cracked – changed.
26 Oct	Black main rotor blade due ultrasonic inspection – replaced. Yellow blade pitch link adjusted
27 Oct	Further track & balance – Blue pitch link adjusted
1 Nov	Unacceptable vertical vibration from main rotor. All four pitch links adjusted.

While it is clear that something odd was going on with the rotor, and that the aircrew were complaining, there is no clear evidence of this in the 1R vibration records. This period corresponds to about 460 "flying days", see Figure 9 and Figure 10 above. In general, the vibration levels were lower than the 0.4 IPS limit, and lower than at other periods in the life of the aircraft.

It may have been that a higher harmonic caused the uncomfortable ride, and hence the pilot complaint, however this has not been investigated further. If this was the case, and it was relevant to the accident, there should be technical log defect records written up by the aircrew noting high vibration.

What is perhaps more remarkable than the vibration levels is that the aircraft was operated over this period with an overall track split in excess of 200mm – greater than that immediately preceding the blade failure.

Conclusions

Availability of Data

The combination of IHUMS groundstation computerised record keeping, augmented by Ken Knight's database management, has provided a clear history of the characteristics of this rotor over an extended period.

Use of the rotor track data retained in the FDR has provided evidence of the rotor behaviour during the last flight.

Behaviour of the Rotor

During the last flight, the yellow blade developed a significant reduction in relative track height. The final overall track split has been calculated to be about 180 mm.

The changes in track and lag between the first and second legs of the penultimate flight may have been related to the defect, however variations such as this can equally be caused by changes in AUW, airspeed or altitude.

The track split was stable during the earlier flights of the 16th July.

Prediction

G-BJVX had been operated with larger track splits. The track pattern of the preceding flight was not a clear indication of the impending failure.

G-BJVX had been operated with higher main rotor vibration. The vibration of the preceding flight was not a clear indication of the impending failure.

From the penultimate flight, the groundstation RTB diagnostics detected a spread in main rotor blade velocities in the cruise and a high vertical vibration at MPOG. Neither would be a cause for alarm as the preceding downloads had been clear and RTB alerts can be spurious.

HYDROGRAPHIC CHART SHOWING AREA SURROUNDING ACCIDENT SITE

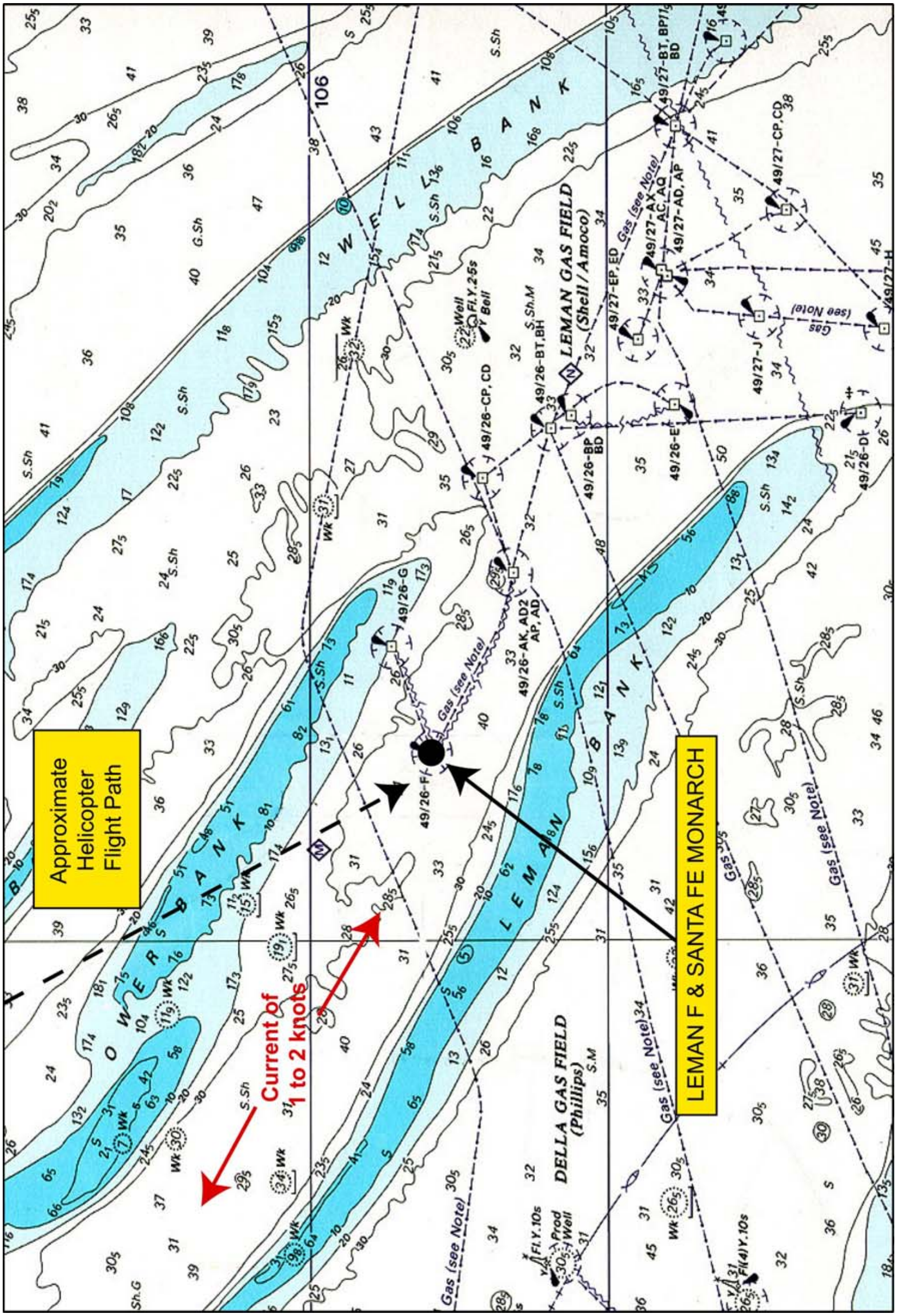

SUNKEN DEBRIS DISTRIBUTION & POSITION RELATIVE TO INSTALLATIONS

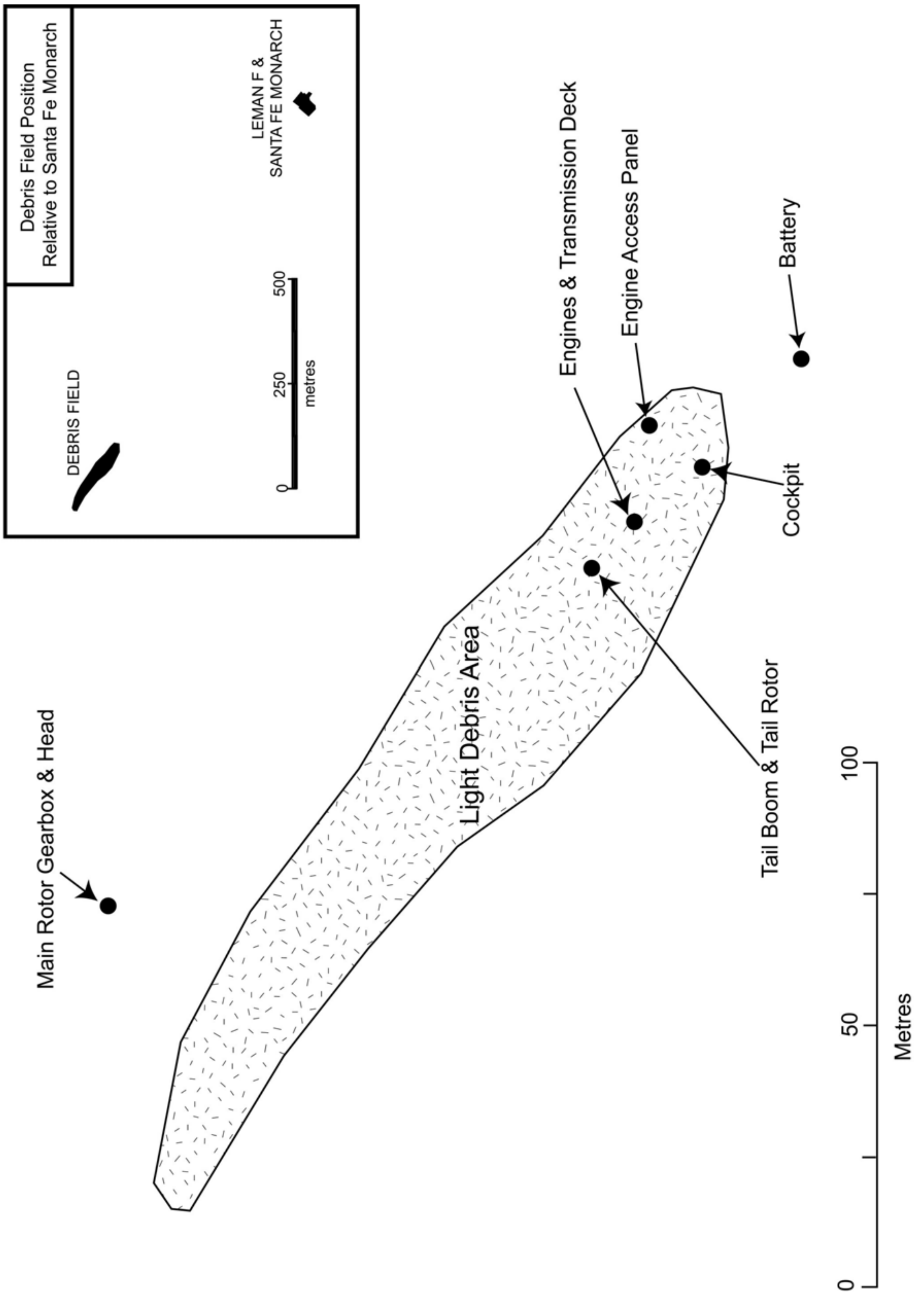

EXTRACT FROM QINETIQ LTD REPORT

EXAMINATION OF SIKORSKY S76 MAIN ROTOR BLADE FAILURE

1. Introduction

An inboard section of a Sikorsky S76 (G-BJVX) main rotor blade was delivered to QinetiQ Cody Technology Park after failing in service. The aircraft was operating over the North Sea when the main rotor blade failed resulting in loss of the aircraft. The Air Accident Investigation Branch (AAIB) organised recovery of the wreckage from the seabed. Upon recovery it was found that three of the main rotor blades showed evidence of superficial damage whereas the fourth was fractured approximately 1950mm from the blade root. The outboard section was not found.

The fractured rotor blade was manufactured from a seam welded titanium alloy (Ti-6Al-4V) spar encased by a composite airfoil. A titanium erosion strip was fitted to the leading edge. It was manufactured in March 1981. In 1999, after accumulating 8,261 hours, the blade suffered a lightning strike while fitted to Sikorsky S76A G-BHBF. It was returned to the manufacturer for inspection after which it was repaired and returned to service. At the time of the failure the blade had accumulated 9,661 hours of use. The airworthiness limitation life of the blade is 28,000 hours.

The following identification markings were observed on the fractured blade upon delivery to QinetiQ;

Top

BLADE SERIAL No. A086-00741A SAC$_{TM}$

Bottom

TRACK +19 MINUTES
BLADE SERIAL No. A086-00741 SAC$_{TM}$
BLADE DWG NO. 76150-09100-041
MFG 3-19-81
REP 11-24-00
RS-0041 - II, III, VI, VII
RS-007 - I, II, III
RS-008 - II
RS-012 - V

2. Visual Examination

The fractured main rotor blade is shown in the as-received condition in figure 1, with the general view of the fracture surface shown in figure 2. The fracture surface was examined using low power stereo microscopy under direct and oblique lighting. Initial observations showed evidence of a granular deposit across the fracture surface of the titanium spar and composite airfoil. The grains appeared to be sand, which was consistent with the report that the wreckage was positioned such that the fractured end of the blade was embedded in the sand of the seabed.

There were two distinct regions observed on the fracture surface. The fracture surface of the leading edge and the majority of the top surface of the spar was relatively flat (perpendicular to the spar surface), while the trailing edge and the majority of the lower surface of the spar was angled at approximately 45° to the spar surface (refer to figure 2). The fracture surface at a 45° angle is typical of overload failure in thin plates. Within the flat fracture surface region at the top surface of the spar, there appeared an area of staining, which can be seen in figure 2 and in more detail in figure 3. With reference to figure 3, evidence of possible beach marks were observed on the trailing edge side of the stain, which is suggestive of fatigue crack propagation. The fracture surface was cleaned in a dilute solution of nitric acid in water to remove the deposits on the surface. Re-examination of the surface showed distinct beach marks leading back to the area that had been stained indicating that this was the origin of the fatigue crack (figure 4).

The macro examination of the fracture surface identified a series of bands across the fatigue region of the crack. In total 63 bands were counted in the trailing edge direction and 61 in the leading edge direction. Of these, 33 in both directions appeared to be larger and more pronounced. These bands on the fracture surface are usually related to increases in the applied load and are typically associated with events such as engine stop/starts or take-off when relatively large loads can be applied before returning to the lower load levels encountered prior to the event.

The fatigue crack origin corresponded with the position of the trailing edge of the titanium erosion strip (figure 5). Figure 6 shows this area in detail. It was observed that at a distance of approximately 20mm from the fracture, the erosion strip began to taper towards the leading edge at an angle of approximately 18°. It was ascertained that this was part of the scarf joint present between the two-part titanium erosion strip. The majority of the area behind this scarf joint taper was filled with a yellow adhesive material (appeared to be painted white) so that it was level with the fibre glass skin and titanium erosion strip in this area. Within this filled region there was a triangular depression at the edge of the fracture surface (figures 6 and 7). Within the triangular depression there was a trough which ran parallel to the edge of the filled region (figure 7), the end of the trough coincided with the origin of the fatigue crack and also a mark on the top surface of the spar (figure 8) which ranged in colour from dark blue at the edge of the fracture to dark orange/light-yellow as it moved from the edge. This colouring was characteristic of heat tinting. Measurements of the thickness of adhesive in this depression found that it varied from 340μm at the apex of the triangle, tapering to 240μm at the edge of the fracture. The thickness in the trough also tapered from 220μm at the apex of the triangle to 150μm just before the edge of the fracture.

Detailed visual examination within the triangular depression showed the presence of a piece of metal protruding from under the titanium erosion strip (figure 7). The metal was approximately 5mm in length running from the edge of the fracture surface to the apex of the depression in line with the tapered scarf joint of the erosion strip. The metal piece appeared to fold under itself at the apex.

Liquid nitrogen was used to embrittle the adhesive allowing removal of the titanium erosion strip from the leading edge of the rotor blade. Figures 9 and 10 show the top surface of the blade in the region of the triangular depression after the erosion strip had been removed. It can be seen that the metal piece that was protruding from the edge of the strip was the edge of a larger piece, approximately 10mm long and 5mm at its widest, which tapered towards its end. The size and shape of the metal piece corresponded to that of the filled region which was present behind the tapered scarf joint of the erosion strip (refer to figure 6). It was also observed that a small area of heat tinting (approximately 0.5mm in diameter) was present at the tip of the metal piece.

The root end of the rotor blade was examined for signs of damage that may have been caused by a lightning strike. The root end of the blade is shown in figure 11. The four holes, containing bushings, allow four through bolts to attach the blade to the spindle. It is sometimes possible for the bushings and bolts to show evidence of arc strikes after rotor blades are struck by lightning. The bushings and bolts were examined and it was found that the bush identified in figure 11 as number 3 (leading edge, inboard), contained a defect, which was examined under high power stereo microscopy. The defect did not show any signs of local heat tinting or melting of the surface which would suggest arcing, which can occur during a lightning strike. There was no corresponding damage observed on the bolt. The bush defect appeared to be a mechanical score and as such appeared to be unrelated to the failure.

3. Scanning Electron Microscope

The fracture surface of the rotor blade was examined in detail with a scanning electron microscope (SEM) in order to confirm that the crack had propagated by fatigue as was suggested by the visual examination. Initially acetate replicas were taken of the fracture surface prior to any cleaning (i.e. the dilute nitric acid wash described during visual examination). The replicas had the dual effect of cleaning the fracture surface of loose debris and obtaining a record of the fracture surface topography. The replicas were carbon coated and examined in the SEM. Examination of the initial replicas of the origin showed the loose debris that was removed from the surface, no fracture surface detail was visible. Repeated replication of the origin failed to show any detail that would indicate the mode of failure, however towards the end of the flat section of the fracture surface on the bottom surface of the blade, some of the replicas showed evidence of striations (figure 12), which confirmed the mode of failure as fatigue.

To examine the fracture surface in detail the fractured end was sectioned chordwise from the main body of the rotor blade. This sample was then sectioned spanwise through the fracture surface to give two samples, the leading edge and the trailing edge. The leading edge sample was approximately 50mm in length and contained the origin, the trailing edge sample was approximately 90mm in length.

Initial examination of the leading edge section in the SEM showed little fracture surface detail around the origin. The majority of the fracture surface was covered by a surface deposit which masked any detail. Figures 13 and 14 show the deposit that was observed. However, there were areas where the surface detail was visible and figure 15 shows an example of the fatigue striations that were observed approximately 15mm from the origin.

Energy dispersive x-ray analysis (EDX) was carried out on the deposit to identify its composition. Figure 16 shows the EDX trace from the deposit, it can be seen that as well as the titanium (Ti) and aluminium (Al) which would be expected there are large peaks for oxygen (O), magnesium (Mg) and calcium (Ca). There are also peaks for carbon (C), silicon (Si), sulphur (S), chlorine (Cl), potassium (K) and iron (Fe).

In order to remove the deposit the fracture surface was cleaned with a dilute solution of nitric acid in water. Re-examination of the surface showed that the majority of the deposit had been removed and that most of the fracture surface detail was evident revealing fatigue striations across the majority of the fracture surface. Figure 17 shows the fracture surface at the fatigue crack origin. A semi-elliptical region of relatively flat topography was present at the origin, measuring approximately 1.23mm in width and 230μm in depth. A detailed view of the fracture surface within this region is shown in figure 18. This region of flat topography corresponded with the area of heat tinting observed on the surface of the spar, which suggested that the microstructure in this region was different from the rest of the spar material.

The spacing of fatigue striations were measured to estimate the number of load cycles required to propagate the crack to failure (appendix A). The fracture was assumed to be two separate cracks both initiating at the same origin and propagating in opposite directions, one towards the trailing edge and the other to the leading edge of the blade. The fracture surface was examined in detail at various points from the origin of the fatigue crack to the end of the fatigue region. Where patches of striations were clearly visible, the spacing was measured and then plotted to estimate the total number of cycles across the fatigue crack. With reference to figure 19, it was evident, especially towards the ends of the cracks, that the striations appeared to consist of regularly repeating units of large striations (yellow) with smaller striations in-between (red). The striation spacing was measured as the distance between the large striations (yellow, figure 19) as these were assumed to be due to one blade rotation, with the finer striations in-between being due to aerodynamic buffeting [1]. Figures 20 and 21 show the striation spacing and the inverse of the striation spacing plotted against distance from the origin for trailing and leading edge cracks. In both cases patches of striations only become clearly visible at distances of approximately 14mm from the origin. A best-fit line was added to the inverse striation data for both half of the cracks and the equation of this line integrated between 14mm and the end of each crack to estimate the number of load cycles required to propagate the crack from approximately 14mm to failure.

Integration of the best-fit curve resulted in an estimate of load cycles required for crack propagation in the leading edge direction from between 14.2mm and 58.3mm from the origin to be 137,402 cycles. In the trailing edge direction an estimate of the load cycles required for crack propagation between 14mm and 84.7mm from the origin was estimated to be 158,824 cycles. The blade rotation was known to be approximately 304 rpm therefore the time required for crack growth could be estimated as 7.5 hours in the leading edge direction and 8.7 hrs in the trailing edge direction. In reality the time for crack propagation would be the same in both directions as they initiated from a single point.

It is possible to extrapolate the best-fit curve back to the origin in order to obtain an estimate for the total number of cycles for crack growth. In this case the origin was taken as being the edge of the changed microstructure (approx. 600μm half length). The estimate obtained for the number of cycles to failure for the leading edge from between 600μm to 58.3mm from the origin was 1,829,071 cycles. In the trailing edge direction an estimate obtained between 600μm to 84.7mm from the origin was 1,848,253 cycles. This corresponds to a time required for crack growth of 100.3 hours in the leading edge direction and 101.3 hrs in the trailing edge direction.

Energy dispersive x-ray (EDX) analysis was carried out on the titanium spar material to confirm its composition. The spectrum obtained from the spar surface identified titanium as the major element present with alloying elements of aluminium and vanadium also present. The spectrum was as expected for the spar material, which was reported as being manufactured from Ti-6Al-4V titanium alloy. The titanium erosion strip was also analysed and confirmed that the material was commercially pure titanium. The metal that was embedded in the adhesive under the erosion strip was also found to be commercially pure titanium.

4. Metallography

The semi-eliptical region of the fracture surface at the fatigue crack origin was sectioned. The sample was polished to a colloidal silica finish and etched with Kroll's etch. Figure 22 shows the cross-section through the origin. It could be seen that there was a change in microstructure at the origin however, the microstructure was not clearly visible at the magnification obtained in the optical microscope. Because of this, the cross-section was examined at higher magnifications in a SEM using back scattered imaging techniques.

Figure 23 shows the images from the SEM. It clearly shows the expected grain structure of Ti-6Al-4V in the bulk of the material and a quadrant in the top right hand corner of martensitic transformed beta. This confirms that the flat region on the fracture surface, at the origin of the fatigue fracture, was a result of a different microstructure at this point.

5. Fourier Transform Infrared Microscopy

Fourier transform infrared (FTIR) microscopy was used to analyse the adhesive in the depression at the fracture origin. Samples were taken from the depression as well as from the filled area behind it and under the titanium erosion strip away from the fracture. Visual examination of the adhesive in the depression showed it to be yellow/brown and relatively hard/brittle when compared to the adhesive under the erosion strip which appeared more yellow in colour and relatively soft. Figure 9 indicates the position of the FTIR samples.

The samples were prepared by producing a fine powder of the adhesive and dispersing in KBr. Figure 24 shows the FTIR spectra obtained. The spectra produced for samples 2, 3 and 4 (filled region and under sheath) were very similar. Sample 1 (depression triangle) also looks similar although the curve was not as clear as the other samples due to the very small quantity of material available. Some extra weak peaks were observed on the curve at approximately 3500, 1482 and 720 cm^{-1}. These could correspond to absorption due to –OH ions or due to nitrogen/oxygen contamination compounds (-NOH) possibly indicating oxidation/degradation. However, it must be noted that these peaks are weak so no strong conclusion can be drawn from them.

The FTIR traces from the failed area, which was carried out by QinetiQ, were sent to Sikorsky for comparison against original M1113 adhesive. Sikorsky agreed that the QinetiQ traces were a good match for the standard M1113 adhesive that they use and that along with the fact that it was yellow in colour suggested that it was probably original adhesive.

6. Discussion

The examination of the Sikorsky S76 (G-BJVX) main rotor blade has shown that failure of the blade occurred due to fatigue crack growth in the titanium spar which initiated from an area of microstructural change. The origin coincided with the heat tinting that was observed in the triangular depression at the edge of the fracture surface which suggests that the change in microstructure at the crack origin was most likely caused by heating and rapid cooling.

Removal of the titanium erosion strip confirmed that there was a triangular piece of metal embedded in the adhesive underneath it, which was found to match the composition of the titanium erosion strip. The size and shape of the embedded titanium matched the filled region behind the triangular depression, which suggested that it should have been in that position rather than embedded in the adhesive. It was ascertained that the position of the fracture was at the scarf joint of the two piece erosion strip and that the

18° angle on the trailing edge of the strip was the start of the tang of the joint for the inboard section of the strip. It was concluded that the embedded section of titanium was the tang of the outboard section of erosion strip that had become folded under the inboard section during manufacturing. This had resulted in the strip material doubling in thickness where it was folded over. The double thickness had occurred where the triangular depression in the adhesive was observed at the edge of the fatigue crack origin. The fatigue crack had initiated in the spar at the rear point of this folded tang. The scarf joint configuration is shown in figure 25 along with the section observed after failure and the likely configuration prior to failure. It is thought that the folded tang of the erosion strip was touching or very close to the titanium spar. The heat tinting at the surface of the spar adjacent to the origin and the heat affected microstructure also at this point indicate a possible scenario whereby current flow during a lightning strike had been able to pass from the leading edge erosion strip to the titanium spar through this folded tang. The heat tinting on the tip of the embedded outboard tang indicated the path of current flow from the erosion strip to the tang, with the current then flowing to the spar through the rear edge of the tang fold. The rapid localised heating and subsequent rapid cooling of the spar material had been sufficient to transform an area at the surface from an equi-axed alpha-beta microstructure to martensite. As well as the martensitic microstructure having a greater susceptibility to fatigue initiation than the alpha-beta microstructure, the heating and cooling would remove the benefits of the shot peening.

Striation spacings were used to give an estimate of the number of cycles the rotor blade had encountered before final failure occurred. Initially a deposit masked the majority of the fracture surface, which inhibited striation counting. The deposit was found to be rich in oxygen, magnesium and calcium. It is likely that this deposit was a combination of magnesium and calcium hydroxide that had been galvanically removed from the seawater and deposited on the fracture surface while the wreckage was on the seabed. Although the fracture surface was masked, the deposit did not appear to do any damage to the surface and the majority was removed by the weak acid rinse.

Striation measurements were carried out at differing distances from the origin. The striations were clearly visible across the majority of the fracture surface towards the ends of the cracks but closer to the origin the striations became less obvious. In the region from the origin until approximately 14mm from the origin, the striations were not clearly visible. Small patches of striation-like features were observed but they were not clearly definable and may have been bands rather than individual striations. The patches were too small to count sufficient striations/bands from which to obtain a confident average spacing. However, from approximately 14mm from the origin to the ends of the cracks, sufficient striations were observed to estimate the total number of load cycles the blade had encountered for crack growth between these points. Using the blade RPM of 304, it was estimated that the time required for crack growth from approximately 14mm from the origin to final failure was 7.5 hours in the leading edge direction and 8.7 hours in the trailing edge direction (table 1). Extrapolating the striation spacings back to the origin is difficult when approximately 14mm of the early crack growth did not reveal striations. However, a best-fit curve for the data from both halves of the cracks was plotted and extrapolated back to 600μm to estimate the total number of load cycles for crack growth. It was estimated that the total number of cycles in the leading edge direction was 1,829,071 and in the trailing edge direction 1,848,253 which can be converted to a time required for crack growth of 100.3 hours in the leading edge and 101.3 hours in the trailing edge (table 1). The steepness of the curve at short crack lengths is likely to generate potential errors and therefore extrapolation to the origin can only be used as a guide to the likely crack life. The extrapolated steep curve in this case results in the striation spacing becoming extremely small towards the origin, which may increase the total number of cycles to a disproportionately large amount. Therefore, only the estimate obtained from the half crack size of approximately 14mm to final failure, in this case 8.7 hours, should be considered as being a good estimate of the crack growth. Any estimates obtained from extrapolation back to the origin must be used cautiously.

The macro examination of the fracture surface identified a series of bands, which may have been related to increased loading such as during take-off or engine stop/starts. In total, 63 bands were counted in the trailing edge direction and 61 in the leading edge direction (average 62). Of these, 33 in both directions appeared to be larger and more pronounced. The service life of the failed rotor blade consisted of numerous short hops between offshore installations and to and from land. In many cases numerous take off and landings are performed without engine stop/starts. With reference to the flight data (appendix B) it can be seen that 62 take off/landings occurred in the final 19.5 hours of the blade and 62 engine stop/starts in the final 69.28 hours (table 1).

With reference to table 1, it can be seen that the time required for total crack growth estimated from the striation measurements is approximately 100 hours, assuming one striation per blade rotation. This suggests that the macro bands are most likely due to engine stop/starts as this number corresponded to approximately 70 flying hours rather than take off/landings, which only corresponded to approximately 19 hours.

Measured feature	Number	Assumed load cycle	Equivalent flying hours (approx)
Trailing Edge			
Striations between 14,030µm and 84,700µm	158,824	Blade rotation	8.7
Striations between 600µm and 84,700µm	1,848,253	Blade rotation	101.3
Macro bands on fracture surface	63	Engine stop/starts	71
		Take off/landings	19.6
Leading Edge			
Striations between 14,238µm and 58,304µm	137,402	Blade rotation	7.5
Striations between 600µm and 58,304µm	1,829,071	Blade rotation	100.3
Macro bands on fracture surface	61	Engine stop/starts	68.6
		Take off/landings	19.25

Table 1. Tabulated data of band / striation measurements.

It must be said that the use of striation counting to estimate crack growth must be used as a guide only. Many assumptions are made about the loading cycle. In this case it has been assumed that each blade revolution produces one striation and that each blade revolution occurs at a speed of 304 RPM. It is possible that some striations are produced by cyclic loads not associated with the blade rotation such as vibration and wind gusts, although in this case that problem was addressed by measuring the distance between the prominent striations and ignoring the 2 to 3 smaller striations that were observed in-between. However, this again is an assumption. The region of the fracture surface adjacent to the origin in which clear striations were not evident was overcome by extrapolating the striation count back to the origin. Extrapolation can only be used as an estimate because it assumes that the crack growth follows the extrapolated curve, which may not be the case. Also the fatigue striation estimate has not taken into account the initial growth of the crack to produce a through crack. In this situation the crack is changing from a single crack front at the through crack position to two separate cracks propagating in opposite directions. This initial through-crack growth is likely to be different from the crack growth in the two opposite propagating cracks.

FTIR was carried out to establish if the adhesive at the failure origin was similar in nature to M1113, which is the adhesive used by Sikorsky during manufacturing. If the adhesive was found to be different it may have indicated that a repair had been carried out after manufacturing. The FTIR traces from the failed area, which was carried out by QinetiQ, were sent to Sikorsky for comparison against original M1113 adhesive. Sikorsky agreed that the QinetiQ traces were a good match for the standard M1113 adhesive that they use and that along with the fact that it was yellow in colour suggested that it was probably original adhesive. However, many commercial epoxy adhesives could give similar traces so it is not conclusive.

To summarise, it appears that a manufacturing anomaly introduced into the main rotor blade in March 1981 at the erosion strip scarf joint had provided a path through which current could flow from the erosion strip to the spar. It is possible that a lightning strike had produced current flow through the anomaly causing a resistance heating effect at the contact point to the spar, which in-turn caused a localised change in the microstructure. This localised change in microstructure had been sufficient to increase the susceptibility of the spar to fatigue at this point. Continued service of the blade led to fatigue initiation and propagation at the anomaly contact point until final failure occurred.

7. Conclusions

7.1 The Sikorsky S76 main rotor blade failed due to fatigue crack growth through approximately 50% of the spar followed by catastrophic overload of the remaining section.

7.2 The fatigue crack initiated from a localised change in the microstructure.

7.3 The change in microstructure occurred at a manufacturing anomaly that had allowed the erosion strip tang to come into contact, or very close to, the titanium spar.

7.4 It is likely that a lightning strike on the rotor blade had produced a flow of current through the anomaly, from the erosion strip to the spar, causing a resistance heating effect similar to a spot weld, which led to the change in the microstructure at the fatigue crack origin.

7.5 Fatigue striation measurements predicted that approximately 1.8 million blade rotations had occurred during growth of the crack from the initial defect 0.6mm half-length to final failure. Assuming a constant blade rotation of 304 rpm, these 1.8 million cycles would have occurred in approximately 100 hours.

7.6 Coarse crack growth bands were measured from close to the origin to final failure. Making the assumption that each band represented an engine stop/start then some 70 hours of crack growth can be predicted to have occurred from close to the origin to final failure.

7.7 Since coarse bands and fine striations are not easy to detect close to the origin this correspondence between two separate measurements of crack growth appears reasonable.

8. Comments and Recommendations

The manufacturing anomaly of the erosion strip, which resulted in failure of the blade, would have been visible on the outer surface of the blade as the outboard scarf joint tang was folded under the inboard. This would have resulted in the outboard erosion strip tang as not being visible.

In order to reduce the re-occurrence of this type of failure on main rotor blades with two-part erosion strips, examination of the scarf joint would be prudent. Examination would identify blades in which any of the scarf joint tangs were not visible. If the tangs are not visible it must be assumed that they are beneath the adhesive and as such have the potential to provide an electrical contact between the erosion strip and the spar and hence have the potential to cause the spar to fail in fatigue if subjected to lightning strikes. Furthermore, even if lightning strikes do not occur the possibility of fretting fatigue occurring where the erosion strip tang and spar are in contact can not be ruled out.

9. Acknowledgements

Flight data (AAIB)
Materials and design advice (Sikorsky)

10. References

[1] ASM Handbook of Case Studies In Failure Analysis Volume

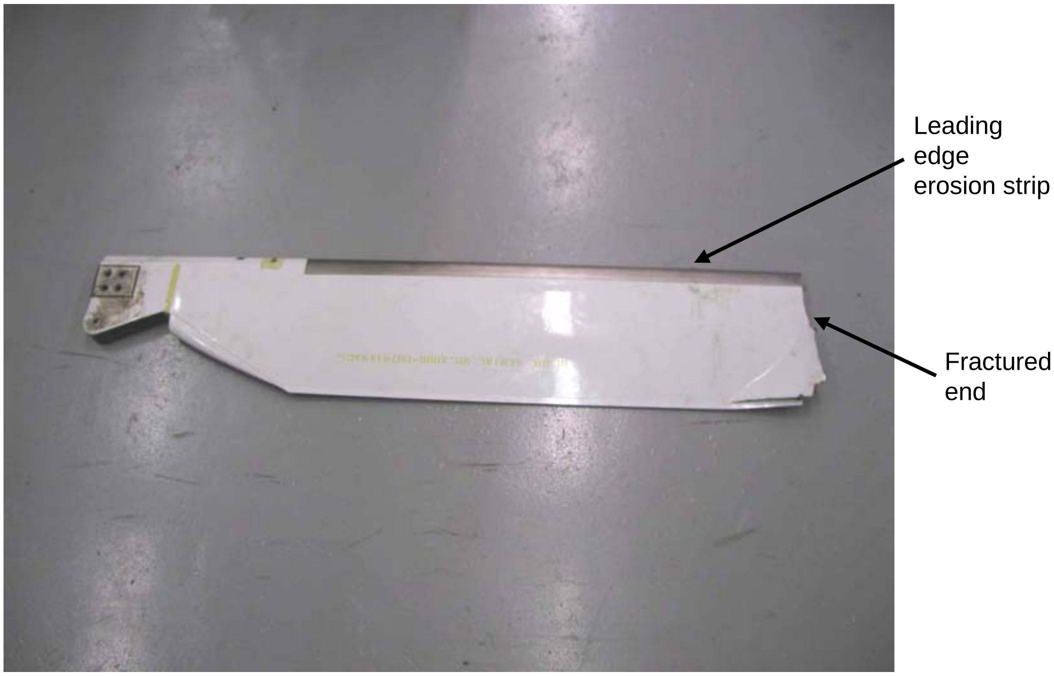

Figure 1. Inboard section of main rotor blade as-received.

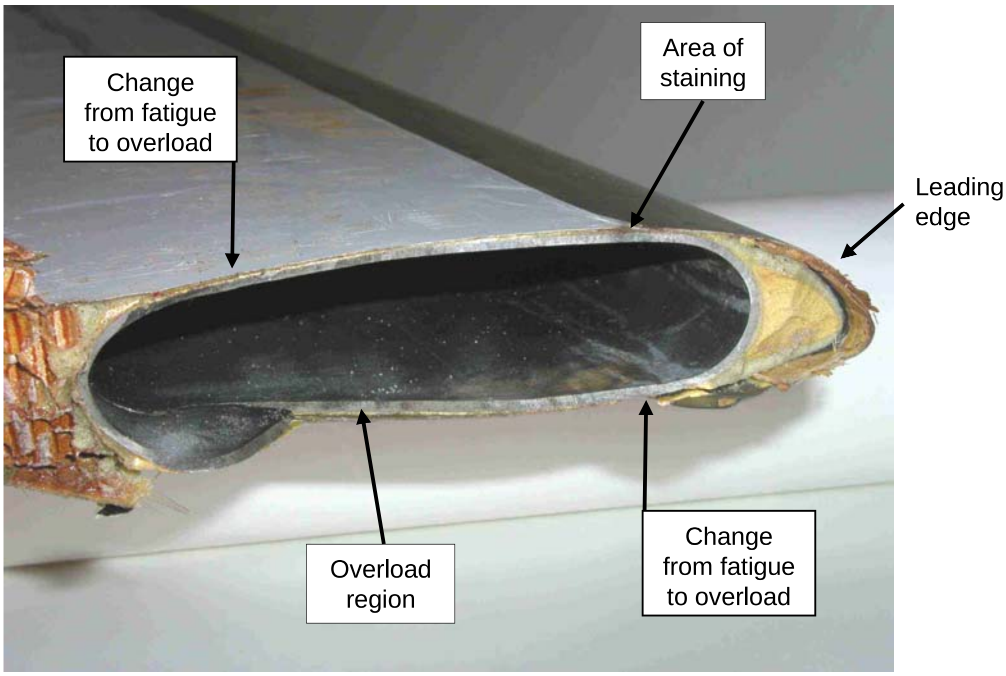

Figure 2. Fracture surface of main rotor blade spar as-received. Arrows indicate position of change in fracture surface

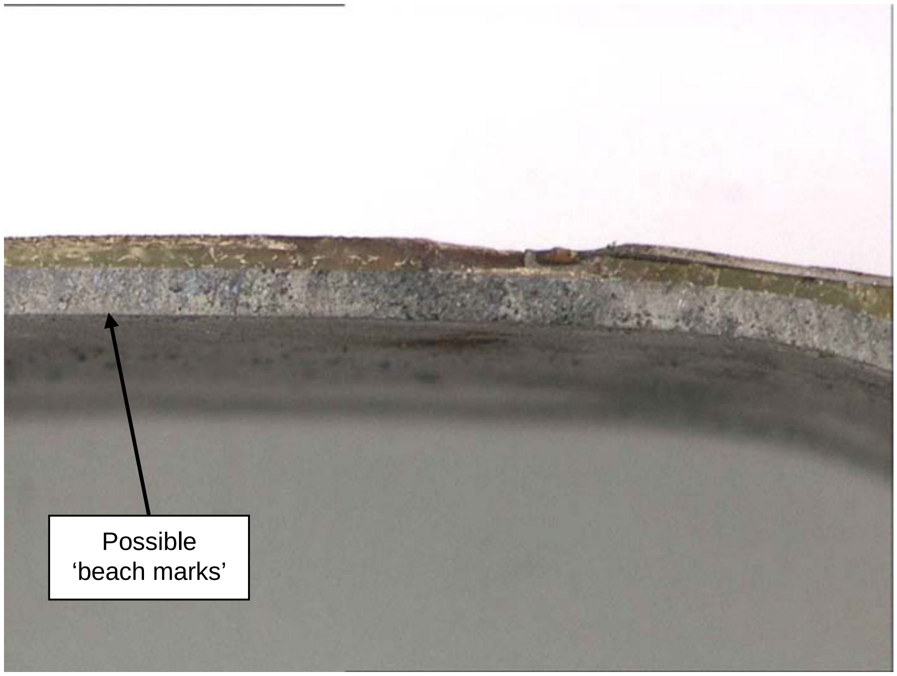

Figure 3. Stain on fracture surface at top of spar (identified in figure 2).

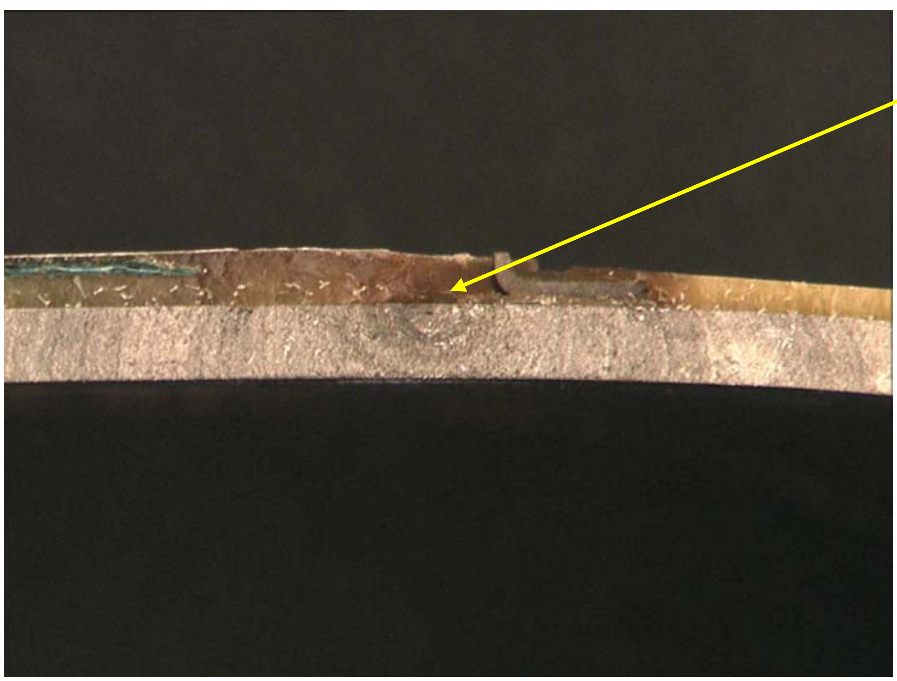

Figure 4. Fracture surface in region of straining (figure 3) after cleaning.

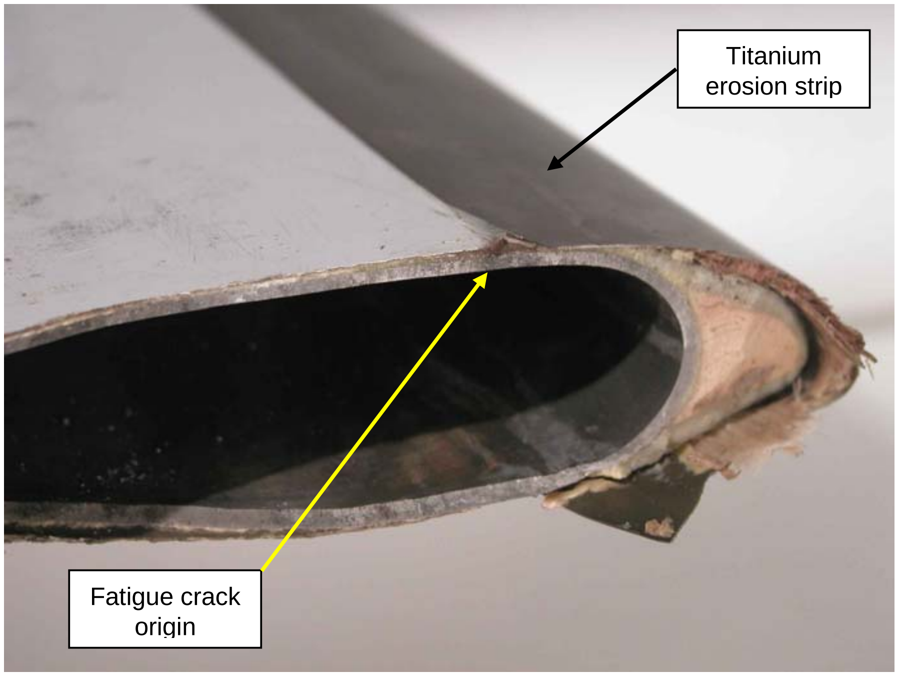

Figure 5. Position of fatigue crack origin with respect to erosion strip.

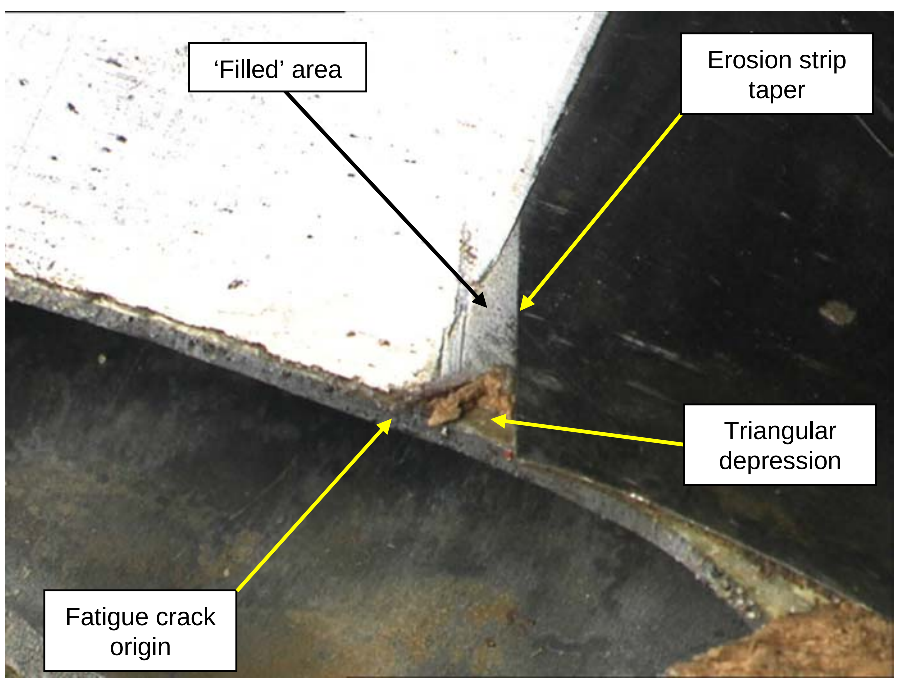

Figure 6. Detail of blade at edge of fracture face

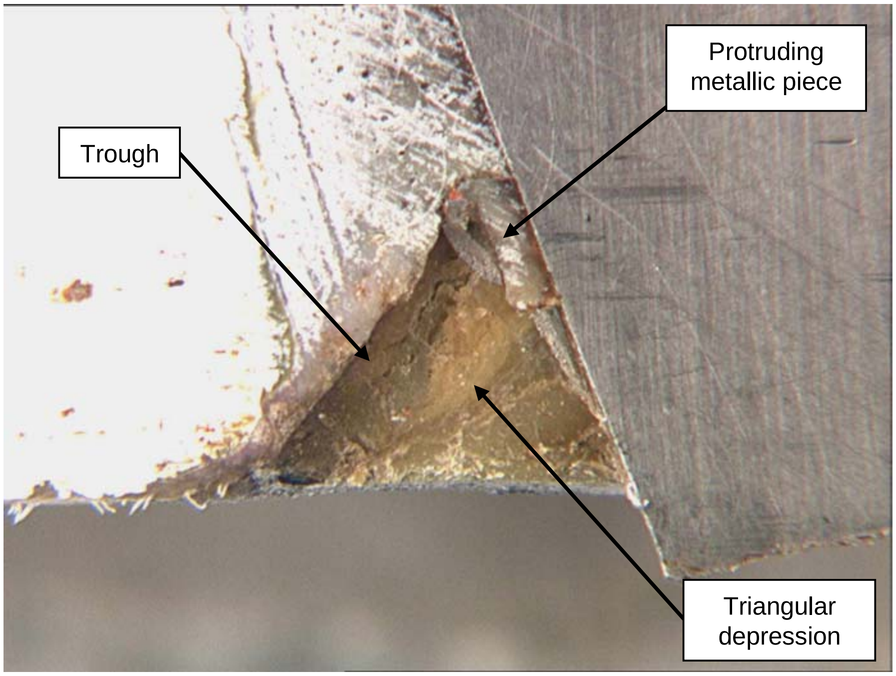

Figure 7. Detail of triangular depression.

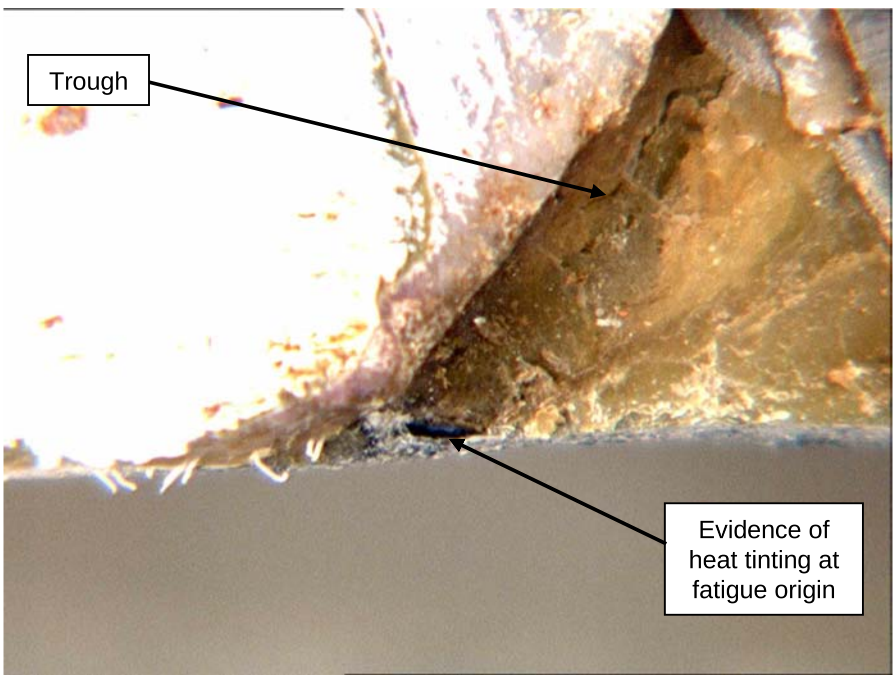

Figure 8. Detail of trough within triangular depression.

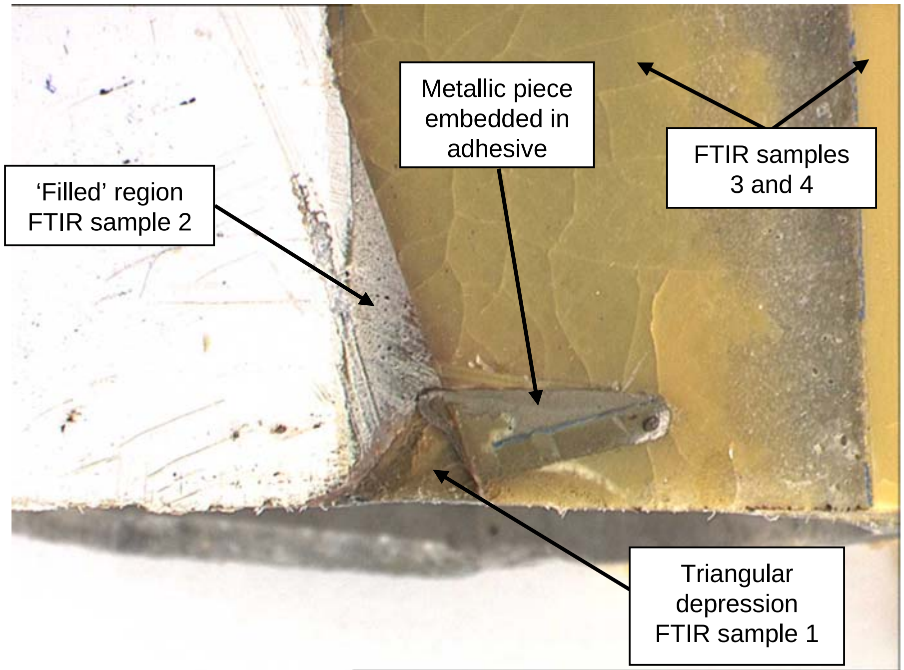

Figure 9. View of blade top surface after removal of erosion strip.

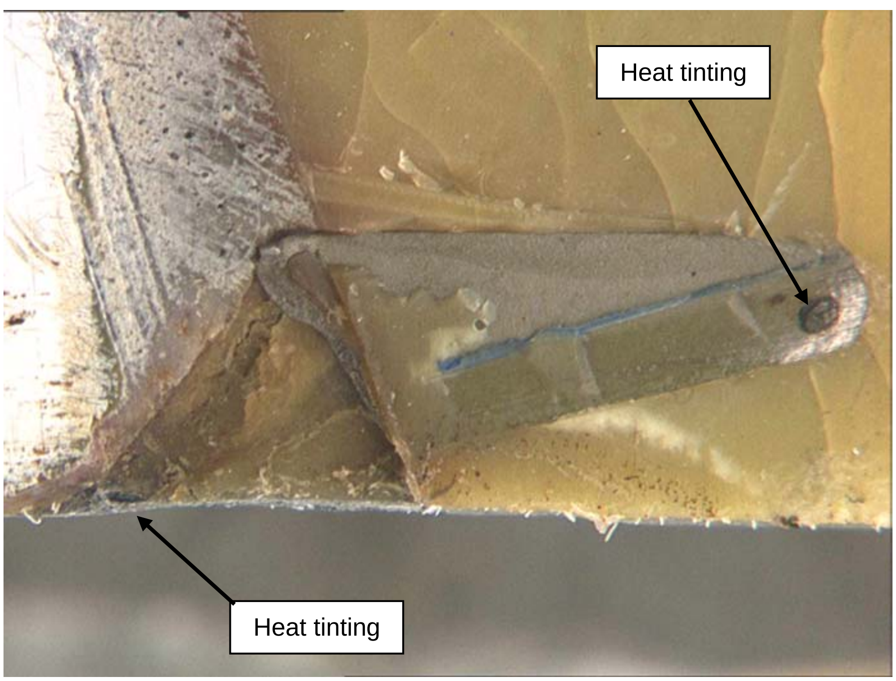

Figure 10. Detail view of figure 9.

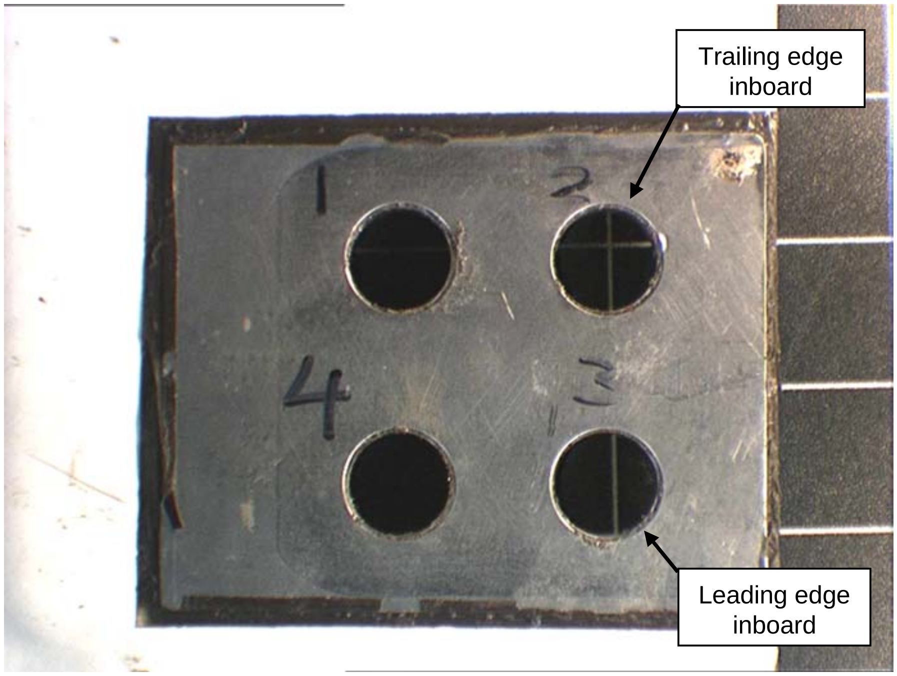

Figure 11. Root end of rotor blade showing position of attachment holes.

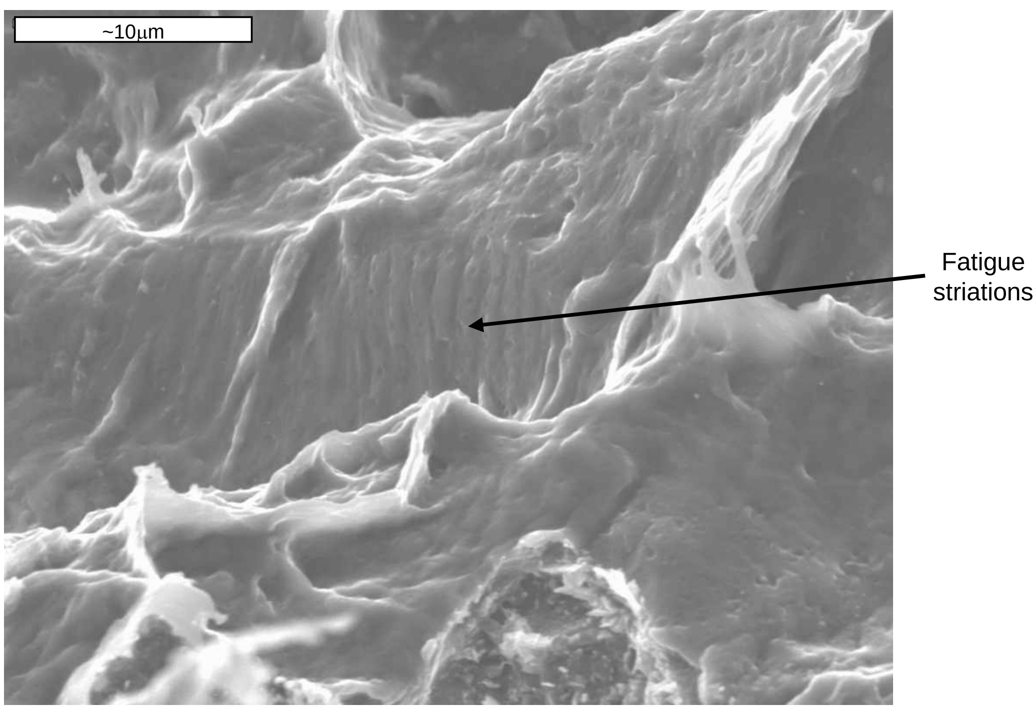

Figure 12. Replica of fracture surface towards end of leading edge crack.

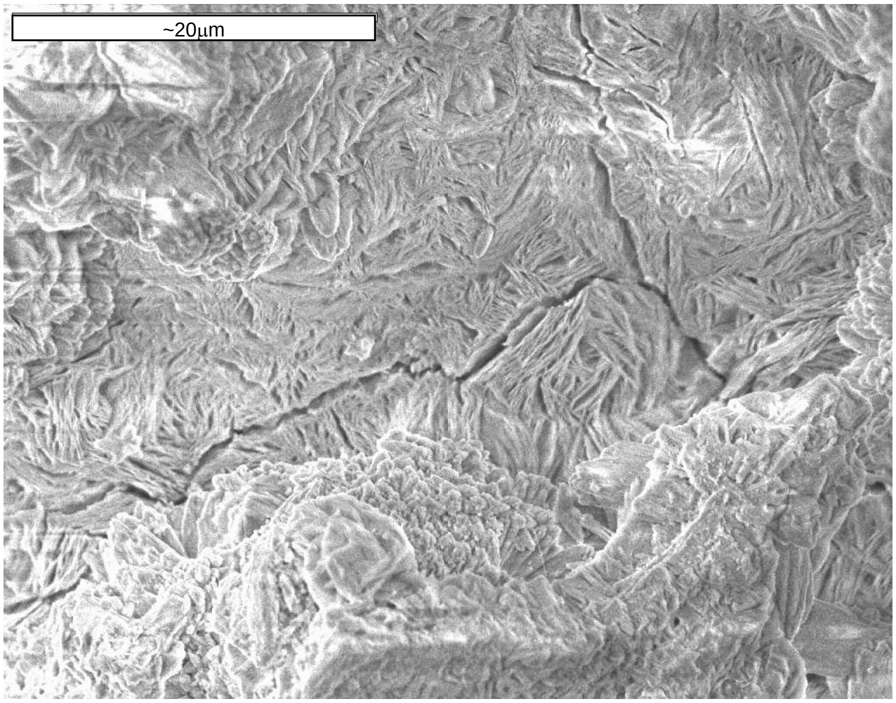

Figure 13. Deposit on fracture surface of rotor blade.

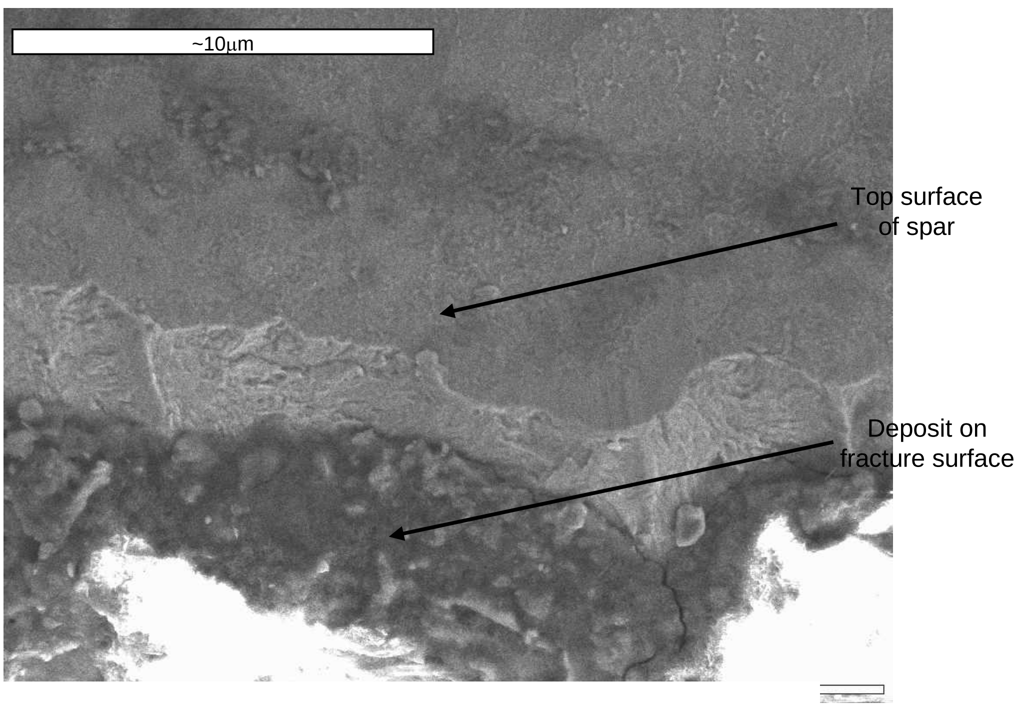

Figure 14. Deposit at origin of fatigue crack.

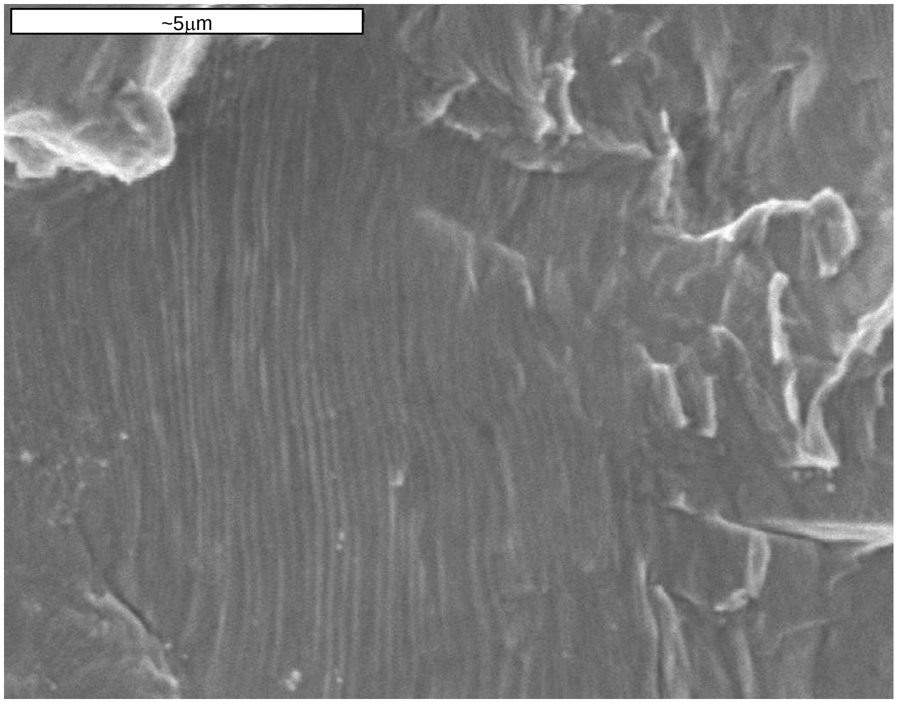

Figure 15. Fatigue striations observed on fracture surface between the deposit.

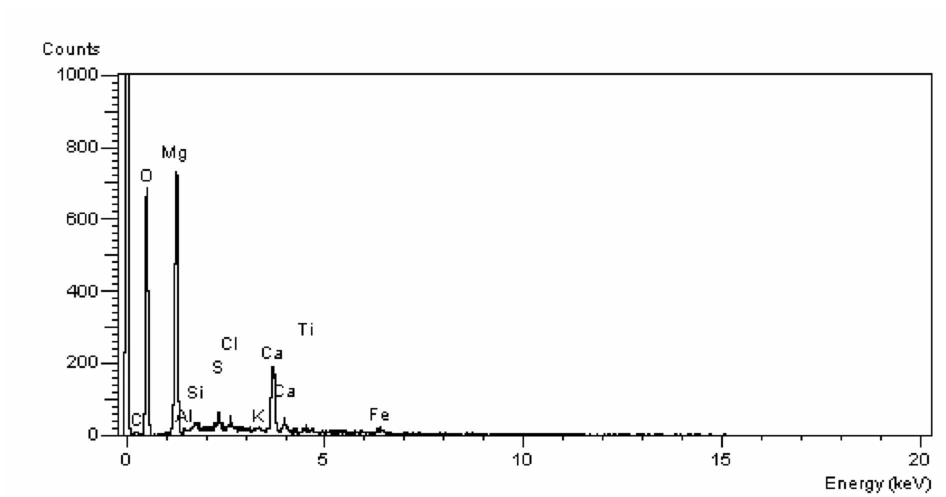

Figure 16. EDX spectrum from fracture surface deposit.

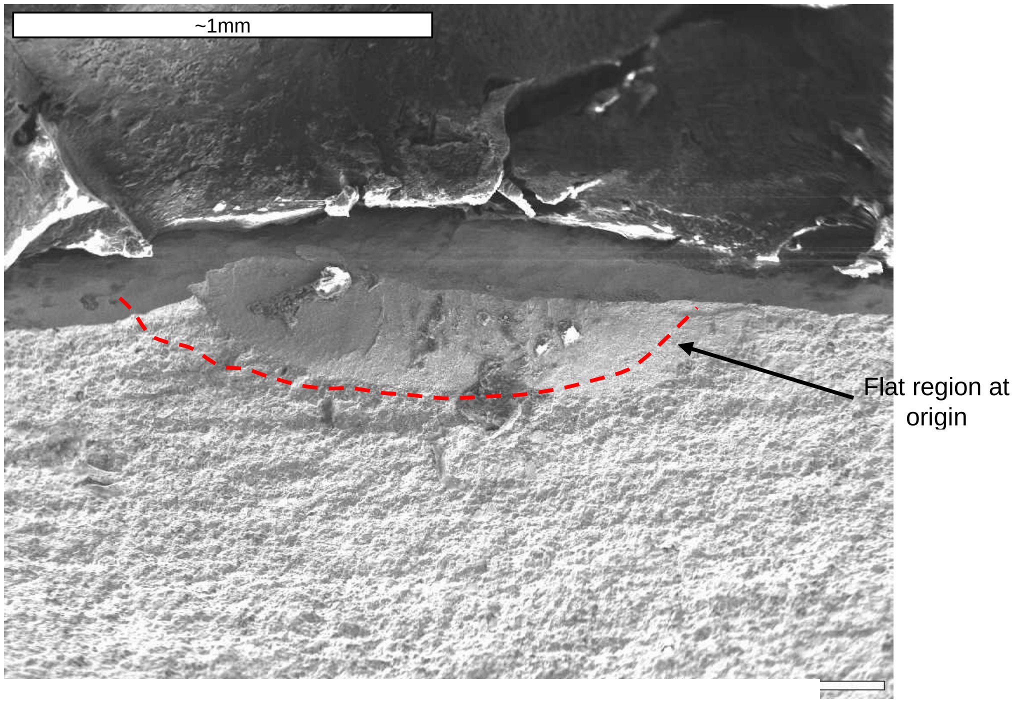

Figure 17. Fracture surface at fatigue crack origin after cleaning.

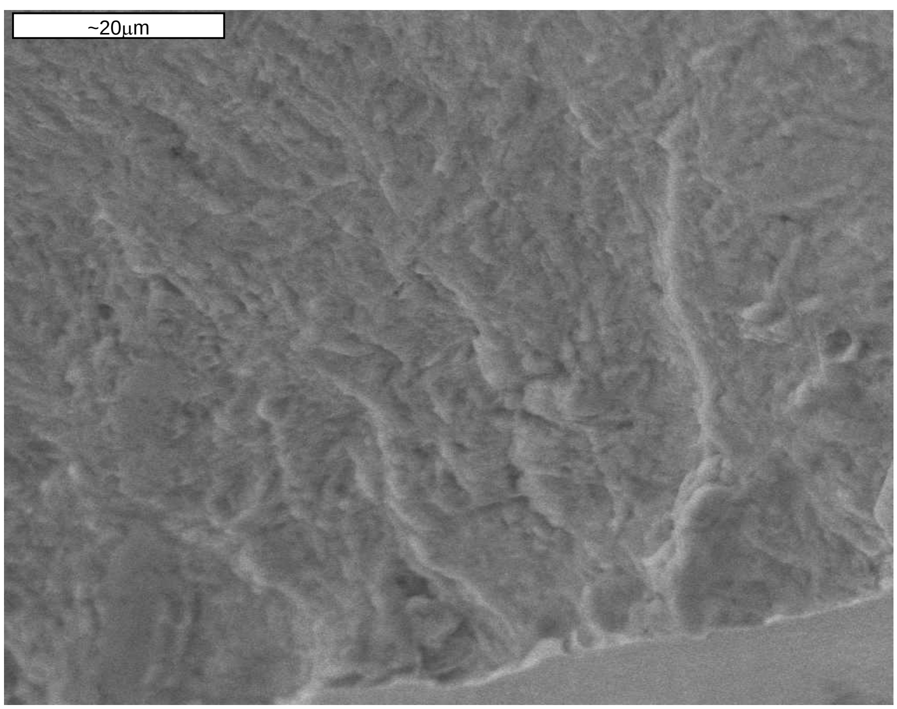

Figure 18. Fracture surface within flat region identified in figure 17.

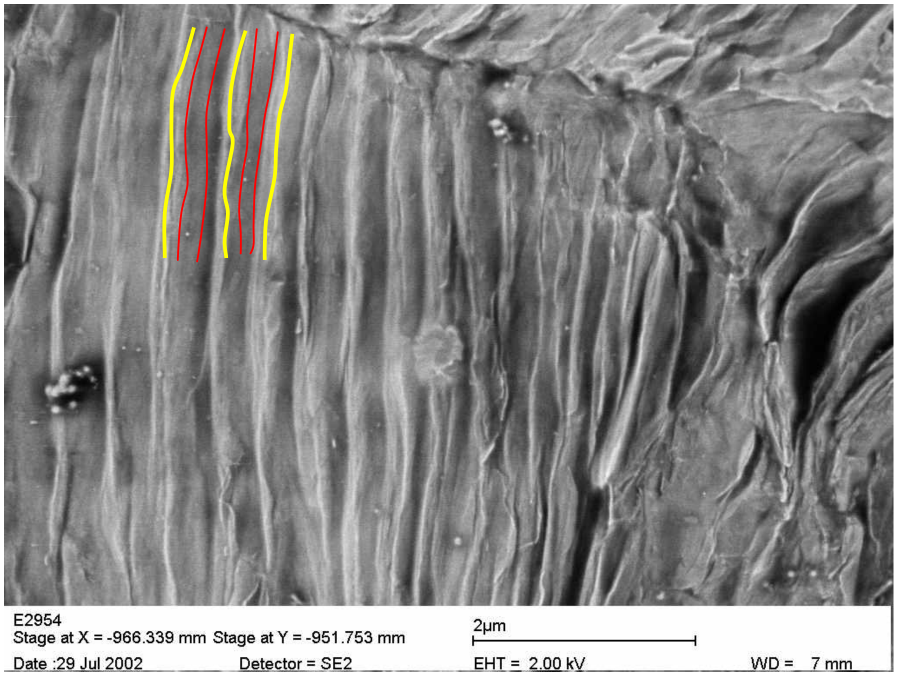

Figure 19. Striations on fracture surface.

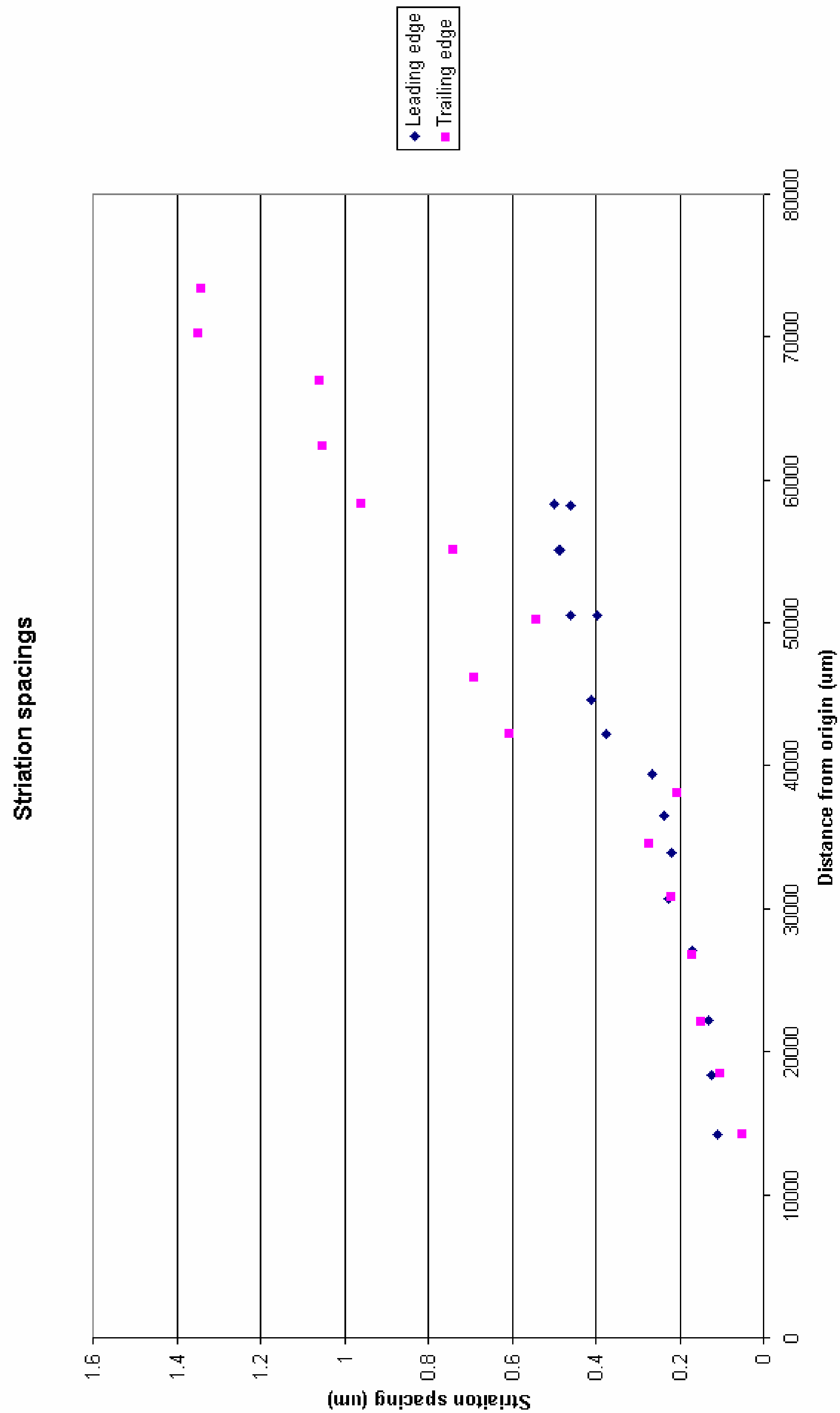

Figure 20. Striation spacing of leading and trailing edge cracks.

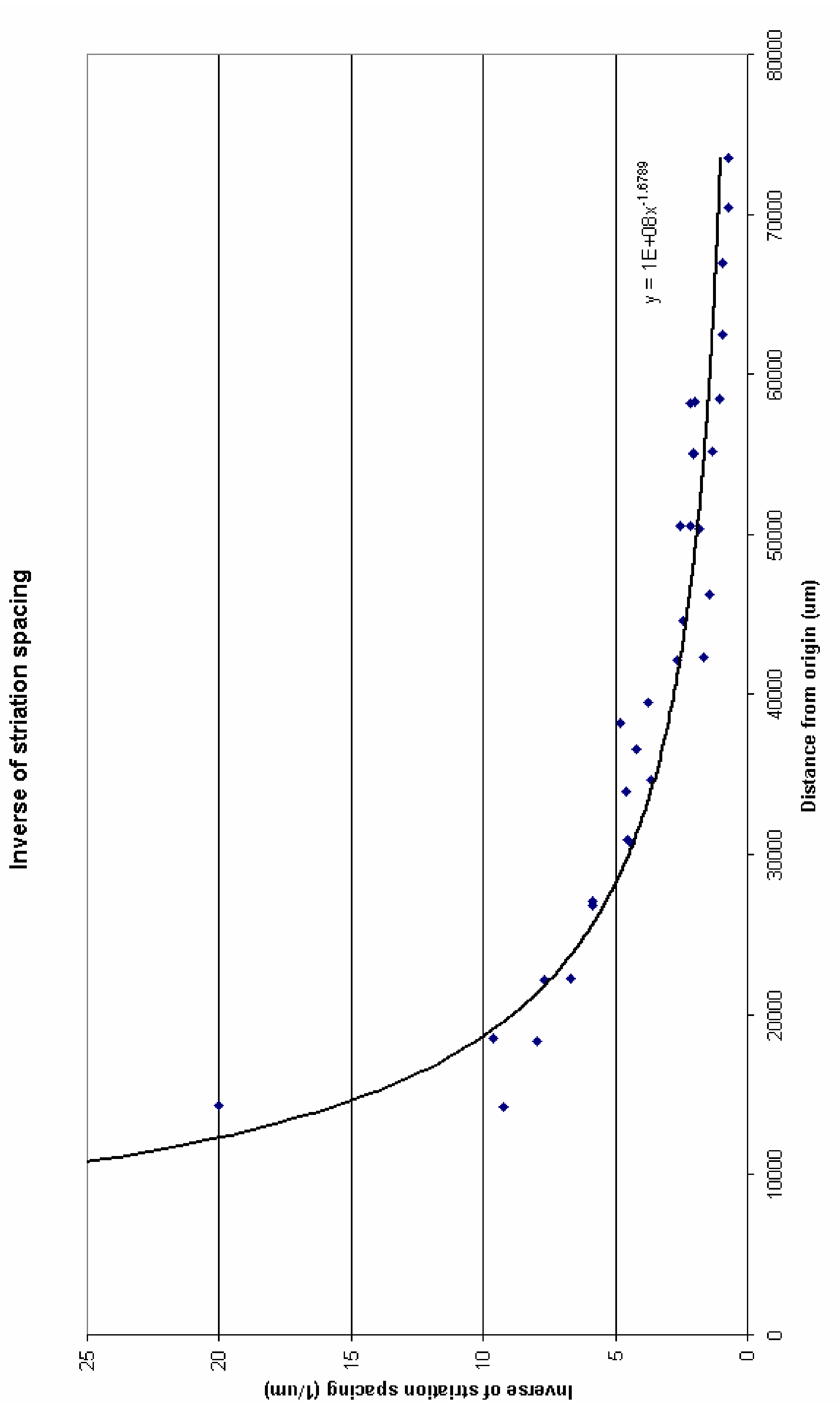

Figure 21. Inverse of striation spacing of leading and trailing edge cracks.

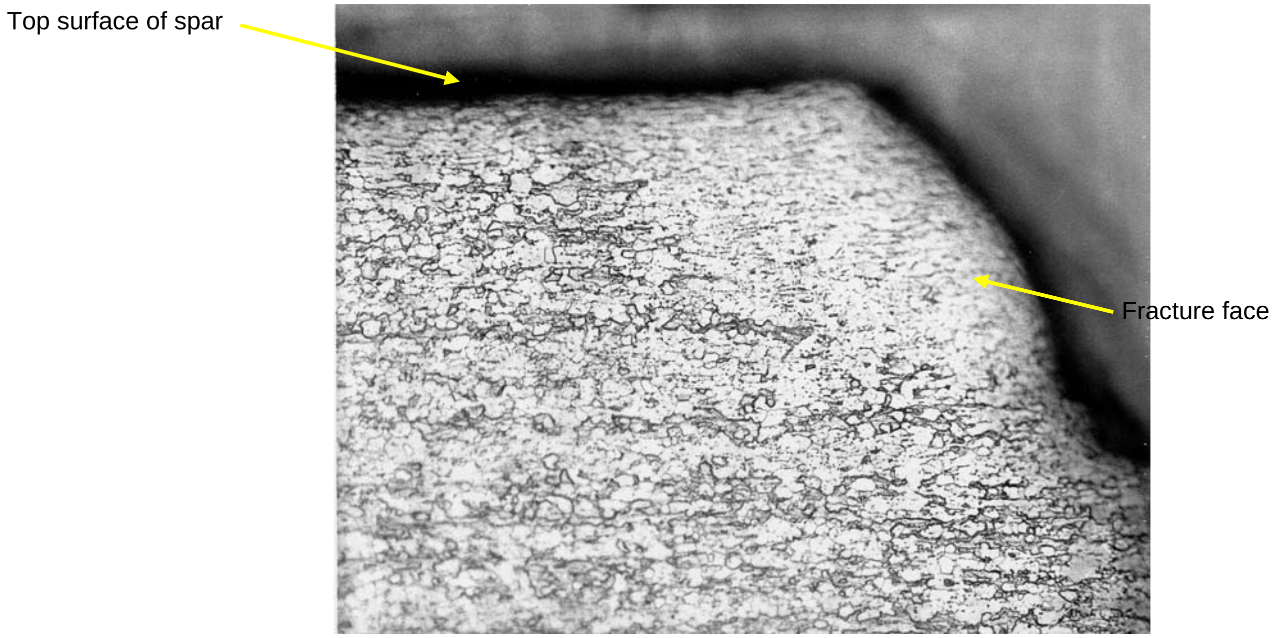

Figure 22. Microstructure at cross-section through fatigue crack origin. Mag x 200

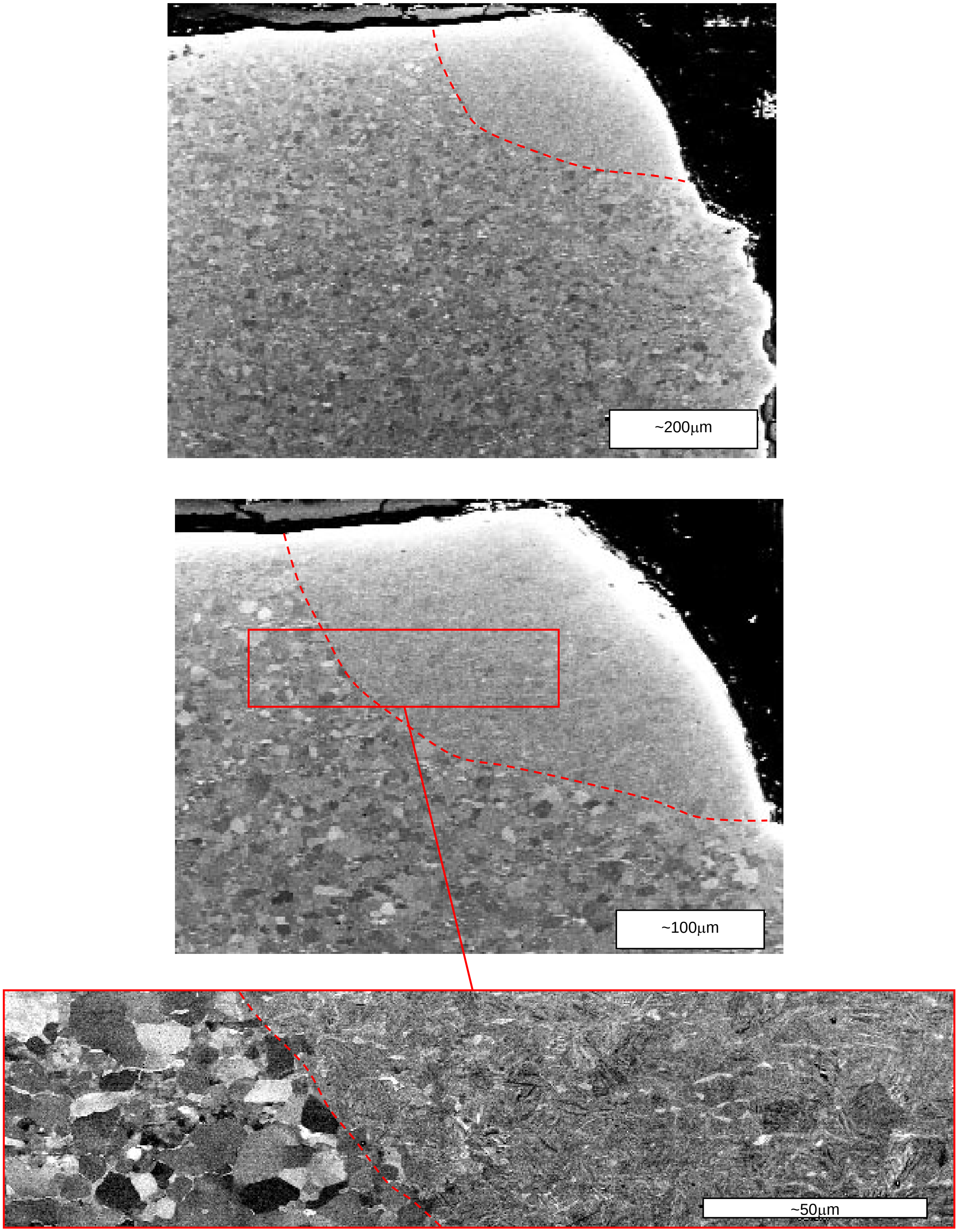

Figure 23. SEM images of microstructure at cross-section through fatigue crack origin.

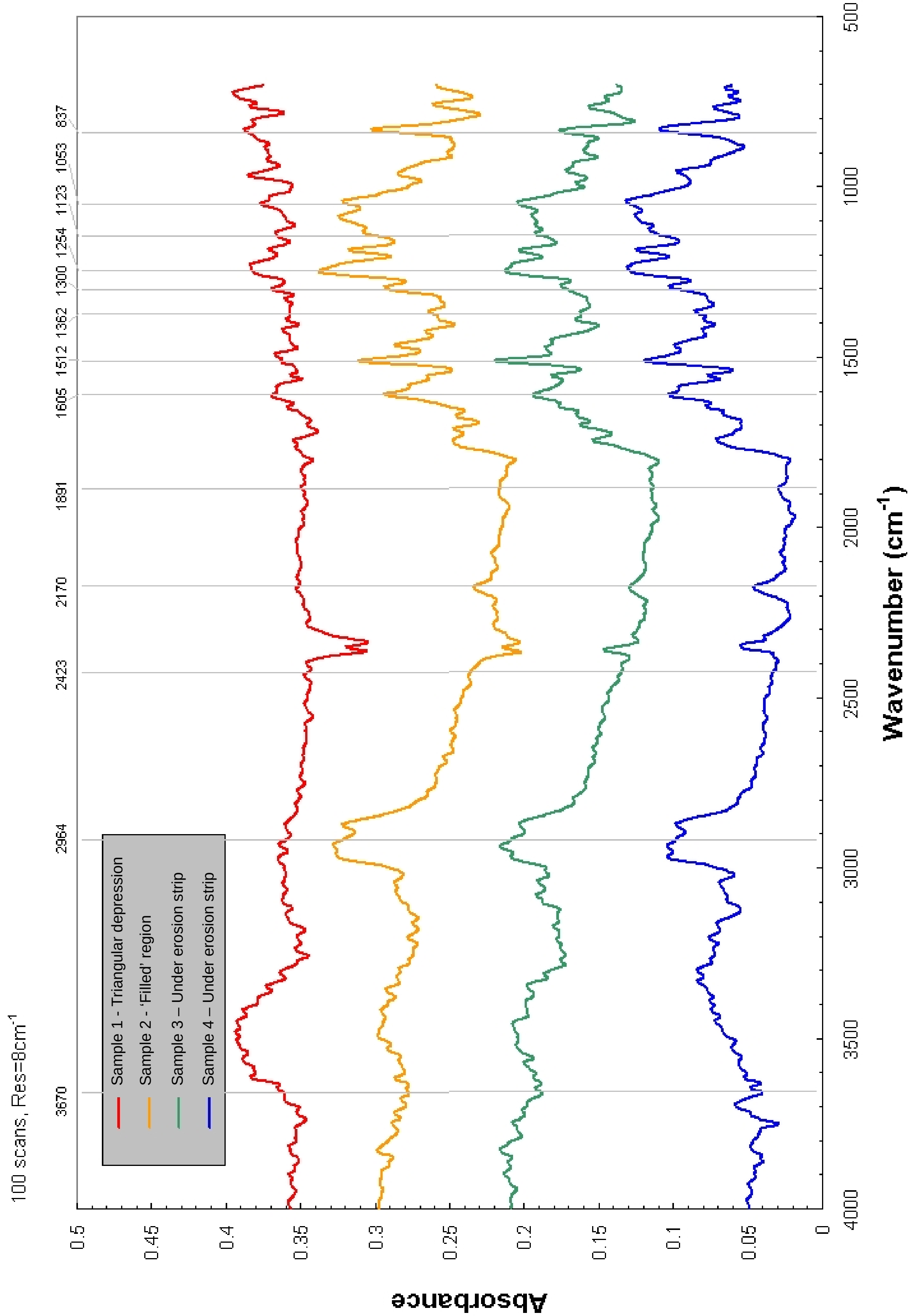

Figure 24. FTIR trace of adhesive at origin of failure.

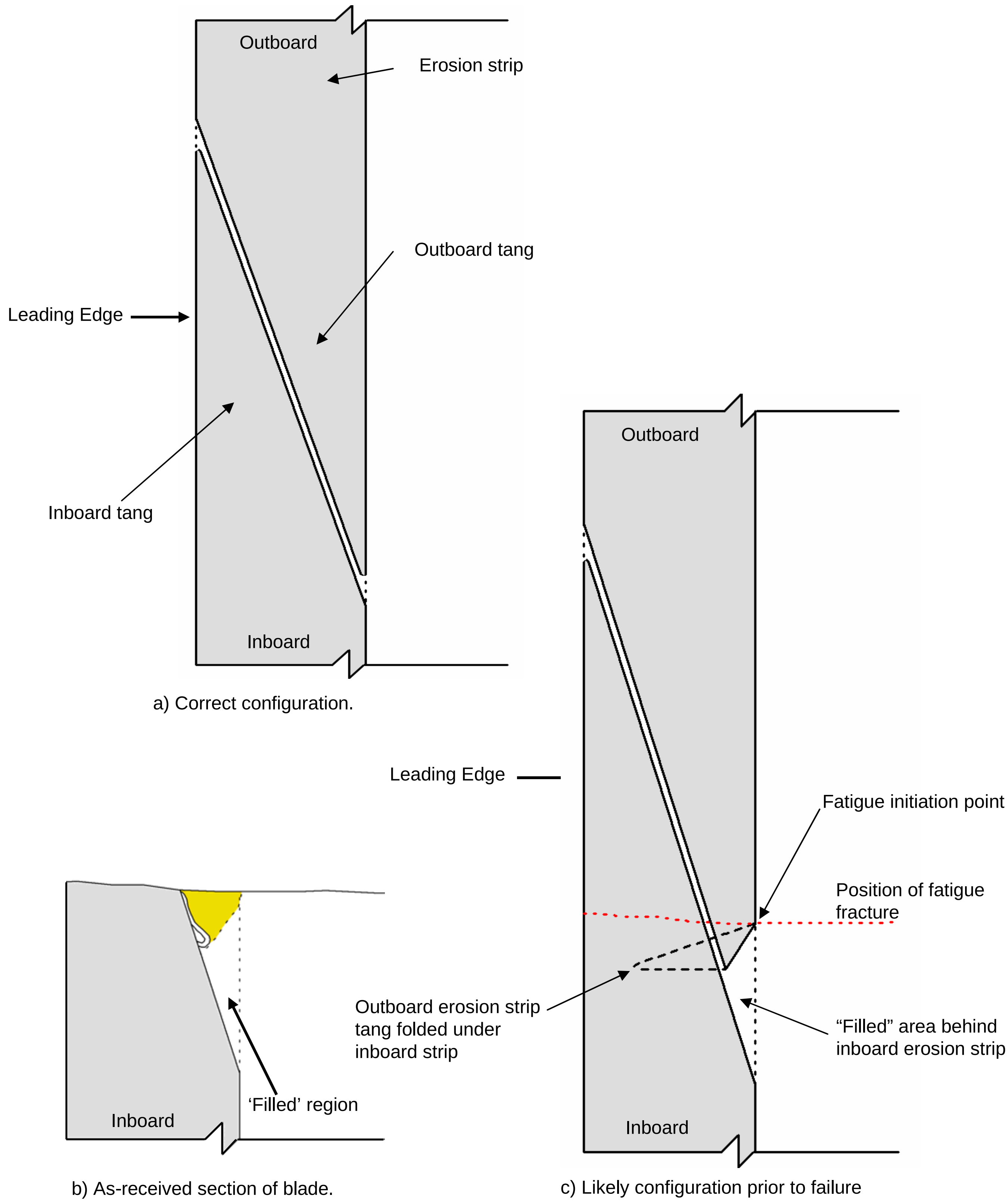

Figure 25. Scarf joint configuration.

APPENDIX A

Striation spacing data

	Distance from origin		Striation spacing	
	mm	μm	μm	1/μm
Leading Edge	58.30	58304	0.5	2
	58.23	58232	0.459	2.178649
	55.06	55061	0.488	2.04918
	55.05	55046	0.484	2.066116
	50.55	50547	0.46	2.173913
	50.50	50501	0.396	2.525253
	44.64	44636	0.41	2.439024
	42.18	42182	0.375	2.666667
	39.46	39462	0.266	3.759398
	36.56	36562	0.237	4.219409
	33.89	33889	0.218	4.587156
	30.76	30763	0.225	4.444444
	27.10	27098	0.171	5.847953
	22.16	22157	0.13	7.692308
	18.35	18349	0.1254	7.974482
	14.24	14238	0.108	9.259259
	9.11	9114	---	---
Origin	0.00	0.00	0.0	0.0
	14.30	14303	0.05	20
	18.52	18522	0.104	9.615385
	22.24	22244	0.15	6.666667
	26.85	26854	0.17	5.882353
	30.92	30920	0.22	4.545455
	34.62	34623	0.273	3.663004
	38.20	38198	0.207	4.830918
	42.35	42349	0.605	1.652893
	46.25	46250	0.69	1.449275
	50.35	50352	0.54	1.851852
	55.16	55161	0.74	1.351351
	58.46	58463	0.96	1.041667
	62.46	62463	1.05	0.952381
	66.99	66990	1.06	0.943396
	70.39	70390	1.35	0.740741
Trailing Edge	73.49	73492	1.34	0.746269

APPENDIX B

Flight Data

Date	Landings (total)	Engine Starts (total)	Hours (total)
16 Jul	13	4	5:20
11 Jul	4 (17)	1 (5)	1:00 (6:20)
10 Jul	2 (19)	1 (6)	1:26 (7:46)
9 Jul	6 (25)	2 (8)	4:02 (11:48)
7 Jul	7 (32)	1 (9)	0:47 (12:35)
7 Jul	4 (36)	1 (10)	0:24 (12:59)
7 Jul	8 (44)	1 (11)	1:31 (14:30)
6 Jul	2 (46)	2 (13)	0:46 (15:16)
5 Jul	16 (62)	6 (19)	4:15 (19:31)
5 Jul	3 (65)	0 (19)	0:17 (19:48)
5 Jul	5 (70)	0 (19)	0:49 (20:37)
4 Jul	6 (76)	2 (21)	2:20 (22:57)
3 Jul	24 (100)	4 (25)	4:39 (27:36)
2 Jul	12 (112)	3 (28)	4:23 (31:59)
27 Jun	10 (122)	2 (30)	1:53 (33:52)
26 Jun	2 (124)	1 (31)	0:28 (34:20)
24 Jun	6 (130)	1 (32)	1:49 (36:09)
14 Jun	10 (140)	4 (36)	3:20 (39:29)
13 Jun	22 (162)	4 (40)	6:09 (45:38)
12 Jun	15 (177)	6 (46)	5:22 (51:00)
11 Jun	16 (193)	3 (49)	3:56 (54:56)
10 Jun	12 (205)	2 (51)	2:48 (57:44)
6 Jun	15 (220)	4 (55)	4:49 (62:33)
5 Jun	4 (224)	2 (57)	2:16 (64:49)
4 Jun	13 (237)	2 (59)	2:08 (66:57)
3 Jun	19 (256)	3 (62)	2:31 (69:28)
31 May	21 (277)	2 (64)	3:01 (72:29)
30 May	8 (295)	1 (65)	1:54 (74:23

CRACK PROGRESSION FORWARDS FROM THE INITIATION POINT TO FINAL FAILURE IN RELATION TO FLYING HOURS (QINETIQ DATA)

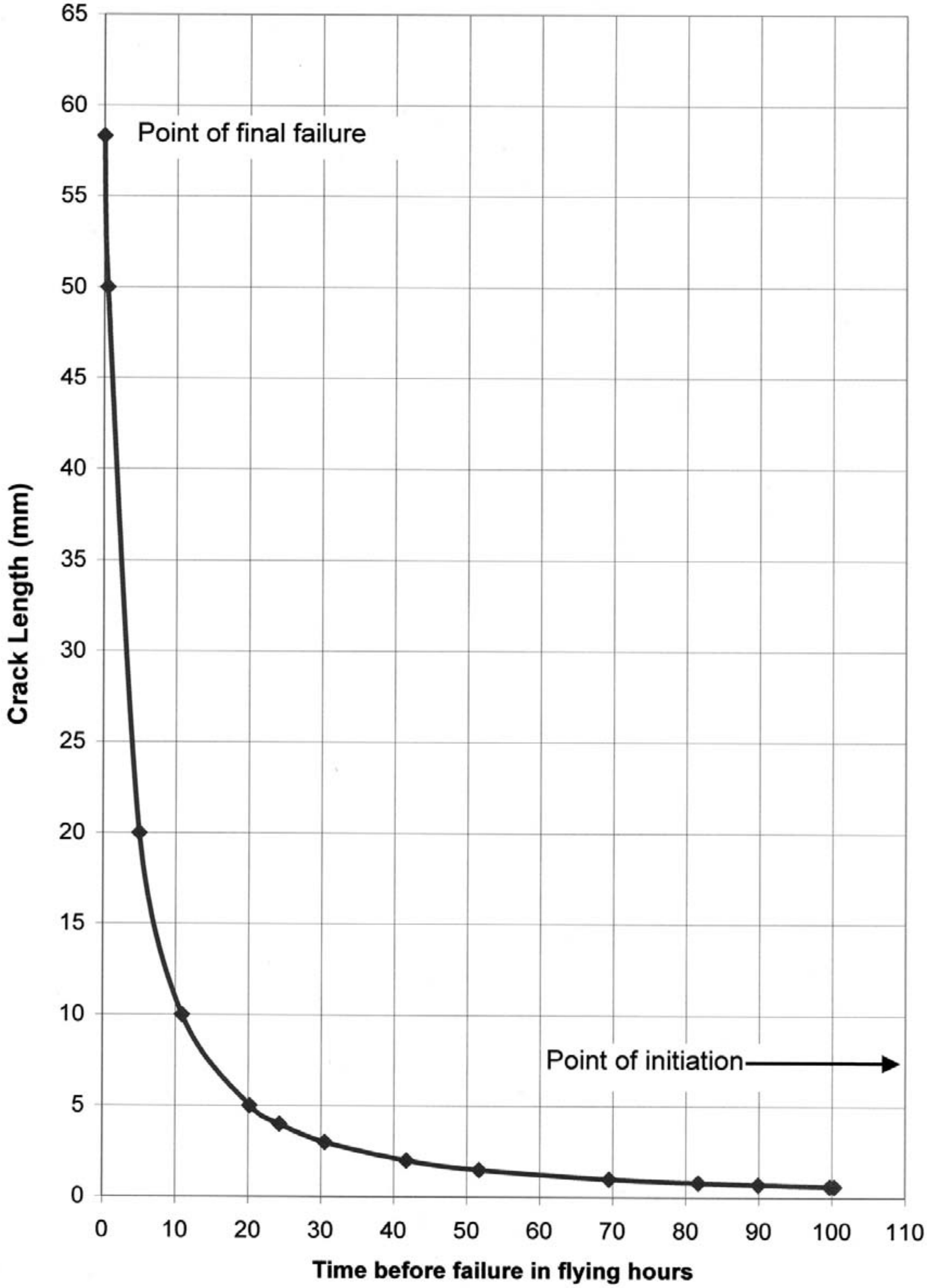

CRACK PROGRESSION REARWARDS FROM THE INITIATION POINT TO FINAL FAILURE IN RELATION TO FLYING HOURS (QINETIQ DATA)

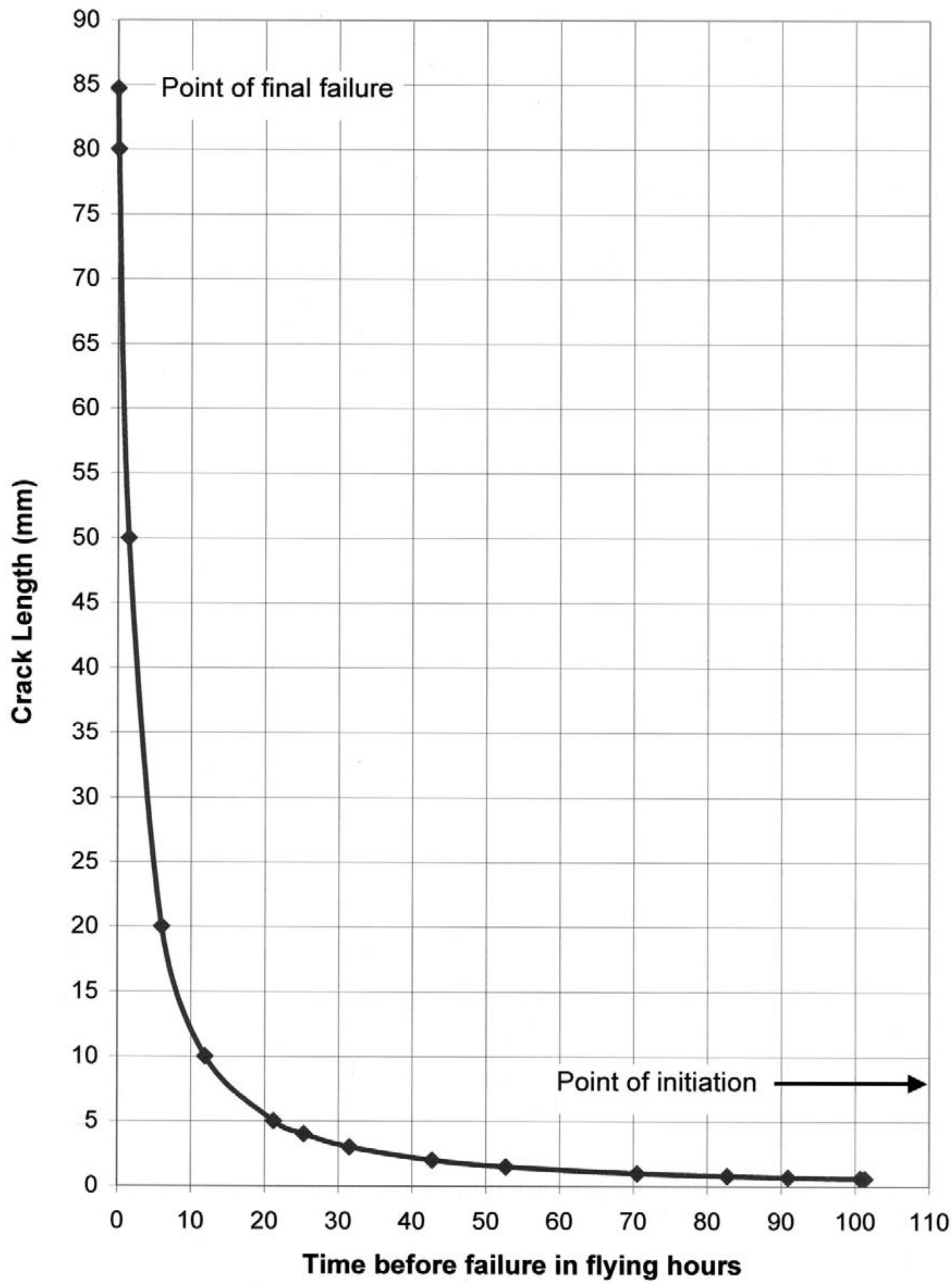

TOTAL CRACK LENGTH IN RELATION TO FLYING HOURS (QINETIQ DATA)

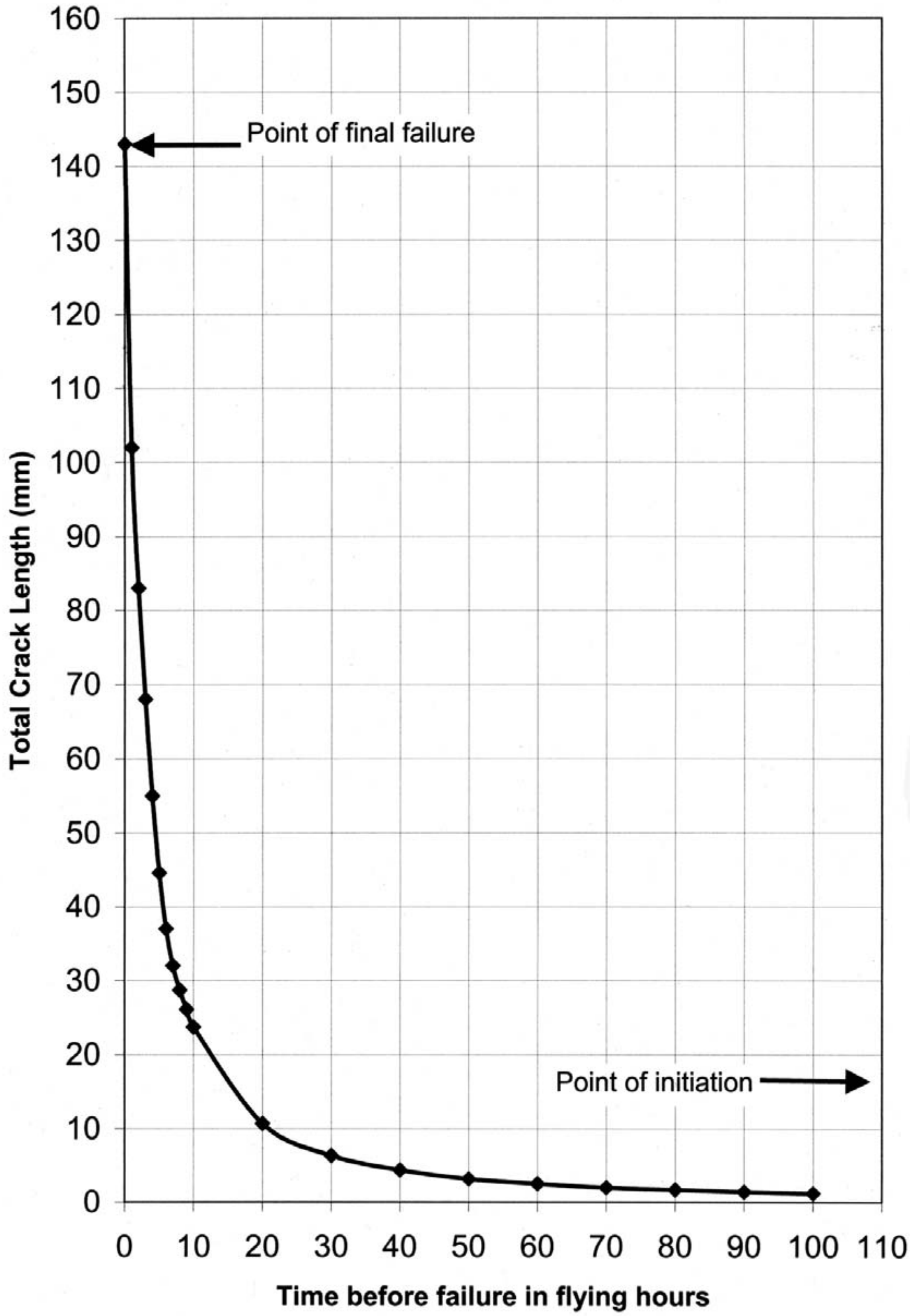

EXTRACT FROM SIKORSKY STRIATION COUNT DOCUMENT

Methods

The fracture surface was lightly brushed with Alconox and rinsed. QinetiQ had cleaned the surface previously in dilute nitric acid. Three sets of cleaning replicas were pulled from the fracture surface. Numerous replicates for the striation count were obtained. These were negative Pt/C shadowed and examined in the TEM[1].

Results

The fatigue zone propagated from a single origin located on the top surface of the spar approximately 35 mm inboard from the leading edge and corresponding with the position of the trailing edge of the titanium erosion strip. The initial propagation was from the origin to the breakthrough of the inside spar wall. Subsequent propagation was from the breakthrough equivalent (BTE) locations laterally in both trailing and leading edge directions. The BTE, occurs at approximately 2.0 mm from the origin.

The estimated number of striations from the origin to the BTE was 49,300. From the BTE the estimated number of striations in the trailing direction was 438,100. The total estimated number of striations on the trailing section inclusive of the origin to final fracture was 487,400. The density at 85mm from the BTE was 1.6 striations/micron. From the BTE the estimated number of striations in the leading edge direction was 529,400. The total estimated number of striations in the leading direction inclusive of the origin to final fracture was 578,700. Data from Sikorsky and QinetiQ at comparable locations is shown in Table 3.

Discussion

Sikorsky Aircraft (TEM) striation data shows that densities (striations/micron) are similar at several locations to the QinetiQ (FEM) data. For example, on the trailing side of the crack at 25 mm BTE the Sikorsky average density was 5.6 and the QinetiQ density was 5.9 and at 36 mm BTE the Sikorsky average was 4.8 as was the QinetiQ. There were also differences such as the average density of 7.7 vs. 3.7 at 33 mm. Beyond 44mm the Sikorsky densities are consistently slightly higher than those from QinetiQ. (Note: To make any direct comparisons between data from the two laboratories, 2 mm was subtracted from locations that were a distance from the origin rather than a distance from the BTE)

The last data point on the trailing side (where the crack was visible) was at 85mm from the BTE (Sikorsky data). The last data point given by QinetiQ was at 71.49mm from the BTE.

[1] Transmission Electron Microscope

The author states in the report, however, that the number of cycles was calculated between 14mm and 82.7mm from the origin (same as 12mm and 80.7 from the BTE).

There are differences in the total numbers of striations calculated. For example, on the trailing edge fracture surface from 12 mm to 85 mm from the Sikorsky observed 226,900 striations while QinetiQ counted 158,824 striations from 12mm to 72mm. On the leading edge fracture surface from 12mm to 68mm Sikorsky observed 334,400 striations and QinetiQ counted 137,402 from 12mm to 56mm.

The differences in densities can be attributed in part to the instrumentation used. The resolution of striations is greater in a TEM than in a FEM[2]. Because of the physics of the electron beam, more subsurface features are resolved in the SEM. Finer surface striations are more resolvable in the TEM. The sample preparation technique involved in TEM also enhances surface features by using Pt/C shadowing.

Total number of striations from the origin to the end of the fatigue zone was 487,400 and 578,700 for the trailing edge and leading edge respectively according to Sikorsky procedure. The formula used by Sikorsky is conservative. By applying that formula to the QinetiQ data the total in the trailing direction is 423,900 and in the leading direction is 287,200. This analysis of the QinetiQ data produces a low count because the integration assumes constant growth rate from the origin to 14mm.

Using the blade RPM of 304, QinetiQ estimated the time required for crack growth from approximately 14 mm from the origin to final failure to be 8.7 hrs in the trailing edge direction and 7.5 hrs in the leading edge direction. Applying that principle to Sikorsky striation data results in the time required for crack growth from the origin to final failure to be 26.7 hrs in the trailing edge direction and 31.7 hrs in the leading edge direction. The propagation time could be longer since fatigue cracks can grow either intermittent or segmental at very slow growth rates resulting in larger striation spacing appearances than the growth rate would indicate.

Conclusions

1. QinetiQ underestimated the number of striations.

2. The differences in striation densities and totals are due to technique, instrumentation, and integration method.

[2] Field emission scanning Electron Microscope

Table 1 Striation Count Results for the Trailing Edge

Distance From Origin (mm)	Average Striation Per Micron	Incremental Distance (mm)	Incremental Count[1]	Comments[2]
0.6	20.0	0.6	12,000	only data point
0.8	20.0	0.8	16,000	only data point
1.5	18.0	0.7	12,600	
1.8	16.3	0.3	4,890	
1.9	20.0	0.1	2,000	only data point
2.0	17.7	0.1	1,770	
Estimated number of striations from origin =			49,300	

Distance From BTE (mm)	Average Striation Per Micron	Incremental Distance (mm)	Incremental Count[1]	Comments[2]
2.0	21.4	2.0	42,800	
4.0	20.9	2.0	41,800	
6.0	11.4	2.0	22,800	
8.0	17.1	2.0	34,200	
10.0	11.2	2.0	22,400	
12.0	15.1	2.0	30,200	
14.0	10.0	2.0	20,000	
16.0	8.6	2.0	17,200	
25.0	5.6	9.0	50,400	
29.0	4.5	4.0	18,000	
33.0	7.7	4.0	30,800	
36.0	4.8	3.0	14,400	
42.0	3.2	6.0	19,200	
44.0	2.4	2.0	4,800	
48.0	2.1	4.0	8,400	
53.0	1.8	5.0	9,000	
56.0	1.8	3.0	5,400	
60.0	1.7	4.0	6,800	
64.0	1.7	4.0	6,800	
73.0	1.5	9.0	13,500	
85.0	1.6	12.0	19,200	rubbed fatigue
93.0				very rubbed, patches of overload
Estimated number of striations from BTE =			438,100	
Total estimated number of striations =			487,400	

1. The fracture surface was very rubbed between the origin and the breakthrough of the wall, therefore the count should be considered a maximum.

2. No overload observed until approximately 75mm, however too rubbed to quantify, appears to be patchy.

Table 2 Striation Count Results for the Leading Edge

Distance From Origin (mm)	Average Striation Per Micron	Incremental Distance (mm)	Incremental Count[1]	Comments[2]
0.6	20.0	0.6	12,000	only data point
0.8	20.0	0.8	16,000	only data point
1.5	18.0	0.7	12,600	
1.8	16.3	0.3	4,890	
1.9	20.0	0.1	2,000	only data point
2.0	17.7	0.1	1,770	
Estimated number of striations from origin =			49,300	

Distance From BTE (mm)	Average Striation Per Micron	Incremental Distance (mm)	Incremental Count[1]	Comments[2]
1.2	17.0	1.2	20,400	only data point, rubbed
1.9	15.3	0.7	10,710	only data point, rubbed
2.5	16.0	0.6	9,600	rubbed
3.0	19.0	0.5	9,500	
8.0	12.5	8.0	100,000	
10.0	11.9	2.0	23,800	
12.0	10.5	2.0	21,000	
16.0	10.7	4.0	42,800	
20.0	9.7	4.0	38,800	
24.0	10.2	4.0	40,800	
29.0	6.8	5.0	34,000	
32.0	7.2	3.0	21,600	
44.0	6.4	12.0	76,800	
45.0	4.2	1.0	4,200	
46.0	4.1	1.0	4,100	
56.0	3.5	10.0	26,250	25% overload
57.0	4.8	1.0	3,600	only data point, 25% o'load
58.0	2.4	1.0	2,400	only data point, rubbed
68.0	3.9	10.0	39,000	
Estimated number of striations from BTE =			529,000	
Total estimated number of striations =			578,700	

1. Count should be considered a minimum due to rubbing.
2. Count reduced to reflect the amount of ductile overload.

Table 3 – Data of Sikorsky vs. QinetiQ at comparable locations

	SIKORSKY		**QINETIQ**	
	DISTANCE FROM BTE (MM)	**AVERAGE STRIATION PER MICRON**	**DISTANCE FROM BTE (MM)**	**AVERAGE STRIATION PER MICRON**
LEADING EDGE	12.0	10.5	12.0	9.3
	16.0	10.7	16.0	8.0
	20.0	9.7	20.0	7.7
	29.0	6.8	29.0	4.4
	32.0	7.2	32.0	4.6
	56.0	3.5	56.0	2.0
TRAILING EDGE	12.0	15.1	12.0	20.0
	25.0	5.6	25.0	5.9
	29.0	4.5	29.0	4.5
	33.0	7.7	33.0	3.7
	36.0	4.8	36.0	4.8
	44.0	2.4	44.0	1.4
	48.0	2.1	48.0	1.9
	53.0	1.8	53.0	1.4
	60.0	1.7	60.0	1.0

Sikorsky S76 Main Rotor Blade Failure – Striation Data Analysis

A Sikorsky S76 main rotor blade failure was examined by QinetiQ and is detailed in QinetiQ report QINETIQ/FST/SMC/LR024608 issue 2 (March 2003). Analysis of striation spacing along the crack length was used to estimate the likely time required for crack growth. Two cracks were present propagating in both trailing and leading edge directions. In both cracks, QinetiQ were unable to observe sufficient clear striations in the region from the origin to approximately 14mm in length to enable an accurate growth rate from origin to failure. The clearly observed striations from approximately 14mm to the ends of both cracks were measured and the crack growth rate for this period determined. The results for this are shown in table 1. The QinetiQ method of determining the total number of striations for crack growth uses a fitted curve power line through the striation density data, with integration of the curve to determine the number of striations. The power curve can be extrapolated back to the origin of the crack in order to estimate the total number of striations for crack growth and hence a total crack growth rate. This was carried out in QINETIQ/FST/SMC/LR024608 issue 2 and the results also shown in table 1.

Sikorsky were given access to the QinetiQ report and analysed the QinetiQ data using their preferred point-to-point method to determine the crack growth rates. However, they also wanted access to the fracture surfaces so that they could carry out their own striation spacing measurements using a transmission electron microscope (TEM) to try to observe striations in the region near the origin where QinetiQ were unable to with a field emission scanning electron microscope (SEM).

Sikorsky took acetate replicas of the fracture surfaces at AAIB premises, however, during the initial examination of the rotor blade (QINETIQ/FST/SMC/LR024608 issue 2), QinetiQ sectioned through the origin of the fatigue cracks after carrying out the striation counting to examine the microstructure. The fatigue origin had to be removed from an epoxy resin mount and combined with the remaining three sections of the fracture surface to reconstruct the original fracture. It must be noted that Sikorsky's replicas and measurements were taken from four sections of the original fracture, of which saw cuts and grinding/polishing of the origin will have removed material.

The Sikorsky results are shown in table 2 using the point-to-point method. Also shown are the results for the power line method, which QinetiQ applied to the Sikorsky data. Figure 1 shows a plot of both QinetiQ and Sikorsky data. It can be seen that the over the period of crack growth from approximately 14mm to the end of the crack, QinetiQ leading edge, trailing edge and Sikorsky trailing edge measurements were comparable. However, Sikorsky measured a slightly higher striation density in the leading edge.

Sikorsky's estimate of the number of striations from the origin to the final failure were significantly lower than QinetiQ's from origin to final failure. As stated in the original QinetiQ report (QINETIQ/FST/SMC/LR024608 issue 2) the QinetiQ measurements from 14mm to final failure can be considered a good estimate of the number of striations present. Any estimates from the origin to 14mm must be used cautiously as assumptions were made that the extrapolated curve fits the actual crack growth. With this in mind, QinetiQ used the Sikorsky results for the period of crack growth at the origin in which clear striations were not observed with the SEM and combined them with the QinetiQ data from approximately 14mm to final crack growth. The results are shown in table 3. The data has also been plotted in figures 1, 2 and 3.

It was clear that Sikorsky had overestimated the fatigue crack length in the leading edge. QinetiQ measured the crack lengths in the trailing edge as 84.7mm and the leading edge as 58.3mm, whereas Sikorsky measured 87mm and 70.0mm respectively. The difference in the trailing edge is most likely due to the fact the Sikorsky made measurements on a reconstructed fracture surface and therefore the difference is unlikely to be significant. However, the difference in the leading edge crack length does not appear to be due to recombining sections of the fracture. Between 58.0mm (end of fatigue crack measured by QinetiQ) and 70.0mm, Sikorsky indicated that 25% of the fracture was overload with fatigue present within. QinetiQ did observe parallel bands running in some areas of the overload crack growth, however the banding did not follow a single direction and did not cross grain boundaries. QinetiQ assumed that the banding was a result of the microstructure of the material, which did show some lamella structure (figure 4) that could be mistaken for striations on an acetate replica. It is therefore assumed that the fatigue crack in the leading edge did end at 58.3mm from the origin and that Sikorsky had observed the material microstructure in the overload region and mistaken it for fatigue striations.

The Sikorsky data used by QinetiQ for the fatigue crack growth near the origin is based on the data reported in Sikorsky Material Analysis Request No. MAR-ON0403251 (26/02/2004). QinetiQ did not have access to TEM photographs with which to verify the striation spacing measurements.

Trailing Edge		
14,030 μm to fatigue end (measured)	158,824 striations	8.7 hrs
Origin to end (extrapolated data)	1,848,253 striations	101.3 hrs
Leading Edge		
14,238 μm to fatigue end (measured)	137,402 striations	7.5 hrs
Origin to end (extrapolated data)	1,829,071 striations	100.3 hrs

Table 1. QinetiQ striation counting measurements using power line method.

Trailing Edge		
Origin to end (point-to-point)	473,760	26.0 hrs
Origin to end (power line)	542,704	29.8 hrs
Leading Edge		
Origin to end (point-to-point)	527,520	28.9 hrs
Origin to end (power line)	537,008	29.4 hrs

Table 2. Sikorsky striation counting measurements.

Trailing Edge		
Origin to end (combined data)	444,712	24.4 hrs
Leading Edge		
Origin to end (combined data)	388,025	21.3 hrs

Table 3. Combined data striation counting measurements using power line method.

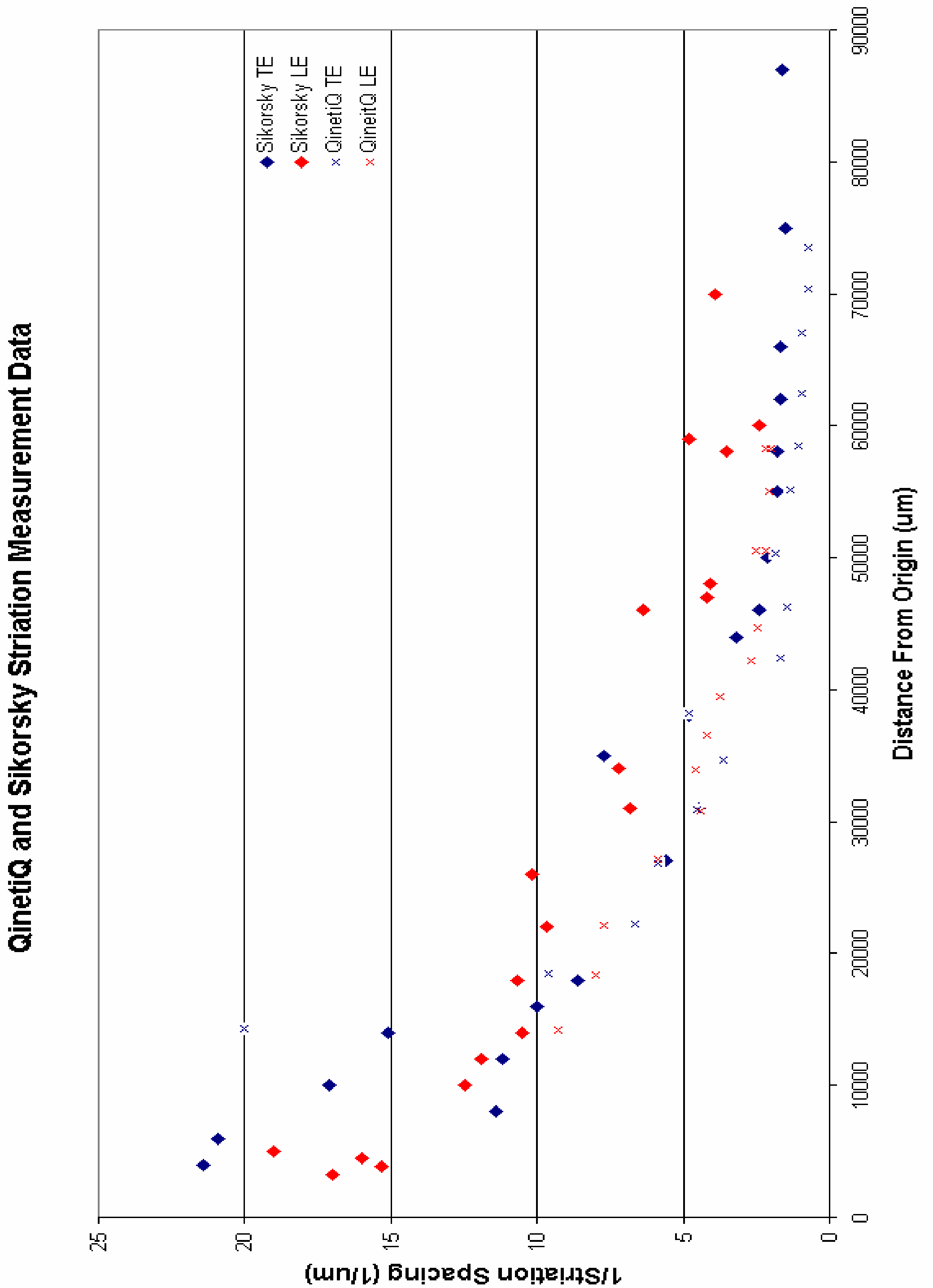

Figure 1. QinetiQ and Sikorsky striation density data.

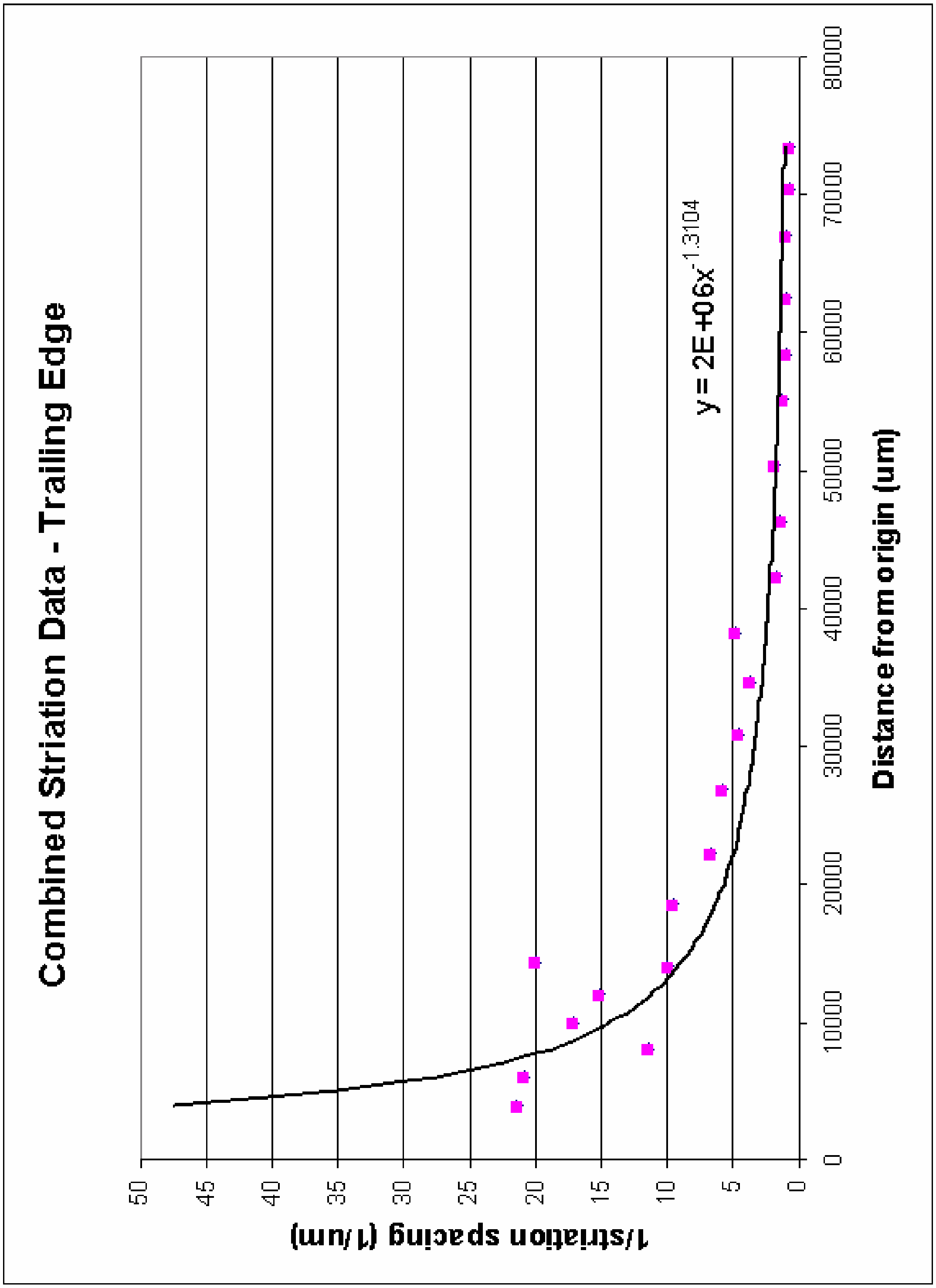

Figure 2. Combined Sikorsky and QinetiQ data for trailing edge crack.

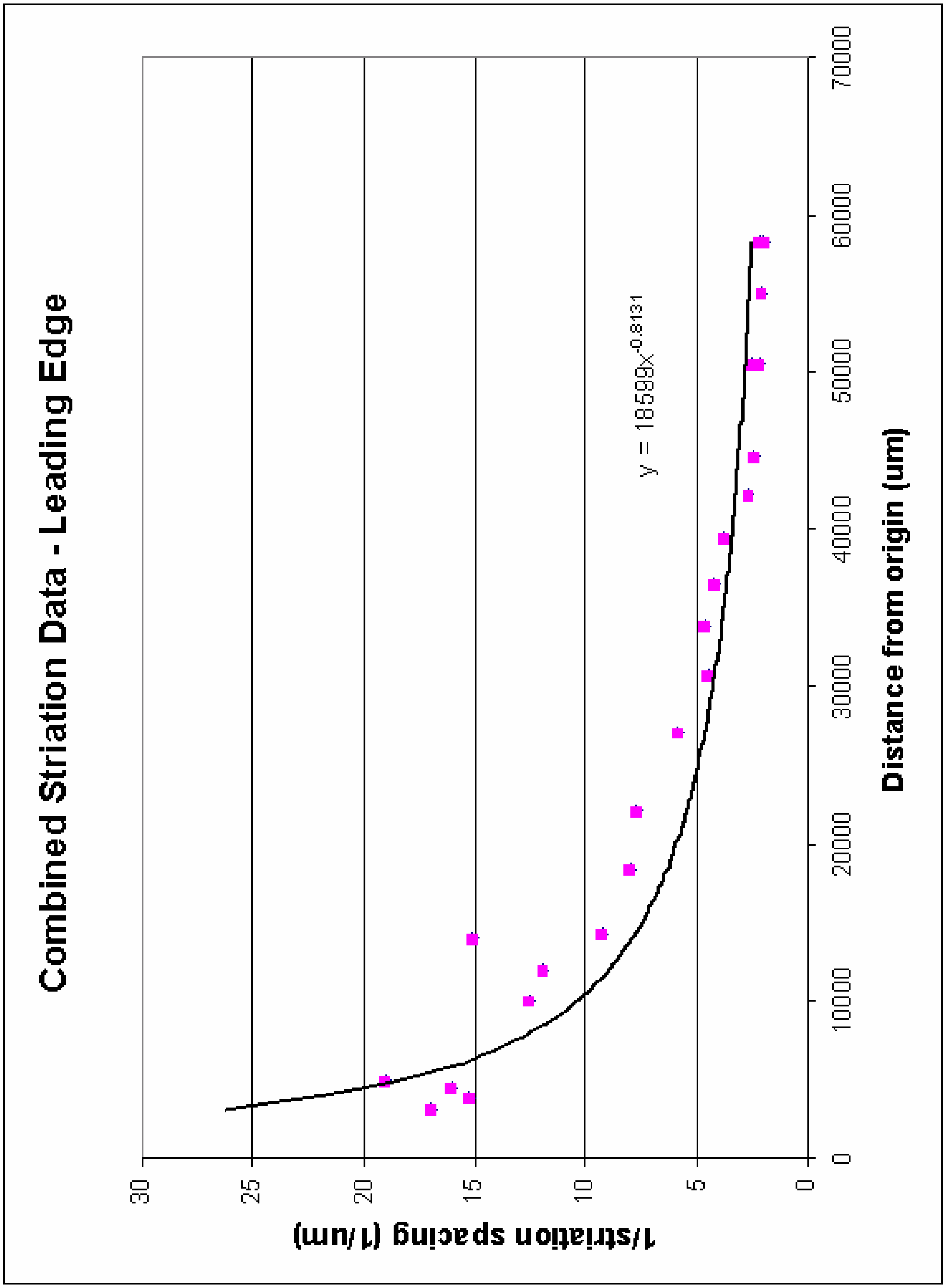

Figure 3. Combined QinetiQ and Sikorsky data for leading edge crack.

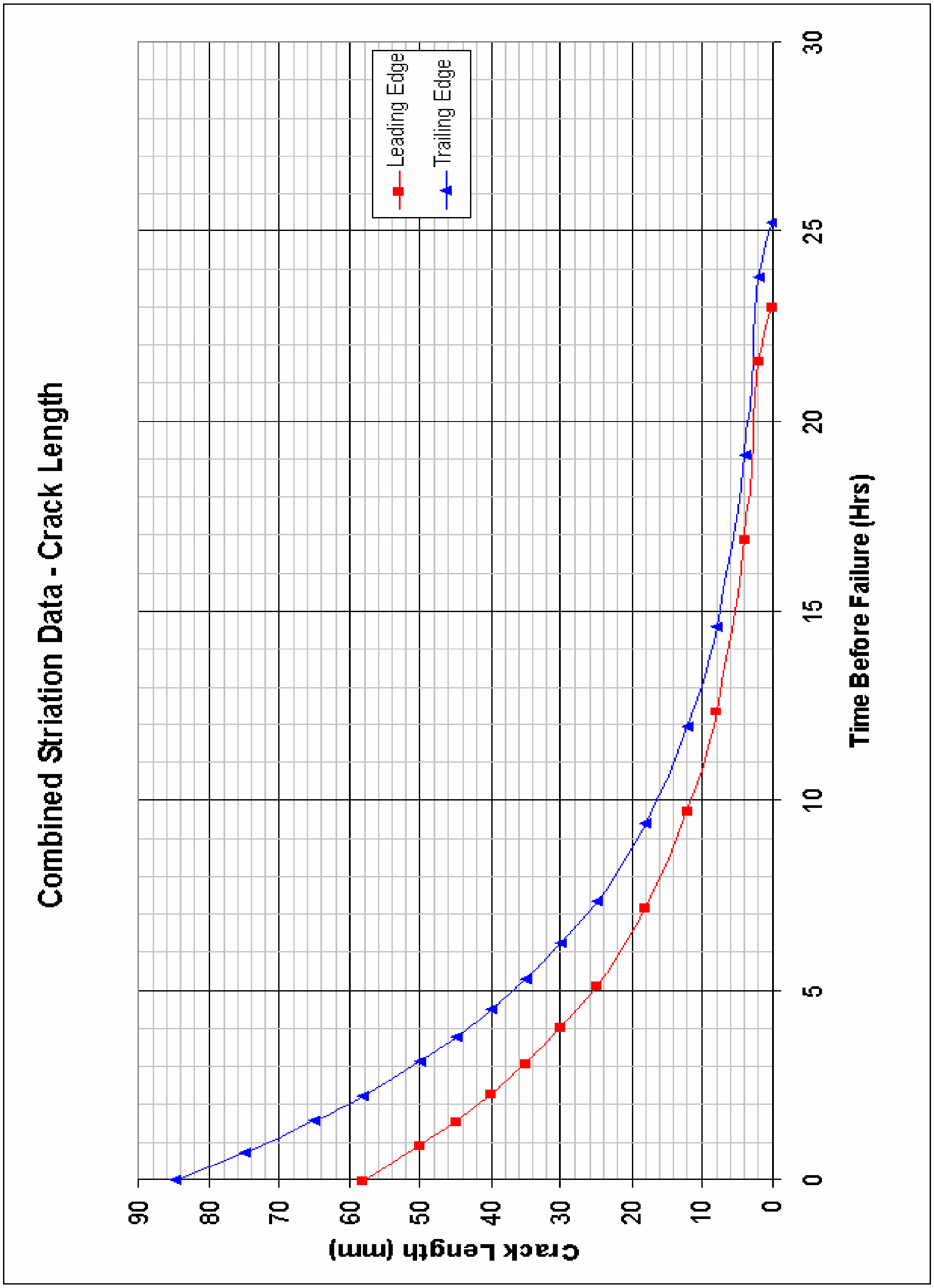

Figure 4. Combined data single power line through both sets of data to estimate likely crack length prior to failure.

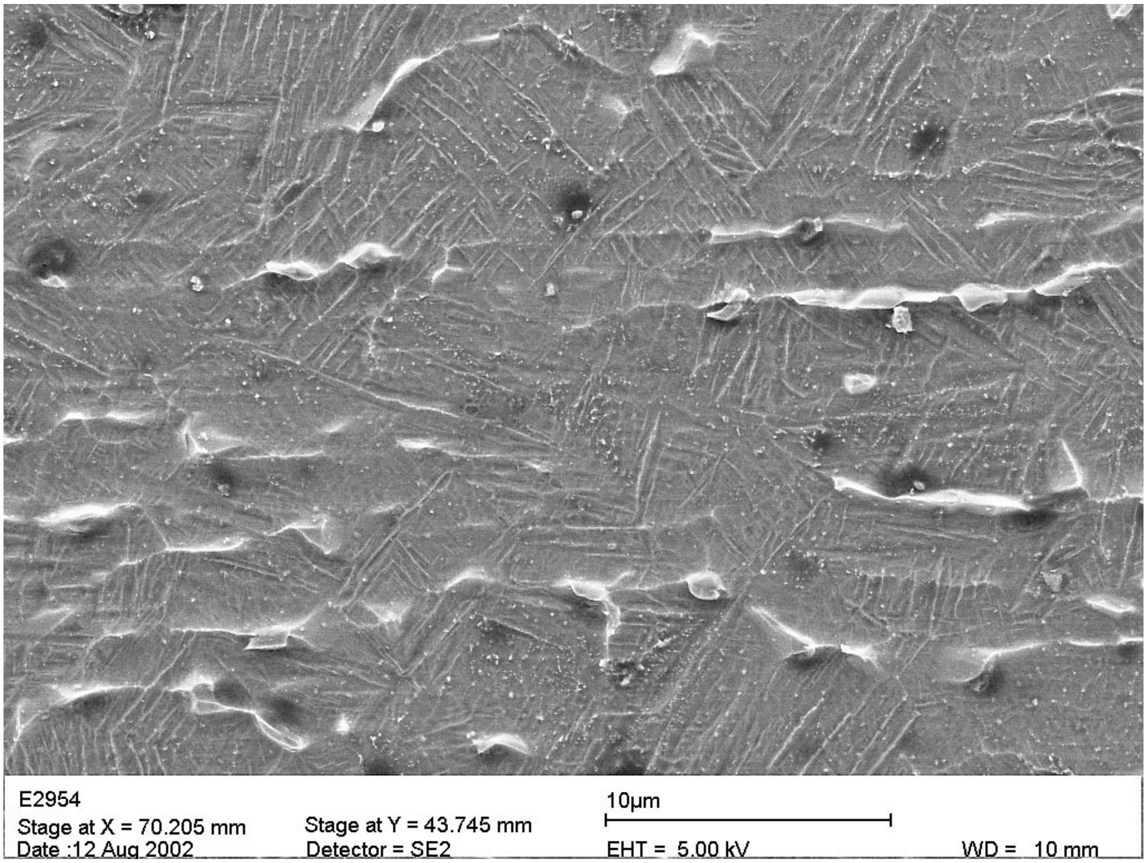

Figure 5. Microstructure of titanium spar showing lamella structure.

Sikorsky S76 Main Rotor Blade Erosion Strip Analysis

Following on from the examination of a Sikorsky S76 (G-BJVX) main rotor blade failure conducted by QinetiQ Cody Technology Park (reference report QINETIQ/FST/SMC/LR024608 – October 2002), a section of the leading edge erosion strip was returned for further analysis. The erosion strip had failed along with the main rotor blade as would be expected, giving a fractured edge (QINETIQ/FST/SMC/LR024608). It was requested that the fracture surface of the erosion strip be examined to determine if it failed due to overload or if there was any element of fatigue crack growth prior to final catastrophic failure.

The erosion strip was manufactured from commercially pure titanium and was approximately 0.45mm in thickness.

Scanning electron microscope (SEM) examination of the erosion strip fracture surface, identified striations, which indicated that the crack growth had occurred by fatigue. In order to make an approximate assessment of the crack growth rate, striation counting was carried out at varying points along the crack length.

Figure 1 shows the section of erosion strip that was examined, with the fracture surface identified. The fatigue crack initiated on the inner surface of the erosion strip approximately 6.7mm from the trailing edge (figure 2). From this point the crack propagated towards the trailing edge for the remaining 6.7mm of strip and towards the leading edge around the nose of the strip. Final catastrophic overload failure occurred when the fatigue crack was approximately 64.3mm (from origin) in length.

The fracture surface had suffered from some post failure mechanical damage, which had destroyed most of the fracture surface detail. This was observed to be most extensive around the origin and top trailing edge of the section. However, despite the damage, sufficient areas of fatigue striations were observed to enable striation spacing measurements to be carried out. Figure 3 shows an example of the striations observed.

Three areas of ductile overload were also observed within the fatigue. These occurred at 45.0 - 46.9mm, 47.2 - 49.0mm and 50.2 - 55.2mm (all measurements from origin) . These static jumps indicated that the fatigue crack propagation changed to overload for short periods of time during crack growth.

Initial analysis of the striation spacing data did not show any consistent pattern in striation spacing against crack length. The spacings appeared to be fairly random, so no useful conclusions could be drawn as to the total number of striations on the fracture surface. There was some doubt as to the validity of the striation spacing determination so a section was cut from the erosion strip and polished so that an examination of the microstructure could be carried out. After etching the polished specimen with Kroll's reagent, an acicular type structure was observed. It was believed that some of the striation spacing measurements may have actually been a feature of the microstructure rather than fatigue striations. With this in mind, the striation spacings were re-measured.

After re-measurement of the striations, the spacings appeared to increase as the crack length increased which is typical of fatigue crack growth. Figures 4 and 5 show the striation spacing and inverse of striation spacing against crack length respectively.

In the region from the origin until approximately 18.5mm from the origin, the striations were not clearly visible. There was a lot of post-failure mechanical damage and the small patches of striation-like features that were observed were not clearly defined. However, from approximately 18.5mm from the origin to the end of the crack, striations were observed which allowed an estimate of the total number of load cycles the erosion strip had encountered between these points. Using the blade RPM of 304, it was estimated that the time required for crack growth from approximately 18.5mm from the origin to final failure was 2.4 hours. Extrapolating the striation spacings back to the origin is difficult when approximately 18.5mm of the early crack growth did not reveal striations. However, a best-fit curve for the data was plotted and extrapolated back to 100μm to estimate the total number of load cycles for crack growth. It was estimated that the total number of cycles was 133,444, which can be converted to a time required for crack growth of 7.3 hours. Any estimates obtained from extrapolation back to the origin must be used cautiously.

The static jumps were removed from the total load cycle estimates. In essence, the total number of striations was calculated between the areas of fatigue crack growth (ie 100μm – 45mm, 46.9mm – 47.2mm, 49mm – 50.2mm and 55.2mm – 64.3mm) based on the best fit curve through the data (figure 5). This assumes that there is no appreciable difference in the fatigue crack propagation before and after the static jump, that is, the crack continues to propagate in a steady state across the whole crack length despite the static jumps. In reality it is possible that after a static jump the fatigue crack would need to initiate again and therefore the total time for crack growth could be considerably longer than the estimated 7.3 hours.

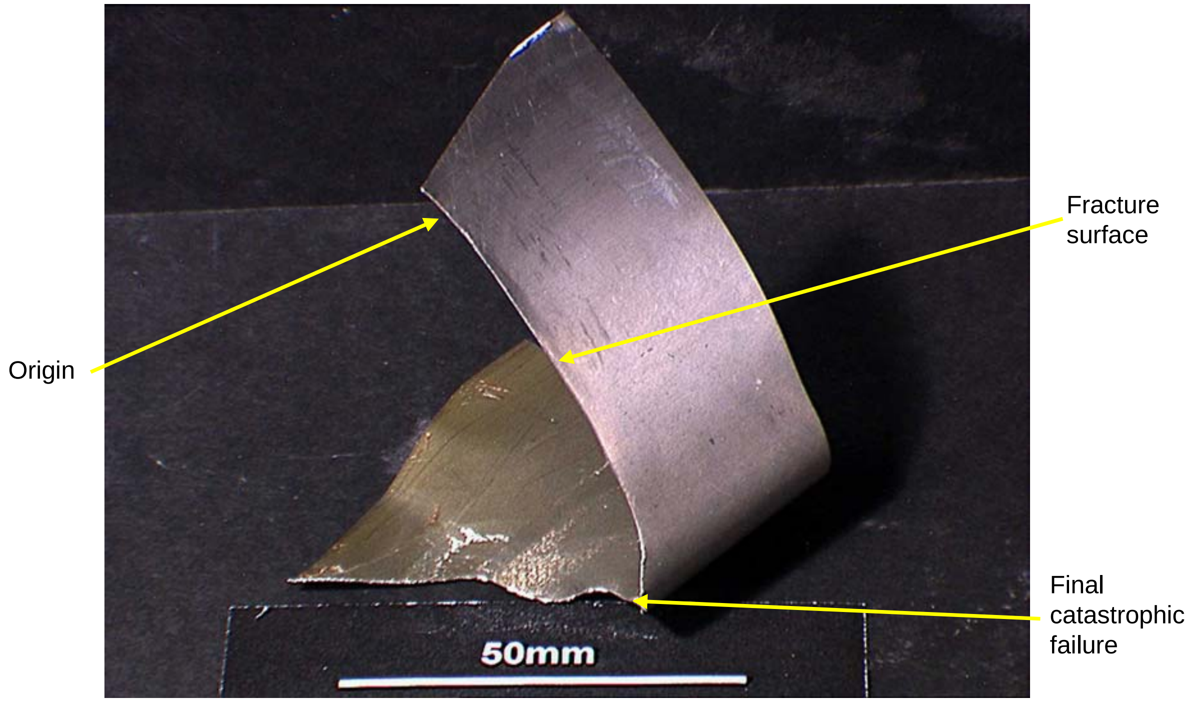

Figure 1. Section of Erosion strip with fractured edge.

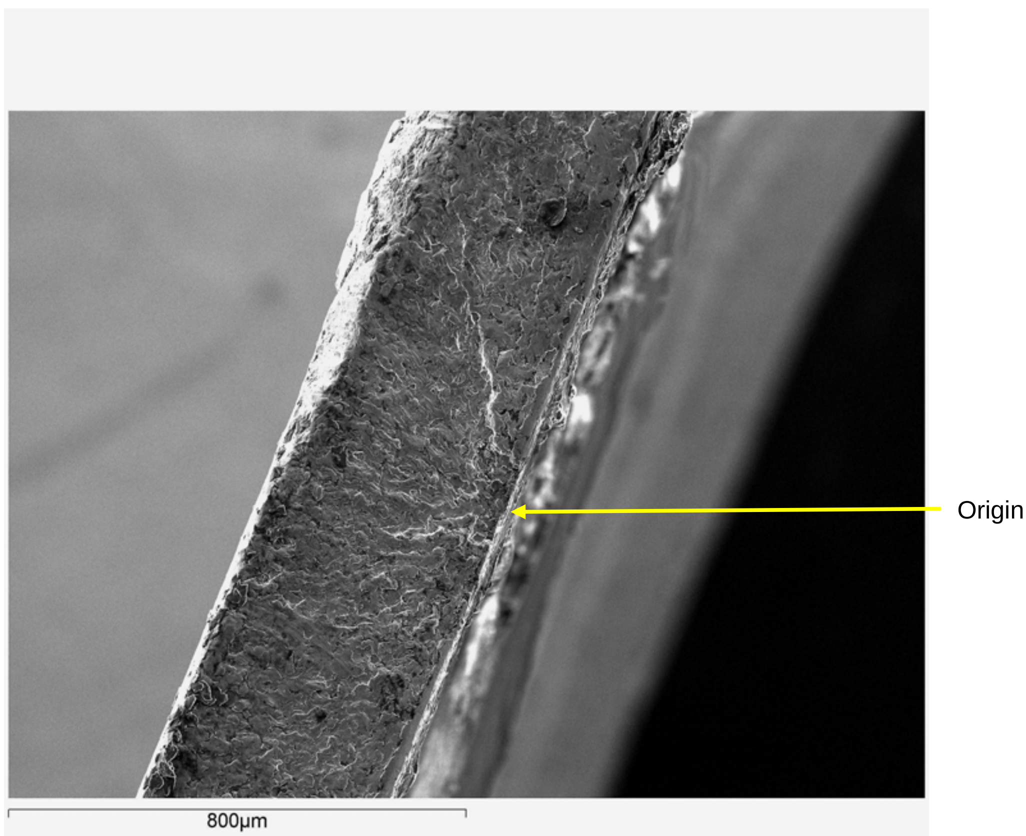

Figure 2. Origin for fatigue crack.

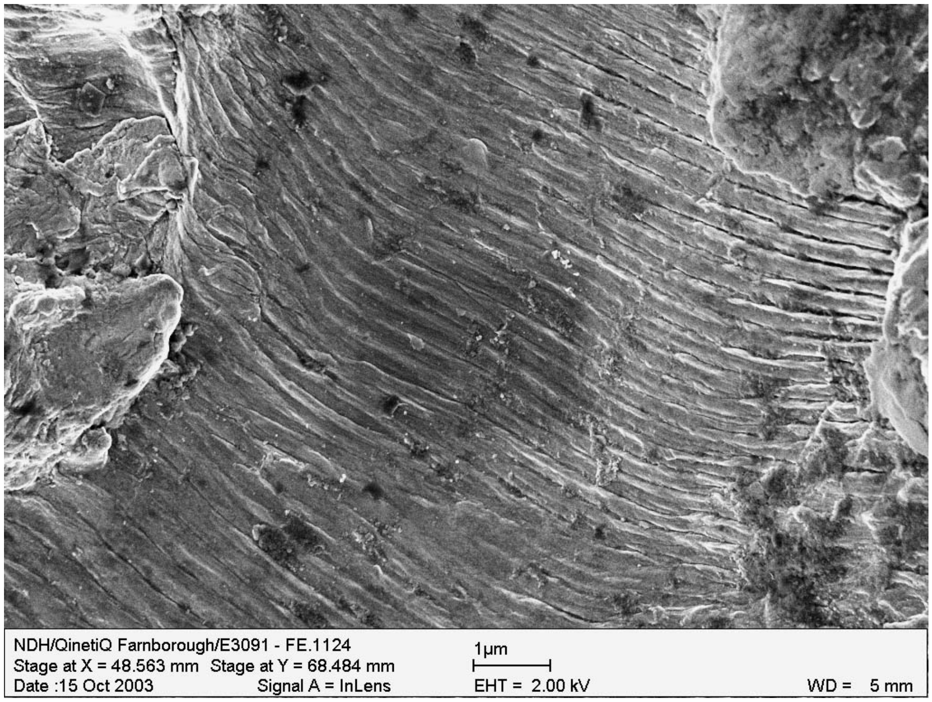

Figure 3. Example of striations observed on fracture surface.

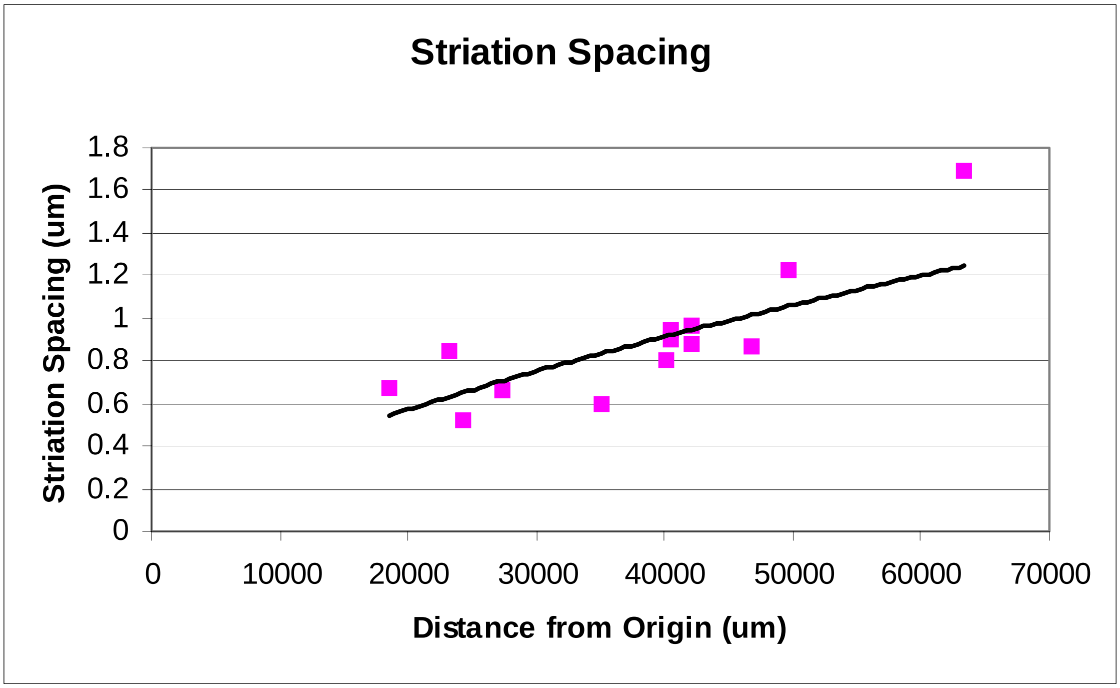

Figure 4. Striation spacing against crack length.

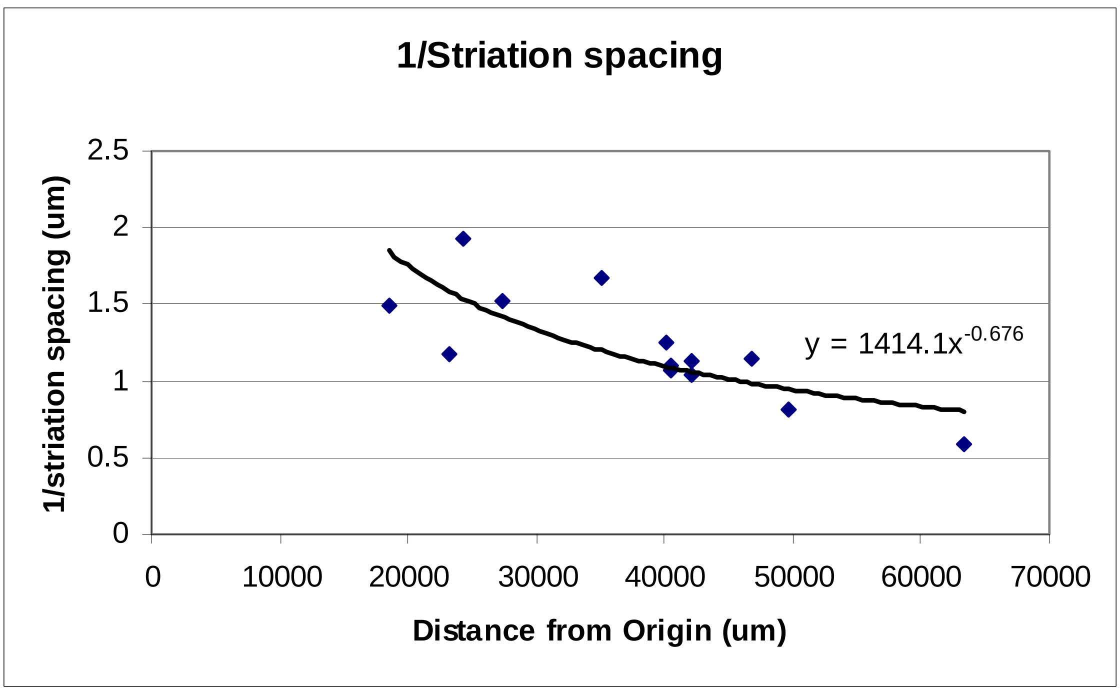

Figure 5. Inverse of striation spacing against crack length.

Sikorsky S76 Main Rotor Blade Failure

A previous QinetiQ investigation into a failed Sikorsky S76 main rotor blade (QINETIQ/FST/SMC/LR024608) found that failure occurred due to a fatigue crack initiating and propagating in the titanium spar. Fatigue striations measurements were carried out and an estimate of the crack life was determined. It was requested that a representative crack at different stages of propagation be introduced into a full size blade at the failure location to determine if the amount of blade droop changed with increasing crack length.
Rotor blade serial no. A086-00180A, which was fitted to the aircraft at the time of the accident but had remained relatively undamaged, was used in this experiment. The blade was bolted to a fixed bed at the root end through three of the available five fastener holes and the tip was allowed to drop freely. The distance from the floor to the top of the blade at the root end was measured as 1159mm. With the blade in the as-received condition, the distance from the top of the blade tip to the floor was measured as 617mm, which represents a natural blade droop of 542mm.

A position at the trailing edge of the erosion strip on the top surface of the blade 1950mm from the root was marked as the origin of the fatigue crack and a 30mm transverse slot was cut into the blade at this point to represent a crack propagating in the leading edge direction for 14mm and the trailing edge direction for 16mm. The distance between the blade tip and the floor was measured and the slot extended to represent increasing crack lengths. In total, the blade droop was measured at four different crack lengths. The different crack lengths are represented in figure 1 and the results of the blade droop are shown in table 1. Figure 2 shows a series of photos taken from a fixed camera position at the various crack lengths. Figure 3a shows the blade tip before cutting and figure 3b shows how the position changed after each cut. For each cut the blade is coloured differently and the results overlaid. The results of the blade droop are also shown in graph form in figure 4.

From the experiment, it was found that at a crack length of 19mm in the leading edge direction and 22mm in the trailing edge direction (cut 2), there was no increase in the blade droop. Fatigue striation measurements carried out in QINETIQ/FST/SMC/LR024608 and reported in QINETIQ/FST/SMC/LR026770 indicated that an approximate time before failure at the crack length of cut 2 was 5hrs 20mins which corresponds to the evening before the day of the accident when a visual inspection of the aircraft was carried out. Approximately one hour before failure, a pre-flight inspection was also carried out. The corresponding crack length at this time (cut 3) produced an increase in blade droop of 23mm over the blade length of approximately 6m.

Figure 1. Cross section through spar showing crack positions.

Cut ID	Crack length (mm) Leading / trailing edge direction	Approx. time before failure (mins)	Blade root distance from floor (mm)	Droop (mm)	Change in droop (mm)
No cut	0	N/A	617	542	0
1	14 / 16	460	617	542	0
2	19 / 22	320	617	542	0
3	44 / 58	60	594	565	23
4	58 / 84	Time of failure	554	605	63

Table 1. Results.

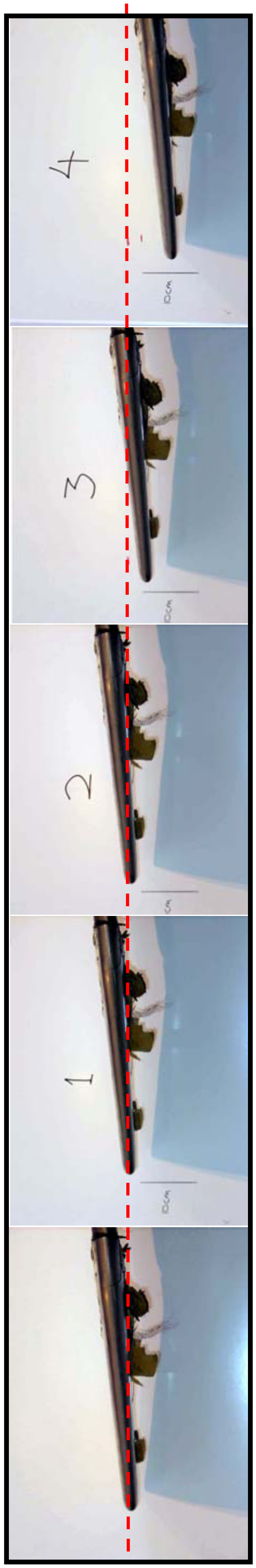

Figure 2. Blade droop at various crack lengths

a)

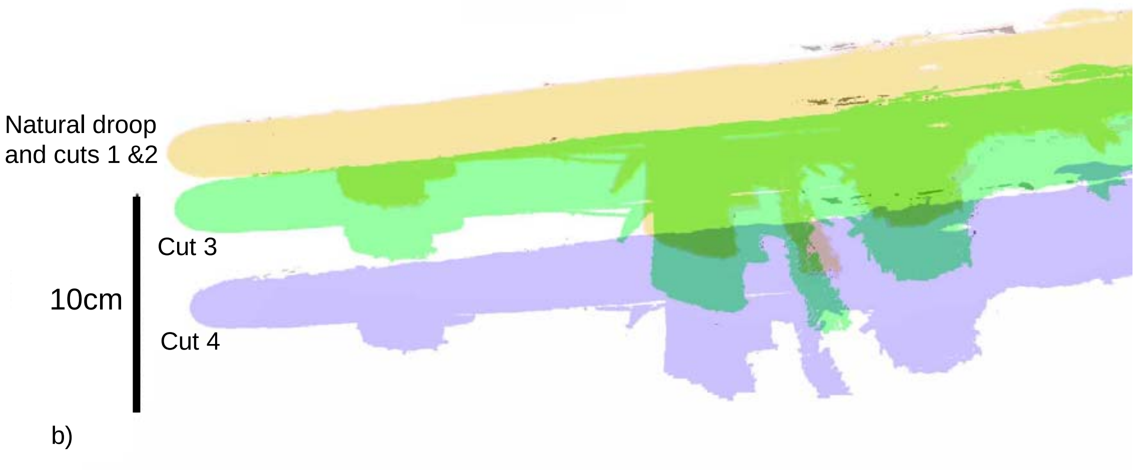

b)

Figure 2. a) blade droop, b) change in droop at different crack lengths.

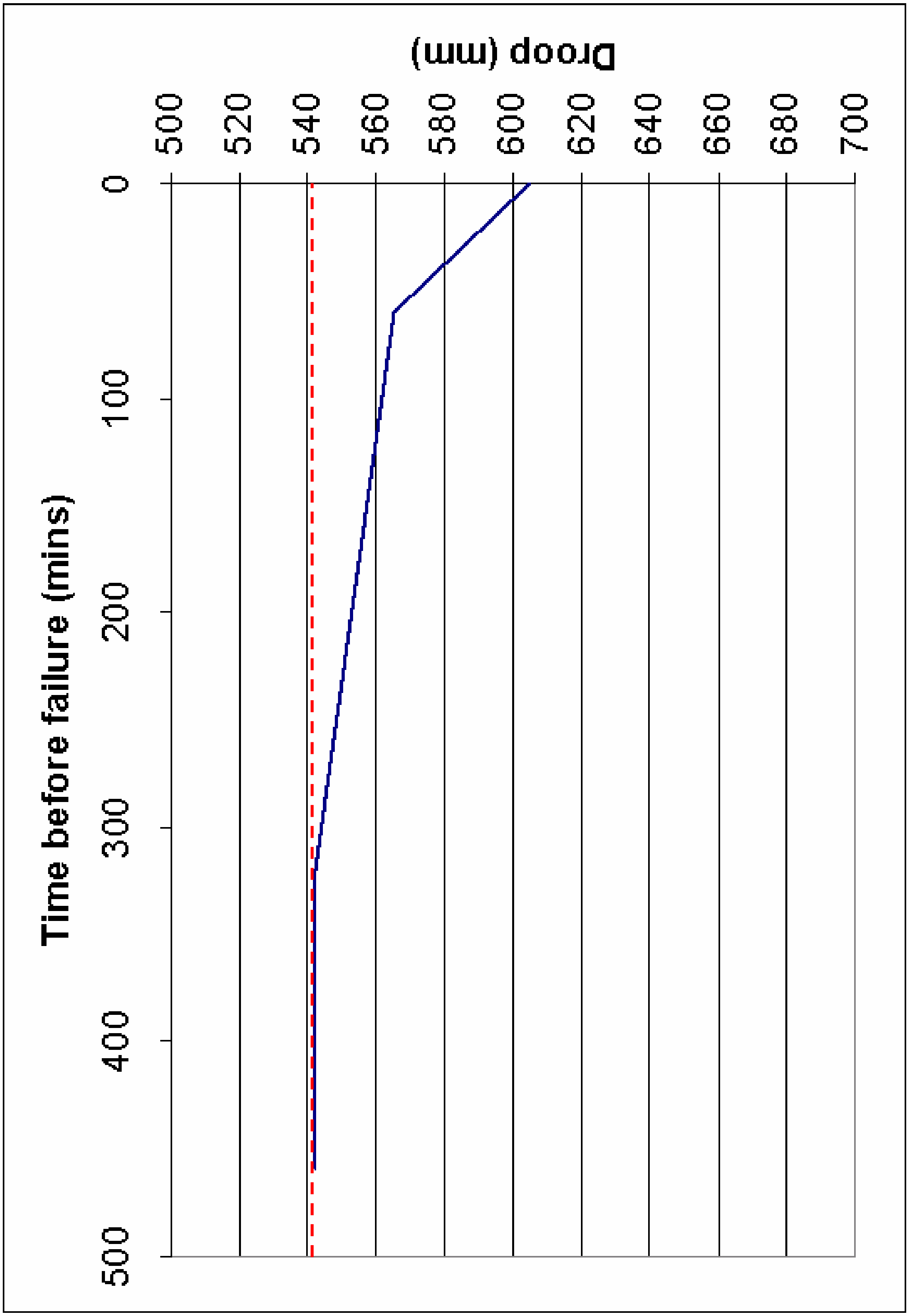

Figure 3. Graph of blade droop results.

In order to cut varying crack lengths in the spar during this experiment the external composite material and titanium erosion strip was also cut. A crack in the composite may not have been present during the actual failure especially around the leading edge and erosion strip and therefore this may have provided some resistance to the drooping that was observed during this experiment. Also the blade was slightly heavier due to ingress of water which may also have increased the amount of droop observed. Finally the “crack” introduce during this experiment was relatively wide (i.e. slitting wheel) when compared to a fatigue crack which may also have affected the degree of droop that was observed.

Unless otherwise indicated, recommendations in this report are addressed to the regulatory authorities of the State having responsibility for the matters with which the recommendation is concerned. It is for those authorities to decide what action is taken. In the United Kingdom the responsible authority is the Civil Aviation Authority, CAA House, 45-49 Kingsway, London WC2B 6TE or the European Aviation Safety Agency, Postfach 10 12 53, D-50452 Koeln, Germany.